Exploiting the Potentiality of
High Valent Transition Metal Halides
in Organic Synthesis

PhD Candidate: Niccolò Bartalucci

PhD Supervisor: Prof. Fabio Marchetti

University of Pisa

Doctoral School in Chemistry and Materials Science

XXXII Cycle

Abstract

Halides of group 5 and 6 transition metals in a +5 or +6 oxidation state (high valent metal halides, HVMH) are strong Lewis acids that can also exploit oxidizing power and halogenating ability, thus constituting potential mediators in various organic transformations. In the framework of our interest in the chemistry of HVMH with different organic functionalities, we have investigated the reactions with compounds bearing unsaturated C–N or C–O bonds. Activation products, like quinoxalinium and imidazolium salts, were obtained from the reactions of HVMH with α-diimines, as a result of intra-/inter-molecular couplings. Also, rare coordination complexes were isolated and characterized, including the first examples of high valent metal fluoride adducts with α-diimines. Unprecedented, "non-classical" coordination compounds were afforded from NbX_5 (X = Cl, Br) and isocyanides. Furthermore, clean CO release at room temperature was observed for the first time from tertiary α-phenylcarboxylic acids upon interaction with HVMH, resulting in either the isolation of stable carbocation salts, or their conversion into more stable hydrocarbons.

Index

1. Introduction

1.1. High Valent Transition Metal Halides

High valent transition metal halides (HVMH), with a metal centre in an oxidation state higher than +4, may represent potential, easily available alternatives to the use of precious elements in organic synthesis. The heavier group 5 and 6 metal halides (i.e., niobium and tantalum pentahalides, molybdenum pentachloride and tungsten hexachloride) combine a strong Lewis acidic character[1–5] with a high oxidation potential,[6–8] and thus are able to promote a wide variety of organic transformations, including the dehydrogenative coupling of arenes[9,10] and other C–C bond forming processes,[11,12] the hydrofunctionalization[13] and hydroaminoalkylation[14,15] of alkenes, the polymerization of alkynes[16,17] and various cycloaddition reactions.[18] Despite being simple and low-cost precursors, HVMH are remarkably air-sensitive, and their handling may be rather difficult: this might be one of the reasons why the chemistry of these compounds is relatively young.[19]

1.1.1. Group 5 Transition Metal Halides

While having received increasingly high attention in the past two decades,[20–22] compounds based on group 5 transition metals still "live in the shadow of metal complexes of group 4" (Kempe et al. 1998, p. 3363).[23] The use of group 5 metal halides in metal-mediated synthesis has been rather circumscribed, when compared to the

group 4 congeners and, within group 5 itself, the prevalent attention has been devoted to vanadium compounds which have found application mainly in industrial processes.[24–28] Nevertheless, the employment of MX_5 (M = Nb, Ta) in both stoichiometric and catalytic reactions has seen a significant growth in the recent past, encouraged by their cheapness and by the substantial non-toxicity of the metal elements.[29,30]

Niobium and tantalum pentahalides present themselves as crystalline solids, with colours ranging from colourless (NbF_5, TaF_5, $TaCl_5$), to yellow ($NbCl_5$, $TaBr_5$), red ($NbBr_5$, TaI_5) and dark brown (NbI_5).[31,32] They are relatively volatile,[33,34] which is indicative of the covalency of the M–X bonds. In the solid state, the structures of MX_5 are oligomeric (pentafluorides are M_4F_{20} tetramers, while the heavier halides are dimers, M_2X_{10}), and the metal centre is hexacoordinated, with some of the halide ligands displaying a bridging coordination (Figure 1).[35–38] They are scarcely soluble in non-coordinating solvents, while, due to their high Lewis acidity, even weak donor atoms can easily break the oligomeric structure:[39–43] this makes them highly susceptible to hydrolysis by even traces of moisture.
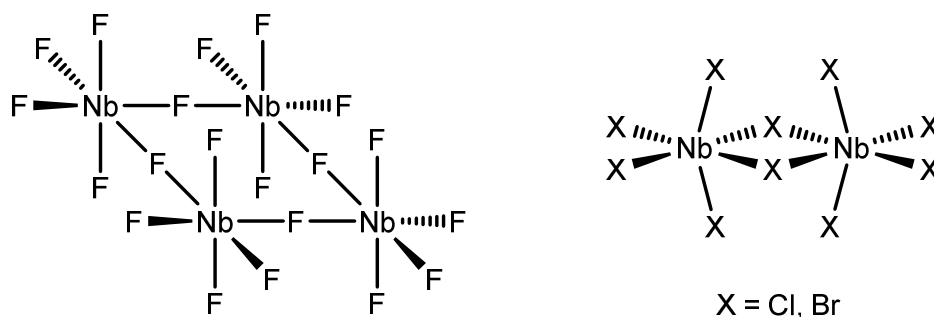

Figure 1. Solid-state structures of niobium pentahalides. Tantalum pentahalides are isostructural.

Given the striking electronic and functional similarities, niobium and tantalum pentahalides have been often compared with their main group isoelectronic counterparts, i.e. group 15 pentahalides.[44] However, despite all of them being strong Lewis acids,[3,4,45] there are some important differences between the more common PX_5 and MX_5 (M = Nb, Ta) that must be pointed out. PF_5 is a colourless gas at room temperature (b.p. = −102°C) and has a trigonal bipyramidal geometry under all conditions. Like niobium and tantalum pentafluorides, it reacts readily with Lewis bases, including F^-, with which forms the stable, non-coordinating PF_6^- anion.[46] Instead, MF_5 can also form the even more stabilizing $M_2F_{11}^-$, analogous to the main group $Sb_2F_{11}^-$, but displaying a higher thermal stability,[47] which allows for the stabilization of unusual, elusive organic cations at room temperature and above.[7,48] PCl_5 is a well-known chlorinating agent,[49] commonly employed in numerous organic protocols for the chlorination of alcohols,[50] carboxylic acids[51] and amino acids.[52] Niobium and tantalum pentahalides may be employed in Cl/O exchange reactions as well (see Section 1.2.2), but their higher M–Cl bond energy (Nb–Cl = 98 kcal/mol, Ta–Cl = 104 kcal/mol; mean bond energies in the gaseous phase have been considered),[53,54] compared to the P–Cl bond energy in PCl_5 (*ca.* 69 kcal/mol),[55,56] results in a more difficult chlorine transfer.[57,58] This makes them poorer chlorinating agents, but may also allow for the stabilization of otherwise reactive cations: $[Cl]^-$ and $[PCl_6]^-$ salts of pyrrolidinium-2-carbonylchloride are prone to degradation at room temperature, due to release of HCl and subsequent condensation reactions, while $[NbCl_6]^-$ and $[TaCl_6]^-$ salts have been reported to be stable up to

80°C.[59] Similar considerations can be made for the comparison between PBr_5 (mean P–Br bond energy = 58 kcal/mol),[56] employed as a brominating agent,[60] and MBr_5 (Nb–Br = 83 kcal/mol, Ta–Br = 87 kcal/mol).[53]

1.1.2.   Group 6 Transition Metal Chlorides

In addition to being strong Lewis acids, molybdenum pentachloride ($MoCl_5$) and tungsten hexachloride (WCl_6) are, when compared to the heavier halides of group 5, more prone to reduction, due to their higher oxidation potential (E($MoCl_5$) = 1.16 V and E(WCl_6) ≈ 1.1 V, *versus* the ferrocene/ferrocenium couple),[6,9] and are characterized by weaker metal-halide bonds,[53,61] thus favouring Cl/O exchange reactions (see Section 1.2.2).

$MoCl_5$ is the highest thermally stable molybdenum chloride,[62] and has a dimeric Mo_2Cl_{10} structure with chloride bridges in the solid state, in analogy with niobium and tantalum pentachlorides (*vide supra*). WCl_6 is one of the few known hexachlorides to be stable at room temperature, and has monomeric, octahedral solid state structure (Figure 2). Both substances are dark, volatile solids under standard conditions.
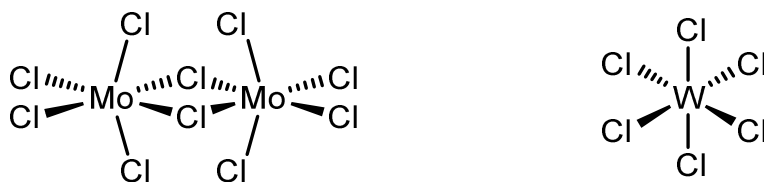

Figure 2. Solid-state structures of molybdenum pentachloride and tungsten hexachloride.

4

1.2. Metal-directed Activation of Organic Moieties

Looking at the d-block transition metal series from left to right, one can notice a trend in the reactivity of the high valent chlorides with organic molecules: taking the interactions with oxygen donors as an example, $TiCl_4$ generally reacts by affording hexacoordinated complexes, and activation of the ligands is observed at high temperature only;[63] $NbCl_5$ and $TaCl_5$ (while still displaying a quite rich coordination chemistry) are able to cleave C–O bonds such as those in alcohols and ethers in relatively mild conditions, but only exploit their Lewis acidity when interacting with stronger C–O bonds (i.e. double bonds of carbonyl compounds);[57,64] instead, in view of the lower M–Cl bond energy (Mo–Cl = 82 kcal/mol, W–Cl = 83 kcal/mol)[53] and the higher oxidation potential, $MoCl_5$ and WCl_6 make possible stoichiometric modifications of simple molecules through unconventional pathways even at room temperature or below. The following sections will try to rationalize the outcomes of the interaction of HVMH with organic substrates, providing an overview of their behaviour with the most common functional groups and organic transformations.

1.2.1. O-H Activation

Within the interaction of HVMH with organic substrates bearing an O–H functionality, it can be observed that the M–X bond energy is of key importance in the determination of the nature of the products. For instance, the highly energetic M–F bonds in niobium or tantalum pentafluorides (Nb–F = 138 kcal/mol, Ta–F = 144 kcal/mol)[53] are not cleaved in the reaction of these halides with simple alcohols such as methanol or ethanol: instead, coordination complexes $MF_5(ROH)$ or $[MF_4(ROH)_4][MF_6]$ (M = Nb, Ta; R = Me, Et) can be obtained, and the O–H bond is thus preserved.[65] This is in line with the documented coordination chemistry of MF_5 with monodentate ligands (L): complexes with 1:1 and 1:2 stoichiometries are generally obtained, the former being $[MF_5L]$ species, assumed to be mononuclear with C_{4v} symmetry, and the latter being ionic species $[MF_4L_4][MF_6]$, with eight-coordinate cations and six-coordinate anions.[66] On the other hand, the M–X bonds in the heavier pentahalides (MX_5, with M = Nb, Ta, Mo; X = Cl, Br) are comparatively weaker, so an HX release is feasible, leading to (halo-) alcoholato[67,68] or carboxylato complexes.[69]

The activation of the O–H bond of an alcohol or a carboxylic acid can also be the preliminary step for a further functionalization of the organic substrate: this strategy has allowed Goldman and co-workers to efficiently synthesize stereohindered amides, such as N-methylated amides and peptides (Figure 3).[70]

6
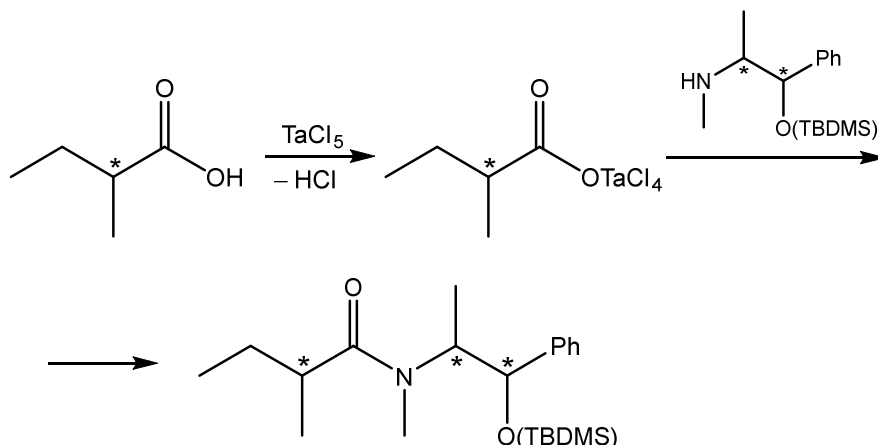
Figure 3. TaCl$_5$-mediated coupling between (S)-(+)-2-methylbutyric acid and TBDMS protected-(1S,2S)-(+)-pseudo-ephedrine.

NbCl$_5$ has also proven itself to be an excellent catalyst for the trimethylsilyl protection of alcohols. The reactions were performed in dichloromethane at room temperature, and reached almost complete conversion within minutes.[71] Although no reaction mechanism was provided, it is observed that the more electron-rich the alcohol, the better the yield, and the shorter the reaction time.

1.2.2.   C-O Activation

Besides the M–X bond energy, another important aspect to consider when evaluating the behaviour of HVMH with oxygen-based moieties, is the remarkable oxophilicity of these metal centres: this characteristic is the reason for the extreme air-sensitivity of high valent metal halides, as they will react almost instantly with even traces of H$_2$O, eventually yielding the stable metal oxide after the release of the corresponding hydrogen halide. Accordingly, the

interaction of metal halides with other O-donors can be driven by the formation of a stable M–O bond: the cleavage of strong metal chloride bonds such as those in $NbCl_5$ (98 kcal/mol) can be balanced by the formation of an even stronger Nb–O bond (184 kcal/mol in gaseous $NbOCl_3$).[53] Such Cl/O exchanges can be exploited as effective synthetic tools for the chlorination of C–O bonds in organic substrates.

In 1992, Jones and co-workers investigated the possibility of obtaining chlorinated alcohols by employing $NbCl_5$, $TaCl_5$, $MoCl_5$ and WCl_6, observing that the chlorination was not only feasible (the 5d metals working better than the 4d ones), but in some cases (i.e. with secondary alcohols) offered selective chlorination, unaccompanied by elimination.[72] A room temperature, $NbCl_5$-mediated chlorination of a hydroxyl moiety was employed for the synthesis of highly desirable β-chloro-α,β-unsaturated ketones (Figure 4).[73]

R = R' = R" = H
R = R' = H, R" = Me
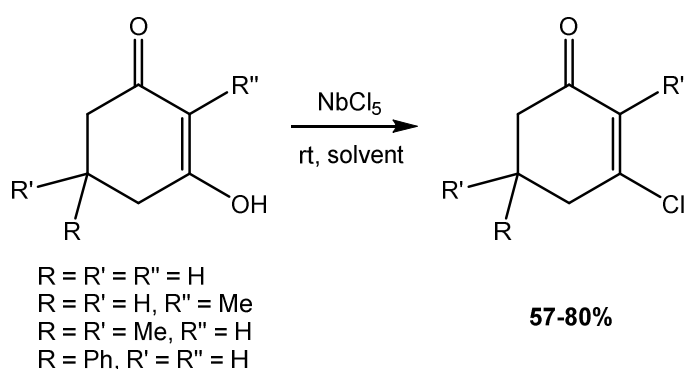R = R' = Me, R" = H
R = Ph, R' = R" = H

57-80%

Figure 4. Synthesis of β-chloroenones promoted by $NbCl_5$.

Group 6 high valent metal chlorides have also been reported as chlorinating agents to access acyl chlorides from carboxylic acids[74,75] and α-ammonium acyl chlorides from some α-amino acids.[76]

8

The high Lewis acidity of $NbCl_5$ was exploited in the catalytic activation of the C–OH bond in benzyl alcohols, allowing for substitution reactions by C-, O-, N- and S-centred nucleophiles.[77] By employing $MoCl_5$ as a catalyst, it is also possible to obtain the substitution using less nucleophilic nitrogen donors, such as sulfonamides and carbamates, while still operating in mild conditions (Figure 5).[78]

R' = H, F, OH, MeO
R" = alkyl, aryl, allyl, alkynyl

65-95%
Nu = RO, RNH_2, RS, RSO_2NH, ROCONH
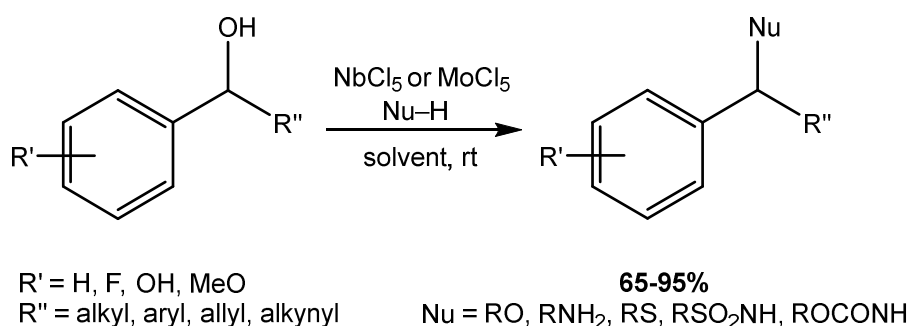
Figure 5. Nucleophilic substitution of benzyl/propargyl alcohols catalysed by MCl_5 (M = Nb, Mo).

Allylic or propargylic alkoxides have been reported to undergo a formal metalla-halo-[3,3] rearrangement when treated with NbX_5 (X = Cl, Br): this leads to the generation of allylic or allenic halides, powerful electrophilic intermediates in organic synthesis (Figure 6). This method allows for the preparation of such highly desirable intermediates from simple alkoxides, which can in turn be obtained from allylic/propargylic alcohols (by deprotonation), or from carbonyl compounds by treatment with vinylmagnesium bromide.[79,80]

Figure 6. Formal NbX$_5$-promoted metalla-halo-[3+3] rearrangement of allylic/propargylic alkoxides to yield allylic/allenic halides (X = Cl, Br).

When simple acyclic ethers interact with MoCl$_5$ or WCl$_6$ at room temperature (and above), the cleavage of C–O bonds can occur as a result of a Cl/O exchang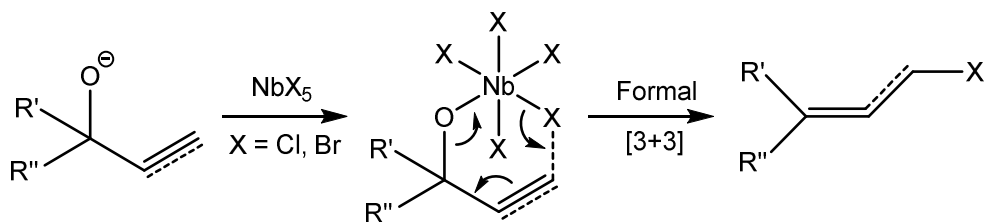e:[81,82] formation of alkyl chlorides can be observed as a result of rupture the C$_{sp3}$–O bond in Et$_2$O (affording EtCl) and *t*-BuMeO (forming both MeCl and *t*-BuCl); aryl ethers such as Ph$_2$O, while able to reduce WCl$_6$ to WCl$_5$(OPh$_2$) following the release of Cl$_2$, are not cleaved even at high temperatures; the resistance of C$_{sp2}$–O bond to cleavage is further confirmed when mixed aryl alkyl ethers, like PhOMe (anisole), are treated with group 6 high valent halides: only MeCl is observed. Furthermore, in aromatic substrates bearing more than one ethereal bond (e.g. bis-alkoxyl derivatives of catechol or BINOL), NbCl$_5$ is reported to be selective for the mono-dealkylation: only one C$_{sp3}$–O bond is cleaved, and the corresponding alkyl chloride is released.[83,84] Conversely, mono-chalcogenoethers are not activated by direct interaction with MX$_5$ (M = Nb; Ta; X = F, Cl, Br), and coordination adducts [MX$_5$(ER$_2$)] (E = S, Se, Te) have been reported.[85]

The ability of NbCl$_5$ of breaking C–O bonds in relatively mild conditions can also be exploited in the MOM (methoxymethyl ether)

10

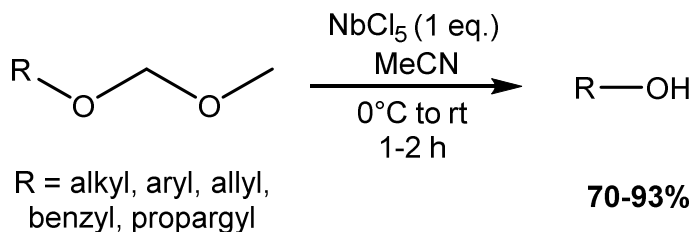deprotection of alcohols, which normally requires harsher conditions and a strongly acidic medium (Figure 7).

$$R\diagdown O\diagdown O\diagdown \xrightarrow[\substack{0°C\ to\ rt \\ 1\text{-}2\ h}]{\substack{NbCl_5\ (1\ eq.) \\ MeCN}} R{-}OH$$

R = alkyl, aryl, allyl,
benzyl, propargyl

70-93%

Figure 7. $NbCl_5$-mediated deprotection of methoxymethyl ethers.

High valent metal chlorides from group 5 and 6 can be also employed catalytically in the cleavage and further functionalization of ethers, by adding an acyl chloride to the reaction mixture: this will result in the formation of an ester, and the metal chloride will be regenerated in the process.[86,87]

If a polyether, like 1,2-dimethoxyethane (dme), is treated with MCl_5 (M = Nb, Ta) at room temperature in a 2:1 ratio (or higher), the formation of 1,4-dioxane occurs, as a consequence of unusual multiple C–O activation of the organic substrate, which also leads to the release of MeCl (Figure 8). The formation of the corresponding metal oxo-chloride coordination adduct, $MOCl_3$(dme), accounts for the abstraction of an oxygen from the starting material, and also serves as a driving force for the overall process. Other 1,2-dialkoxyalkanes, like diglyme, 1,2-diethoxyethane or 1,2-dimethoxypropane have also been shown to undergo the same kind of process.[88] Instead, by treating 1,2-dialkoxyethanes ($ROCH_2CH_2OR$, R = Me, Et) with niobium and tantalum pentafluorides, ionic derivatives $[MF_4(k^2\text{-}ROCH_2CH_2OR)_2][MF_6]$ are obtained at room temperature: the

activation of the organic substrate yielding 1,4-dioxane is still observed, but it only occurs upon heating. In accordance with the general trend, these reactions are driven by the nature of the halide: given the stronger M–X bonds, the $[MF_5]$ frame is preserved and the formation of alkyl fluorides is disfavoured, thus the rearrangement gives selectively dialkylethers OR_2 (R = Me, Et) instead (Figure 8).[58]
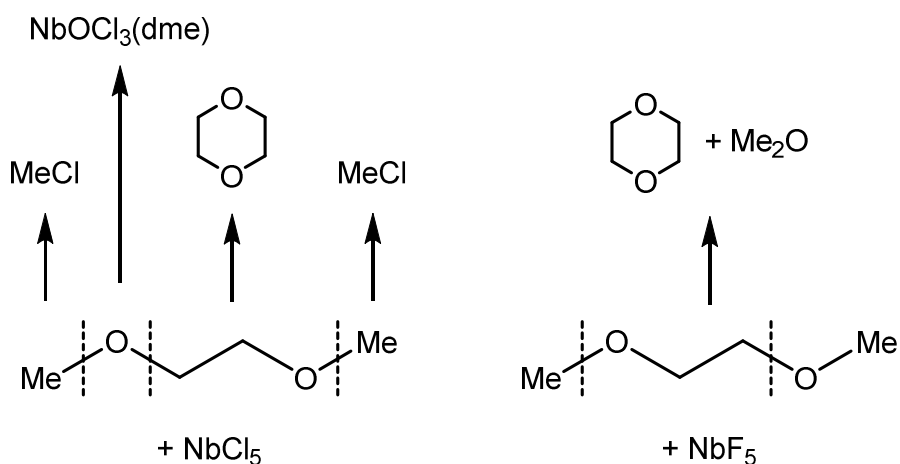
Figure 8. Fragmentation reactions of 1,2-dimethoxyethane (dme) in the presence of NbX_5 (X = Cl, F).

Analogous carbon-chalcogen bond cleavage can be observed in ditelluroether $CH_2[CH_2Te(t\text{-}Bu)]_2$, which is decomposed in the presence of $TaCl_5$ to multiple products, including the dealkylated $[(t\text{-}Bu)Te(CH_2)_3Te][TaCl_6]$, as a result of Te–C bond cleavage.[85]

Cyclic ethers like 1,4-dioxane can themselves interact with high valent metal halides: in this respect, group 5 heavier pentahalides may behave as typical Lewis acids, i.e. they are able to coordinate oxygen donors affording simple, mononuclear adducts.[19] However, either a thermal treatment or the use of an excess of organic reactant may

12

result in C–O activation processes, especially in smaller, more strained cyclic compounds: both 1,3-dioxolane and tetrahydrofuran (thf) form $MX_5(L)$-type coordination adduct when added in a 1:1 ratio to niobium or tantalum pentahalides, but the 1,3-dioxolane adduct yields bis(chloromethyl) ether upon heating,[89] and thf undergoes polymerization when added in an excess with respect to the metal halide (see Section 1.2.6).[90] Group 6 halides like $MoCl_5$ instead, promote a room temperature C–O activation in thf regardless of the stoichiometry, and 1,2-dichlorobutane is formed, together with molybdenum oxo-chloride, $MoOCl_3$, which can bind excess thf.[91]

As particularly strained cyclic ethers, epoxides undergo ring opening reactions when interacting with high valent metal halides: in 2007, Constantino and co-workers have shown that $NbCl_5$ can be employed as an efficient Lewis acid catalyst to perform the ring opening of variably substituted epoxides, obtaining a range of different outcomes, including chlorohydrins and rearrangement products. A tentative mechanism for α-pinene oxide was also proposed: as a probable first step, the coordination of $NbCl_5$ to the oxygen atom is suggested.[92] While investigating stoichiometric reactions of a selection of simple epoxides with niobium and tantalum pentahalides, we have found out that the ring opening occurs with insertion into a M–X bond (when X = Cl, Br): in particular, the reaction of 1,2-epoxybutane with MCl_5 (M = Nb, Ta) proceeds with a regioselective insertion of the epoxide into an M–Cl bond, with the chloride attacking the less hindered carbon (Figure 9).[93] In the case of niobium and tantalum pentafluorides, the generally stronger M–F bonds are not prone to insertion, and again, the $[MF_5]$ frame is preserved: instead,

NbF$_5$ promotes a Meinwald-type rearrangement of 2,3-dimethyl-2,3-epoxybutane into methyl tert-butyl ketone.[94]
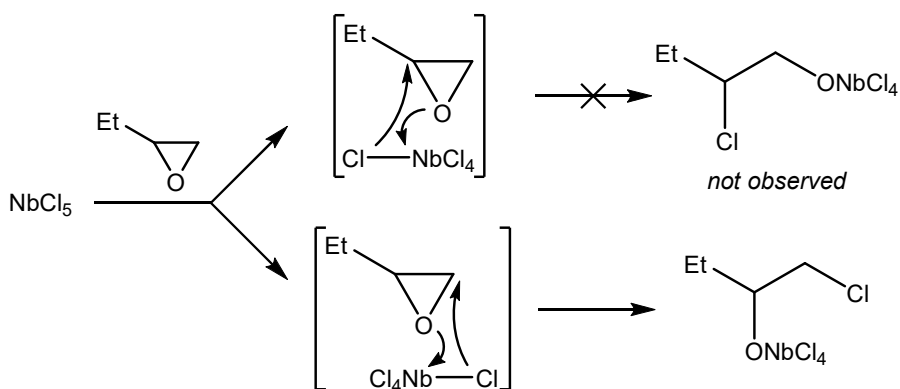
Figure 9. Possible modes of insertion of 1,2-epoxybutane into the Nb–Cl bond of NbCl$_5$.

Niobium and tantalum pentachlorides have also proven to be good catalysts for the regioselective ring opening of epoxides by aromatic amines, which allows for the synthesis in mild conditions of synthetically relevant β-amino alcohols.[95,96]

Often by exploiting their marked Lewis acidic character, high valent metal halides are reported as catalysts in several transformations involving carbonyl groups.

NbCl$_5$ catalytically activates aldehydes towards nucleophilic attack by α-diazoesters, allowing β-ketoesters to be obtained in good yields by carrying out the reactions at room temperature in dichloromethane, with a reasonably low catalyst loading (5 mol%). The authors suggest a plausible coordination of the carbonyl oxygen to the Nb(V) centre, thus enhancing the electrophilicity of the carbon and allowing for the C–H insertion of the nucleophile (ethyl diazoacetate).[97]

14

The same authors were also able to exploit the Lewis acidity of NbCl5 in the promotion of the Knoevenagel condensation between aldehydes and β-diketones/β-ketoesters, being able to carry out the reaction in mild, solvent-free conditions (Figure 10).[98]

R = Me, Ph, OEt
R' = Me, Ph, OEt, OMe
R'' = Ph, Cy, n-heptyl, p-Tol, p-ClC$_6$H$_4$, p-OMeC$_6$H$_4$, o-NO$_2$C$_6$H$_4$

62-90%
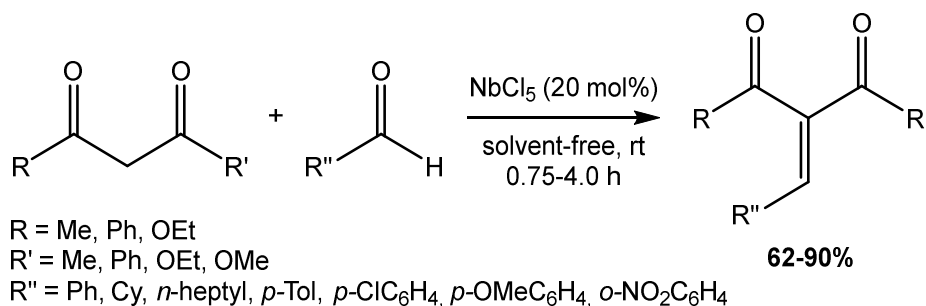
Figure 10. Solvent-free NbCl5-catalysed Knoevenagel condensation between 1,3-dicarbonyl compounds and aldehydes.

Various other condensation and multicomponent reactions involving the activation of carbonyl compounds by niobium pentachloride as a Lewis acid have been documented: NbCl5 has been employed as a catalyst for the room temperature, solvent-free synthesis of triarylmethanes from N,N-dimethyl- or N,N-diethylaniline and a selection of aromatic aldehydes (Baeyer condensation).[99] Bis(indolyl)methanes have been obtained as well from aromatic aldehydes and NbCl5 as a catalyst, by treatment with two equivalents of indole in methanol at ambient temperature.[100]

A one-pot, three-component Mannich reaction between acetophenone, substituted benzaldehydes and a variety of aromatic amines was reported for the synthesis of β-aminoketones in ethanol at room temperature, employing NbCl5 (10 mol%) as a catalyst (Figure 11).[101]
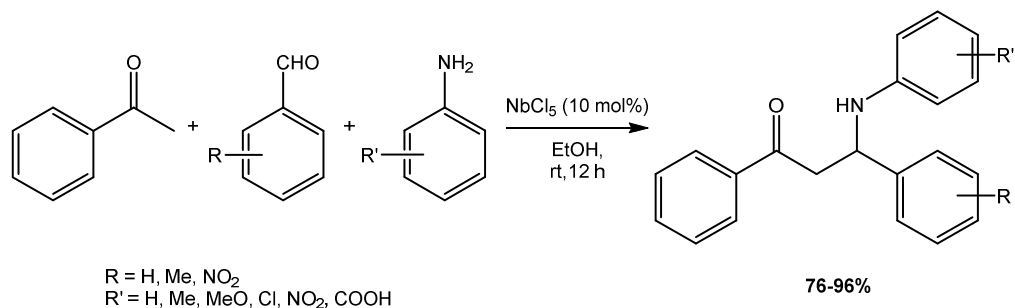
Figure 11. Direct Mannich reaction of various aryl aldehydes and aromatic amines with acetophenone catalysed by niobium pentachloride, to synthesize β-amino carbonyl compounds.

The NbCl$_5$-catalysed condensation of a variety of aromatic, aliphatic and allylic amines with 1,3-dicarbonyl compounds, occurring at room temperature without any additional solvent, has been exploited for the chemo- and regioselective synthesis of enamine derivatives (β-enaminones and β-enamino esters).[102]

The three-component reaction of carbonyl compounds, amines and diethyl phosphite (Kabachnik-Fields reaction), catalysed by NbCl$_5$ under solvent-free conditions, was reported by Zhang and co-workers as a mild protocol for the preparation of a wide variety of α-aminophosphonates in good to excellent yields in short time (Figure 12). α-Aminophosphonates are a recurring motif in various bio-active compounds, and have been employed as substitutes for the corresponding α-amino acids and as intermediates in organic synthesis.[103]

16

Figure 12. NbCl$_5$-catalysed Kabachnik-Fields reaction for the one-pot synthesis of α-aminophosphonates under solvent-free conditions.

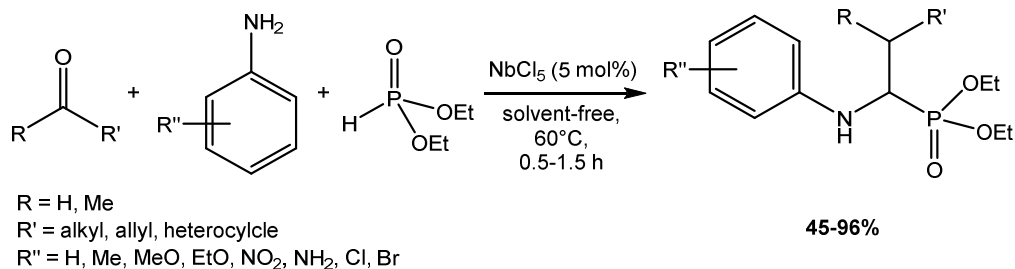Lewis acid-catalysed cyanosilylation of aldehydes and ketones has been carried out using NbF$_5$ as a catalyst: the reaction has been reported to proceed at room temperature, in solvent-free conditions with a low catalyst loading (0.5-1 mol%), and almost quantitative conversion could be attained in 20 minutes.[104] The same reaction has also been reported employing NbCl$_5$/phytic acid as a reusable homogeneous catalyst.[105]

WCl$_6$ activates carbonyl compounds towards nucleophilic attack from sulfonamides, to attain the synthesis of N-sulfonyl imines. In the proposed mechanism, WCl$_6$ acts as a Lewis acid catalyst, and it was found to be suitable for recovery and recycling in up to four successive runs.[106]

It should however be noted that group 6 high valent metal chlorides, other than being potent Lewis acids, also display a lower M–Cl bond energy when compared to their group 5 congeners (*vide supra*): because of this feature, a Cl/O exchange is also feasible when MoCl$_5$ and WCl$_6$ interact with carbonyl compounds. It was initially reported by Jung and collaborators that by treating cyclic ketones with WCl$_6$, it was possible to obtain vinyl chlorides or *gem*-dichlorides, according to

the steric hindrance of the starting material.[107] More recently, our group has contributed to the field by reporting a stoichiometric 1:2 reaction between MoCl$_5$ and a selection of simple ketones, R$_2$C=O: the outcome is the formation of *gem*-dichlorides (R$_2$CCl$_2$) as a result of a Cl/O exchange, which also forms MoOCl$_3$. The latter is then able to coordinate another equivalent of ketone to form the neutral adduct MoOCl$_3$(O=CR$_2$) (Figure 13).[108]
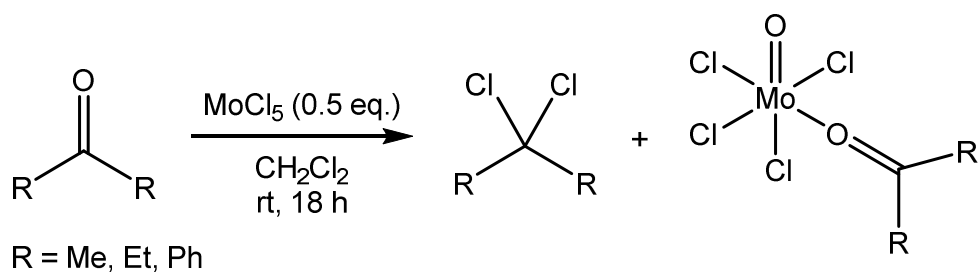
Figure 13. Synthesis of *gem*-dichlorides from ketones mediated by MoCl$_5$.

Carboxylic acid derivatives like amides and esters were also investigated in the same work: chloriminium salts were obtained as a consequence of a single chlorine transfer to the amide substrate per metal centre. While it was possible to isolate stable chloriminium salts originating from tertiary (i.e. N,N-disubstituted) amides, those generated from secondary amides like acetanilide showed tendency to undergo self-condensation to yield acylamidinium salts.[109] Evidences of Cl/O exchange were also observed for the interaction of MoCl$_5$ with esters (i.e. formation of MoOCl$_3$) but attempts at identifying and isolating any chlorinated organic derivative were unsuccessful.[110]

It is noteworthy that the "amide" C=O bond in lactams appears to be somewhat less reactive towards chlorination by molybdenum

18

pentachloride, when compared to the C=O bond in ketones. This was shown by the reaction of the MoCl$_5$ with isatin (1H-indole-2,3-dione): only the "ketone" C=O bond is chlorinated, while the "amide" C=O is left intact (Figure 14).
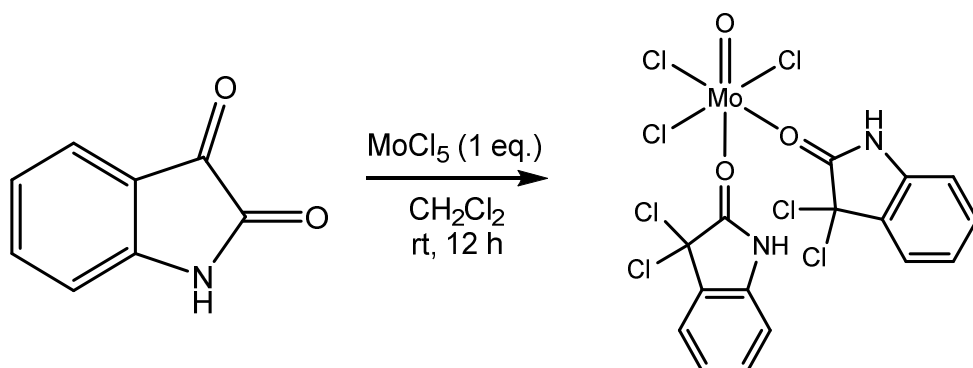
Figure 14. Reaction of MoCl$_5$ with isatin (1H-indole-2,3-dione).

The sensitivity of high valent transition metal halides to oxygen has been exploited on organic substrates (containing the C=O moiety) that can undergo dehydration: NbCl$_5$ forms a coordination complex with N,N'-dicyclohexylurea (dcu), and when a solution of said complex is treated with excess triethylamine, dicyclohexylcarbodiimide (dcc) is formed, together with NbOCl$_3$, upon release of HCl;[111] benzonitrile has been obtained by dehydration of benzamide promoted stoichiometrically by NbCl$_5$ or WCl$_6$: the reaction proceeds with formation of NbOCl$_3$ or WOCl$_4$, respectively, and release of HCl.[112]

TaCl$_5$ and NbCl$_5$ were both found to be active in the catalytic acylation of alcohols and phenols by acetic anhydride.[113,114] The reactions were performed at room temperature in dichloromethane, and reached almost complete conversion in a few hours, showing numerous advantages (e.g. a broader functional group tolerance)

when compared to previously known protocols requiring stoichiometric or excess reagents and harsher conditions (e.g. strong bases). The same strategy was later extended to the acetylation of other nucleophiles besides alcohols: amines and thiols have also shown comparable results under the same reaction conditions (Figure 15).[115] We have recently reported an example of deacetylation promoted by $NbCl_5$ or $NbBr_5$: when treated with equimolar amounts of the niobium halide at room temperature, acetylsalicylic acid underwent loss of the acetyl group, which was released as the corresponding acetyl halide. After hydrolysis of the reaction mixtures, salicylic acid was recovered as the sole organic product.[69]

$$R\text{—}NuH \ + \ Ac_2O \ \xrightarrow[\substack{CH_2Cl_2 \\ \text{rt, 1-3 h}}]{NbCl_5 \ (10 \ mol\%)} \ R\text{—}Nu$$

Nu = O, S, NH   **85-96%**
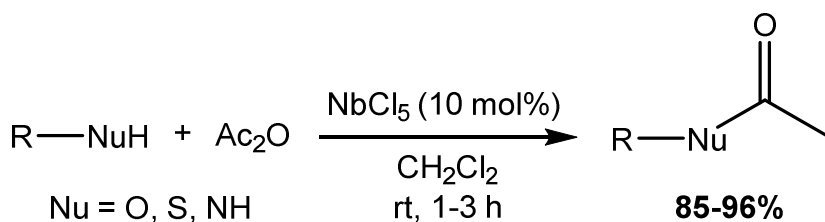
Figure 15. Acetylation of alcohols, thiols and amines with acetic anhydride, catalysed by $NbCl_5$.

Acetylation, and more in general acylation of arenes and heterocycles was also achieved *via* Friedel-Crafts reaction catalysed by $NbCl_5$, with $AgClO_4$ as an additive: the authors propose a mechanistic pathway in which a chloride from $NbCl_5$ is abstracted by $AgClO_4$, leading to the catalytically active species $[NbCl_4][ClO_4]$. This protocol allows for a catalyst loading as low as 1 mol%, and employs anhydrides as acylating reagents. Carboxylic acids can also be directly used, by adding *p*-nitrobenzoic anhydride to obtain the *in situ* formation of the mixed anhydride.[116] A $NbCl_5$-catalyzed Friedel-Crafts reaction was

20

further exploited by Da Silva Barbosa and co-workers by using a bifunctional electrophile, an α,β-unsaturated carboxylic acid, to achieve the cascade intermolecular alkylation/intramolecular acylation of aryl substrates, leading to indanones as final cyclization products (Figure 16).[117] Other examples of one-pot, multicomponent cascade reactions promoted by high valent metal halides will be discussed in the following (see Section 1.2.3).
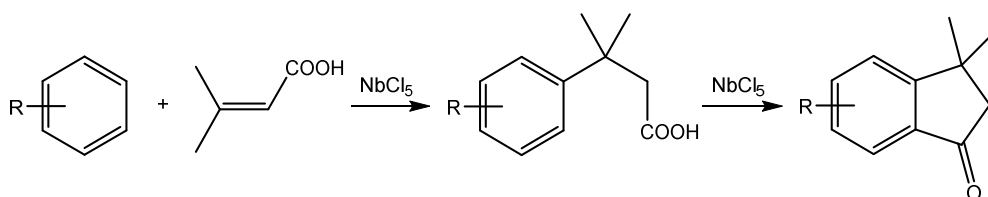
Figure 16. Proposed pathway for the NbCl₅-catalysed Friedel-Crafts intermolecular alkylation followed by intramolecular acylation leading to indanones.

1.2.3.   Cycloaddition / Cyclization Reactions

Cycloaddition reactions are one of the simplest and most economical strategies for the synthesis of heterocyclic compounds, including several biologically relevant molecules: pyrimidines have been commonly synthesized with this method, as a result of a metal-assisted interaction of an alkyne unit with two nitrile units.[18]

Obora and collaborators have reported a NbCl₅-mediated [2+2+2] cycloaddition of terminal/internal alkynes with aryl nitriles. Unlike previously reported procedures, this protocol chemo- and regioselectively yielded substituted pyrimidines, without undesired

pyridine (cycloaddition of two alkyne units and one nitrile unit) or benzene (alkyne cyclotrimerization) derivatives: the authors suggest that this is due to the high Lewis acidity of $NbCl_5$ towards the nitrile group, which results in a dimerization of the latter as a first step (Figure 17). Optimal pyrimidine yields were obtained by adding $NbCl_5$ in six batches (each 0.2 mmol, one every 2 h, 1.2 mmol total), using the nitrile as a solvent, and operating at 60 °C for 22 h.[118]
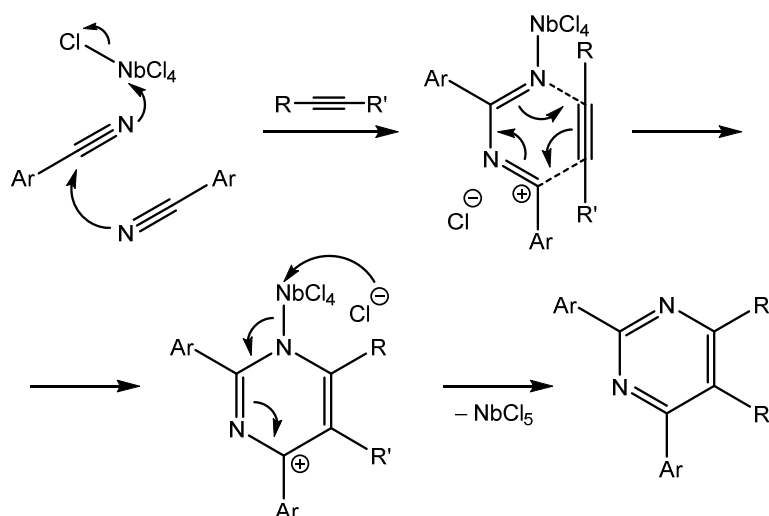
Figure 17. Proposed mechanism for the [2+2+2] cycloaddition of alkynes and aryl nitriles mediated by $NbCl_5$.

The same authors have later proposed a "catalytic version" of the aforementioned process, employing 20 mol% $NbCl_5$ with $FeCl_3$ as an additive, thus exploiting the different affinities of the two Lewis acids towards different substrates. The method was also extended to alkyl and vinyl nitriles, albeit with lower yields.[119]

Niobium pentachloride has also been reported as a pre-catalyst in cycloaddition reactions driven by low-valent niobium species: the catalytically active species in the 2:1 ratio reaction between alkynes

22

and nitriles, which afforded pyridine derivatives, is generated *in situ* by employing NbCl$_5$ (20 mol%) in the presence of Zn and Ph$_2$Si(OMe)$_2$;[120] cyclohexadienes have been synthesized from alkenes and terminal[121] or internal alkynes[122] in cycloaddition reactions catalysed by a NbCl$_5$/(TMS)$_3$SiH and a NbCl$_5$/Zn/PCy$_3$ system, respectively; in one particular case, i.e. the reaction between *tert*-butylacetylene and a selection of aliphatic alkenes, the proposed low-valent niobium active catalyst was generated directly by the alkyne, without using any external reducing agent.[123]

Strained polycyclic compounds, investigated as components for high-energy hydrocarbon fuels used in rocket systems, have been obtained from the homodimerization of 1,3,5-cycloheptatrienes, passing through tandem [6+2] and [4+2] cycloadditions: niobium and tantalum pentachlorides can promote such dimerization selectively towards one homodimer, while other metal catalysts drive the rearrangement towards a different homodimer (Figure 18).[124]
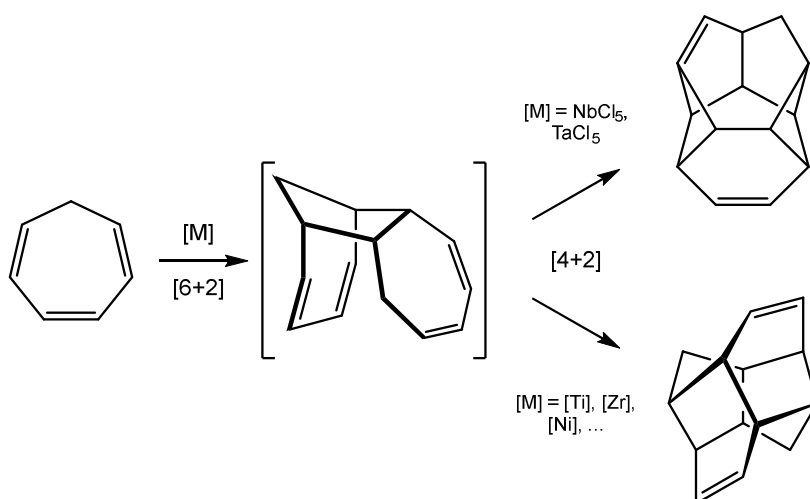

Figure 18. Influence of the metal catalyst on the outcome of the homodimerization of 1,3,5-cycloheptatriene.

The catalytic carboxylation of epoxides is known in the literature as a method for the synthesis of cyclic carbonates: from Aresta's seminal work in the early 2000s,[125] Nb(V) species have been investigated as potential catalysts for the process, in the presence of a nucleophilic co-catalyst. The $NbCl_5/NBu_4Br$ system was found to be very efficient for the synthesis of variably substituted propylene carbonates at low temperatures and low CO_2 pressure (Figure 19).[126] Several modifications have then been applied to the method, like the use of imidazolium bromides as nucleophiles, which allowed for even milder reaction conditions (room temperature, 4 bar CO_2 pressure),[127] and the implementation of carboxymethyl-cellulose-supported imidazolium-based ionic liquids, in order to improve the robustness and reusability of the catalytic system.[128]
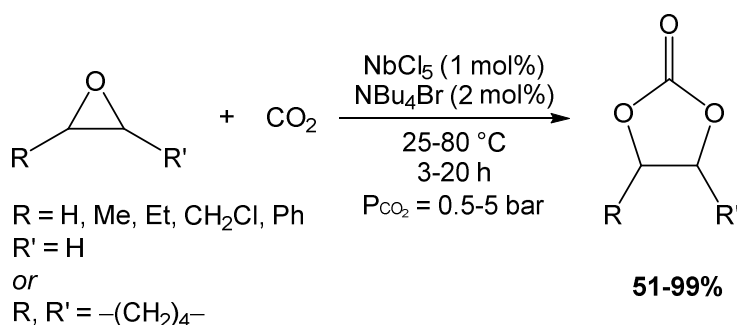
Figure 19. The $NbCl_5/NBu_4Br$ system as a catalyst for the solvent-free carboxylation of epoxides to cyclic carbonates.

Moreover, Basset and collaborators have reported a thorough mechanistic investigation, proposing a dual role of the nucleophilic co-catalysts (i.e. performing a nucleophilic ring-opening of the epoxide at the beginning of the catalytic cycle, and coordinating the metal centre in the final, rate-determining step of the cyclization). The involvement

24

of a second Nb centre in the CO_2 insertion step is also suggested on the basis of computational and experimental results.[129]

An analogous system, NbCl$_5$/NBu$_4$I, was studied for the catalytic cycloaddition of CO_2 to aziridines: the protocol allowed for the synthesis of N-tosyloxazolidinones from the corresponding N-tosylaziridines, but though NbCl$_5$ provided complete regioselectivity, the system based on Nb(OEt)$_5$ granted overall better yields.[130]

Epoxides are also involved in the synthesis of 4-chloro-5,6-dihydro-2*H*-pyran derivatives, by reaction with homopropargylic alcohols, promoted by niobium pentachloride: in the tentative mechanism proposed by the authors, NbCl$_5$ both facilitates the ring opening of the epoxide by coordinating the oxygen atom, and provides the chloride nucleophile (Figure 20).[131]

Figure 20. Tentative mechanistic pathway for the NbCl$_5$-promoted synthesis of dihydropyran derivatives, by the reaction of homopropargylic alcohols and epoxides.
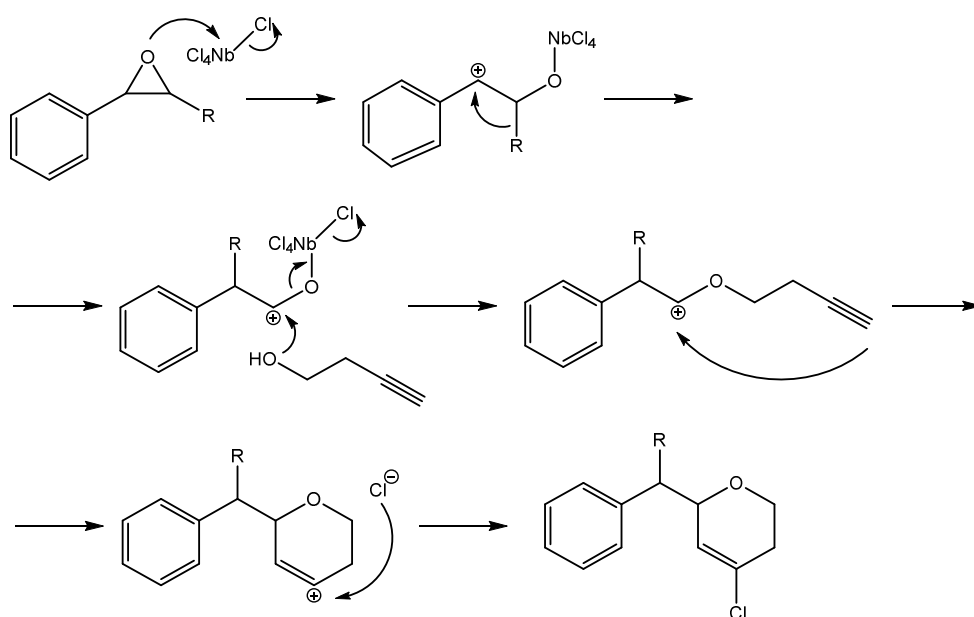
The Prins cyclization is an acid-catalysed addition of alkenes/alkynes to carbonyl compounds, and it is one of the most important synthetic routes for the preparation of six-membered tetrahydropyran derivatives: a procedure based on $TaCl_5$-SiO_2 was proposed in order to avoid the use of mineral acids or expensive reagents, and relied on microwave heating in a solvent-free environment to achieve the formation of cyclic 1,3-diol derivatives from formaldehyde and variably substituted styrenes;[132] 4-chlorotetrahydropyrans were prepared from aldehydes and 3-buten-1-ol using niobium pentachloride (20 mol%) as promoter, in a reaction consisting of hemi-acetal formation and subsequent Prins-type cyclization, occurring at ambient temperature.[133]

A prominent field in modern synthetic methodology, for which high valent metal halides have been investigated as Lewis acidic catalysts, is multicomponent reactions (MCRs): an MCR is usually defined as a process in which three or more reactants are combined in one pot, in order to form a product that has structural characteristics of each employed reagent, generating structural complexity in a selective and atom-economical fashion. One of the first examples of niobium pentachloride being employed as a catalyst in an MCR has been reported by Yadav and co-workers: the synthesis of 3,4-dihydropyrimidinones from aldehydes, 1,3-dicarbonyl compounds and (thio)urea, known as the Biginelli reaction, was achieved with 5 mol% $NbCl_5$ in ethanol at room temperature, in good to excellent yields, while displaying tolerance towards a wide range of substrates including aromatic, aliphatic, and heterocyclic aldehydes (Figure 21).[134] More recent reports suggest that molybdenum pentachloride

(5 mol%) is also an active catalyst for the same reaction, although refluxing acetonitrile is needed to successfully carry out the reaction.[135]
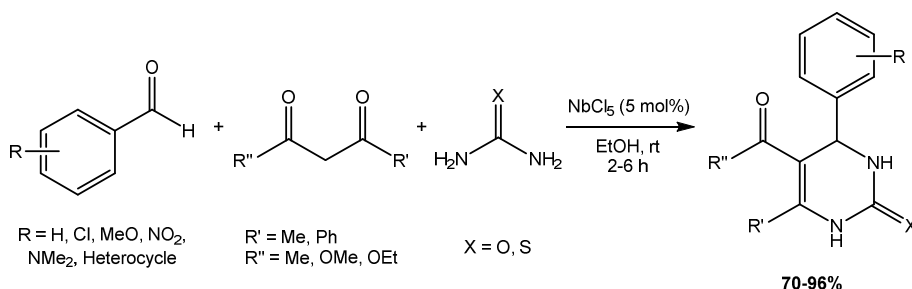
Figure 21. Three-component synthesis of 3,4- dihydropyrimidinones catalysed by $NbCl_5$.

The group of Da Silva-Filho in particular has been very active in the MCR field, demonstrating how a variety of polyheterocycles, such as coumarins,[136,137] tetrahydroquinolines,[138] tetrahydropyridines,[139] chromenes,[140,141] 4*H*-pyrans,[142] and phloroglucinol derivatives,[143] can be obtained with this strategy, starting from simple building blocks such as aldehydes, alcohols, amines and 1,3-dicarbonyl compounds (Figure 22). All reactions are carried out in mild conditions, at room temperature, using acetonitrile or dichloromethane as a solvent and employing 0.25 to 1 equivalents of $NbCl_5$. The proposed mechanism involves, in almost every case, the coordination of the Lewis acid to the aldehyde carbonyl, thus enabling a Knoevenagel condensation forming an intermediate which can then react further undergoing a Michael addition, or a Diels-Alder-type cycloaddition.
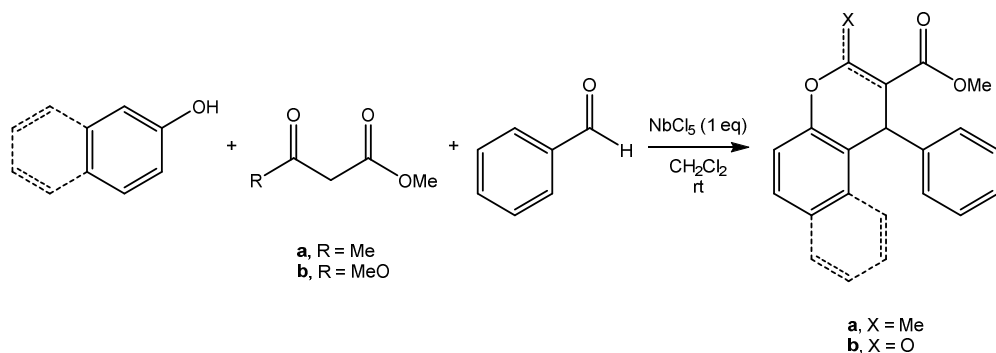
Figure 22. Multicomponent synthesis of chromenes (**a**) and coumarins (**b**) mediated by niobium pentachloride.

Some of the polyheterocycles obtained *via* this protocol have found application as organic dyes: quinoline derivatives can be obtained when one of the MCR partners is a terminal alkyne (i.e. phenylacetylene), as a result of the nucleophilic attack of the latter on an imine, formed *in situ* from the condensation of an aldehyde with a substituted aniline, in the presence of NbCl₅ (for the proposed mechanism, see Figure 23);[144–146] a selection of fluorescein dye derivatives has been prepared from the NbCl₅-catalysed cyclization of substituted phenols and phthalic anhydride derivatives, and tested for employment in dye-sensitized solar cells (DSSCs),[147] and as blue-light-induced photoinitiators;[148] a Mannich-type MCR involving benzaldehyde, aniline and 1,3-dicarbonyl derivatives in the presence of NbCl₅ (25 mol%), in acetonitrile at ambient temperature, has been reported to yield pyrrolo-[3,2-*b*]pyrroles, which are considered to be promising compounds for their potential applications in organic electronics.[149]
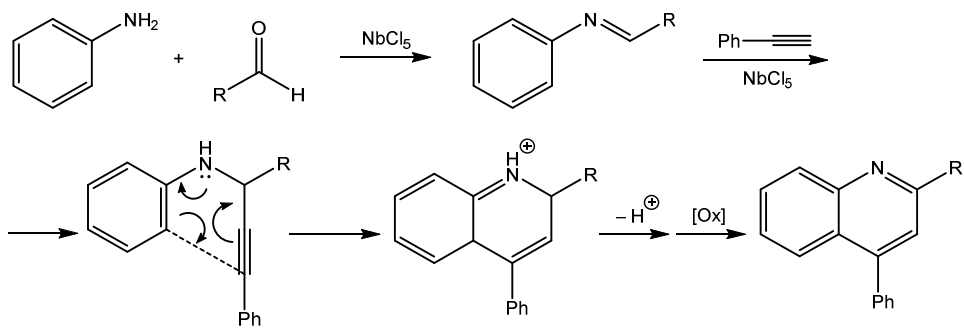
Figure 23. Proposed reaction mechanism for the NbCl$_5$-promoted multicomponent cyclization of anilines, aldehydes and phenylacetylene, yielding quinoline dye derivatives.

Recent reports by Manisankar and Kamble have further demonstrated the potentiality of MCRs in the synthesis of even more complex structures, as results of one-pot, four-component reactions in the presence of NbCl$_5$: biologically important spyro pyrazoles have been prepared from substituted isatins, 1,3-dicarbonyls, hydrazines and either 2-hydroxy-1,4-naphthaquionone or malononitrile, with 6% weight NbCl$_5$ and ethanol as a solvent, at 80°C;[150] the solvent-free, room temperature synthesis of benzylpyrazolyl coumarin derivatives has been carried out starting from 4-hydroxycoumarin, ethyl acetoacetate, hydrazines and aromatic aldehydes, catalysed by the NbCl$_5$/AgClO$_4$ couple (1 mol% and 3 mol%, respectively).[151]

One-pot cyclization reactions catalysed by high valent transition metal halides have also been exploited in the synthesis of xanthene derivatives, namely dibenzoxanthenes and xanthenediones. 14-Aryl-14*H*-dibenzo[*a,j*]xanthenes can be obtained from β-naphthol and aromatic aldehydes, using WCl$_6$ (1 mol%) as a catalyst, at 110°C without any additional solvents.[12] A modification of this procedure was later proposed by a different research group: by employing

dichloromethane as a solvent, and $NbCl_5$ as a catalyst (albeit in a higher loading, 25 mol%), the reaction could be carried out at ambient temperature (Figure 24).[152] By exploiting a similar protocol, which involves the one-pot cyclization of 1,3-cyclohexanedione with aromatic and heterocyclic aldehydes, xanthenedione derivatives can be synthesized: the reaction requires 2 hours in refluxing acetonitrile, and relies on niobium pentachloride (25 mol%) as a catalyst.[153]

WCl_6 (1 mol%)
solvent-free, 110°C
4-60 min

or

$NbCl_5$ (25 mol%)
CH_2Cl_2, rt
24-48 h

R = H, F, Cl, Br, Me, *t*-Bu, Ph
OMe, SMe, NO_2, NMe_2

70-97%
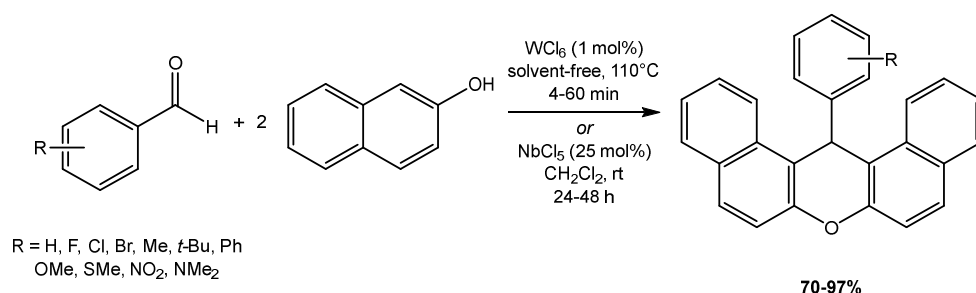
Figure 24. Dibenzoxanthenes synthesis from β-naphthol and arylaldehydes, catalysed by high valent transition metal halides.

A one-pot process mediated by $NbCl_5$ as a Lewis acid, involving a tandem Claisen rearrangement/cyclization reaction, has been reported for the biomimetic cascade conversion of natural lawsone (2-hydroxy-1,4-naphthoquinone) ethers into dunnione and nor-β-lapachone, two biologically active natural products.[154,155]

1.2.4. C-C Activation

High valent molybdenum and tungsten centres are widely known in the field of olefin metathesis and act as core motifs for the molybdenum/tungsten imido-alkylidene catalysts that granted Richard

Schrock the Nobel Prize in 2005.[156] Nevertheless, there are relatively few reports in the literature about the direct employment of a simple, homoleptic high valent metal halide precursor in a carbon-carbon bond activation reaction. Greish and collaborators have reported a procedure which relies on WCl_6 dissolved in ionic liquids to obtain the co-metathesis of ethylene and olefinic compounds (ethenolysis). However, the reaction suffers from a relatively poor conversion, and it is also accompanied by double bond shift, generating olefins which are as well able to participate in the metathesis reaction, and finally yielding a mixture of different products.[157] A silica-supported $MoCl_5$ catalytic system, operating in the presence of Me_4Sn, was reported by the group of Bykov for the metathesis of terminal and internal alkenes. The generation of the active catalyst is believed to occur *via* the interaction of molybdenum pentachloride with the surface hydroxyl groups of SiO_2, with the release of two equivalents of HCl per $MoCl_5$ molecule; Me_4Sn present is then able to methylate the molybdenum centres to afford a $[MoCl(CH_3)_2]$ fragment; then, α-H elimination occurs, and the catalytically active molybdenum alkylidene fragment is generated (Figure 25).[158] The aforementioned catalytic system has been applied to the metathesis reaction of 1,7-octadiene, which proceeds along two pathways: the formation of the chain growth product, 1,7,13-tetradecatriene, and the intramolecular cyclization to cyclohexene. The stereochemistry of the process was also studied, and it was observed that the Z-stereoisomer of 1,7,13-tetradecatriene appears to be more prone to undergo cyclization to cyclohexane.[159] The same group also reported an investigation on the cyclododecene co-metathesis with 1-hexene, yielding the biologically relevant 1,13-octadecadiene along with other chain extension products.[160]

31
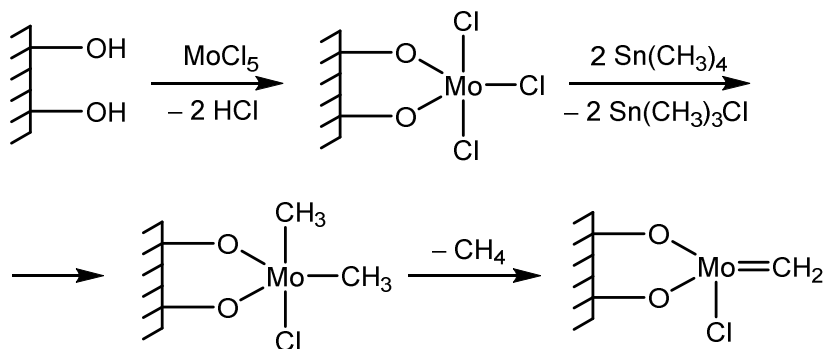
Figure 25. Proposed pathway for the generation of the catalytically active species in a MoCl$_5$/SiO$_2$-Me$_4$Sn system for olefin metathesis.

A somewhat related system, based on NbCl$_5$ supported on SiO$_2$ or Al$_2$O$_3$, was reported for the alkylation of aromatic compounds with alkenes: by employing this heterogeneous catalyst at room temperature, benzene and toluene could be converted, by treatment with 1-hexene, into their mono- and disubstituted derivatives, the latter being the more favourable products.[161]

In a recent contribution by Obora and co-workers, niobium pentachloride was employed as a catalytic precursor, together with trimethylsilyl chloride, zinc and benzyl dichloride, to attain the ring closing metathesis (RCM) of N,N-diallyl-*p*-toluenesulfonamides: the *in situ* generated catalyst allowed for the quantitative conversion of the organic substrate into 3-pyrroline derivatives, using thf as a solvent and heating at 60°C for 2 hours.[162] The same group was able to exploit the Lewis acidity of NbCl$_5$ towards alkenes in the promotion of the secondary amide formation reaction from alkenes and nitriles. The reactions occurred at room temperature over 24 hours, using the aromatic/aliphatic nitrile as a solvent, and the organic product is recovered after hydrolysis. The authors also suggest a plausible

reaction mechanism, involving the activation of the double C–C bond of the olefin by coordination of NbCl5 to the less substituted carbon atom. A carbocation transposition is however possible, and this accounts for the fact that two isomers of the secondary amide can be observed (Figure 26).[163]
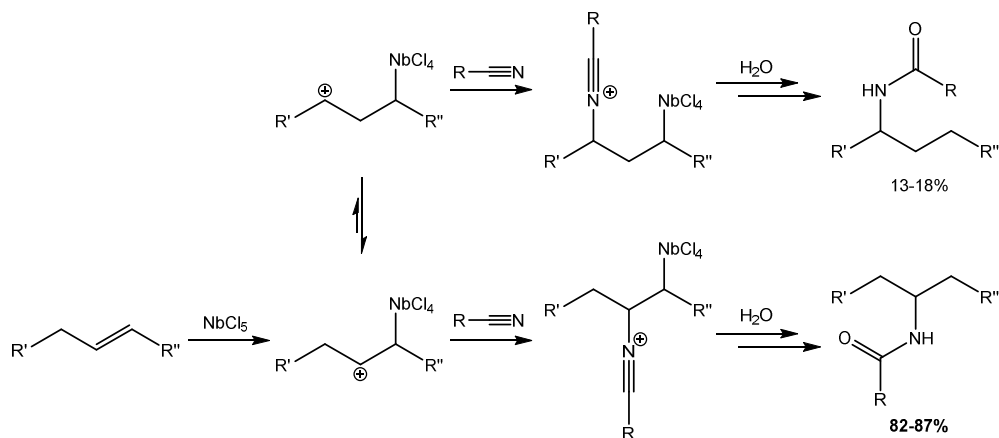
Figure 26. Suggested mechanistic pathway for the NbCl5-mediated amidation of alkenes with aromatic and aliphatic nitriles.

Carbon nucleophiles have also been reported to react with alkenes in the presence of TaCl5 as a catalyst: the group of Sultanov has documented a series of additions of different organometallic reagents to terminal alkenes and norbornenes, by employing 5 mol% TaCl5 in thf at room temperature. This protocol has allowed the authors to obtain carbomagnesation,[164–167] carboalumination[168] and carbozincation[169] of the substrates, in high yields and good stereoselectivity, and the reaction is believed to occur through a tantalacyclopentane intermediate.

An intramolecular hydrofunctionalization of alkenes bearing a nucleophilic substituent on the backbone has been reported by

Amatore and co-workers, relying on a NbCl$_5$/AgNTf$_2$ catalytic system.[13] This protocol allowed for the preparation of heterocyclic (furans, pyrans, pyrrolidines, piperidines, lactones and lactams) and spirocyclic compounds, following the addition of an O–H bond (from an hydroxyl or a carboxyl group), or N–H bond (amino or amido group) to an unsaturated C–C bond, with formation of five- or six-membered cycles, the former being generally favoured (Figure 27). Notably, tantalum(V) derivatives have been recently described as hydrofunctionalization catalysts, in the synthesis of substituted amines *via* hydroaminoalkylation of alkenes.[14,15] However, TaCl$_5$ itself (or other high valent metal halides) does not appear to be active in such transformations.

NuH = OH, NHR, COOH, CONHR
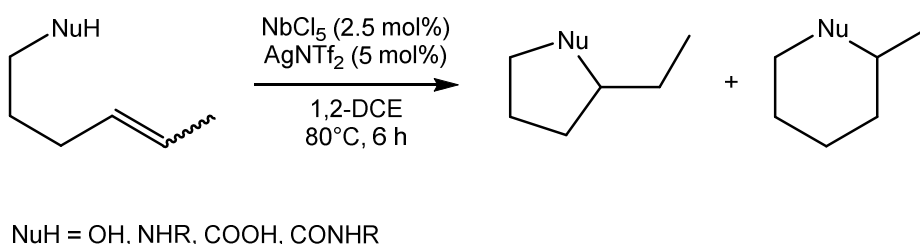
Figure 27. Intramolecular hydrofunctionalization of alkenes catalysed by NbCl$_5$ in the presence of AgNTf$_2$.

An example of C–C bond cleavage promoted by high valent transition metal halides has been reported a few years ago by our group, in the framework of our investigation of the reactivity of MX$_5$ (M = Nb, Ta; X = Cl, Br) with a selection of α-amino acids: their 1:1 reactions resulted in the formation of the iminium salts [RCH=NR′R″][MX$_6$], as a consequence of a selective C*–C(O) bond cleavage. In contrast to the well-known decarboxylation reactions, in which the carboxyl group is

lost in the form of CO_2, in this reaction the latter is apparently preserved as a formate ligand: this was suggested after the isolation of a niobium formate derivative, identified as co-product of the reaction between $NbCl_5$ and N,N-dimethyl-L-phenylalanine (Figure 28).[170]
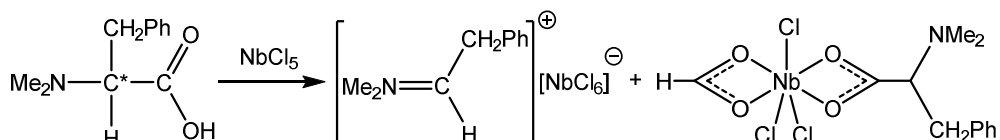
Figure 28. Activation of N,N-dimethyl-L-phenylalanine by interaction with $NbCl_5$, with formation of an iminium salt and a niobium formate derivative.

1.2.5. C-H Activation

The possibility to directly introduce new functional groups in organic substrates *via* direct C–H bond functionalization is a highly attractive strategy in modern synthetic chemistry. The first step that has to be tackled in this regard is the cleavage of the C–H bond itself, which is in general poorly reactive due to a large kinetic barrier, associated with the nonpolar nature of this bond: in this context, transition metals can play a pivotal role.[171]

Regarding the reactivity of niobium pentahalides in the activation of inert C_{sp3}–H bonds, a recent computational study investigated the gas-phase activation of methane by the concerted metalation-deprotonation (CMD) reaction pathway, the outcome being the $NbX_4(CH_3)$ complex, with release of the corresponding hydrogen halide. The study concluded that the initial electrostatic interaction

35

between NbX_5 and CH_4, which has a crucial role in the whole activation process, is favoured by the increase of the electronegativity in the halogen ligand series. Moreover, steric hindrance caused by the larger, less electronegative halogens, decreased the entity of the Nb–C interaction. The electronegativity of the halides ultimately appears to have an influence on both the kinetics and the thermodynamics of the process (i.e. the reactions with CH_4 are exothermic for NbF_5 and $NbCl_5$, and endothermic for the remaining halides).[172]

From an applicative point of view, the possibility of installing a new C–C bond in place of an inert C–H is a current topic in synthetic methodology.[173] Currently employed cross-coupling protocols often involve expensive, functionalized starting materials (e.g. boronic acids in the Suzuki-Miyaura cross-coupling), and rely mainly on precious late transition metals: the development of feasible methodologies to circumvent these limitations would be advisable. In this context, Shi and co-workers reported an investigation on a selection of transition metals, including $NbCl_5$ and $TaCl_5$, in the direct functionalization of aromatic C–H bonds and subsequent cross-coupling with an aryl bromide.[174] The reactions were carried out in the arene as a solvent, at 80°C for 48 hours, using 10 mol% MCl_5 (M = Nb, Ta) together with bathophenanthroline (4,7-diphenyl-1,10-phenanthroline, 30 mol%) and potassium *tert*-butoxide (3 equivalents), and afforded biphenyls in low to moderate yields (Figure 29). However, a relatively poor regioselectivity and narrow functional group tolerance, would limit the applications of this methodology.
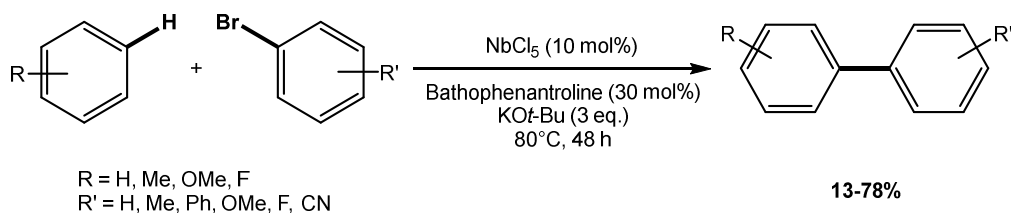
Figure 29. Direct C–H functionalization/cross-coupling of arenes with aryl bromides through NbCl$_5$ catalysis.

A different class of direct C–H activation/C–C formation, for which high valent metal halides have received considerable attention, is the oxidative (dehydrogenative) aromatic coupling: for this reactions, MoCl$_5$ was first proposed as a promoter by Kumar and Manickam, who reported the oxidative trimerization of *o*-dialkoxybenzenes to hexaalkoxytriphenylenes. The products could be obtained in good to excellent yields in very short reaction times, by using one equivalent of MoCl$_5$ in dichloromethane at ambient temperature (Figure 30).[175]
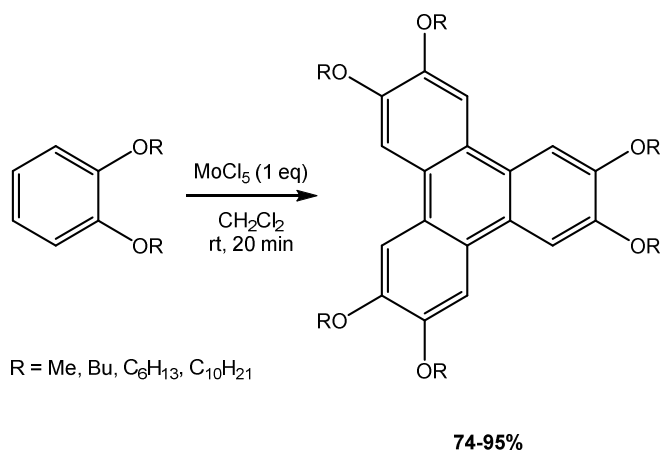
Figure 30. MoCl$_5$-mediated oxidative aromatic coupling of 1,2-dialkoxybenzenes to hexaalkoxytriphenylenes.

Over the past two decades, the group of Waldvogel extensively investigated the role and potentiality of MoCl5 in the mediation of oxidative aromatic coupling.[9,10] Catechol ketals were first considered as a substrate, undergoing oxidative trimerization to yield triphenylene ketals.[176] These C3v-symmetric scaffolds, in their *all-syn* configuration (i.e. with three functional groups on the same face of the molecule), are highly desirable for the supramolecular binding of C3- and pseudo-C3-symmetric molecules (e.g. caffeine or explosives).[177] However, when performing the reaction with stoichiometric MoCl5 in CH2Cl2 for 20 minutes, the desired products are obtained in relatively low yields (20-40%) and in a statistical mixture of *all-syn* and *anti,anti,syn* isomers in a 1:3 ratio (Figure 31). Further improvements on the reaction were made by employing TiCl4 as an additional Lewis acid in order to preserve the electrophilicity of MoCl5: with this strategy, both the overall yield and the selectivity towards the *all-syn* isomer were enhanced (up to 17:1 ratio).[178] Moreover, the authors also propose a metal template process to isomerize the undesired *anti,anti,syn* isomer and ultimately obtain up to 96% yield in the *all-syn* product.[179]

Figure 31. Triphenylene ketal isomers originated from the MoCl5-mediated oxidative trimerization of functionalized catechol ketals (FG = functional group).

The same group also reported that, when more substituted, electron-rich arenes are involved, a dehydrodimerization occurs to afford substituted biphenyls: starting from iodoarenes, the reaction was carried out employing 1.2 equivalents of MoCl$_5$ and very mild conditions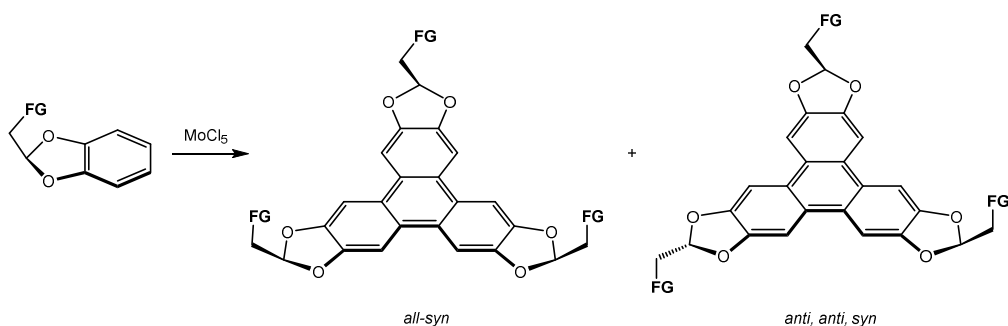 (0°C in dichloromethane for 40 minutes), and the corresponding iodobiaryls could be isolated in moderate to good yields (Figure 32).[180] The effect of different protective groups for the phenolic substituents was also investigated systematically: acetals/ketals, triisopropylsilyl, alkoxycarbonylmethyl and 2-chloroethyl systems were all found to be compatible with the MoCl$_5$-mediated oxidative aromatic coupling, thus enlarging the scope of the reaction.[181] More recently, a protocol to implement the dehydrogenative aromatic coupling into a flow chemical process was developed, in order to benefit from the high reaction rate of MoCl$_5$, while having an easy work-up method (direct column chromatography). MoCl$_5$ was employed as a single-use solid bed, and given the short reaction times, it was possible to avoid the use of anhydrous solvents: these features allowed for an easy-to-perform and automated reaction method, with comparable yields to the batch protocol.[182] An electrochemical approach, with a molybdenum-based anode, was also proposed as an alternative to the MoCl$_5$-mediated protocol, allowing for the conversion of a broad range of substrates and a more environmentally friendly process, by avoiding large amounts of reagent waste.[183] It is noteworthy that, while similar in many regards, the electrochemical method and the classical, stoichiometric one follow two distinct reaction mechanisms, and are thus not completely interchangeable. The MoCl$_5$-mediated version

appears to be somewhat more selective towards the formation of products with a larger number of newly-formed C–C bonds.[184]
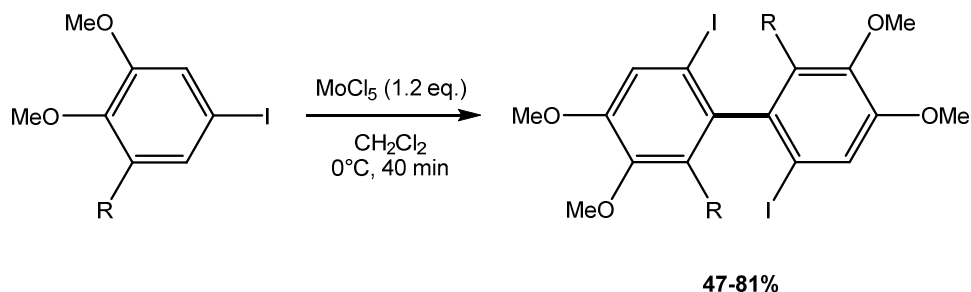
Figure 32. MoCl$_5$-mediated dehydrodimerization of iodobenzenes to iodobiphenyls.

Intramolecular dehydrogenative coupling is also very well documented: by treating organic substrates bearing two aryl substituents close to one another with either MoCl$_5$ or the MoCl$_5$/TiCl$_4$ system, five- to eight-membered rings were formed as a consequence of a double C–H bond activation, followed by direct C–C bond formation. With this strategy, dibenzocycloheptenes,[185,186] 2,2'-cyclolignanes,[187] fluorene derivatives,[188] phenanthrene derivatives,[189,190] carbazoles[191] and spirocyclic compounds[192,193] have all been synthesized from the suitable bis-aryl starting materials (Figure 33). In almost all cases, reactions were conducted in dichloromethane in mild conditions (0°C to ambient temperature), and afforded the products in moderate to good yields.

Cross-coupling is also possible for particular substrates, as it was demonstrated for the cyclization of some thiophene derivatives with veratrole (1,2-dimethoxybenzene).[194]
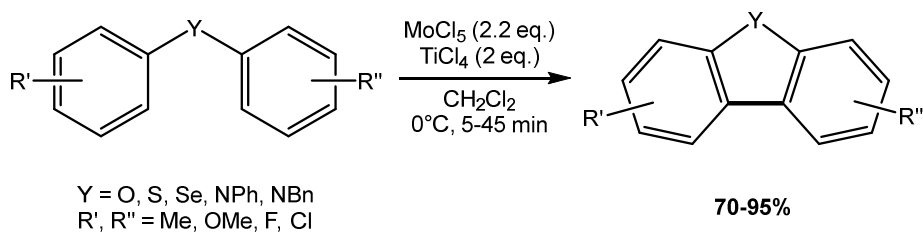
Figure 33. Synthesis of dibenzo-heterofluorenes *via* dehydrogenative coupling mediated by the MoCl$_5$/TiCl$_4$ system.

In order to overcome the formation of undesired chlorinated by-products, occurring in particular when very electron-rich aryl systems are involved, Waldvogel and co-workers also developed a molybdenum(V) fluoroalkoxy reagent, [(CF$_3$)$_2$CHO]$_2$MoCl$_3$, obtained from MoCl$_5$ and 1,1,1,3,3,3-hexafluoroisopropanol (HFIP).[195] By employing this reagent, yields and selectivities in favour of the non-chlorinated products were significantly improved: this behaviour found confirmation in the electrochemistry of [(CF$_3$)$_2$CHO]$_2$MoCl$_3$, which is reported to have both a cleaner voltammogram (i.e. fewer electroactive species) and an higher peak potential (E = 1.22 V vs. ferrocene), when compared to MoCl$_5$ (E = 1.16).[9]

The oxidative aromatic coupling is often referred to as Scholl reaction,[196] even though some mechanistic studies have evidenced how the two reactions may actually rely on slightly different mechanisms, the oxidative aromatic coupling occurring through a radical cation mechanism with an oxidant as a mediator, and the Scholl reaction being mediated by Brønsted or Lewis acids (with or without the use of an additional oxidant), and supposedly occurring *via* an arenium cation intermediate.[197–199] The dual nature of MoCl$_5$, being it both a Lewis acid and an oxidant, is presumably the reason

why reactions mediated by this compound are not easily categorized as one or the other type of mechanism.

Nevertheless, the Scholl reaction appears to be majorly involved in the functionalization of large dendritic polycycles,[196] as it was reported for the formation of new C−C bonds in extensively conjugated polyarenes.[200,201]

Experimental evidences of the ability of high valent transition metal halides to activate amine C−H bonds have been documented by our group in the past few years. The Lewis acidity and oxidizing power of WCl_6 are involved in the generation of a iminium derivative, $[PhCH=N(CH_2Ph)_2][WCl_6]$, from tribenzylamine, following the activation of a benzylic hydrogen which is formally transferred to a second equivalent of the starting amine, yielding $[(PhCH_2)_3NH][WCl_6]$. The proposed mechanism suggests that the reaction proceeds *via* a tribenzylamine radical cation intermediate, generated by WCl_6, which is in turn reduced to the $[W^VCl_6]^-$ anion; a subsequent hydrogen atom transfer occurs between two equivalents of the tribenzylamine radical cation (Figure 34).[202] A similar outcome has been observed from the non-selective interaction of $NbCl_5$ with tribenzylamine: the iminium derivative $[PhCH=N(CH_2Ph)_2][NbCl_6]$ was isolated as the main product. The expected co-formation of Nb(IV) species could not be ascertained in this case; nevertheless, a salt containing the $[Nb^{IV}Cl_6]^{2-}$ anion was isolated from the reaction of $NbCl_5$ with triethylamine, confirming that the Nb(V) to Nb(IV) reduction may be working in the activation reactions of trialkylamines.[203]

42
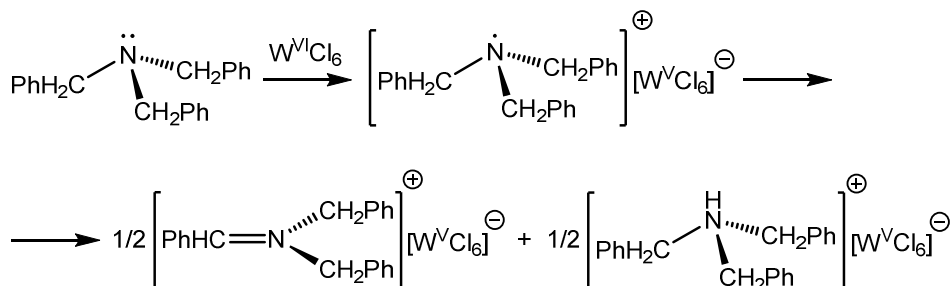
Figure 34. Proposed pathway for the generation of an iminium derivative from tribenzylamine *via* WCl$_6$-promoted benzylic C–H activation.

TaCl$_5$ can activate the rather unreactive C$_{sp3}$–H bonds in acetonitrile towards deprotonation from triethylamine, leading to the isolation of the tantalum vinylimido complex [HNEt$_3$][(Et$_3$N{CH$_2$}CN)TaCl$_5$].[204] The reactivity was also investigated with aryl nitriles, employing a TaCl$_5$/PPh$_3$ system: in the case of benzonitrile, a zwitterionic tantalum enediimido complex was obtained, after double C–C bond formation between two activated nitrile fragments (Figure 35).[3]
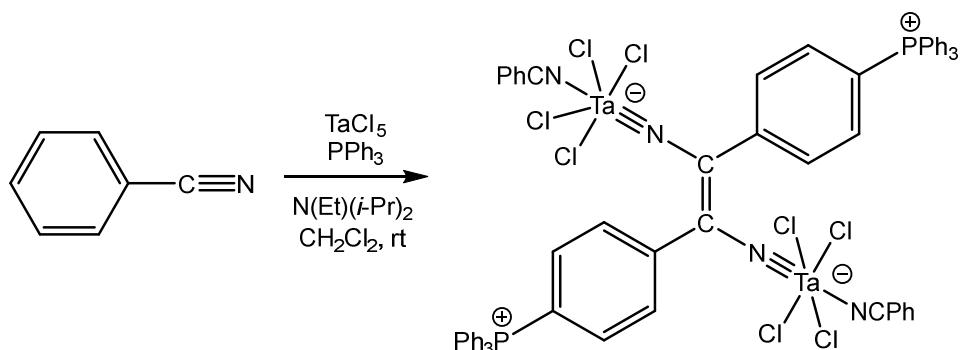
Figure 35. Formation of a zwitterionic tantalum(V) enediimido compound following C–H activation of benzonitrile by the TaCl$_5$/PPh$_3$ system.

The synthesis of γ,δ-unsaturated-β-ketoesters has been achieved by a NbCl$_5$-catalysed insertion of ethyl diazoacetate into aldehydes C–H

bonds. Under the optimised conditions, the methodology allowed for the obtainment of the desired products in moderate to good yields, while maintaining a broad substrate tolerance thanks to the mild operating conditions (Figure 36).[205]
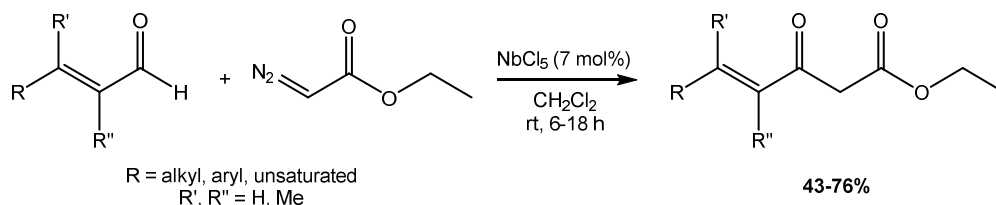
Figure 36. NbCl$_5$-catalysed C$-$H insertion of ethyl diazoacetate into α,β-unsaturated aldehydes, to obtain γ,δ-unsaturated-β-ketoesters.

A heterolytic C$_{sp3}$$-$H bond activation of acetone has been reported from our laboratory, when the acetone adducts [MX$_5$(Me$_2$CO)] (M = Nb, Ta; X = F, Cl, Br) are treated with ketones: the reactions then proceed with the formation of a new C$-$C bond, generating metal derivatives containing aldolate ligands.[57]

A C$-$H activation is believed to be involved in the self-protonation of some N-alkyl substituted ureas promoted by WCl$_6$. In particular, the protonated tetraethylurea (teu) derivative [teuH][WCl$_6$] was isolated in moderate yields from the equimolar reaction of the two precursors, in dichloromethane at room temperature. The presence of a W(V) anion suggests that the reaction occurs *via* an oxidation step, in which the radical cation of tetraethylurea, [teu]$^{•+}$, is formed: such a radical can abstract a hydrogen from an additional equivalent of teu, leading to the [teuH]$^+$ cation. This hypothesis was further supported by spectroscopic evidences of products containing the [CH$_2$=N] moiety in the reaction mixture.[206,207]

44

Group 6 high valent chlorides have also been investigated as catalysts for the oxidative chlorination of C–H bonds: $MoCl_5$ was employed with a chlorine dioxide/dimethylformamide system for the ring chlorination of terpenes, although it was outperformed by $CeCl_3$ for both yield and selectivity;[208] better results were obtained when a $MoCl_5$/NaClO system was tested for the allylic chlorination of terpenes: when conducting the reactions at ambient temperature (or below) with 0.5 equivalents of $MoCl_5$ in a 1:1 dichloromethane/water mixture, natural terpenes were converted in the corresponding chlorides in moderate to good yields, although in some cases (i.e. with α- and β-pinene), a ring opening rearrangement occurred (see Section 1.2.2), resulting in lower yields.[209]

Ring chlorination of pyridines, following the activation of C_{sp2}–H bonds, is also reported to be feasible with WCl_6 as a catalyst, but very harsh conditions appear to be required (175°C for 6 hours, employing chlorine gas).[210]

1.2.6. Polymerization

Among the different classes of polymers, polyacetylenes have an historical relevance as one of the first conductive organic polymers: the discovery of their high electrical conductivity upon doping was a milestone in the field, and was awarded with the Nobel Prize in Chemistry in 2000.[211] From a synthetic point of view, group 6 high valent metal chlorides have been known as pre-catalysts for the polymerization of acetylenes since the late 70s: the group of Higashimura initially documented the WCl_6-catalysed polymerization

of phenylacetylene, and was able to obtain high molecular weight polymers (7000-15000 g/mol).[212] $MoCl_5$ was tested as a catalyst as well, but was found to be less active, hinting to a possibly different mechanism of action. The study was later extended to different aryl acetylenes, namely β-napthylacetylene[213] and diphenylacetylene[214], from which high molecular weight polymers with similar properties to poly(phenylacetylene) were obtained. The polymerization of *tert*-butylacetylene was studied as well, and $MoCl_5$ was found to be a better catalyst for this reaction.[215] Likewise, $MoCl_5$ proved to be more efficient in the polymerization of oxygen-containing acetylenes, such as propiolic acid.[216] The influence of additives such as Ph_4Sn was evaluated: the pre-mixing of a small amount of the latter with WCl_6 (or $MoCl_5$) before the addition of the monomer, resulted in a remarkably accelerated polymerization, leading to polymers with molecular weights greater than 10000 g/mol.[217]

Since these seminal reports, many research groups have contributed to the field over the past 40 years, greatly enhancing the range of alkynes that can undergo polymerization using $MoCl_5$ or WCl_6 as pre-catalysts (with or without Ph_4Sn as an additive). Tang and collaborators have reported several application of functionalized polyacetylenes, obtained by the WCl_6/Ph_4Sn system: polyacetylenes with liquid crystalline properties have been obtained by the polymerization of [((4′-cyano-4-biphenylyl)oxy)carbonyl]-1-alkynes in dioxane;[218] by conducting the polymerization of phenylacetylene in the presence of short carbon nanotubes, the latter could be solubilized by effect of the wrapping of soluble polymer chains;[219] diphenylacetylenes bearing stereogenic menthyl ([1R,2S,5R]-2-isopropyl-5-methylcyclohexyl) groups were polymerized to obtain

46

products with chiroptical and luminescence properties (Figure 37);[220] tetraphenylene-decorated polyacetylenes exhibited fluorescent and photoluminescent properties, and were investigated as potential fluorescent chemosensors for the detection explosives, thanks to their signal-amplifying effect and high binding capability.[221] The vast majority of these polymerization reactions are conducted in toluene at 80°C for 24 hours, and no significant improvements have appeared in the literature in the past four decades.[222]
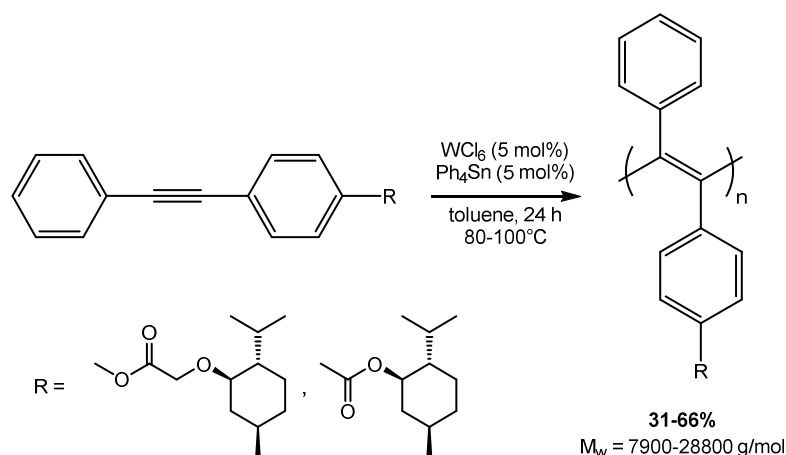
Figure 37. Synthesis of helical and luminescent poly(diphenylacetylenes) bearing menthyl pendants, catalysed by WCl_6/Ph_4Sn.

While the WCl_6/Ph_4Sn combination has proven to be an efficient catalytic system over the years,[223] both WCl_6 and $MoCl_5$ exhibit enhanced catalytic activity also in the presence of other additives, such as $EtAlCl_2$: the group of Gal has successfully employed these systems for the polymerization of acetylenes with biphenyl[224] and 4-phenoxyphenyl substituents.[225] In the latter case, the $MoCl_5$/$EtAlCl_2$ catalytic system was found to be better performing, in agreement with

previous observations of molybdenum catalysts being more reactive towards oxygen-containing substrates (*vide supra*).

Phenylacetylenes bearing ester functionalities, including pentafluorophenyl benzoates, which conferred enhanced solubility to the final polymer, were also synthesized by employing WCl_6/Ph_4Sn as a catalyst (Figure 38).[226] Co-polymers, obtained from varying ratios of different monomers, could also be prepared with reasonable yields following this procedure.[227] Ferrocene-functionalized acetylenes (i.e. phenylferrocenylacetylene) have also been reported to react in the presence of catalytic amounts of WCl_6, although the resulting reaction is an oligomerization, leading, in rather low yields, to products with five repeating units.[16]
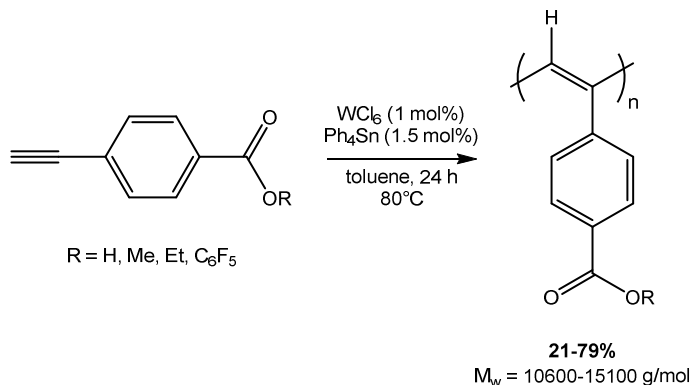
Figure 38. WCl_6/Ph_4Sn-catalysed synthesis of poly(phenylacetylenes) featuring ester side groups.

When compared to those generated by other metal catalysts, such as palladium or rhodium catalysts, polyacetylenes synthesized employing $MoCl_5$ or WCl_6 tend to assume a *trans*-rich stereoconfiguration of the polymer chain (Figure 39).[226,228,229] This feature appears to be however accompanied by an overall lower

stereoregularity, with respect to Pd- and Rh-based, *cis*-rich polyacetylenes.[230]
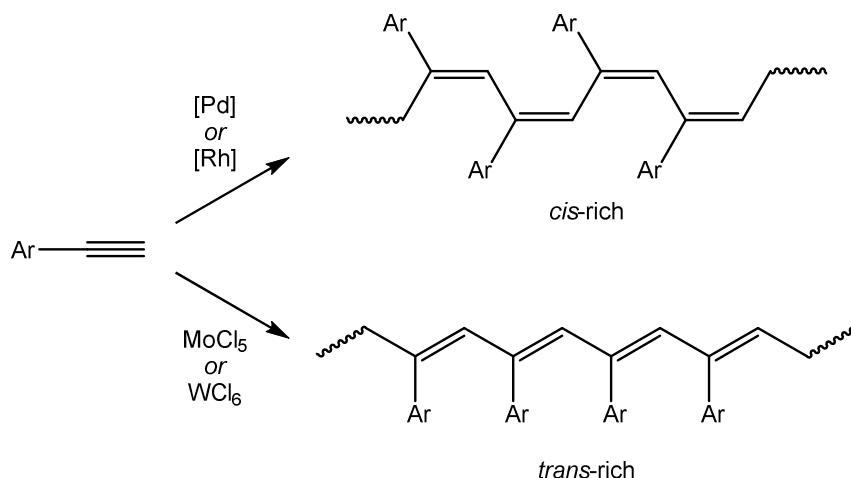
Figure 39. Comparison between the stereoconfiguration of the carbon backbone in Pd-/Rh-based and Mo-/W-based polyacetylenes.

Group 5 metal halides have also been considered as catalysts for the polymerization of acetylenes: in particular, Sakaguchi and co-workers have documented several transformations of internal alkynes, employing $NbCl_5$ and $TaCl_5$ as catalytic precursors, in the presence of various additives, and conducting the reactions in the common conditions for these polymerizations (toluene, 80°C, 24 hours, *vide supra*). The $TaCl_5$/*n*-Bu_4Sn system has been found to be the most effective for the polymerization of variably substituted diphenylacetylenes: different analogues, bearing alkyl side chains,[231] annulated aromatic rings,[232] and electron-donating and withdrawing groups,[233] have been prepared with this method. $NbCl_5$/*n*-Bu_4Sn and WCl_6/Ph_4Sn were also considered with heterocycle-[234] or fluorenyl-containing acetylenes.[235]

Among functionalized polyacetylenes, high-molecular-weight polymers of trimethylsilylacetylenes have received attention for their air and thermal stability, and particularly for their high gas permeability. High valent halides of group 5 metals have been demonstrated to be excellent catalysts for this polymerization, being able to afford the product in almost quantitative yield, by carrying out the reactions in toluene at 80°C over 24 hours, and by employing 2 mol% MX_5 (M = Nb, Ta; X = Cl, Br).[222] Derivatives of the aforementioned polymers, bearing similar gas permeability properties, have been prepared in the more recent years, and in most cases, niobium and tantalum pentahalides have again emerged as the most suitable catalytic systems: poly(1-(3,3,3-trifluoropropyldimethylsilyl)-1-propyne) was obtained in good yields using a $TaCl_5$/Ph_3Bi system as a catalyst (2 mol%) in toluene at room temperature, and it exhibited a good selectivity for some gases (e.g. CO_2);[236] germanium analogues, have been synthesized by polymerization of trimethylgermyl-1-propyne in almost quantitative yield, in the presence of $NbCl_5$ or $TaCl_5$ (the two metal halides appear to promote the polymerization with a different stereochemistry, $NbCl_5$ being more prone to yield *cis*-rich polymers);[237] co-polymers of trifluoropropyldimethylsilyl-1-propyne with trimethylsilyl-1-propyne have been prepared in moderate to good yields with $TaCl_5$/Ph_3Bi,[238] while more soluble derivatives of the same co-polymer where obtained employing $NbCl_5$/Ph_3SiH;[239,240] block co-polymers of trimethylsilyl-1-propyne and 4-methyl-2-pentyne, obtained from $NbCl_5$-based catalysts, have been also studied, in order to increase the resistance of the sylilated polymer to higher hydrocarbons.[241]

50

Interestingly, it was observed that the gas permeability of some of these polymers can be enhanced by adding of $TaCl_5$, $NbCl_5$, and $MoCl_5$ to the polymer itself: gel formation occurred upon addition, as a consequence of the coordination with metal chloride particles. The resulting materials displayed a higher gas permeability when compared with the original polymer membranes, without any significant decrease in the gas selectivity. [242]

The ability of niobium and tantalum pentahalides to promote the cyclotrimerization of alkynes has been exploited to obtain hyperbranched poly(alkenephenylene)s from diynes (Figure 40):[243] $TaBr_5$ in particular was found to be the most suitable, single-component catalyst for the reactions, which were carried out in toluene at room temperature, and were also performed starting from silole-[244] and tetraphenylene-containing diynes.[245] The same concept was also exploited for the crosslinking of alkyne-terminated polyimides, by using $TaCl_5$ as a catalyst under thermal treatment.[246]
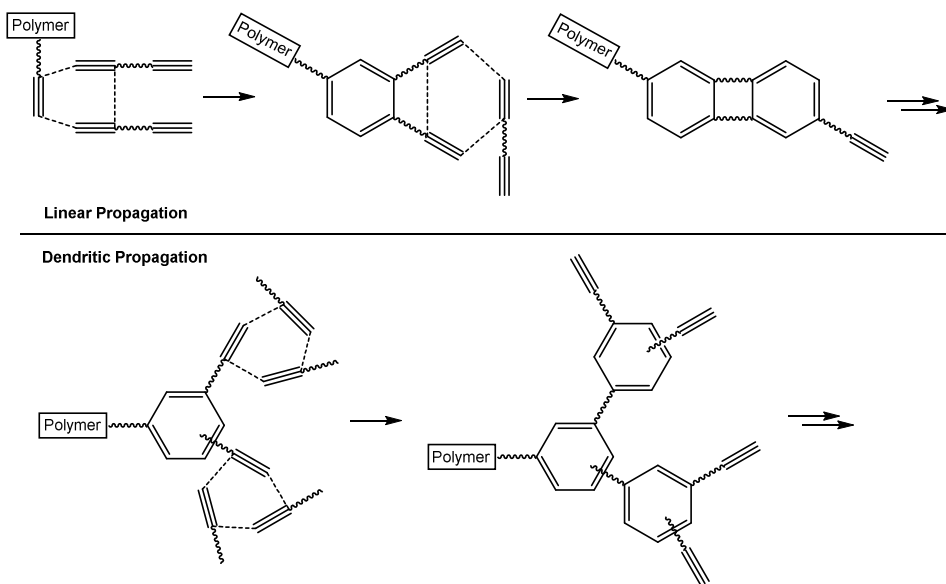
Figure 40. Linear and branched propagation patterns for the TaBr$_5$-catalysed polycyclotrimerization of diynes.

Catalytic systems based on MoCl$_5$ and WCl$_6$ have been reported for the ring opening metathesis polymerization (ROMP) of cyclic olefins: the effect of various additives has been systematically investigated, evidencing how different organometallic cocatalysts (i.e. organoaluminum, organotin) can influence the stereochemistry of the resulting polyolefin.[247,248] As of today, WCl$_6$-based three- or four-component catalysts are commonly employed, also including an alcohol (generally ethanol) as an initiator and a linear olefin (i.e. 1-hexene) as chain transfer reagent, to control the molecular weight of the polymer.[249,250]

While various niobium(V) and tantalum(V) complexes are active pre-catalysts for the polymerization of acyclic olefins,[251–253] the high valent metal halides themselves do not exhibit a prominent catalytic activity for this kind of reaction: both NbCl$_5$ and NbF$_5$ have been

investigated in the polymerization of ethylene, in the presence of methylaluminoxane (MAO) as a co-catalyst and 1,2-dichloroethane as a re-activator, in chlorobenzene at 50 °C: a very low activity was found for $NbCl_5$, while NbF_5 was practically inactive.[254] $NbCl_5$ and $TaCl_5$ were also studied for the cationic polymerization of *p*-methoxystyrene, but both were found unable to control the polymerization.[255] Nevertheless, our group has reported the room temperature polymerization of β-pinene, employing $NbCl_5$ as a catalyst in a very low concentration (0.05 mol%), in toluene as a solvent and without any additive.[256]

Both group 5 and 6 high valent metal chlorides have been known to promote the ring opening polymerization (ROP) of tetrahydrofuran since the 1960s,[257,258] but it was not until recently that the mechanism of said process was investigated: NMR studies have suggested that the polymerization is propagating from a zwitterionic species when TaF_5 (the best performing among the high valent metal halides) is employed, while when $NbCl_5$ or TaX_5 (X = Cl, Br) are used, halide migration and formation of ionic species is observed (Figure 41). With TaF_5 (0.25 mol%), by carrying out the reaction in bulk at room temperature, thf is rapidly polymerized (16% conversion was reached after 1 hour, and 36% after 3 hours), and a high molar mass poly(thf) (67100 g/mol) could be recovered.[90]
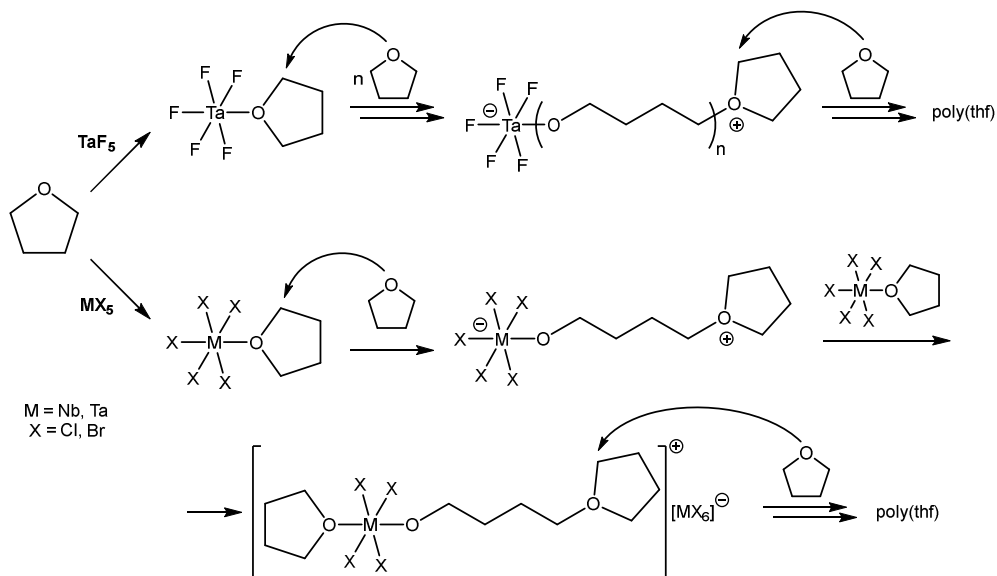
Figure 41. Different propagating species involved in the ring opening polymerization (ROP) promoted by high valent transition metal halides.

1.2.7.   C-N Activation

Among the most common transformations occurring *via* C–X bond activation, the transition metal catalysed activation of a C–N bond has emerged as a versatile tool in synthetic methodology, also due to the numerous sources of different functional groups bearing a C–N bond.[259] Some C–N bonds are relatively easy to break, like those of aziridines: these three-membered rings are intrinsically strained, and this enables facile C–N bond activation in the presence of transition-metal complex. TaCl$_5$ supported on SiO$_2$ has been utilized as a catalyst for the ring opening of aziridines with aromatic amines, leading to 1,2-diamines in high yields. Moreover, a high regioselectivity was observed, either towards the product of the attack

of amines at the less hindered carbon atom, in the case of unsymmetrical aliphatic aziridines, or at the benzylic carbon, in the case of 2-arylaziridines. The reactions were carried out in dichloromethane at room temperature, an relied on a rather low catalyst loading (2.5 mol%).[260]

Imines represent a much less investigated class of compounds regarding the C–N bond activation, and given their analogy to carbonyl compounds, high valent metal halides are potentially suitable promoters for transformations involving this class of organic substrates.

Andrade and co-workers reported an $NbCl_5$-mediated allylation of aldimines, performed in dichloromethane at −15°C and using allyltri-*n*-butylstannane, and affording homoallylic amines in good yields and high selectivity.[261] The role of $NbCl_5$ is supposedly that of exploiting the classic Lewis acid behaviour, by interacting with the nitrogen atom and forming an iminium salt, thus facilitating the nucleophilic attack on the carbon. The authors also propose that the interaction with the stannane occurs through an *antiperiplanar* transition state, which would explain the *syn* selectivity when substituted allylstannanes (i.e. crotylstannane) are employed.[262]

The outcome of the direct interaction of imines with $TaCl_5$ and NbX_5 (X = Cl, F) has been recently investigated by our group: iminium salts, with $[MX_6]^-$ anions, have been isolated in around 50% yields. The hydrogen source for the observed protonation could be attributed either to dichloromethane or adventitious water, but self-protonation following the activation of the imine reactant is also a possibility: this was suggested by the isolation of the niobium(V) azavinylidene

species [Ph$_2$C=NH$_2$][NbCl$_5$(N=CPh$_2$)], generated from the reaction of NbCl$_5$ with benzophenone imine (Figure 42).[263]

55%
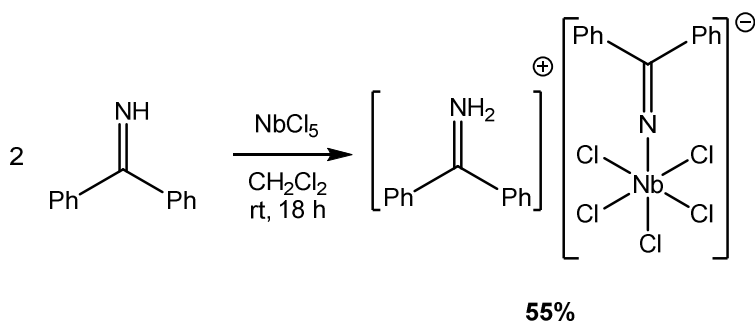
Figure 42. NbCl$_5$-mediated self-protonation of benzophenone imine into an iminium salt with a niobium(V) azavinylidene anion.

Like its group 5 congeners, WCl$_6$ too promotes the activation of C–N bonds of imines, and iminium salts were obtained in moderate yields from a selection of variably substituted imines. However, when WCl$_6$ reacted with benzophenone imine, in dichloromethane at room temperature, another product (other than the aforementioned iminium salt) was isolated in comparable amounts: the aza-2-allenium salt, [Ph$_2$C=N=CPh$_2$][WCl$_6$], generated by self-condensation of the imine reagent after release of N$_2$.[264] The proposed reaction mechanism, based on Density Functional Theory (DFT), suggests an initial C-chlorination of the C=N moiety, followed by a nucleophilic attack on the same carbon by a second equivalent of benzophenone imine, and the formation, after release of HCl, of the aza-2-allenium cation and a tungsten imido anion, [WCl$_5$(NH)]$^-$. The latter, in the presence of unreacted WCl$_6$, is finally converted in the [WCl$_6$]$^-$ anion, and N$_2$ is released (Figure 43).

56
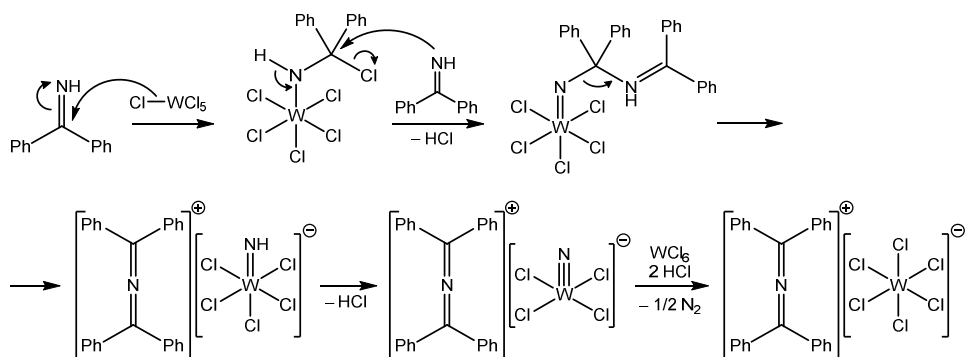
Figure 43. DFT-supported mechanism for the formation of an aza-2-allenium salt from the reaction of benzophenone imine with WCl_6.

While equimolar reactions of lactams with niobium pentahalides proceed with the formation of coordination compounds, a cleavage of the C–N amide bond was observed for the 3:2 ratio reaction of ε-caprolactam with $NbCl_5$, with subsequent ring opening (Figure 44).[64] When $MoCl_5$ was allowed to interact with δ-valerolactam, only protonation products could be observed, and in low yields.[265] These products appear to be originating by a poorly efficient self-protonation mechanism, involving N–H bond cleavage: as an indirect proof, the same reaction conducted on a N-substituted lactam, N-methylpyrrolidinone, did not undergo self-protonation, but was instead subject to previously mentioned Cl/O exchange (see Section 1.2.2).
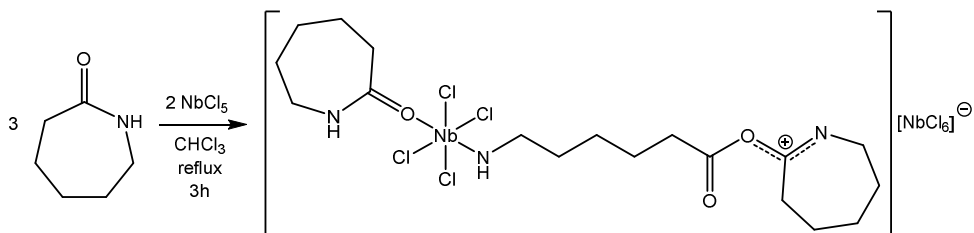
Figure 44. $NbCl_5$-mediated C–N cleavage and ring opening of ε-caprolactam.

1.2.8. C-F Activation

The C–F bond is one of the strongest single bonds that can be found in an organic molecule, and its challenging activation arouses interest not only from an academic point of view, but also for its potential implications in the abatement of air pollutants such as chlorofluorocarbons (CFCs).

NbCl5 has been proposed as a pre-catalyst for the reductive cleavage of aromatic C–F bonds in fluorobenzenes. The reactions were carried out in 1,4-dioxane at 100°C for 4 hours, and LiAlH4 was employed as a reductant: low valent niobium species, whose formation is believed to take place *in situ*, are suggested as active species in the defluorination.[266]

The same protocol also found application in the activation of trifluoromethyl groups attached to aromatic rings, widely recognized as one of the most inert examples of organofluorine compounds: activation reactions involving these benzylic C–F bonds are rather scarce in the literature.[267] By employing NbCl5 (0.3 equivalents) and LiAlH4 (6 equivalents) in refluxing dioxane, *o*-aryltrifluorotoluene derivatives were converted into fluorenes in moderate to good yields, as a consequence of a double activation of C–F and C–H bonds, followed by C–C coupling (Figure 45).[268] Biologically and pharmaceutically relevant N-fused indole derivatives have been also prepared by a similar methodology.[269]
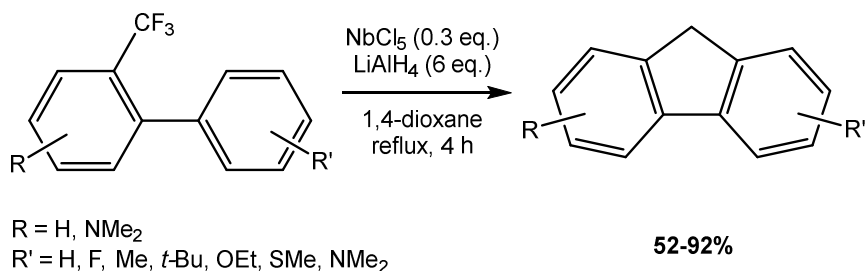
Figure 45. NbCl$_5$-catalysed synthesis of fluorenes by reductive activation of C–F and C–H bonds of *o*-aryltrifluorotoluenes.

More recently, high valent metal halides were investigated for the catalysis of the defluorinative triallylation of trifluorotoluene derivatives: NbCl$_5$ again emerged as the most suitable catalyst, and a protocol involving 10 mol% of the latter, and 5 equivalents of allyltrimethylsilane, in 1,2-dichloroethane at ambient temperature, allowed to attain benzylic triallylation in moderate yields. Release of trimethylsilyl fluoride, which accompanied the cleavage of the C–F bonds, was detected *via* NMR. Analogues bearing mono- or difluoromethyl groups (in place of the trifluoromethyl group) where studied as well, but they were observed to yield, respectively, the corresponding mono- or diallylated products in a lower yield, when compared to the triallylation reaction.[270]

1.2.9. Oxidation

As already mentioned in the previous sections, high valent metal halides can display a remarkable oxidizing behaviour: while this is not so surprising for group 6 metal halides, given their documented oxidation potential (E(MoCl$_5$) = 1.16 V and E(WCl$_6$) ≈ 1.1 V, *versus*

the ferrocene/ferrocenium couple, see Section 1.1.2), the same behaviour is not as well explored for the halides of group 5 metals. Nevertheless, evidences of redox activity have been reported also for niobium and tantalum pentahalides: it has been shown by our group that NbF_5 can promote the oxidation of monocyclic arenes, including benzene, affording the $[Nb_2F_{11}]^-$ salts of the corresponding radical cations (Figure 46). Niobium pentafluoride exhibits the dual activity of oxidizing agent and precursor to the stabilizing counterion $[Nb_2F_{11}]^-$: the formation of the latter is probably the driving force for the whole process, and its interaction with the radical cations leads to their kinetic inertness, which allows them to resist in chloroform solutions for long periods.[48,271]

R = R' = R" = H
R = R" = H; R' = OMe
R = H; R' = OEt, R" = Me
R = F, R' = OMe, R" = F

9-75%
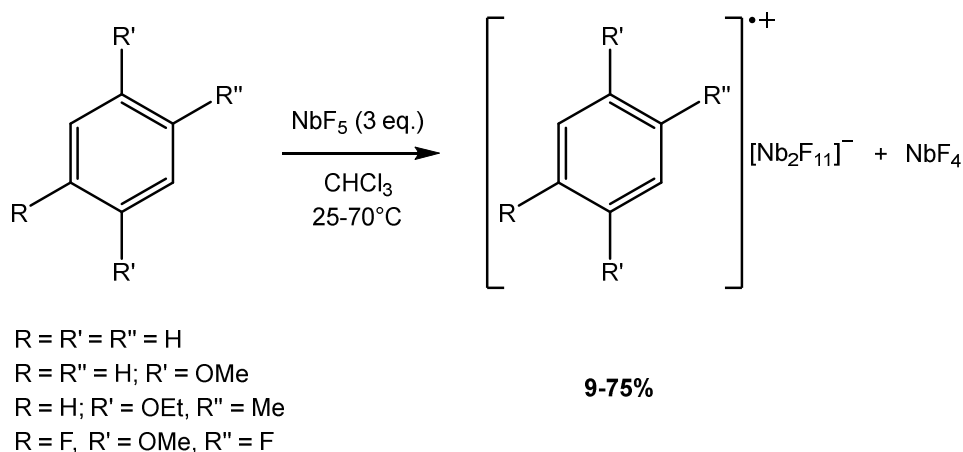
Figure 46. NbF_5-promoted oxidation of monocyclic arenes to stabilized radical cation salts.

A subsequent EPR/DFT study allowed for the detection and recognition of long-lived salts of radical cations, generated by one-electron oxidation of variably substituted monocyclic arenes promoted by MX_5 (M = Nb, Ta; X = F, Cl).[7] In the case of 1,3-

60

dimethoxybenzene, the generated radical cation was able to abstract an hydrogen from the reaction medium, thus affording the protonated dimethoxybenzene cation salt, $[2,4\text{-}(MeO)_2C_6H_5][M_2F_{11}]$ (M = Nb, Ta), at room temperature in chloroform. Although the product was only recovered in a rather low isolated yield (around 30%), such a cation is normally only stable in very acidic media, i.e. H_2SO_4 or 1,1,3,3-hexafluoroisopropanol (HFIP).[272]

Redox processes appear to be involved in the reactions of NbF_5 with imines: in particular, in its reaction with N-benzylidene-*tert*-butylamine, PhCH=N(*t*-Bu), evidences of the presence of benzonitrile, PhC≡N, could be detected *via* NMR after hydrolysis of the reaction mixture. This could hint at a potential C_{sp2}–H activation, providing the hydrogen source for the observed formation of iminium salts (see Section 1.2.7).[263] This hypothesis is further supported by the detection of benzonitrile (NMR and GC-MS analyses) from the hydrolysis of reaction mixture generated by the interaction of the same imine with WCl_6. Moreover, the IR spectra (measured before the water treatment) suggested the presence of a nitrilium group, and subsequent DFT calculations confirmed the possibility of [PhC≡N(*t*-Bu)]$^+$ being formed after C–H activation of the imine. Benzonitrile is then formed upon hydrolysis by loss of the *tert*-butyl group from the nitrilium cation (Figure 47).[264]
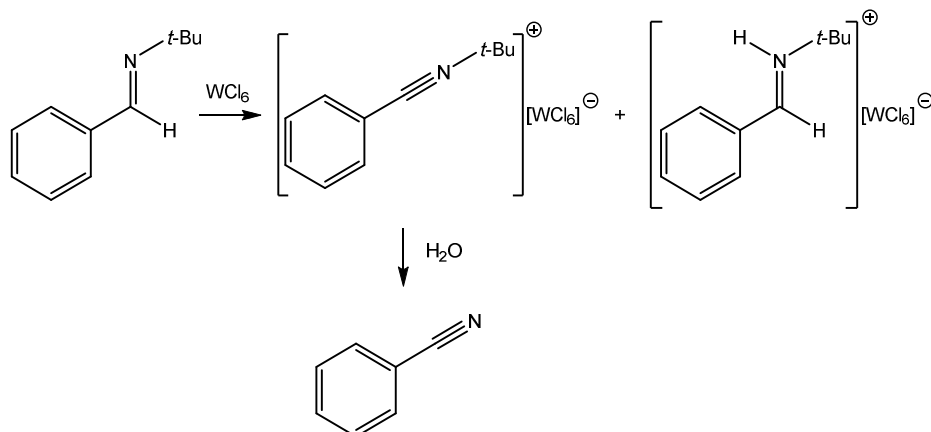
Figure 47. Possible pathway to the WCl_6-promoted formation of a nitrilium cation from N-benzylidene-*tert*-butylamine, and hydrogen transfer to form an iminium derivative.

High valent metal halides have been reported as catalysts in several procedures involving the oxidation of S-containing compounds. $TaCl_5$ catalyses the oxidation of halides (X^-, X = Br, I) into halonium ions (X^+) with H_2O_2: this strategy was employed in the oxidative deprotection of dithioacetals, which afforded carbonyl compound when treated with catalytic amounts of $TaCl_5$/NaI (10 mol%) and H_2O_2 (20 equivalents) in a water/ethyl acetate mixture at ambient temperature.[273] The *in situ* generated I^+ reacts with the dithioacetal and a iodosulfonium complex is formed. The carbonyl compound is recovered upon hydrolysis (Figure 48). In a more recent development, $NbCl_5$ was found to be even more catalytically active that $TaCl_5$ under analogous conditions, the former being able to deprotect also dithioacetals derived from aldehydes, and acyclic dithioacetals.[274] The $NbCl_5$/NaI and $TaCl_5$/NaI were also tested for the oxidative dethioacetalization of 2-silylated 1,3-dithianes by H_2O_2: despite being very active, the group 5 based catalysts caused overoxidation of

62

some substrates, with undesired cleavage of the C–Si bond, and for this reason, a milder, Fe(III)-based catalyst was ultimately chosen.[275]
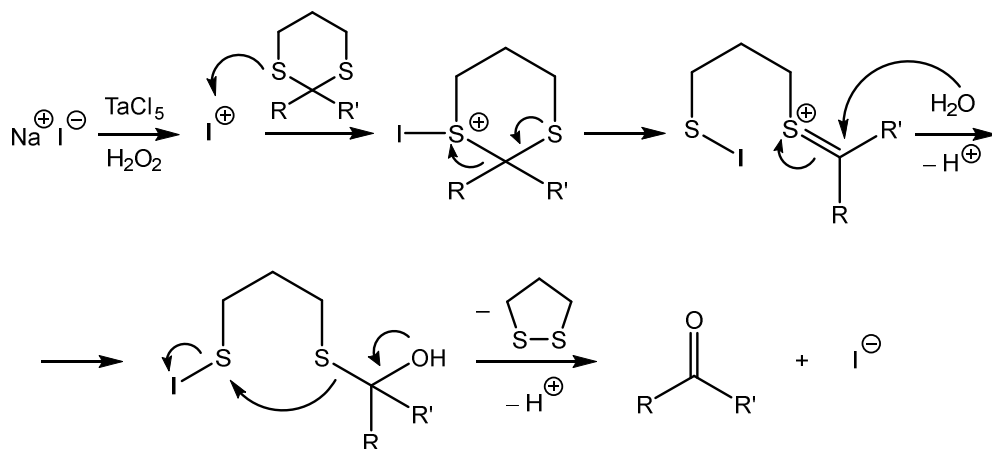
Figure 48. Proposed mechanistic pathway for the oxidative dethioacetalization catalysed by $TaCl_5$ and NaI with aqueous H_2O_2.

As an extension to the aforementioned method, the same authors also investigated the oxidation of sulfides under similar reaction conditions, using H_2O_2 and MCl_5 (M = Nb, Ta) as a catalyst in the presence or absence of NaI: by properly tuning the reaction conditions, sulfoxides and sulfones could be selectively obtained, the choice of the solvent being a critical aspect (i.e. sulfoxides are almost quantitatively obtained when performing the reactions in acetonitrile, while sulfones are the only product when methanol is employed) (Figure 49).[276] A niobium (or tantalum) peroxide complex, formed by reaction of MCl_5 with hydrogen peroxide (or with an organic peroxide, generated *in situ* by reaction of H_2O_2 with the solvent), is believed to be the active oxidizing species. The presence of NaI is found to be detrimental to the reaction: sulfides are converted to iodosulfonium ions under these conditions, and are thus not available for the

reaction with the peroxide complex.[277] Interestingly, if the same conditions (i.e. MCl$_5$/H$_2$O$_2$, in the absence of NaI) are applied to dithioacetals, oxidation at the sulfur atoms is observed, and bis-sulfonylmethylene compounds are obtained.[278] The NbCl$_5$/H$_2$O$_2$ system has also been applied, in the presence of (aza)crown ethers, to the desulfurization of diesel fuel, attaining the decrease of the total sulfur content in the model mixtures down to 13% of the initial amount.[279–281]
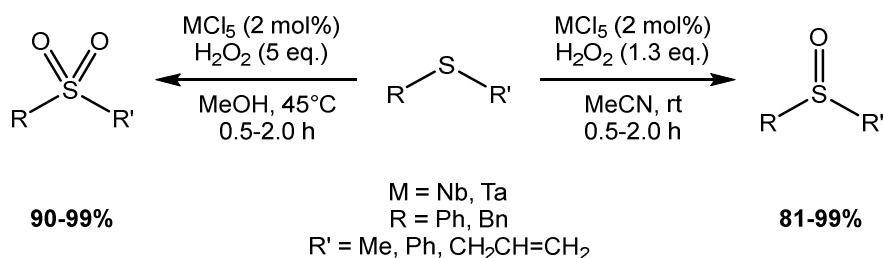
Figure 49. MCl$_5$-catalysed (M = Nb, Ta) oxidation of sulfides to sulfones and sulfoxides.

TaCl$_5$/NaI is also reported to promote the reverse reaction, i.e. the deoxygenation of sulfoxides to sulfides: when carrying out the reaction in acetonitrile at room temperature, TaCl$_5$ can react with sulfoxide in a 1:2 ratio, abstracting two equivalents of oxygen and thus being converted into TaO$_2$Cl. This allows for the formation of sulfoxides in almost quantitative yields in a few minutes.[282] The protocol is an improvement on a precedent method employing a TaCl$_5$/In system.[283,284]

Group 6 high valent metal chlorides, being characterized by a high oxidation potential (*vide supra*), can act themselves as oxidants towards S-containing substrates. A MoCl$_5$-mediated oxidative

64

treatment of diaryldisulfides was reported to obtain thianthrenes, as a consequence of oxidative coupling. The protocol, consisting of treatment of the organic substrate in dichloromethane at room temperature with stoichiometric MoCl₅ (together with TiCl₄ as an additive in some instances), allowed for the high yield conversion of symmetric 1,2-diaryldisulfides, with electron-donating substituents strongly enforcing the coupling in the *para* position (Figure 50).[285]

R = Me, MeO, Cl, OCH₂COOEt
R' = H *or* R' = R

45-98%
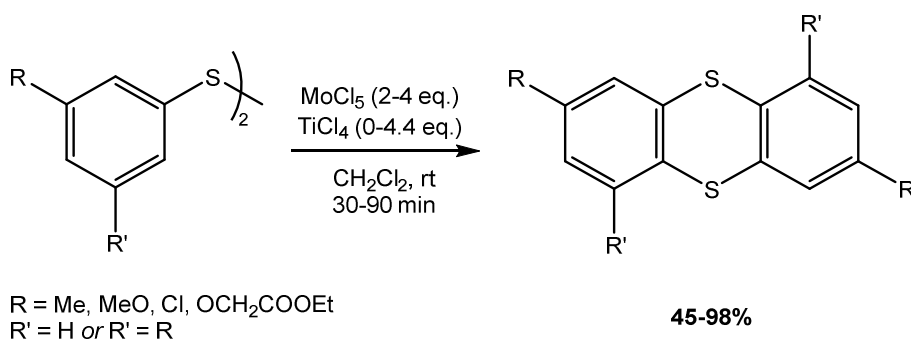
Figure 50. MoCl₅-mediated oxidative conversion of 1,2-diaryldisulfides into thianthrenes.

Diaryldisulfides can also be cross-coupled to substituted, electron-rich arenes or heterocycles, in order to obtain non-symmetrical sulfides, in an oxidative sulfenylation reaction promoted by MoCl₅ (3 equivalents) and TiCl₄ (additive, 3.3 equivalents) (Figure 51). The synthesis provides moderate to good yields, and appears to be tolerant towards numerous substituents or protecting groups. A dialkyldisulfide has been also included in the scope, as well as diphenyldiselenide.[286]

R = H, Me, F, I   Y = CH₂=CH₂, O, NTs, NMs
E = S, Se   R' = H, Me, *t*-Bu, Ph, MeO, Br, I

21-67%
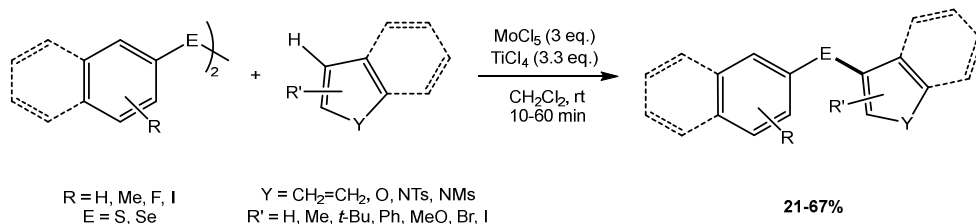
Figure 51. Oxidative chalcogenation of substituted arenes and heterocycles, affording diarylchalcogenides, promoted by MoCl₅ and TiCl₄.

The synthesis of thia- and selenaheterocycles was also achieved by adapting the protocol to the intramolecular cyclization of disulfides/diselenides. Five- to seven- membered heterocycles were obtained in good yields and mild reaction conditions, with MoCl₅ (and TiCl₄ as an additive) resulting again to be the best suited promoter.[287]

66

2. Aim of the Thesis

By combining the numerous, peculiar features of high valent metal halides, the synthesis of complex organic products, which are usually prepared exploiting more complicated synthetic protocols, could be achieved in a simple and straightforward way. Investigating the chemistry of group 5 and 6 high valent metal halides may have both a practical and a scholarly interest: it implies the exploration of previously unknown reactivity aspects, given the relatively low amount of both fundamental and applied research in this field, when compared to more common metal precursors (i.e. group 4 transition metals or late transition metals). Moreover, the implementation of easily available, low-cost and virtually environmentally compatible metal promoters in catalytical or even stoichiometric processes can be advantageous with respect to the use of precious and toxic low valent metals such as rhodium, iridium or palladium.

Given our interest, in the recent years, in the behaviour of HVMH towards organic molecules bearing unsaturated C–Y bonds (Y = N, O), we herein report an investigation over a selection of different substrates (i.e. α-diimines, isocyanides, carboxylic acids): their proneness to undergo diverse reactivity patterns when interacting with metal halides will be discussed, in an attempt to rationalize the conditions favouring the formation of coordination adducts or possible activation products.

3. Result and Discussion

3.1. α-Diimines

α-Diimines (also called 1,4-diaza-1,3-dienes, DADs) represent an interesting class of organic compounds, whose steric and electronic properties can be adjusted by varying the substituents on the N=C–C=N skeleton (Figure 52).[288,289] Their robustness and versatility render them as one of the most versatile classes of ancillary, chelating ligands in coordination chemistry,[290] forming complexes with metal centres from the main groups,[291–293] transition metals,[294] lanthanides[295,296] and actinides.[297,298] These complexes find application in metal-assisted organic synthesis, being involved in stoichiometric as well as catalytic transformations.[299–303]
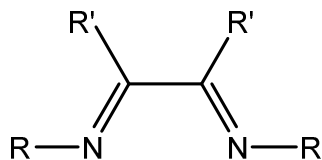
Figure 52. Generic structure of an α-diimine (1,4-diaza-1,3-diene, DAD)

Concerning their interaction with metal centres, α-diimines are considered to be redox non-innocent ligands,[304,305] as they can undergo two stepwise, mono-electron reductions to radical anion, and enediamido dianion (overall two-electron reduction),[288] possibly determining some ambiguity in the assignment of the oxidation states (Figure 53).
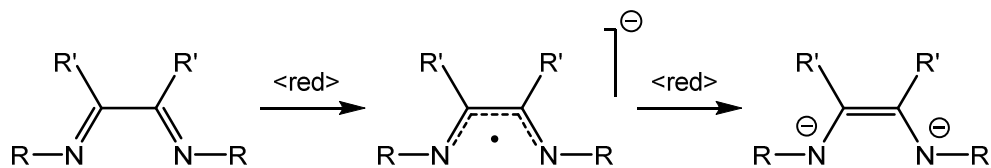
Figure 53. Single-electron reduction steps of α-diimines.

Conversely, the oxidation behaviour of α-diimines has not been clearly addressed so far, and information about this aspect is rather sparse in the literature.[295,306]

In this setting, reactivity studies of α-diimines with metal centres in a high oxidation state (+4 or higher), which may act as oxidants, are quite rare in the literature, being limited to MO_2Cl_2 derivatives,[307,308] and mixed chloro-phosphine complexes.[309] Regarding homoleptic, high valent transition metal chlorides, only those of group 4 metals have been considered for the direct interaction with α-diimines.[310,311] The reactivity of this class of ligands with group 5 and 6 metal chlorides (MCl_5, M = Nb, Ta, Mo, and WCl_6) has received considerable attention in the recent years. However, all the described reactions have been carried out in the presence of reductants (e.g. Zn/Hg,[309] Na,[312] Na/naphthalene,[313]) or chlorine-abstracting agents (1-methyl-3,6-bis(trimethylsilyl)-1,4-cyclohexadiene, MBTCD),[5,314–317] thus entailing the reduction, by one or two electrons, of the metal centre. This strategy is necessary to quench the activation ability of the high valent metal chlorides, allowing for the isolation of coordination compounds containing intact, redox active α-diimine ligands.

3.2. Reactions of WCl₆ with α-Diimines

The first example of direct interaction, i.e. in the absence of any additional reactants, of two N-aryl substituted α-diimines with a high valent metal chloride is herein described.[318] By reaction with WCl₆, at room temperature in dichloromethane, N,N′-bis(2,6-diisopropylphenyl)-1,4-diaza-1,3-butadiene (DAD$_{Dipp}$) and 2,3-bis(2,6-diisopropylphenylimino)butane ($_{Me}$DAD$_{Dipp}$) were converted into the quinoxalinium salts [{2,6-C₆H₃(CHMe₂)₂}N(CR')₂NCC(CHMe₂)(CH)₃C][WCl₆] (R' = H, **1a**; R' = Me, **1b**) (Figure 54).

R' = H, DAD$_{Dipp}$
R' = Me, $_{Me}$DAD$_{Dipp}$

R' = H, **1a** (60%)
R' = Me, **1b** (45%)
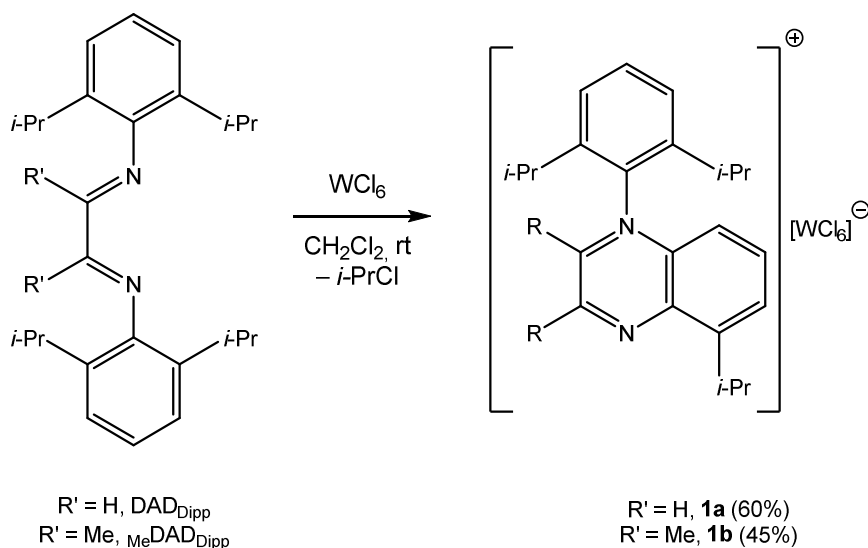
Figure 54. WCl₆-promoted intramolecular cyclization of N-aryl α-diimines into quinoxalinium salts.

The formation of isopropyl chloride was detected by means of NMR and GC-MS analyses on the liquids (distilled under vacuum) from the WCl₆/DAD$_{Dipp}$ and WCl₆/$_{Me}$DAD$_{Dipp}$ reaction mixtures in CD₂Cl₂. The same approach was applied to reaction mixtures of WCl₆ with

different α-diimines, and limited amounts of alkyl halides were detected in most cases (see Section 5.2), hinting at possible differences in the reactivity (*vide infra*).

Compound **1a** was isolated and characterized *via* IR and NMR spectroscopy, and single crystals suitable for X-ray diffraction were collected: its crystal structure consists of an ionic packing of [{2,6-$C_6H_3(CHMe_2)_2$}N(CR')$_2$NCC(CHMe$_2$)(CH)$_3$C]$^+$ cations and [WCl$_6$]$^-$ anions (Figure 55). While the anion has already been described in miscellaneous salts,[264,319] the cation represents the first example of crystallographically characterized N-aryl-quinoxalinium ever reported. Its bonding parameters do not significantly differ from those previously reported for N-alkyl-quinoxalinium cations (relevant bond lengths and angles of **1a** are reported in Table 1).[320–323]
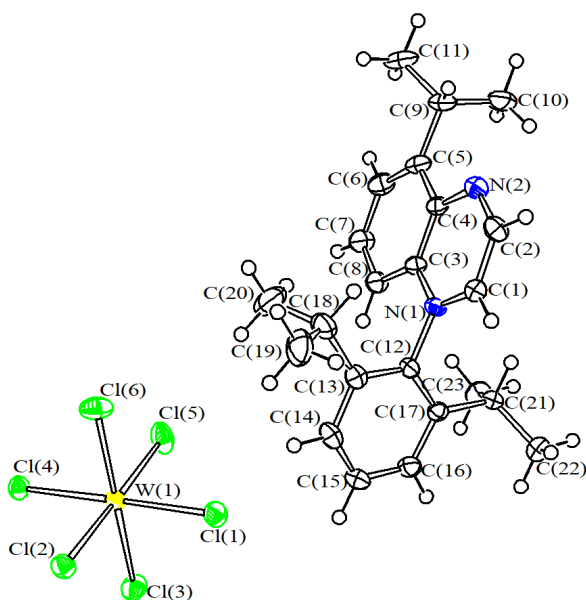
Figure 55. ORTEP drawing of the crystal structure of **1a**. Displacement ellipsoids are at the 50% probability level. Only one of the two independent molecules present within the unit cell is represented.

Table 1. Selected bond distances (Å) and angles (deg) for **1a**.

Bond Distances (Å)			
W(1)–Cl(1)	2.3224(16)	W(1)–Cl(2)	2.3478(15)
W(1)–Cl(3)	2.3083(16)	W(1)–Cl(4)	2.3309(15)
W(1)–Cl(5)	2.3133(17)	W(1)–Cl(6)	2.3083(17)
C(1)–C(2)	1.411(9)	C(3)–C(4)	1.424(8)
C(1)–N(1)	1.327(8)	C(4)–N(2)	1.359(8)
C(2)–N(2)	1.314(9)	C(3)–N(1)	1.385(8)
C(4)–C(5)	1.434(9)	C(5)–C(6)	1.363(10)
C(6)–C(7)	1.405(10)	C(7)–C(8)	1.366(9)
C(8)–C(3)	1.411(9)	N(1)–C(12)	1.471(8)
Angles (deg)			
Cl(1)–W(1)–Cl(4)	178.97(6)	Cl(2)–W(1)–Cl(5)	178.81(6)
Cl(3)–W(1)–Cl(6)	179.65(7)	C(2)–C(1)–N(1)	119.7(6)
C(1)–N(1)–C(3)	120.3(5)	N(1)–C(3)–C(4)	117.7(5)
C(3)–C(4)–N(2)	121.5(6)	C(4)–N(2)–C(2)	118.2(6)
N(2)–C(2)–C(1)	122.7(6)	C(3)–C(4)–C(5)	119.0(6)
C(4)–C(5)–C(6)	117.5(6)	C(5)–C(6)–C(7)	122.7(6)
C(6)–C(7)–C(8)	121.8(6)	C(7)–C(8)–C(3)	117.3(6)
C(8)–C(3)–C(4)	121.7(6)		

Quinoxalinium salts have several potential applications, ranging from synthetic chemistry, as photo-initiators[324] or as oxidants,[325,326] to pharmaceuticals[327,328] and chemosensors.[329] Common synthetic strategies to access quinoxaliniums involve N-alkylation of the corresponding quinoxaline,[328] or direct condensation of α-diketones with N-substituted 1,2-phenylenediamines:[327] these strategies have been scarcely applied for the synthesis of N-aryl quinoxalinium salts, and only a few examples are available in the literature.[330,331]

In order to understand the mechanistic pathway leading to the intramolecular cyclization of DAD$_{Dipp}$, several experiments, including electrochemical analyses and EPR spectroscopy, and DFT calculations were performed. The cyclic voltammetry of DAD$_{Dipp}$ in dichloromethane revealed, in addition to the documented reduction behaviour, the presence of an irreversible oxidation process (E = 1.63 V, measured *versus* Ag/AgCl): this peak could be attributed to the presumably generated radical cation, which rapidly undergoes degradation, as pointed out by the appearance, in the second scan toward negative potentials of a 2-cycle voltammetric experiment, of a reduction peak at −0.33 V (Figure 56).
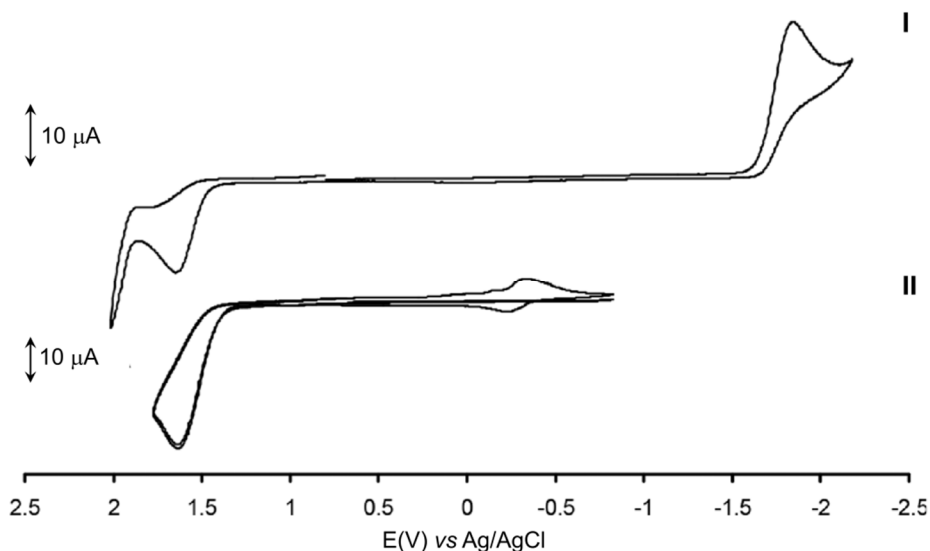
Figure 56. Cyclic voltammograms of DAD_{Dipp} recorded at a Pt electrode in CH_2Cl_2 solution containing 0.2 M [n-Bu$_4$N][PF$_6$]. Scan rate 0.1 V/s.
I) Cyclic voltammetry obtained starting the scan toward negative potentials from +0.8 V; **II**) 2-cycle voltammetry between −0.8 and 1.8 V.

It should be noted that the value of oxidation potential of DAD_{Dipp} would allow, in principle, a chemical oxidation by WCl_6 (E ≈ 1.6 V vs Ag/AgCl/KCl in dichloromethane).[6] Nevertheless, no radical cationic derivatives of DAD_{Dipp} could be detected from the EPR analysis on the mixture with WCl_6 in dichloromethane, and neither electrochemical or chemical oxidation (using NOBF$_4$, i.e. a common oxidizing agent, with a comparable oxidation potential to that of WCl_6)[6] ultimately led to the formation of the quinoxalinium cation featured in **1a**. This combined evidence suggest that, despite the fact that **1a** contains a W(V) anion, its generation cannot be the consequence of a simple electron transfer from DAD_{Dipp} to W(VI).

Following these experimental observations, DFT calculations were carried out to determine key intermediates along a plausible mechanistic pathway to the formation of **1a** (Figure 57; for details on the calculated intermediates, see Section 5.11). The most likely first step, following the initial WCl$_6$---DAD$_{Dipp}$ interaction (Figure 108, p. 210), appears to be a chlorination of the N=C–C=N skeleton (intermediate **A**, Figure 109, p. 210). Experimentally, the reaction of DAD$_{Dipp}$ with a chlorinating agent, i.e. PCl$_5$, in dichloromethane, selectively proceeds with a Cl/H substitution at one imine carbon: the resulting chlorinated α-diimine, however, does not undergo further rearrangements, hinting that the formation of **1a** is not a product of simple chlorine transfer either. Following chlorination of the organic substrate, one-electron transfer from the newly formed ligand to the metal centre can occur, along with the migration of another chloride from the metal to an isopropyl-substituted carbon atom (intermediate **B**, Figure 110, p. 211). Then, the presence of both an activated aromatic ring and a formally anionic nitrogen atom would favour the intramolecular cyclization (intermediate **C**, Figure 111, p. 211). Finally, the aforementioned release of isopropyl chloride (*vide supra*) can take place, probably acting as the driving force for the whole process: such elimination generates a radical (intermediate **D**, Figure 112, p. 212) which could be oxidized to the final quinoxalinium cation either by WCl$_5$ ($\Delta G = -7.5$ kcal/mol), or most likely by still unreacted WCl$_6$ ($\Delta G = -40.8$ kcal/mol).
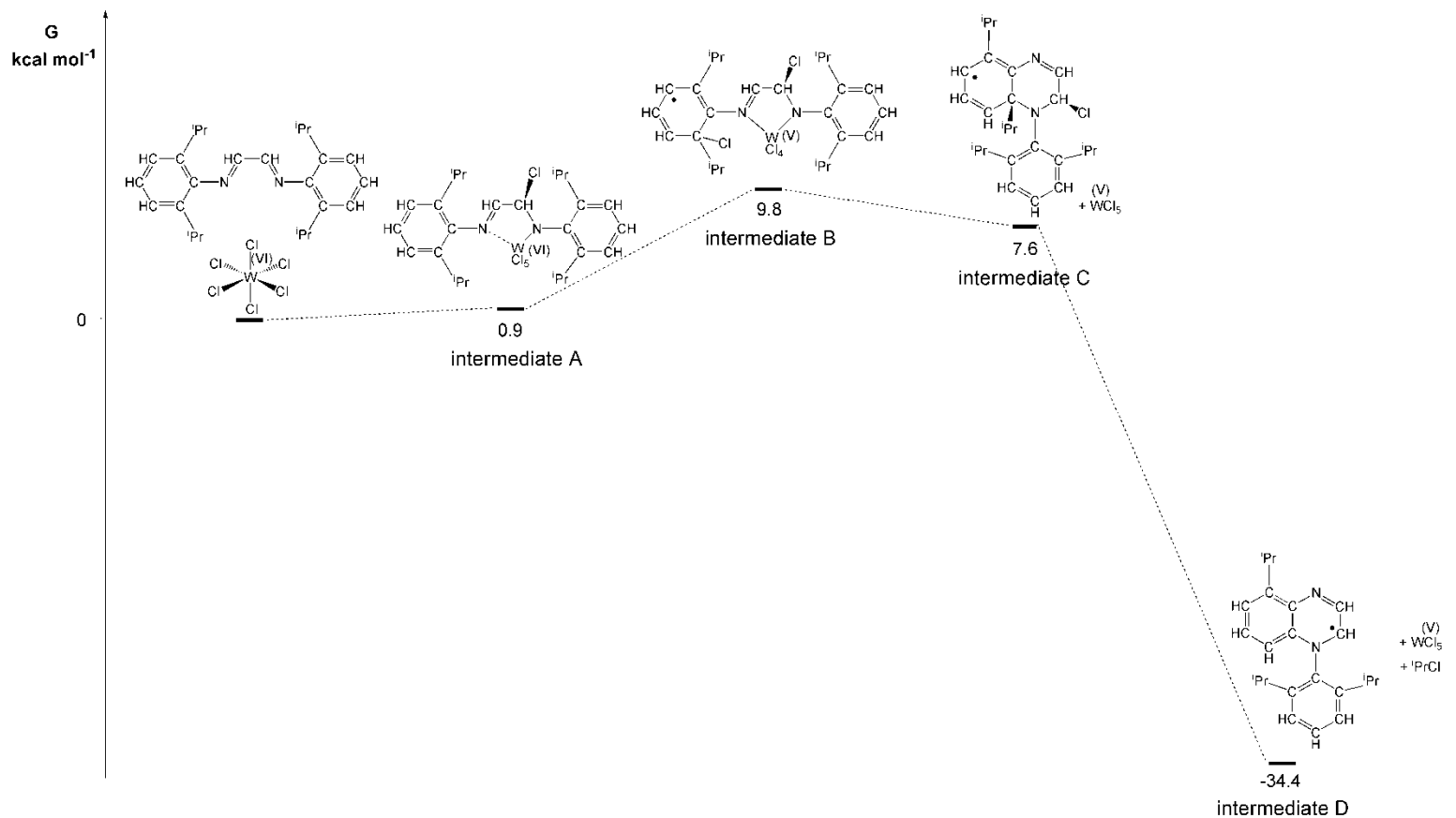
Figure 57. Relative Gibbs energies of DFT-optimized intermediates along the proposed pathway for the WCl_6-mediated conversion of DAD_{Dipp} to quinoxalinium salt **1a**. C-PCM/ωB97X calculations, dichloromethane as continuous medium.

The W(IV) coordination complex $WCl_4(DAD_{Dipp})$, **2a**,[5] was identified as a side-product of the synthesis of **1a**. In regulating the **1a/2a** ratio, the solvent polarity played a crucial role: in fact, while **2a** is observed in small amounts when performing the reaction in dichloromethane, if toluene is employed **2a** becomes the major product (60% yield). By performing the same reaction with DAD_{Dep} in toluene, the W(IV) complex $WCl_4(DAD_{Dep})$, **2b**, is obtained in 40% yield (Figure 58). This strategy may provide an alternative route to $W^{IV}Cl_4(DAD)$ coordination compounds, in the absence of Cl-abstracting reagents.[5]

R = *i*-Pr, DAD_{Dipp}
R = Et, DAD_{Dep}

R = *i*-Pr, **2a** (60%)
R = Et, **2b** (40%)
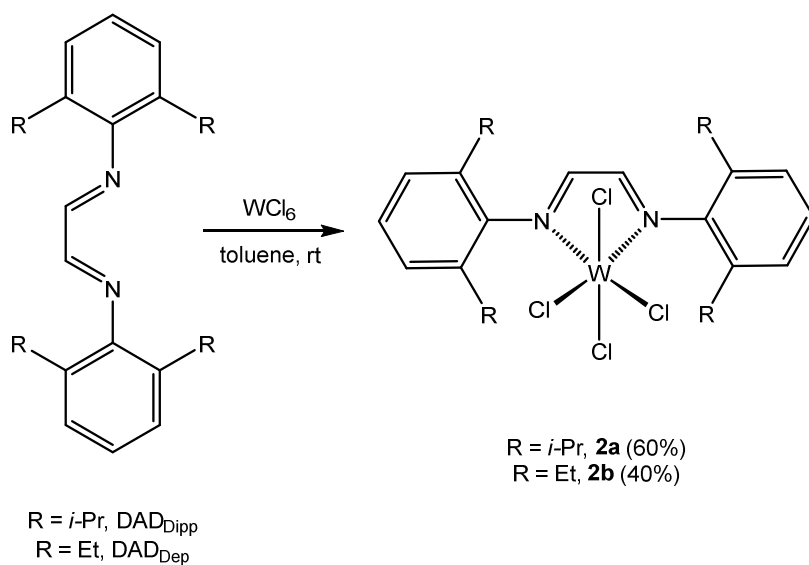
Figure 58. Synthesis of $W^{IV}Cl_4(DAD)$ coordination complexes by direct interaction of WCl_6 with α-diimines in toluene.

The new compound **2b** was fully characterized by analytical and spectroscopic techniques, and its crystal structure was ascertained *via* X-ray diffraction (Figure 59, Table 2). The structure of **2b** bears striking analogies to that of previously reported **2a**.[5]

78

Figure 59. Crystal structure of **2b** with key atoms labelled.

Table 2. Selected bond distances (Å) and angles (deg) for **2b**.

Bond Distances (Å)			
W(1)–Cl(1)	2.351(3)	W(1)–Cl(2)	2.349(3)
W(1)–Cl(3)	2.296(3)	W(1)–Cl(4)	2.250(3)
W(1)–N(1)	2.032(10)	W(1)–N(2)	2.054(9)
N(1)–C(1)	1.344(15)	N(2)–C(2)	1.351(15)
C(1)–C(2)	1.381(17)		
Angles (deg)			
Cl(1)–W(1)–Cl(2)	169.60(11)	Cl(3)–W(1)–N(1)	161.7(3)
Cl(4)–W(1)–N(2)	160.9(3)	Cl(3)–W(1)–Cl(4)	110.88(12)
N(1)–W(1)–N(2)	73.7(4)	W(1)–N(1)–C1)	120.1(8)
N(1)–C(1)–C(2)	113.4(11)	C(1)–C(2)–N(2)	113.3(10)
C(2)–N(2)–W(1)	118.9(8)		

The unexpected outcome of the WCl_6-promoted activation of DAD_{Dipp} prompted us to extend the investigation to other α-diimines: the direct interaction of WCl_6 with N,N′-bis(xylyl)-1,4-diaza-1,3-butadiene, DAD_{Xyl}, was studied in a room temperature reaction in dichloromethane (xylyl = 2,6-dimethylphenyl). The iminomethyl-imidazolium salt [(Xyl)NCHCHN(Xyl)CCHN(Xyl)][WCl_6], **3**, was obtained in 47% yield (Xyl = 2,6-$C_6H_3Me_2$) (Figure 60).[332]

3 (47%)
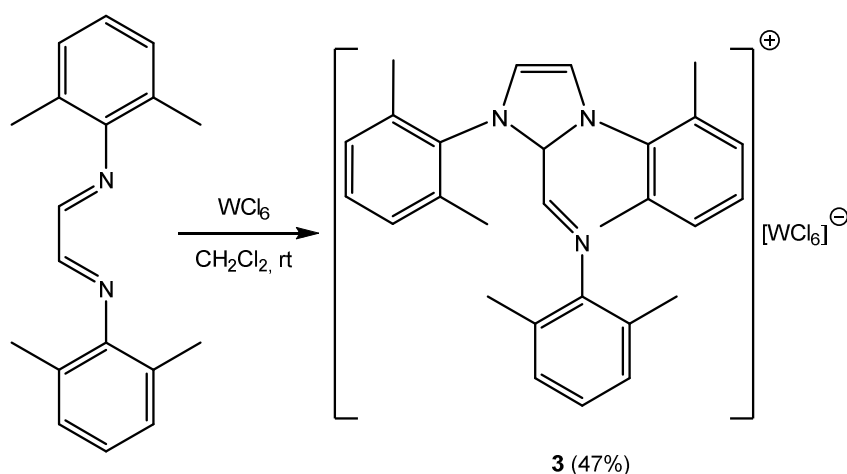
Figure 60. WCl_6-directed conversion of DAD_{Xyl} into imidazolium salt **3**.

The iminomethyl-imidazolium cation is formally generated by the intermolecular cyclization of two DAD_{Xyl} units, accompanied by elimination of one [N-Xyl] fragment. In order to understand the destiny of such fragment, the WCl_6/DAD_{Xyl} reaction mixture was monitored *via* NMR spectroscopy in CD_2Cl_2: besides the signals relative to **3**, the presence of an additional, xylyl-containing species was detected. The methyl groups of this species appeared to be significantly deshielded (3.43 ppm in the ^{1}H NMR), hinting at the co-formation of a metal-bound amide or imide. DFT calculations provided further insight on the nature of such species, which will be discussed later in the

80

document. The imidazolium salt **3** was isolated and characterized by IR, ^{1}H and ^{13}C NMR spectroscopy, and a X-ray diffraction study was performed on a single crystal (Figure 61, Table 3).
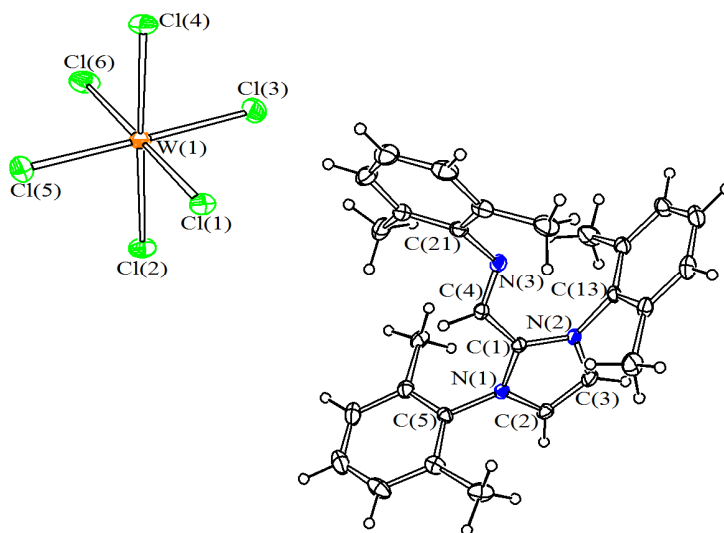
Figure 61. ORTEP drawing of the molecular structure of the imidazolium salt **3**, with key atoms labelled.
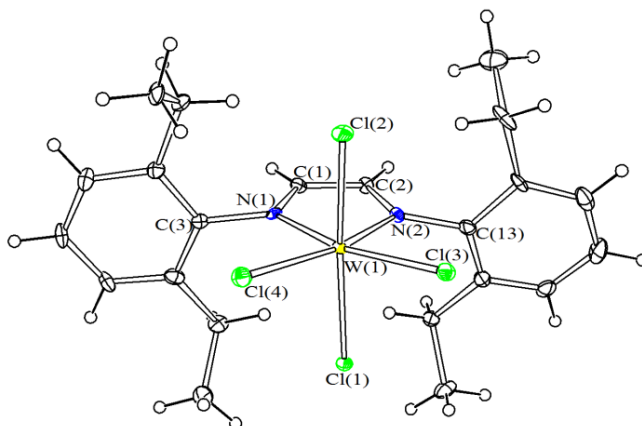
Table 3. Selected bond distances (Å) and angles (deg) for **3**.

Bond Distances (Å)			
W(1)–Cl(1)	2.3420(8)	W(1)–Cl(2)	2.3302(9)
W(1)–Cl(3)	2.3149(9)	W(1)–Cl(4)	2.3319(9)
W(1)–Cl(5)	2.2921(10)	W(1)–Cl(6)	2.3263(9)
C(1)–N(1)	1.346(4)	N(1)–C(2)	1.371(4)
C(2)–C(3)	1.352(5)	C(3)–N(2)	1.369(4)
N(2)–C(1)	1.346(4)	C(1)–C(4)	1.461(4)
C(4)–N(3)	1.264(4)	N(3)–C(21)	1.432(4)
N(1)–C(5)	1.454(4)	N(2)–C(13)	1.453(4)

Angles (deg)			
Cl(1)–W(1)–Cl(6)	179.16(4)	Cl(2)–W(1)–Cl(4)	177.86(3)
Cl(3)–W(1)–Cl(5)	178.89(4)	C(1)–N(1)–C(2)	109.7(3)
N(1)–C(2)–C(3)	106.3(3)	C(2)–C(3)–N(2)	108.2(3)
C(3)–N(2)–C(1)	108.7(3)	N(2)–C(1)–N(1)	107.0(3)
N(1)–C(1)–C(4)	123.8(3)	N(2)–C(1)–C(4)	129.2(3)
C(1)–C(4)–N(3)	120.4(3)	C(4)–N(3)–C(21)	118.9(3)

The solid-state structure of **3** consists of an ionic packing of $[WCl_6]^-$ anions and $[(Xyl)NCHCHN(Xyl)CCHN(Xyl)]^+$ cations. The crystallographic determination of the latter is unprecedented. The geometry and the bonding parameters within the imidazolium skeleton and the xylyl groups are within expectation. The C(4)–N(3) bond (1.264(4) Å) holds substantial imine character, the C(4) atom exhibiting pure sp^2 hybridization (C(1)–C(4)–N(3) = 120.4(3) °).

While being a rare transformation, the conversion of α-diimines into iminomethyl-imidazolium salts has already been reported in the literature (for different α-diimines), being promoted by Brønsted or Lewis acids (i.e. HCl, $AlCl_3$).[333,334]

DFT calculations have been performed to elucidate the reaction pathway leading to **3** (Figure 62, for details on the computed intermediates, see Section 5.11, Figure 113-Figure 118).
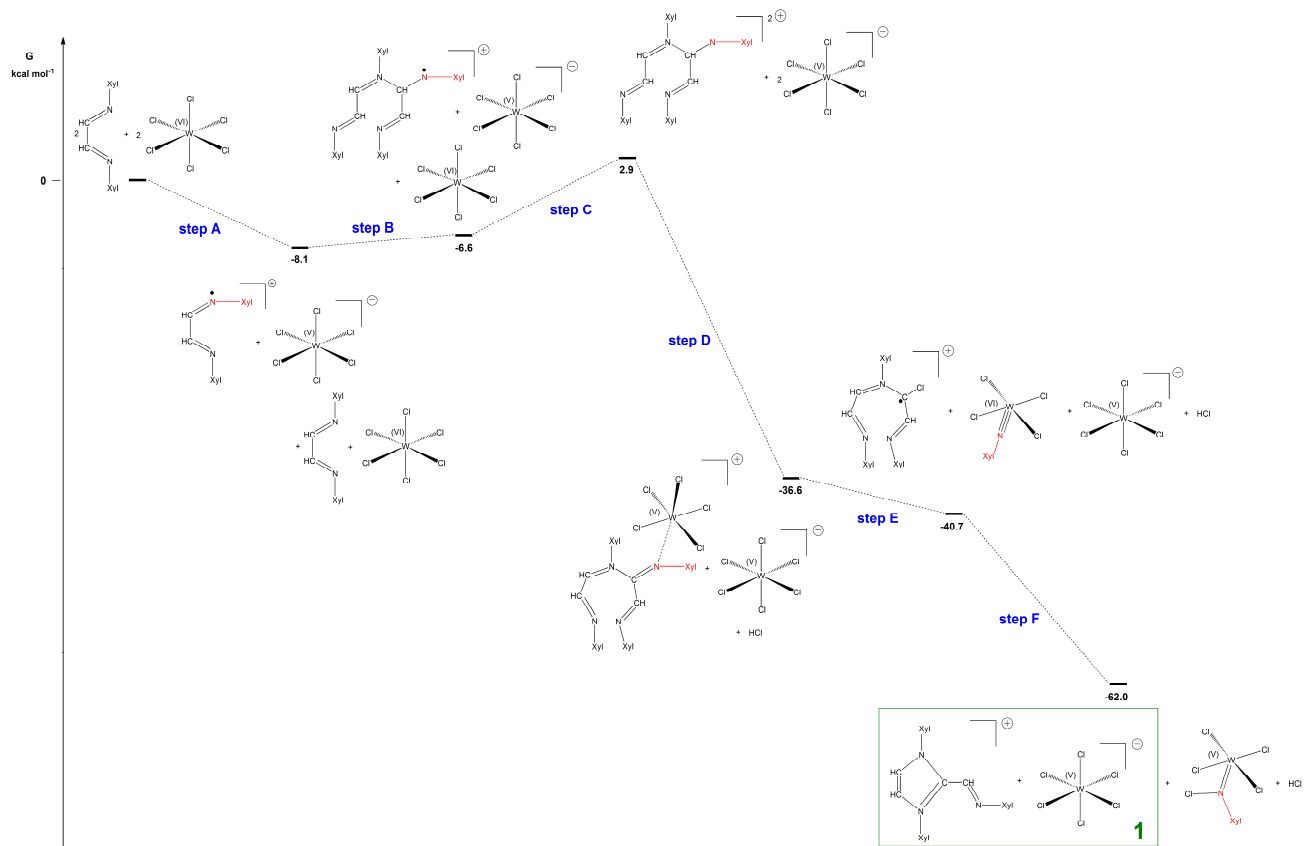
Figure 62. Relative Gibbs free energies of proposed intermediates for the WCl$_6$-mediated conversion of DAD$_{Xyl}$ to the imidazolium salt **3**. C-PCM/ωB97X calculations, dichloromethane as continuous medium. Xyl = 2,6-C$_6$H$_3$Me$_2$.

The reaction presumably starts with a mono-electronic oxidation of DAD$_{Xyl}$ by WCl$_6$, affording the corresponding radical cation [DAD$_{Xyl}$]$^{•+}$ and the W(V) species [WCl$_6$]$^−$ (step **A** in Figure 62, and Figure 113 in Section 5.11, p. 213). A new C–N bond is then formed as a consequence of the coupling of [DAD$_{Xyl}$]$^{•+}$ with still unreacted DAD$_{Xyl}$, thus generating the radical cation [XylNCHCHN(Xyl)CH(NXyl)CHNXyl]$^{•+}$ (step **B**, and Figure 114, p. 213). The latter may be further oxidized by WCl$_6$ to the corresponding dication (step **C**, Figure 115, p. 214): though this step has a slightly positive ΔG, subsequent loss of H$^+$ as HCl (by reaction with [WCl$_6$]$^−$) renders the overall process thermodynamically favourable (Step **D**). The formation of an adduct between WCl$_5$ and the [N(Xyl)C(CHNXyl)NXylCHCHNXyl]$^+$ cation (Figure 116, p. 214) is preliminary to the mono-electronic reduction of the organic frame by W(V), accompanied by Cl/[N-Xyl] exchange: the W(VI)-imido complex W(NXyl)Cl$_4$ and the chlorinated radical cation [XylNCHCHN(Xyl)C(Cl)CHNXyl]$^{•+}$ (Figure 117, p. 215) are thus generated (step **E**). The electron poor, Cl-bound carbon can be attacked intramolecularly by the imine nitrogen, and a subsequent electron exchange between the organic intermediate and the W(VI)-imido complex would lead to the final five-membered ring closing (step **F**). A formal migration of the chlorine atom from the organic cation to W^{VI}Cl$_4$(NXyl) appears to be energetically favoured, resulting in W^{V}Cl$_4$(NClXyl) (Figure 118, p. 216): the formation of the latter would account for the deshielded methyl signals in the NMR spectrum (*vide supra*), compatible with a W(V) N-chloro amide.

It can be concluded that at least two different activation pathways are viable following the direct interaction of WCl_6 with N-aryl α-diimines, i.e. intramolecular rearrangement to quinoxalinium (Figure 54) or intermolecular coupling leading to imidazolium (Figure 60). The reactions of WCl_6 with other α-diimines were non-selective, and led to complicated mixture of products. In only one case, i.e. the reaction of WCl_6 with 2,3-bis(2,6-dimethylphenylimino)butane, $_{Me}DAD_{Dep}$, was it possible to identify and isolate [(2,6-$C_6H_3Et_2$)NH=CMeCMe=N($C_6H_2Et_2$Me)][WCl_6], **4**, as low-yielding product, resulting from a different type of activation (for further information, see Section 5.2 and Figure 95, Table 14, in Section 5.10, p. 185).

It should be mentioned here that the known activation reactions of α-diimines are quite rare in the literature,[335,336] and are usually limited to C–C[314,315,337,338] and C–Cl[339,340] couplings on the N=C–C=N backbone. Examples of cyclizations similar to those promoted by WCl_6 are rather scarce: a $FeCl_2$-promoted trimerization of a N-aryl α-diimine was reported to yield a tri-cyclic dipyrrolopyrrole;[341] 2,3-bis(diphenylphosphino)-1,4-diazadienes have been shown to undergo an intramolecular [4+2] cycloaddition between the α-diimine unit and the N-aryl substituent, upon coordination of the phosphine groups to group 10 metal complexes.[342,343]

3.3. Reactions of MCl$_5$ (M = Mo, Nb, Ta) with α-Diimines

The reactions of a series of α-diimines with MoCl$_5$ have been evaluated, under analogous conditions to those employed for the reactions with WCl$_6$ (dichloromethane, ambient temperature, no additional reactant). DAD$_{Dipp}$ and DAD$_{Xyl}$ where tested first, but their direct interaction with MoCl$_5$ resulted in complicated mixtures of products. Instead, by reaction with MoCl$_5$, DAD$_{Dep}$ and DAD$_{tBu}$ (N,N′-bis(*tert*-butyl)-1,4-diaza-1,3-butadiene) were converted into their N-protonated derivatives, [DAD(H)]$_2$[Mo$_2$Cl$_{10}$] (DAD = DAD$_{Dep}$, **5a**; DAD = DAD$_{tBu}$, **5b**), in good yields (Figure 63).

R = 2,6-Et$_2$C$_6$H$_3$, DAD$_{Dep}$
R = *t*-Bu, DAD$_{tBu}$

R = 2,6-Et$_2$C$_6$H$_3$, **5a** (68%)
R = *t*-Bu, **5b** (78%)
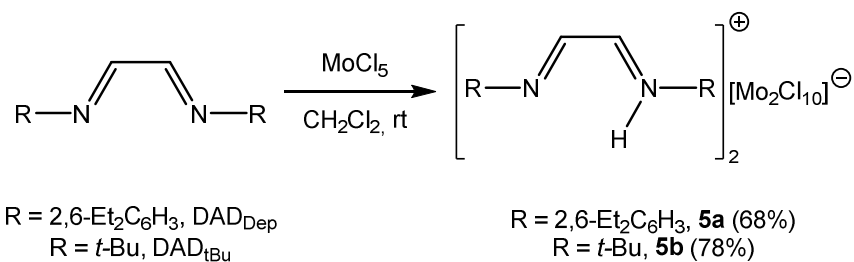
Figure 63. MoCl$_5$-promoted conversion of α-diimines in salts containing protonated α-diiminium cation.

The oxidizing power of MoCl$_5$ is likely to promote the abstraction of an electron from the α-diimine: subsequent hydrogen capture by the resulting radical cation from the reaction medium would generate the protonated cations of **5a-b**, following a pathway frequently observed in HVMH-promoted oxidation reactions performed in chlorinated solvents (see Section 1.2.9). Concerning the Mo(IV) anion, it is documented in the literature that the formal "[MoCl$_5$]$^-$" anion actually exhibits a dinuclear [Mo$_2$Cl$_{10}$]$^-$ structure,[344–346] hence the proposed formula for **5a-b** in Figure 63.

Characterization of **5a-b** was accomplished by means of elemental analysis, IR spectroscopy and magnetic susceptibility determination, together with DFT calculations: both asymmetric and symmetric stretching bands of the imine groups were observed in the solid-state IR spectrum of **5b**, respectively at 1667 and 1599 cm^{-1}, in agreement with the simulated spectrum. Only the symmetric vibration mode could be detected in the spectrum of **5a** (1586 cm^{-1}). The N–H stretching gave an absorption in the 3150-3250 cm^{-1} region in both spectra. Moreover, the magnetic susceptibility values for **5a-b** were fully consistent with those available in the literature for a Mo(IV)-chloride species.[91,347–349] All attempts to obtain suitable crystals of **5a-b** for X-ray diffraction were unsuccessful: solid-state structures could not thus be determined, and DFT calculated structures are herein proposed in their place (Figure 64).
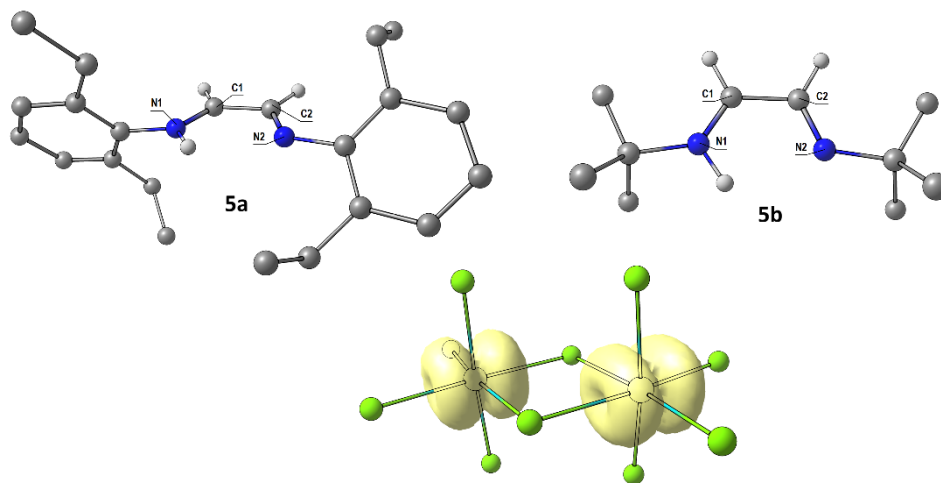
Figure 64. DFT-optimized structures (C-PCM/ωB97X calculations) of the cations and the anion within **5a** and **5b** with spin density surface (isovalue = 0.01 a.u.).

The study of the direct interactions of α-diimines with HVMH was further extended to the pentachlorides of group 5 metals, i.e. NbCl$_5$ and TaCl$_5$. The reactions of these metal halides with DAD$_{Dipp}$, performed in dichloromethane at room temperature, proceeded with activation of the organic substrate, affording a complicated mixture of products. From the NbCl$_5$/DAD$_{Dipp}$ reaction mixture, it was possible to identify [{2,6-C$_6$H$_3$(CHMe$_2$)$_2$}N(CH)$_2$NCC(CHMe$_2$)(CH)$_3$C][NbCl$_6$], **6**, NbCl$_4$(DAD$_{Dipp}$), **7**, and [DAD$_{Dipp}$(H)][NbCl$_6$], **8a** (Figure 65). The tantalum analogue [DAD$_{Dipp}$(H)][TaCl$_6$], **8b**, was isolated in very low yield from the TaCl$_5$/DAD$_{Dipp}$ reaction. Carrying out the reactions at different temperatures (e.g., at − 60 °C, or 80 °C in 1,2-dichloroethane) did not substantially affect the final composition of the reaction mixtures. Products **6**, **7**,[314] and **8a-b** were all identified by X-ray diffraction (details on the crystal structures are provided in Section 5.10, from Figure 96 to Figure 99, and corresponding Tables).
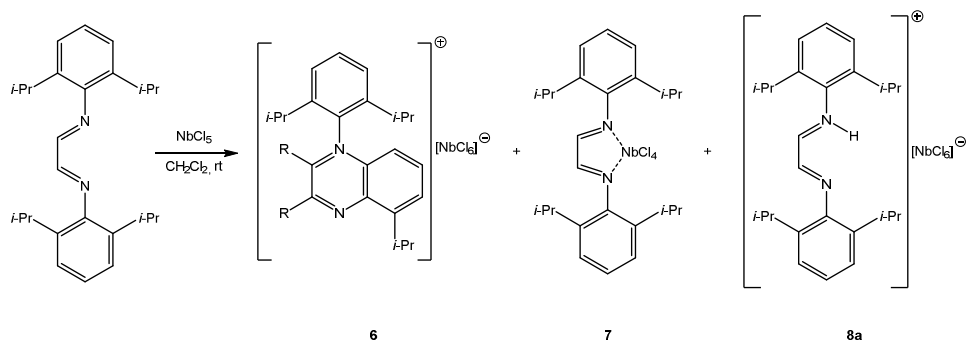
Figure 65. Products generated in the non-selective activation of DAD$_{Dipp}$ promoted by NbCl$_5$.

The outcome of the NbCl$_5$-directed activation of DAD$_{Dipp}$ bears some striking resemblances to that of the WCl$_6$/DAD$_{Dipp}$ reaction (see previous section, 3.2): the quinoxalinium cation featured in **6** is completely analogous to the one in **1a** (Figure 55), and it is likely

generated following a similar reaction pattern, involving an intramolecular cyclization and the release of the isopropyl unit. The latter was detected by GC-MS as isopropyl chloride in the final reaction mixture. Moreover, EPR studies suggested the presence of the isopropyl radical, following the identification of the coupled $[(CH_3)_2CHC(CH_3)_2]^{\cdot}$ radical at $-60\ °C$ (see Section 5.3, Figure 93-Figure 94, pp. 151-152). The co-formation of the Nb(IV) complex **7**, other than being similar to compound **2a** obtained from the WCl_6/DAD_{Dipp} reaction, provides further proof of the occurred redox process.

Similarities between WCl_6 and $NbCl_5$ in their behaviour with α-diimines can also be observed in the reaction with DAD_{Xyl}. Although the reaction mediated by $NbCl_5$ led once again to the formation of several products, the iminomethyl-imidazolium salt $[(Xyl)NCHCHN(Xyl)CCHN(Xyl)][NbCl_6]$, **9**, could be isolated in low yield and X-ray characterized (Figure 66; for details on the crystal structure, see Section 5.10, Figure 100 and Table 20, p. 193).
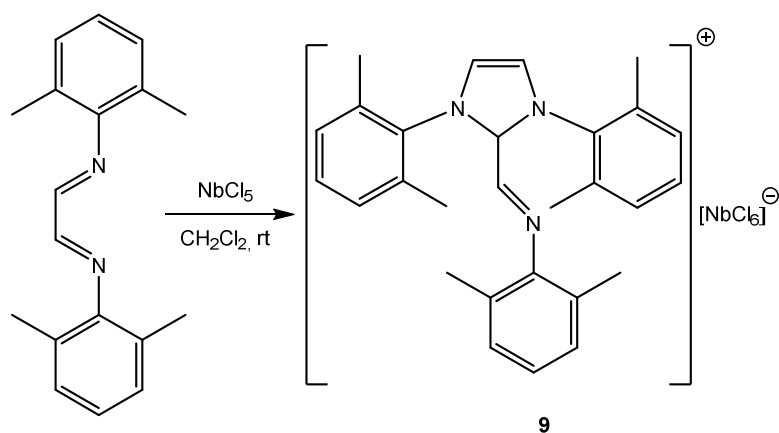
Figure 66. Non-selective, $NbCl_5$-mediated intermolecular cyclization of DAD_{Xyl} to imidazolium.

3.4. Synthesis and Characterization of Coordination Complexes with α-Diimines

During the investigation of the direct interactions of α-diimines with group 5 high valent metal halides, rare examples of coordination complexes were obtained. The factors stabilizing coordination products with respect to activation reactions will be herein discussed.[350]

From the 1:1 reaction of a selection of N-aryl α-diimines with NbF$_5$ in dichloromethane at ambient temperature, the ionic derivatives [NbF$_4$(DAD)$_2$][NbF$_6$] (DAD = DAD$_{Dipp}$, **10a**; DAD$_{Xyl}$, **10b**; DAD$_{Mes}$, **10c**) were obtained in high yields (**Figure 67**) (DAD$_{Mes}$ = N,N'-bis(2,4,6-trimethylphenyl)-1,4-diaza-1,3-butadiene). These represent rare examples of metal complexes with both fluoride and α-diimine ligands, and, to the best of our knowledge, the first example of a high valent metal fluoride coordination compound with an α-diimine.

Ar = 2,6-(*i*-Pr)$_2$C$_6$H$_3$, DAD$_{Dipp}$
Ar = 2,6-(Me)$_2$C$_6$H$_3$, DAD$_{Xyl}$
Ar = 2,4,6-(*i*-Pr)$_3$C$_6$H$_2$, DAD$_{Mes}$

Ar = 2,6-(*i*-Pr)$_2$C$_6$H$_3$, **10a** (82%)
Ar = 2,6-(Me)$_2$C$_6$H$_3$, **10b** (84%)
Ar = 2,4,6-(*i*-Pr)$_3$C$_6$H$_2$, **10c** (91%)
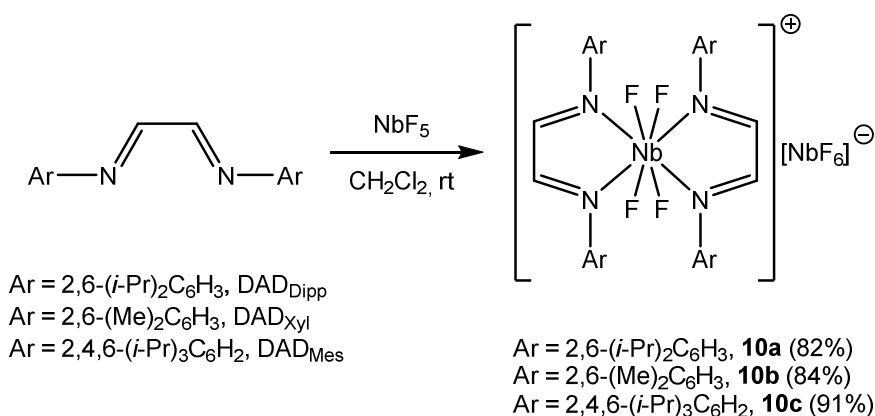
Figure 67. Ionic coordination complexes obtained from the direct interaction of α-diimines with NbF$_5$.

To verify the proposed stoichiometry of the cations in **10a-c**, we repeated the reactions employing different Nb/DAD molar ratios (e.g. 1:2 or 2:1): in all cases, **10a-c** were always obtained in lower yields, and in admixture with unidentified by-products. Moreover, computational studies confirmed the greater stability of the $[NbF_4(DAD)_2]^+$ cations, with respect to the $[NbF_4(DAD)]^+$ cations, in agreement with the experimental data (Equation 1).

$$[NbF_4(DAD)]^+ \quad + \quad DAD \quad \rightleftharpoons \quad [NbF_4(DAD)_2]^+$$

Equation 1. Calculated relative stability of the proposed cations for 10a-c. DAD = DAD_{Dipp}, $\Delta G = -15.9$ kcal/mol; DAD_{Xyl}, $\Delta G = -21.0$ kcal/mol; DAD_{Mes}, $\Delta G = -19.7$ kcal/mol.

Compounds **10a-c** were characterized by elemental analysis, solid-state IR and multinuclear NMR (CD_3CN solution) spectroscopy. The two α-diimine ligands were found to be equivalent, as only one set of signals was present in the ^1H and ^{13}C NMR spectra. The ^{19}F NMR spectra exhibited a decet at *ca.* 102 ppm (I_{Nb} = 9/2), typical of the NbF_6^- anion,[43,66,170,351,352] and one additional resonance ascribable to the cation (in the 144-156 ppm range). The presence of NbF_6^- was further confirmed by the appearance of the typical heptet at *ca.* 1555 ppm in the ^{93}Nb spectra.[66,351,352] The $^1J_{NbF}$ coupling constant displayed the same value (*ca.* 338 Hz) in both ^{19}F and ^{93}Nb NMR spectra.

Ionic adducts **10a-c** were all scarcely soluble in organic solvents, which rendered the recrystallization procedures very difficult. In the absence of X-ray diffraction data, DFT calculated structures are proposed for the cations (the cation in **10b** is shown in Figure 68; for

DFT calculated structures of the cations in **10a** and **10c**, see Section 5.11, Figure 119 and Figure 120, pp. 217-218).
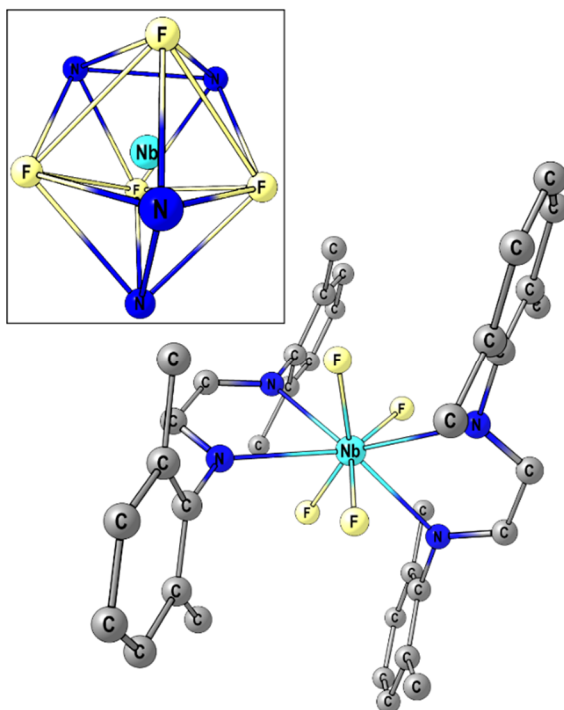
Figure 68. DFT-optimized geometry for the cation $[NbF_4(DAD_{Xyl})_2]^+$ within **10b** (C-PCM/ωB97X, dichloromethane as continuous medium). Hydrogen atoms are omitted for clarity. Selected bond lengths (Å): Nb-F 1.888, 1.888, 1.888, 1.888; Nb-N 2.400, 2.402, 2.402, 2.402; C=N 1.271, 1.271, 1.271, 1.271. Selected angles (°): N-Nb-N (*chelate*) 67.5, 67.6; F-Nb-F (*trans*) 145.2, 145.3. Inset: polyhedron around the metal centre.

The proposed structures for **10a-c** are in line with those of previously reported $[NbF_4(L-L)_2][NbF_6]$ compounds (L-L = bidentate ligand), featuring an eight-coordinated metal centre in the cation.[43,66,352] The cations in **10b** and **10c** display a high symmetry (D_{2d}) around the niobium centre, the fluorine and nitrogen ligands describing a trigonal

dodecahedra. The symmetry is lower in **10a** (D_2) due to the steric bulk of the isopropyl groups.

The differences between NbF_5 and $NbCl_5$ in the reaction with α-diimines could be ascribed to the strength of the Nb–F bond, compared to the Nb–Cl bond (see Section 1.1.1): stronger metal-halide bonds could prevent halogen transfer reactions and stabilize the coordination adducts, thus inhibiting activation routes, and this notwithstanding the fact that NbF_5 can behave as an oxidant.

A stable coordination adduct was also obtained from the reaction of DAD_{Dipp} with $NbOCl_3$. By replacing two of the chloride ligands in $NbCl_5$ with an oxide ligand, the oxophilicity of the metal centre decreases and the remaining Nb–Cl bonds are reinforced:[53] this is probably the reason why $NbOCl_3$ turns out to be less prone to ligand activation. As an example, $NbOCl_3(thf)_2$ is stable in a tetrahydrofuran solution,[353] while, in the same conditions, $NbCl_5(thf)$ initiates the ring opening polymerization of tetrahydrofuran (see Section 1.2.6).

Thus, the 1:1 interaction between $NbOCl_3$ and DAD_{Dipp} in dichloromethane at room temperature led to the isolation in moderate yields of $NbOCl_3(DAD_{Dipp})$, **11**, for which a crystal structure was obtained (Figure 69; relevant bonding parameters are reported in Table 4).
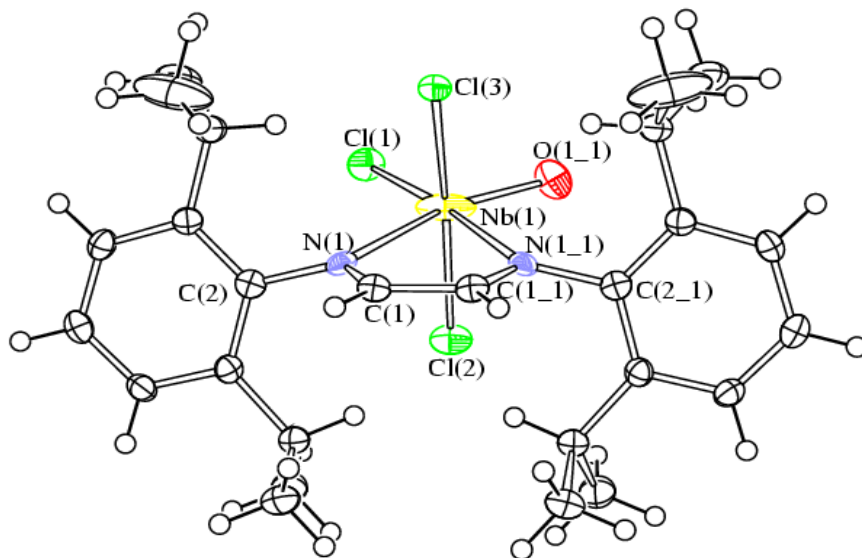
Figure 69. Molecular structure of $NbOCl_3(DAD_{Dipp})$, **11**, with key atoms labelled. Displacement ellipsoids are at the 50% probability level.

Table 4. Selected bond lengths (Å) and angles (deg) for **11**.

Bond Distances (Å)			
Nb(1)–Cl(1)	2.176(3)	Nb(1)–O(1_1)	1.874(8)
Nb(1)–Cl(2)	2.3415(16)	Nb(1)–Cl(3)	2.3876(15)
Nb(1)–N(1)	2.417(4)	Nb(1)–N(1_1)	2.417(4)
N(1)–C(1)	1.283(5)	N(1)–C(2)	1.449(5)
C(1)–C(1_1)	1.469(8)		
Angles (deg)			
Cl(2)–Nb(1)–Cl(3)	161.03(6)	Cl(1)-Nb(1)-N(1_1)	172.32(12)
O(1_1)–Nb(1)–N(1)	154.5(3)	O(1_1)–Nb(1)–Cl(1)	103.5(3)
N(1)–Nb(1)–N(1_1)	70.25(15)	Nb(1)–N(1)–C(1)	113.7(3)
Nb(1)–N(1)–C(2)	130.0(2)	C(1)–N(1)–C(2)	115.8(3)
N(1)–C(1)–C(1_1)	120.8(2)		

In **11**, the C–C and C–N bond lengths in the DAD$_{Dipp}$ ligand are very close to the values of a non-coordinated DAD$_{Dipp}$ (i.e. compatible with two C=N double bonds and a C–C single bond).[354] This finds confirmation in the solid-state IR spectrum, which displays a typical C=N absorption at 1626 cm^{-1}. Consequently, the N$_{sp2}$–Nb interaction would be considered as a dative bond,[355–357] in agreement with the relatively long Nb–N distance (2.417(4) Å) observed in **11** (e.g. when compared to complexes formally containing a reduced [DAD]$^{2-}$ ligand, such as NbCl$_3$(DAD$_{tBu}$)(thf), featuring considerably shorter Nb–N distances).[358] The niobium centre is only slightly (0.272 Å) out of the N=C–C=N plane: coplanarity or small deviations are expected for metal centres bound to neutral α-diimine ligands, while reduced [DAD]$^{2-}$ ligands can enforce the metal more than 1 Å out of the plane.[314,358] All this evidence suggests an Nb(V) centre with a neutral DAD$_{Dipp}$ ligand. The Nb–O bond length (1.874(8) Å) is compatible with a double bond, as expected for oxido ligands:[355,359–361] this is further confirmed by an absorption at 960 cm^{-1} in the solid-state IR spectrum, ascribable to the Nb=O moiety. In the solid state, the complex adopts a distorted octahedral geometry, the three chlorides displaying a *mer* arrangement around the niobium centre, and the oxido and α-diimine ligands sharing the same plane. The presence of a single isomeric form, presumably the same *mer* isomer, is observed in the solution as well by ^{1}H, ^{13}C and ^{93}Nb NMR experiments in CD$_2$Cl$_2$. Indeed, DFT calculations confirmed the *mer* geometry of **11** to be about 3.3 kcal/mol more stable than the alternative *fac* configuration.

Finally, the direct interaction of α-diimines with niobium/tantalum pentabromides was evaluated. The reactions were complicated by the

occurrence of activation pathways, as evidenced by the NMR analyses. Nevertheless, it was possible to obtain coordination compounds from the 2:1 molar reaction of MBr_5 and DAD_{Dipp} in dichloromethane at room temperature: the ionic adducts $[MBr_4(DAD_{Dipp})][MBr_6]$ (M = Nb, **12a**; M = Ta, **12b**) were isolated in 25-30% yields (Figure 70).

M = Nb, **12a** (31%)
M = Ta, **12b** (24%)
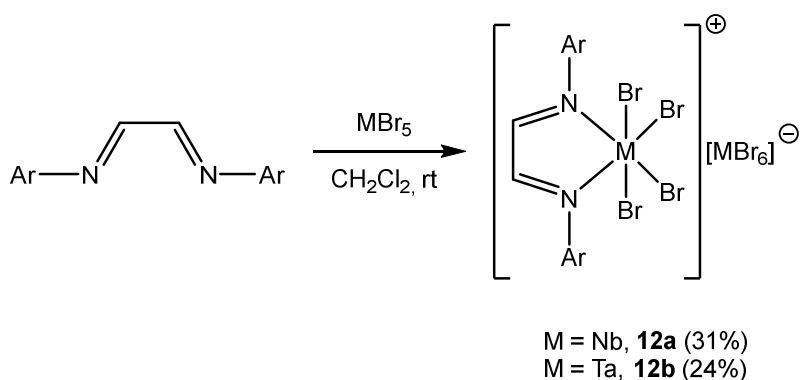
Figure 70. Formation of ionic coordination adducts from the reaction of DAD_{Dipp} with MBr_5 (M = Nb, Ta).

Contrary to our findings for the NbF_5 derivatives, in this case DFT calculations revealed the $[MBr_4(DAD_{Dipp})]^+$ cations to be more stable, when compared to $[MBr_4(DAD_{Dipp})_2]^+$ cations (Equation 2).

$$[MBr_4(DAD)]^+ \; + \; DAD \; \rightleftharpoons \; [MBr_4(DAD)_2]^+$$

Equation 2. Calculated relative stability of the proposed cations for **12a-b**. M = Nb, ΔG = 17.1 kcal/mol; Ta, ΔG = 20.3 kcal/mol.

Niobium and tantalum pentabromides display both lower metal-halide bond energy and a lower oxidation potential when compared to the corresponding pentafluorides and pentachlorides (see Section 1.1.1): while some activation processes may still be viable (i.e. as a

consequence of halide transfer reactions), the decreased oxidizing power allows for the obtainment of coordination compounds from MBr_5 and α-diimines, albeit in rather low yields. This evidence corroborates the idea that, in order to selectively address the reaction pathways to well-defined activation products, both the oxidation potential and the halogenating ability (towards the organic ligand) of the metal species should be exploited.

Compounds **12a-b** were characterized by spectroscopic techniques, as well as single crystal X-ray diffraction (**12a** is shown in Figure 71, Table; the isostructural compound **12b** is reported in Section 5.10, Figure 101 and Table 22).

Both compounds have the same structure, consisting of an ionic packing of $[MBr_6]^-$ anions and octahedral $[MBr_4(DAD_{Dipp})]^+$ cations. In the latter, rather long M–N bond distances can be observed, and the metal centres are almost coplanar with the N=C–C=N backbone: in analogy to the considerations made for **11** (*vide supra*), in both the **12a** and **12b** cations, the DAD_{Dipp} ligand can be considered as a neutral one, coordinating the M(V) centres *via* dative bonds.
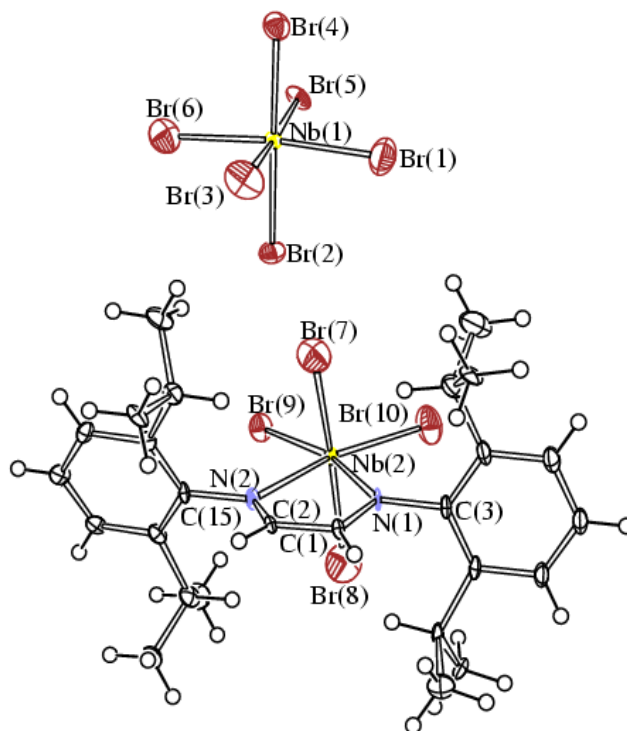
Figure 71. Molecular structure of **12a**, with key atoms labelled.
Displacement ellipsoids are at the 50% probability level.

Table 5. Selected bond lengths (Å) and angles (deg) for **12a**.

Bond Distances (Å)			
Nb(1)–Br(1)	2.428(6)	Nb(1)–Br(2)	2.542(5)
Nb(1)–Br(3)	2.423(6)	Nb(1)–Br(4)	2.457(5)
Nb(1)–Br(5)	2.551(4)	Nb(1)–Br(6)	2.452(6)
Nb(2)–Br(7)	2.384(6)	Nb(2)–Br(8)	2.384(7)
Nb(2)–Br(9)	2.388(4)	Nb(2)–Br(10)	2.367(5)
Nb(2)–N(1)	2.31(3)	Nb(2)–N(2)	2.31(2)
N(1)–C(1)	1.28(4)	N(2)–C(2)	1.25(4)
C(1)–C(2)	1.43(4)		

Angles (deg)			
Br(1)–Nb(1)–Br(6)	173.4(2)	Br(2)–Nb(1)–Br(4)	177.68(18)
Br(3)–Nb(1)–Br(5)	177.8(2)	Br(7)–Nb(2)–Br(8)	169.6(2)
Br(9)–Nb(2)–N(1)	163.6(6)	Br(10)–Nb(2)–N(2)	161.0(6)
N(1)–Nb(2)–N(2)	70.5(8)	Nb(2)–N(1)–C(1)	114.9(19)
Nb(2)–N(1)–C(3)	126.2(17)	C(1)–N(1)–C(3)	118(3)
Nb(2)–N(2)–C(2)	116(2)	Nb(2)–N(2)–C(15)	126.0(17)
C(2)–N(2)–C(15)	118(2)	N(1)–C(1)–C(2)	119(3)
N(2)–C(2)–C(1)	120(3)		

3.5. Reactions of NbX$_5$ (X = Cl, Br) with isocyanides

In order to further explore the behaviour of high valent metal halides towards organic molecules bearing unsaturated C–N bonds, we have focused our attention on investigating the reactions of isocyanides with group 5 metal halides. Isocyanides belong to a unique class of stable organic compounds bearing a formally divalent carbon, similar to that of carbenes and carbon monoxide.[362] Being a highly reactive class of compounds, isocyanides have been involved in a wide variety of reactions,[363] including cycloadditions,[364] MCRs,[365] and radical reactions.[366] Moreover, since their electronic properties are similar to those of the CO ligand, isocyanides display a rich organometallic chemistry.[367–370] Being π-acceptor ligands, a considerable part of the chemistry of isocyanides with metal centres involves low- or zero-valent metals, and this also applies to the metals of group 5.[371] While some chemistry with high valent niobium or tantalum complexes (mainly metallocenes) has been investigated,[372,373] to the best of our knowledge, reactions between isocyanides and high valent metal halides have been barely explored hitherto.

Given this premise, we have studied the 1:1 reaction of NbX$_5$ (X = Cl, Br) with 2,6-dimethylphenyl isocyanide, CNXyl, in toluene at ambient temperature, and thus obtained the coordination complexes NbX$_5$(CNXyl) (X = Cl, **13a**; X = Br, **13b**) (Figure 72).[374] The products were isolated in moderate to good yields as yellow/orange solids, and characterized by spectroscopic techniques, as well as X-ray diffraction.
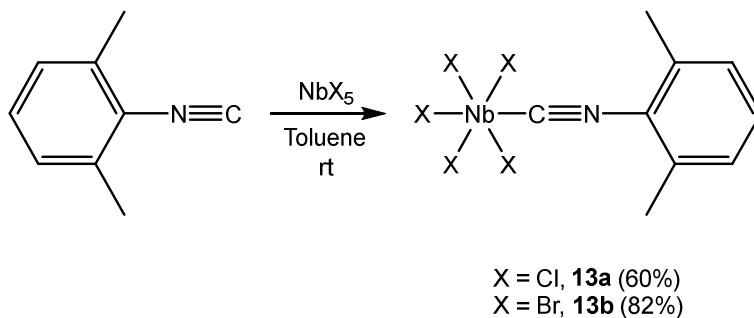
Figure 72. Synthesis of coordination compounds from NbX_5 (X = Cl, Br) and xylyl isocyanide.

^{1}H NMR studies of **13a-b** (C_6D_6 solution) show significantly lower chemical shifts for the CNXyl resonances upon coordination to the niobium centre, with respect to the free ligand. Each [93]Nb spectrum consists of a single resonance (−124 ppm for **13a**, and 479 ppm for **13b**).

Compounds **13a-b**, while scarcely soluble in benzene and toluene, have a good solubility in chlorinated solvents. However, they do not appear to be indefinitely stable in such environment: when the complexes were stored in dichloromethane at ambient temperature, progressive degradation occurred over 24 hours, as immediately evident by colour change (from yellow/orange to green). IR analyses on the residues revealed the disappearance of the C≡N absorption, and the occurrence of new absorptions around 1650 cm^{-1}, implying a lower carbon-nitrogen bond order. NMR analyses were unproductive, due to the presence of a complicated mixture of species. These results suggest that the coordinated isocyanide, activated by the interaction with the niobium centre, undergoes addition reactions, possibly involving the solvent as a nucleophile.

However, a CD_2Cl_2 mixture of $NbCl_5$ and CNXyl could be NMR characterized at room temperature, immediately after addition of the reactants at $-30\ °C$ (see Section 5.5 for details). Under these conditions, the ^{93}Nb NMR spectrum featured a sharp resonance at around 0 ppm, typical of the $[NbCl_6]^-$ anion.[59,64,170,352,375] The presence of the latter may suggest the formation of the ionic coordination compound $[NbCl_4(CNXyl)_2][NbCl_6]$, rather than the neutral **13a**, probably favoured by the relatively higher polarity of dichloromethane (compared to benzene). $NbX_5(L)$ and $[NbX_4(L)_2][NbX_6]$ can be considered as isomers generated, respectively, from formal symmetric and asymmetric cleavage of Nb_2X_{10} (i.e. the dinuclear structure of NbX_5, X = Cl, Br) upon addition of a neutral ligand L (Figure 73).[19,41,66,352,376] Only one of the two modes is generally adopted, depending on the nature of L. However, isomerism between the neutral and the ionic species was previously observed in solution for NHC derivatives.[377,378] It should be also noted that $[NbCl_4(CNXyl)][NbCl_6]$, containing a pentacoordinated cation, could in principle be generated as well, considering the steric hindrance exerted by the CNXyl ligand.
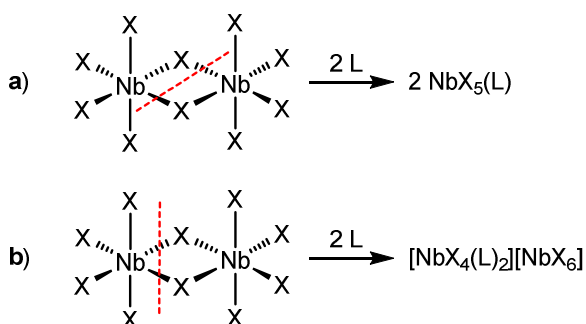
Figure 73. Symmetric (**a**) and asymmetric (**b**) cleavage of the dinuclear structure of NbX_5 (X = Cl, Br) upon addition of a neutral ligand L.

Given the observed lower stability of **13a-b** in chlorinated solvents (with respect to benzene/toluene), it can be concluded that the ionic derivatives are possibly more prone to nucleophilic attack compared to the neutral ones, ultimately resulting in the degradation.

The molecular structures of **13a** and **13b** are shown in Figure 74 and Figure 75, respectively; relevant bonding parameters are reported in Table 6 and Table 7. These crystal structures are among the rare cases of crystallographic characterization of a niobium pentahalide coordination compound containing a neutral carbon ligand, the only other example being $NbCl_5(IPr)$ (IPr = 1,3-bis(2,6-diisopropylphenyl)imidazol-2-ylidene).[379] The structure of **13a** resembles that of a previously reported niobium cyclopentadienyl complex, $NbCp*Cl_4(CNXyl)$.[373] Both complexes **13a** and **13b** display a slightly distorted octahedral geometry, the equatorial halides being bent to a small degree away from the axial halide, towards the isocyanide ligand. This configuration is often found in NbX_5 complexes with a monodentate, neutral ligand. [42,57,373,377,379] Notably, the $Nb–C_{CNXyl}$ distances in **13a-b** are significantly longer compared to known $Nb(V)–C_{carbene}$ bonds[380] and even $Nb(V)–C_{alkyl}$ σ-bond distances;[381–383] comparable $Nb–C$ bond lengths are found in the analogous $Nb–C_{CNXyl}$ interaction in $NbCp*Cl_4(CNXyl)$ (2.245(10) Å) and in the $Nb–C_{NHC}$ contact of $NbCl_5(IPr)$ (2.396(12) Å).

The C–N bond lengths found in the complexes deserve some comment: the C(1)–N(1) contacts (1.143(6) for **13a**, and 1.114(16) Å for **13b**, in agreement with a triple bond)[373] are shorter than the one found in the non-coordinated ligand (1.160 Å). Indeed, solid-state IR

analyses of **13a** and **13b** revealed absorptions relating to the C≡N bond stretching at 2221 and 2209 cm^{-1}, respectively, these values being considerably higher compared to non-coordinated 2,6-dimethylphenylisocyanide (2121 cm^{-1}).
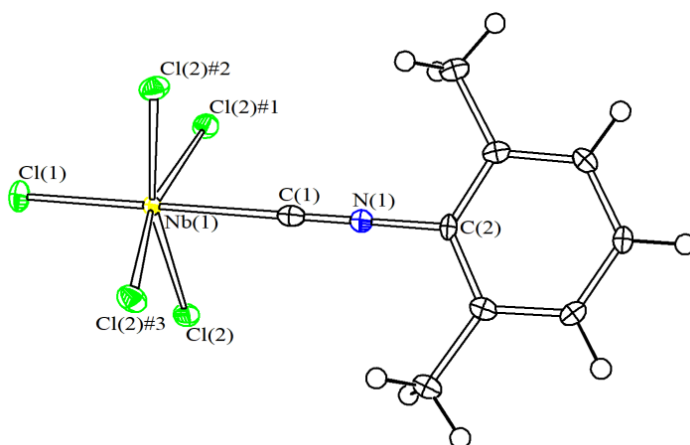
Figure 74. Molecular structure of **13a** with key atoms labelled. Displacement ellipsoids are at the 50% probability level. Symmetry transformations used to generate equivalent atoms: #1 -x+1,y,-z+3/2; #2 -x+1,y,z; #3 x,y,-z+3/2.

Table 6. Selected bond lengths (Å) and angles (deg) for **13a**.

Bond Distances (Å)			
Nb(1)–Cl(1)	2.2738(11)	Nb(1)–Cl(2)	2.3257(6)
Nb(1)–C(1)	2.319(5)		
C(1)–N(1)	1.143(6)	C(2)–N(1)	1.400(5)
Angles (deg)			
Cl(1)–Nb(1)–C(1)	180.0		
Cl(2)–Nb(1)–Cl(2)#2	164.12(3)	Cl(2)#1–Nb(1)–Cl(2)#3	164.12(3)
Nb(1)–C(1)–N(1)	180.0	C(1)–N(1)–C(2)	180.0
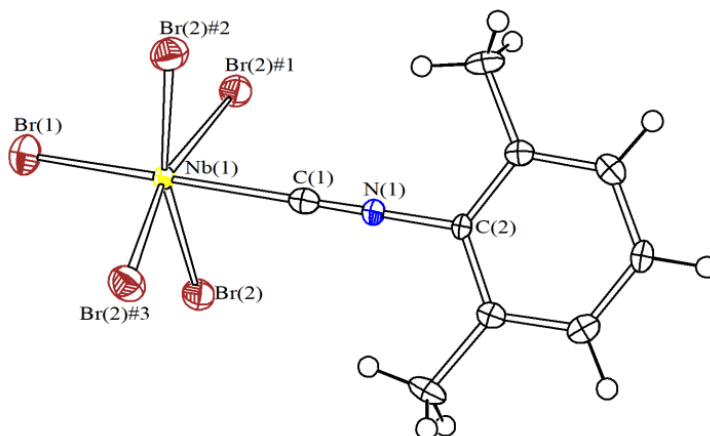
Figure 75. Molecular structure of **13b** with key atoms labelled. Displacement ellipsoids are at the 50% probability level. Symmetry transformations used to generate equivalent atoms: #1 -x+1,y,-z+3/2; #2 x,y,-z+3/2; #3 -x+1,y,z.

Table 7. Selected bond lengths (Å) and angles (deg) for **13b**.

Bond Distances (Å)			
Nb(1)–Br(1)	2.3937(16)	Nb(1)–Br(2)	2.4639(7)
Nb(1)–C(1)	2.329(12)		
C(1)–N(1)	1.114(16)	C(2)–N(1)	1.393(14)
Angles (deg)			
Br(1)–Nb(1)–C(1)	180.0		
Br(2)–Nb(1)–Br(2)#2	163.68(6)	Br(2)#1–Nb(1)–Br(2)#3	163.68(6)
Nb(1)–C(1)–N(1)	180.0	C(1)–N(1)–C(2)	180.0

Compounds **13a** and **13b** were also investigated in the framework of a combined synthetic/theoretical study on possible back-donation in d^0 complexes.[374] For high valent transition metal complexes, it has been generally accepted that the formal d^0 electronic configuration would suppress the back-donation. In some NHC complexes, however, contacts between the four equatorial chloride ligands and the carbene carbon were observed, and found to be within the sum of the van der Waals radii of the respective atoms.[378,379,384,385] This behaviour was attributed to a π-interaction between the chloride lone pairs and the p-orbital of the carbene carbon. Such an interligand interaction has been considered to be a form of back-donation, made possible by the electron density on the Cl-ligands, in spite of the formal absence of d electrons at the metal centre.[379] Indeed, the isocyanide carbons in **13a-b** display C–X contacts with the four equatorial X-ligands (3.049 and 3.141 Å for **13a** and **13b**, respectively) which are smaller than the sum of the van der Waals radii of the corresponding atoms (X = Cl, sum = 3.45 Å; X = Br, sum = 3.55 Å).[386] Previous theoretical studies on a selection of $NbCl_5$ complexes with π-acceptor ligands,[387] using the Charge Displacement (CD) approach,[388–390] revealed that Nb(V) is indeed capable of back-donating electronic density to the π-acid ligand from its d orbitals (partially filled up by the chloride electrons), this contribution being in some cases coexisting with (or replaced by) the interligand interaction with the equatorial chlorides. It should be noted that analogous back-bonding from metal-chloride bonds to a carbon ligand was previously proposed for the pentacoordinated complex $VOCl_3(IMes)$ (IMes = 1,3-dimesitylimidazol-2-ylidene), in which the

vicinity of the equatorial and axial ligands should not be ascribable to steric reasons.[384]

Starting from this premise, the Nb–C bonds in compounds **13a-b** were theoretically analysed by employing the Natural Orbitals for Chemical Valence-Charge Displacement (NOCV-CD)[391] approach and the Natural Bond Orbital (NBO)[392] method to calculate atomic charges, orbital populations and orbital-orbital interactions. The theoretical analysis confirmed and quantified the presence of X → L and M → L interactions (L = CNXyl): despite the lengthening of the triple bond being due to the high polarization effect of the metallic fragment, the isocyanide accepts a non-negligible amount of electronic density (calculations on **13a** are represented in Figure 76). Different contributions to this back-donation can be identified: the electron density is partially deriving from the Cl_{cis} → CNXyl direct interligand interaction (component **B** in Figure 76),[387] from a standard M → L back-donation (component **C**), and finally from a third type of back-donation, whose electronic flux starts from Cl_{trans}, passes through the d_{yz} orbital of the metal and ends up on the π^* orbital of CNXyl (component **D**).
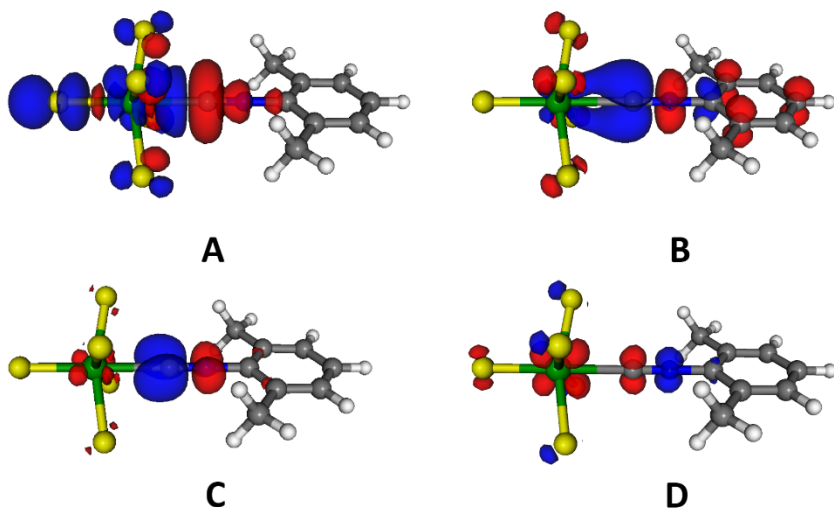
Figure 76. Isodensity surfaces (±0.0010 e/au) for the most relevant bonding components in **13a**. Accumulation regions: blue; depletion regions: red. A) Nb ← CNXyl σ-donation; B) Cl_{cis} → CNXyl interligand interaction; C) Nb→ CNXyl π-back-donation; D) Cl_{trans} → Nb→ CNXyl back-donation.

Further theoretical analyses on **13b** and other two non-synthesized complexes, i.e. $[NbF_5(CNXyl)]$ and $[NbI_5(CNXyl)]$, revealed that the amount of back-donation increases with the increase of the atomic weight of the halide, possibly assuming a more relevant role in the stabilization of the heavier complexes. However, this trend is apparently in conflict with the experimental data for **13a-b** (i.e. solid-state IR spectra, crystal structures): while a shortening of the C–N bond lengths is occurring in both complexes, the C–N bond length in **13b** is considerably shorter than that in **13a**. In both complexes, the polarization overcomes the back-donation,[393] but to different extents, as the CNXyl ligand in **13b** receives, in fact, less back-donation (contrary to the theoretical prediction). The explanation to this effect stems from the crystal packings (Figure 77): in fact, in **13b**, the bromine in *trans* position with respect to CNXyl, Br_{trans}, is involved in

108

intermolecular short contacts with the Br$_{trans}$ of other two molecules of **13b** (Br$_{trans}$–Br$_{trans}$ = 3.626 Å). This interaction is not present in **13a**, in which the Cl$_{trans}$ are not involved in any short contacts.
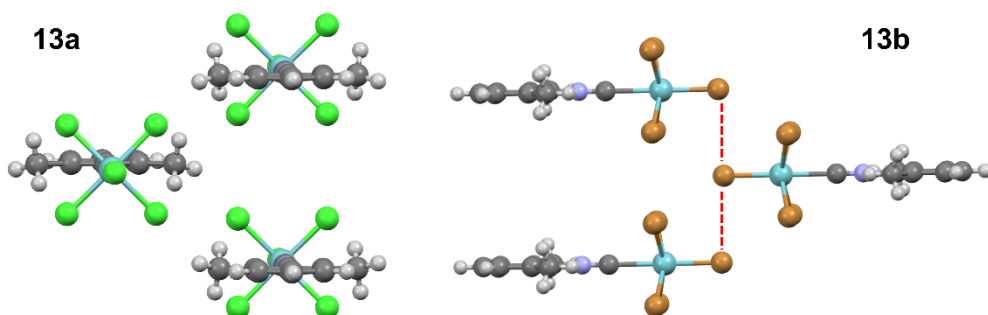
Figure 77. Crystal packings for **13a** and **13b**. Short contact between Br$_{trans}$ is highlighted (red dashed line).

As mentioned above, the lone pairs of X$_{trans}$ are involved in the back-donation (component **D**, Figure 76). Therefore, if in the solid state the Br$_{trans}$ of **13b** is involved in other interactions, it will contribute to the back-bonding to a lesser extent, resulting in a shortening of the C–N bond. On the other hand, considering a single, isolated molecule (i.e. the theoretical scenario), the lone pairs of Br$_{trans}$ would be available for the back-donation, and cause a lengthening of the C–N bond in **13b**, analogous to what observed in **13a**.

3.6. Reactions of HVMH with α-Phenylcinnamic Acid

Having found unusual behaviour arising from the interactions of HVMH with different classes of organic substrates with unsaturated C–N moieties, we were convinced that interesting reactivity could also be observed with molecules bearing unsaturated C–O bonds. Oxygen-containing organic species are often the object of investigation when very oxophilic high valent metal halides are considered (see Section 1.2), but, among this category, carboxylic acids have received relatively less attention, despite being key functional groups in organic chemistry. It is documented that NbF_5 forms coordination adducts with carboxylic acids, while the latter, by interaction with $NbCl_5$, undergo release of HCl, resulting in the formation of metal carboxylates, i.e. a typical behaviour for transition metal chlorides (see Section 1.2.1). Instead, group 6 metal chlorides promote Cl/O exchange in simple carboxylic acids, affording the corresponding acyl chlorides (Section 1.2.2). However, much less is reported in the literature about the interaction of HVMH with more complex carboxylic acids (and their corresponding acyl chlorides), i.e. bearing additional, adjacent functionalities.

We found out that a commercially available α,β-unsaturated carboxylic acid, i.e. α-phenylcinnamic acid (PhCH=CPhCOOH), undergoes one-pot, cascade reactions directed by high valent metal halides, and is finally converted into different polycyclic compounds, featured by local structural differences depending on the nature of the metal halide system.[394]

110

α-Phenylcinnamoyl chloride, PhCH=CPhCOCl, was obtained from PhCH=CPhCOOH by room temperature treatment with PCl$_5$, and then allowed to react with NbF$_5$ in chloroform at reflux temperature. Colour change evidenced a progressive conversion of the organic reactant. Subsequent water treatment and chromatographic separation allowed for the recovery, in moderate yield, of the polycyclic compound **14** (Figure 78).
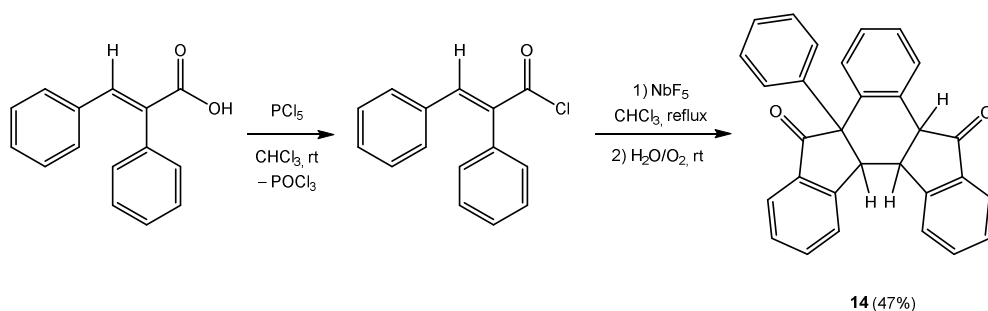
Figure 78. Conversion of α-phenylcinnamic acid into polycyclic compound **14**, mediated by the PCl$_5$/NbF$_5$ system.

The solid-state IR spectrum of **14** features a single, broad signal in the carbonyl range (1713 cm^{-1}), accounting for both C=O groups. Although not novel,[395] **14** has not been crystallographically characterized previously: the molecular structure, obtained by single crystal X-ray diffraction, is shown in Figure 79 (selected bond lengths and angles are in Table 8). Despite being a chiral molecule, the crystal structure represents a racemic mixture of the *SSSS* and *RRRR* enantiomers, crystallizing in the centrosymmetric space group P2$_1$/c. In CDCl$_3$ solution, a single set of ^{1}H NMR signals is observed, which could be ascribed to the aforementioned mixture of enantiomers.
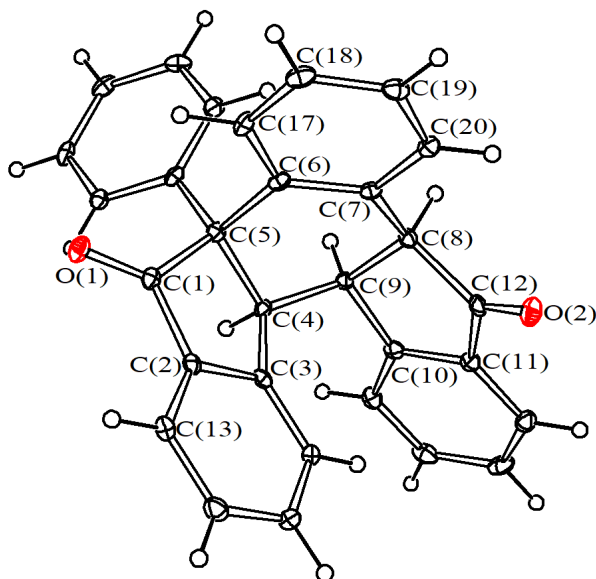
Figure 79. Molecular structure of **14** with key atoms labelled. Displacement ellipsoids are at the 30% probability level.

Table 8. Selected bond lengths (Å) and angles (deg) for **14**.

Bond Distances (Å)			
C(1)–O(1)	1.217(3)	C(12)–O(2)	1.210(3)
C(1)–C(2)	1.466(4)	C(1)–C(5)	1.546(4)
C(4)–C(5)	1.559(3)	C(4)–C(9)	1.534(3)
C(8)–C(9)	1.540(3)	C(8)–C(12)	1.532(3)
C(11)–C(12)	1.476(4)		
Angles (deg)			
C(1)–C(5)–C(6)	103.7(2)	C(4)–C(5)–C(6)	110.2(2)

Compound **14** was previously obtained in strongly Brønsted[395] or Lewis[396] acidic media, therefore we believed that NbF$_5$, as a Lewis acid, must play a crucial role along the reaction pathway. Moreover, no reaction was observed when PhCH=CPhCOCl was treated in the same conditions as those for the synthesis of **14** (i.e. refluxing chloroform, in the presence of POCl$_3$), but without the addition of NbF$_5$. In order to trace a plausible reaction pathway leading to **14**, we carried out a DFT study (Figure 80; detailed calculated intermediates are shown in Figure 121-Figure 126 in Section 5.11, pp. 219-221): an intramolecular Friedel-Crafts cyclization of PhCH=CPhCOCl (compound **A** in Figure 80) to 2-phenylindenone (**B**) *via* HCl release is a feasible first step ($\Delta G = -19.1$ kcal mol^{-1}). This is in agreement with the literature, as 2-phenylindenone was already reported to be a precursor for **14**.[395,396] 2-phenylindenone should then undergo dimerization through a *head-to-head* Diels-Alder cyclization in order to generate **C**: a possible transition state for this annulation step was preliminary determined without the presence of metal fragments (**TS** in Figure 80), but the activation barrier was found to be fairly high in energy (around 34 kcal/mol). This energy barrier was significantly lowered when NbF$_5$ was introduced into the model (to 28.1 kcal/mol when NbF$_5$ is coordinated to the diene, **TS-NbF$_5$-diene** in Figure 80; to 24.1 kcal/mol if NbF$_5$ interacts with the dienophile, **TS-NbF$_5$-dienophile**): the cycloaddition step is thus facilitated, enabling the access to **C**. The subsequent re-aromatization of the arene fragment, occurring *via* hydrogen migration, yields **14**: this final, downhill step ($\Delta G = -26.5$ kcal/mol) is likely to represent the driving force for the entire process.
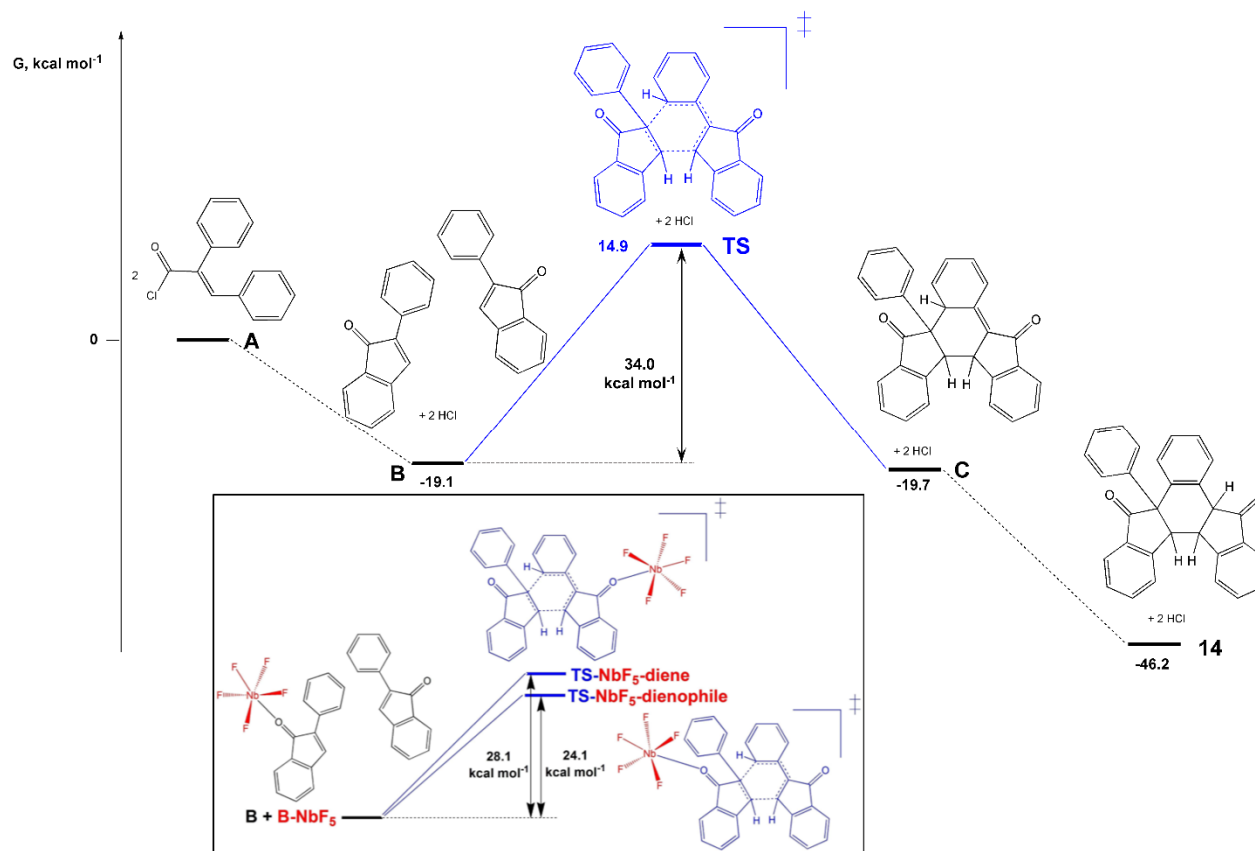
Figure 80. Relative Gibbs free energies of proposed intermediates for the conversion of α-phenylcinnamoyl chloride to **14**. C-PCM/ωB97X calculations, chloroform as continuous medium. Inset: effects of NbF_5 in the annulation step.

114

According to these DFT studies, NbF$_5$, as a Lewis acid, plays a pivotal role in the conversion of PhCH=CPhCOCl into **14**, i.e. by O-coordinating the carboxyl group of the diene/dienophile, allowing for the Diels-Alder annulation. Given the fact that WCl$_6$, other than being a Lewis acid, is also a good chlorinating agent, its direct interaction with the carboxylic acid, PhCH=CPhCOOH, was evaluated for the synthesis of **14**. Being employed as a sole reagent, WCl$_6$ would exploit a) its chlorinating ability in a *in situ* Cl/O exchange with PhCH=CPhCOOH, to afford PhCH=CPhCOCl, and then b) its Lewis acidity, to promote the same conversion obtained with NbF$_5$. As a further advantage, one equivalent of WCl$_6$ could, in principle, act as a chlorinating agent towards two equivalents of acid, the former being converted into the stable WO$_2$Cl$_2$.[397,398] Thus, by adopting the same conditions employed for the NbF$_5$-promoted cyclization, the reaction of PhCH=CPhCOOH with WCl$_6$ was carried out in a 2:1 molar ratio. However, the subsequent hydrolytic treatment, in the presence of air, and chromatographic purification did not lead to the isolation of **14**. Instead, the related polycyclic products **15** (in 51% yield) and **16** (13%) were obtained (Figure 81).
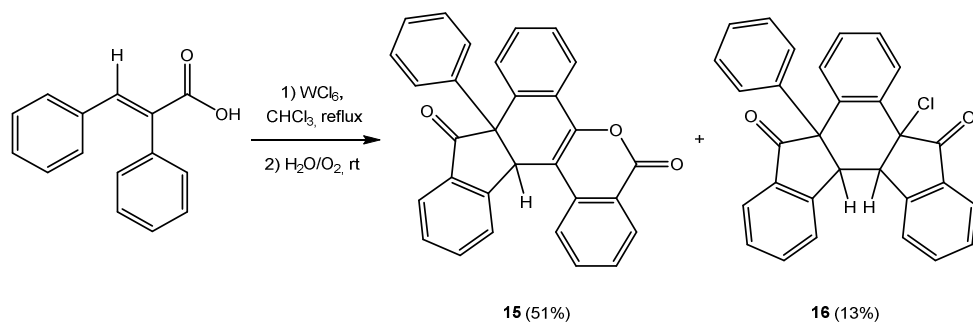
Figure 81. WCl$_6$-promoted conversion of α-phenylcinnamic acid into polycyclic compounds **15** and **16**.

The final outcome was not substantially affected when the reaction was performed in a 1:1 molar ratio. The identity of **15** and **16** was ascertained by IR and NMR spectroscopy, and by X-ray diffraction analyses on single crystals. The solid-state IR spectrum of **15** featured an intense, broad band accounting for the carbonyl group (at 1712 cm^{-1}) and a medium absorption (1646 cm^{-1}) ascribable to the non-aromatic, alkenyl moiety. The carbonyls in **16** gave rise to two intense absorption bands, at 1732 and 1713 cm^{-1}. Diagnostic signals were detected in the ^{1}H NMR spectra of both compounds: the spectrum of **15** is characterized by a singlet at 4.95 ppm, accounting for the unique non-aromatic proton; in **16**, instead, the two adjacent C_{sp3}–H generate doublet resonances at 4.47 and 4.36 ppm ($^3J_{HH}$ = 6.7 Hz). While the molecular structure of **15** has already been reported in the literature,[399] the published structure was measured at room temperature: a low temperature (–170°C) acquisition is reported for completeness sake in Section 5.10, Figure 102, with relevant bonding parameters are given in Table 24 (p. 199). Instead, the crystallographic characterization of **16** is unprecedented: a view of the structure is shown in Figure 82 (selected bonds and angles in Table 9). Analogously to **14**, **15** and **16** feature, respectively, two and four chiral centres: their solid-state structures are racemic mixtures of *RS* and *SR* enantiomers (**15**) and of *SSRR* and *RRSS* enantiomers (**16**), crystallizing in the centrosymmetric space groups P2$_1$/c and P2$_1$/n, respectively.
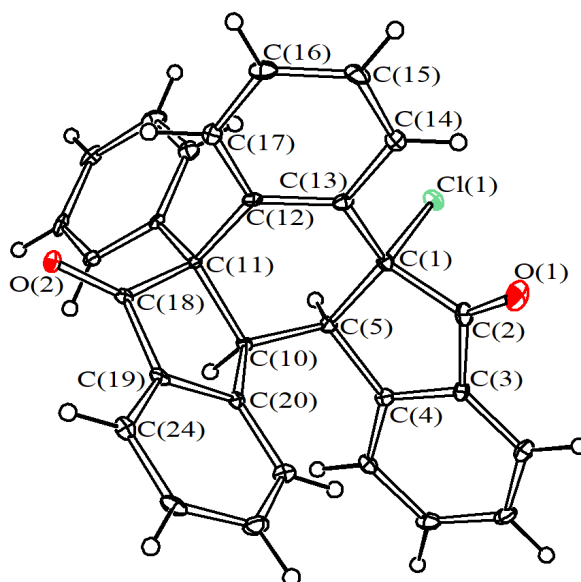
Figure 82. Molecular structure of **16** with key atoms labelled. Displacement ellipsoids are at the 30% probability level.

Table 9. Selected bond lengths (Å) and angles (deg) for **16**.

Bond Distances (Å)			
C(2)–O(1)	1.192(5)	C(18)–O(2)	1.213(5)
C(1)–Cl(1)	1.847(4)	C(1)–C(2)	1.552(6)
C(2)–C(3)	1.471(6)	C(10)–C(11)	1.556(5)
C(11)–C(12)	1.538(5)	C(11)–C(18)	1.548(5)
Angles (deg)			
C(12)–C(11)–C(18)	106.3(3)	C(12)–C(11)–C(10)	110.1(3)

Finally, the reactivity of PhCH=CPhCOOH with PCl$_5$/NbCl$_5$ (i.e. analogous to the PCl$_5$/NbF$_5$ system employed for the synthesis of **14**) was evaluated: the reaction turned out to be poorly selective, generating a complex mixture of products. Among these, instrumental techniques (ESI-MS, ^{1}H NMR) allowed for the identification of the polycycles **15** and **17**, which could be isolated only in low yields, after work-up (Figure 83). Compound **17** (phenylcinnamalone) and substituted derivatives have been previously obtained from PhCH=CPhCOCl only under solvent-free, harsh conditions.[399,400]
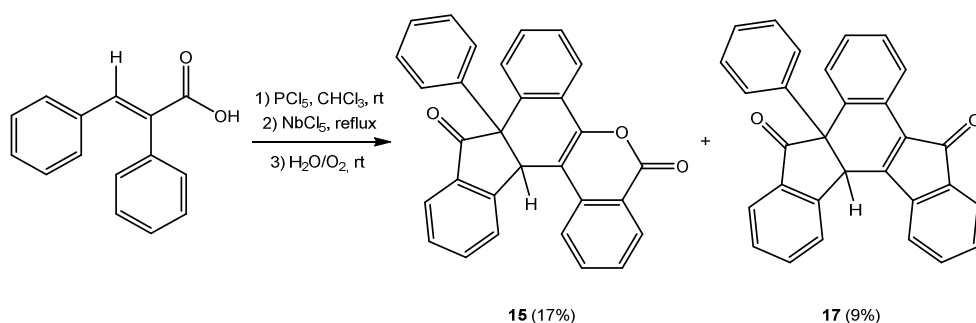
Figure 83. PCl$_5$/NbCl$_5$-promoted cyclization of α-phenylcinnamic acid into products **15** and **17**.

Products **15**, **16** and **17** bear striking similarities to **14**, and it could be supposed that **14** is indeed a common precursor to all three. Product **17** could be envisaged as the result of the dehydrogenation of **14**, possibly occurring in the oxidative, aerobic environment during the water treatment.[399] Hydrochlorination of the newly formed double bond can occur, to yield **16**. HCl is generated during the formation of **14**, see Figure 80; moreover, it would also be present in the hydrolytic mixture as a consequence of the degradation of WCl$_6$. Finally, **15** appears to be the product of a Baeyer-Villiger type lactonization, perpetrated by hydroperoxide species possibly generated during the

dehydrogenation step in the presence of O_2.[399,401,402] To verify this hypothesis, the hydrolytic treatment of the WCl_6/PhCH=CPhCOOH reaction mixture was repeated under rigorous exclusion of O_2 (degassed water, N_2 atmosphere): only **14** was detected in the reaction mixture, together with minor products not including **15-17**.

It can be then concluded that WCl_6 can convert PhCH=CPhCOOH into **15** as a consequence of a cascade process, involving Cl/O exchange to generate PhCH=CPhCOCl, formation of **14** (presumably through a similar pathway to that described in Figure 80), and final lactonization to **15**. This latter process could not be promoted by niobium derivatives, probably due to their insufficient oxidation potential in this environment. Moreover, this Baeyer-Villiger type oxidation appears to occur at room temperature, promoted by aqueous tungsten species, and exploiting air as the external oxygen source. This set of conditions is quite unusual: although in some procedures a Baeyer-Villiger lactonization has been carried out at room temperature employing O_2 and aldehydes as external sources,[403,404] drastic conditions (120° C, in the presence of indium-based catalysts) are usually required for the lactonization of derivatives of **14**.[399]

Attempts to unambiguously identify the tungsten species formed upon hydrolytic treatment have been unsuccessful: WCl_6 is expected to release the chloride ligands (as HCl) upon water treatment,[405,406] and polynuclear tungstates are reported to form at acidic pH values.[407] Indeed, alkaline environment did inhibit the lactonization reaction: no traces of **15** were detected when the hydrolytic treatment of the

WCl$_6$/PhCH=CPhCOOH mixture was performed with a diluted NaHCO$_3$ water solution.

It has to be pointed out that the reactivity of α-phenylcinnamic acid with high valent metal halides is somewhat unique: differently substituted α,β-unsaturated carboxylic acids were also investigated under analogous conditions, by treating them with WCl$_6$. However, these reactions did not proceed any further than the Cl/O exchange, all providing the corresponding acyl chlorides (see Section 5.7), the only exception being tetrolic acid (2-butynoic acid, MeC≡CCOOH), which underwent hydrochlorination of the C≡C bond, to afford MeC(Cl)=CHCOOH, **18** in 72% yield (Figure 84).

18 (72%)
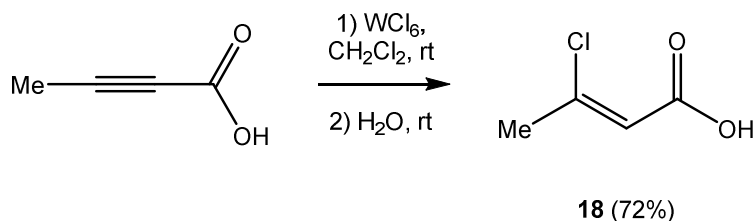
Figure 84. Hydrochlorination of MeC≡CCOOH to MeC(Cl)=CHCOOH mediated by WCl$_6$.

Product **18** has been characterized both spectroscopically and by single crystal X-ray diffraction. A view of the molecular structure is given in Figure 103, with relevant bonding parameters reported in Table 25 (see Section 5.10, p. 200).

3.7. Reactions of HVMH with α-Phenylacetic Acids

In the framework of our investigation on the interactions of HVMH with carboxylic acids bearing additional, adjacent functionalities, we have observed that a unique chemistry is enabled by the presence of at least one phenyl substituent in the α-position to the carboxyl group: by reaction with HVMH at room temperature in dichloromethane, a series of tertiary α-phenyl carboxylic acids was preliminarily converted into the corresponding acyl halides, and then underwent further transformation, accompanied by the release of carbon monoxide.

While not as frequently observed as the more common decarboxylation,[408–410] the decarbonylation reaction is a known transformation for carboxylic acids, and it has been previously exploited to access valuable alkenes[411–413] and C–C coupling products.[414,415] These reactions usually require harsh conditions (150-300 °C), and rely on precious, low valent transition metal compounds as catalysts. When no other additives are involved, the process is believed to proceed through metal-carboxylate intermediates,[416,417] as it was reported for the gas-phase decarbonylation of a palladium-acetate complex upon thermal decomposition.[418] Acyl chlorides have been reported to undergo metal-mediated decarbonylation as well,[419] proceeding upon thermal treatment *via* an oxidative addition mechanism.[410,420]

Initially, triphenylacetic acid, Ph$_3$CCOOH, was treated with equimolar amounts of WCl$_6$. The room temperature reaction in dichloromethane generated the trityl salt [Ph$_3$C][WOCl$_5$], **19**, and trityl chloride, Ph$_3$CCl,

20, in a 1:2 molar ratio according to the ^{1}H NMR analysis (Figure 85). Evolution of carbon monoxide was detected and estimated by GC analysis.
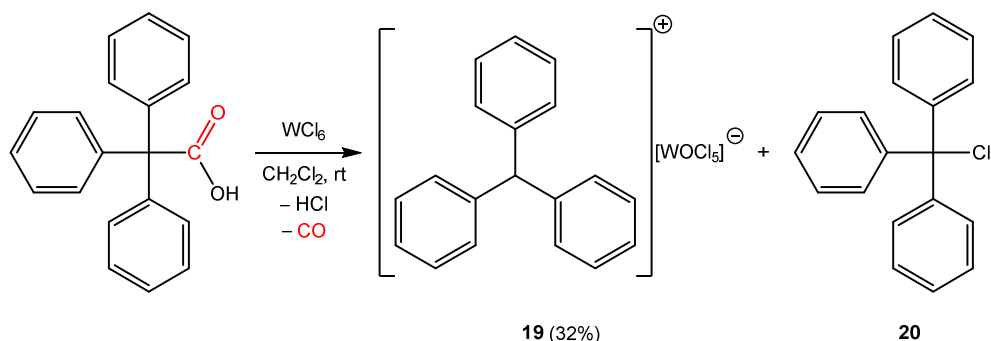
Figure 85. WCl$_6$-mediated room temperature release of carbon monoxide from triphenylacetic acid, affording **19** and **20**.

To the best of our knowledge, the room temperature release of CO *via* carbocation formation from triphenylacetic acid, and, more in general, from tertiary carboxylic acids, is unprecedented.[421]

After work-up, it was possible to retrieve **19** in 32% yield, which was characterized by analytical and spectroscopic methods. The solid-state structure was also determined, by single crystal X-ray diffraction (Figure 86; selected bond lengths and angles in Table 10). In the solid state, the trityl salt **19** consists of an ionic packing of trityl cations, [Ph$_3$C]$^+$,[422–425] and [WOCl$_5$]$^-$ anions:[76] though the structure of this salt is unprecedented, both ions have already been documented in the literature as part of different salts, and here their bonding parameters are in agreement with previous reports.
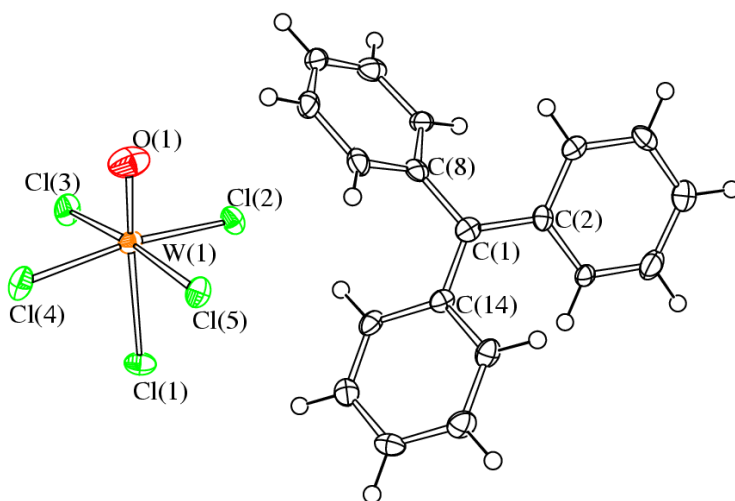
Figure 86. Molecular structure of [Ph$_3$C][WOCl$_5$], **19**, with key atoms labelled. Thermal ellipsoids are at the 50% probability level.

Table 10. Selected bond lengths (Å) and angles (deg) for **19**.

Bond Distances (Å)			
W(1)–O(1)	1.650(4)	W(1)–Cl(1)	2.4898(16)
W(1)–Cl(2)	2.3171(16)	W(1)–Cl(3)	2.3401(15)
W(1)–Cl(4)	2.3154(18)	W(1)–Cl(5)	2.3280(15)
C(1)–C(2)	1.445(9)	C(1)–C(8)	1.449(9)
C(1)–C(14)	1.443(9)		
Angles (deg)			
O(1)–W(1)–Cl(1)	173.91(17)	Cl(3)–W(1)-Cl(5)	172.86(6)
Cl(2)–W(1)-Cl(4)	170.21(6)	C(2)–C(1)–C(14)	121.1(6)
C(8)–C(1)–C(14)	118.8(6)	C(2)–C(1)–C(8)	120.0(6)

A plausible reaction pathway for the WCl$_6$-mediated decarbonylation of Ph$_3$CCOOH is proposed, on the basis of experimental evidence and DFT calculations (Figure 87; intermediates are shown in Figure 127-Figure 135 in Section 5.11, pp. 222-226). After an initial interaction between WCl$_6$ and Ph$_3$CCOOH *via* the carbonyl oxygen (intermediate **a** in Figure 87), chlorine transfer is viable (**b**): following formal elimination of HCl, generation of Ph$_3$CCOCl (**c**), along with WOCl$_4$, is highly favourable, and leads to a stationary point. The intermediate formation of Ph$_3$CCOCl was also experimentally verified by IR/NMR monitoring the WCl$_6$/Ph$_3$CCOOH reaction. Moreover, the reaction of WOCl$_4$ with freshly prepared Ph$_3$CCOCl (from Ph$_3$CCOOH and PCl$_5$) finally afforded a mixture of **19** and **20** (see Section 5.8). It should be noted here that, in the present case, the decarbonylation of Ph$_3$CCOCl cannot occur through the generally accepted and observed oxidative addition mechanism,[419] as the tungsten centre in WCl$_6$ (and WOCl$_4$) is already in its maximum oxidation state (+6). At this stage, the coordination of Ph$_3$CCOCl to WOCl$_4$ (intermediate **d**) would be slightly favourable from a thermodynamic point of view, but calculated equilibria involving **d** resulted to be unproductive. Instead, a chloride exchange between Ph$_3$CC(O)Cl and WOCl$_4$ (transition state **ts1**) may generate the salt [Ph$_3$CCO][WOCl$_5$] (**e**): the latter features an acylium ("oxocarbonium") cation, whose existence (and tendency to lose CO) was previously demonstrated by Olah.[426] Indeed, the decomposition of [Ph$_3$CCO]$^+$ to [Ph$_3$C]$^+$ and CO (intermediate **f**) would act as the driving force for the whole process. Finally, a chloride exchange in the resulting trityl salt **19** provides the way to trityl chloride, **20**, and WOCl$_4$ (**g**), which is in agreement with the experimental (NMR) observation.
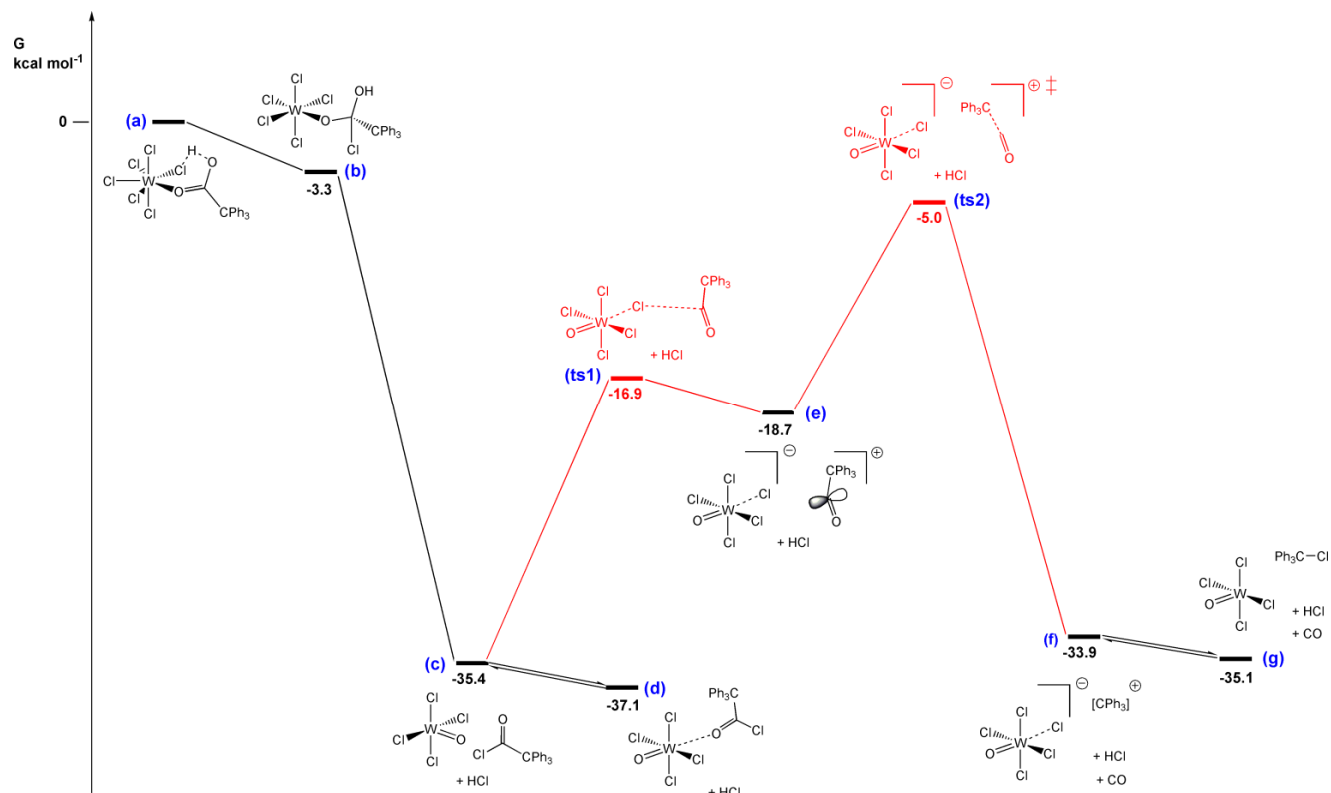
Figure 87. Relative Gibbs free energies of DFT-calculated intermediates along the reaction pathway for the conversion of WCl$_6$ and Ph$_3$CCOOH into [Ph$_3$C][WOCl$_5$], **19**, Ph$_3$CCl, **20**, and WOCl$_4$. Transition states in red. C-PCM/ωB97X calculations, dichloromethane as continuous medium.

Furthermore, the reactivity of Ph$_3$CCOOH was investigated with different HVMH as well, namely MoCl$_5$, WOCl$_4$, NbCl$_5$, and NbF$_5$. By carrying out the reactions under analogous conditions to those employed for the WCl$_6$/Ph$_3$CCOOH reaction (i.e. dichloromethane, ambient temperature), clean CO extrusion was detected (by gas chromatography), and different salts containing the trityl cation were obtained (Figure 88).[427]
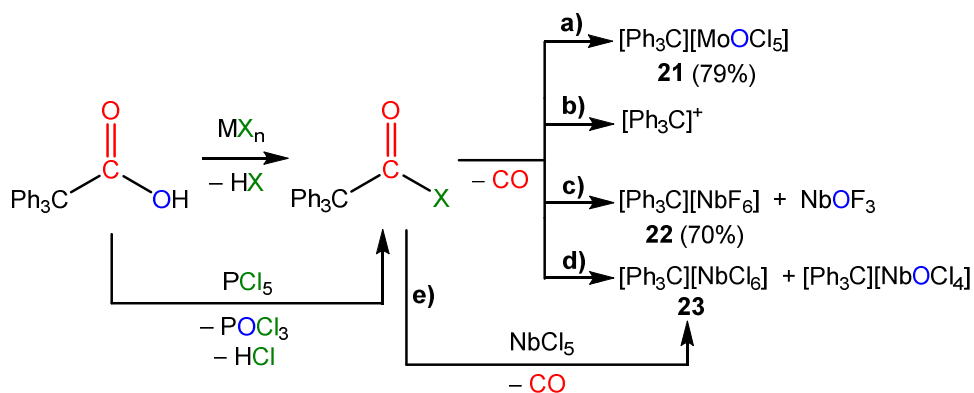
Figure 88. Decarbonylation of Ph$_3$COOH and Ph$_3$COCl by room temperature reactions with HVMH.
MX$_n$ = MoCl$_5$ (**a**); WOCl$_4$ (**b**); NbF$_5$ (**c**); NbCl$_5$ (**d**).

Presumably, these reactions proceed through a similar pattern to that described for the WCl$_6$/Ph$_3$CCOOH reaction: thus, the preliminary formation of Ph$_3$CCOX (X = Cl or F), resulting from X/O exchange between the organic substrate and the metal halide, is likely to precede the CO release step. Indeed, Ph$_3$CCOCl was detected in the reactions involving MoCl$_5$ and NbCl$_5$ (pathways **a** and **d** in Figure 88). Detection of the acyl fluoride derivative supposedly generated by NbF$_5$/Ph$_3$CCOOH (pathway **c**) was unsuccessful. However, it has to be mentioned that an elusive adduct between Ph$_3$CCOF and SbF$_5$ was described by Olah to promptly decarbonylate to [Ph$_3$C]$^+$.[428]

The MoCl$_5$/Ph$_3$CCOOH reaction led to the isolation, in good yield, of [Ph$_3$C][MoOCl$_4$], **21** (pathway **a**, Figure 88), which was characterized by elemental analysis, IR and NMR spectroscopy, and X-ray diffraction (Figure 89; relevant bonding parameters in Table 11). Bearing some similarities with **19**, the solid-state structure of **21** is constituted by an ionic packing of [Ph$_3$C]$^+$ cations and [MoOCl$_4$]$^-$ anions. The latter bears a square-pyramidal geometry, in agreement with various, previously reported [MoOCl$_4$]$^-$ salts.[67,429–431] The Mo–O bond distance is compatible with the double bond typical of an oxido ligand,[432,433] and this finds confirmation in the IR spectrum (ν = 993 cm^{-1}, Mo=O).[91,434,435] Although [MoOCl$_4$]$^-$ anions have also been reported to manifest in the solid state as dimeric {[MoOCl$_4$]$^-$}$_2$ units, infinite {[MoOCl$_4$]$^-$}$_\infty$ chains or weakly bound adducts (i.e. with a donor atom of the cation or a co-crystallized solvent molecule),[430,431] the one in **21** is an isolated, monomeric [MoOCl$_4$]$^-$ anion.
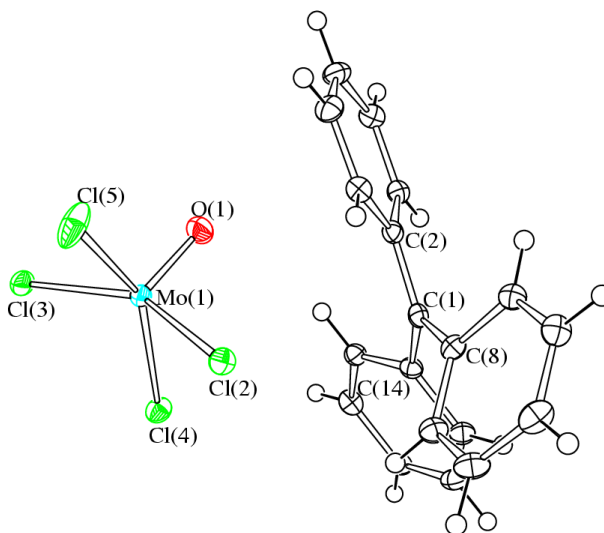
Figure 89. Molecular structure of [Ph$_3$C][MoOCl$_4$], **21**, with key atoms labelled. Thermal ellipsoids are at the 50% probability level.

Table 11. Selected bond lengths (Å) and angles (deg) for **21**.

Bond Distances (Å)			
Mo(1)–O(1)	1.6549(14)	Mo(1)–Cl(2)	2.3527(5)
Mo(1)–Cl(3)	2.3484(5)	Mo(1)–Cl(4)	2.3427(5)
Mo(1)–Cl(5)	2.3320(6)	C(1)–C(2)	1.444(2)
C(1)–C(8)	1.455(2)	C(1)–C(14)	1.442(2)
Angles (deg)			
O(1)–Mo(1)–Cl(2)	105.27(5)	O(1)–Mo(1)–Cl(3)	104.49(5)
O(1)–Mo(1)–Cl(4)	105.66(5)	O(1)–Mo(1)–Cl(5)	105.51(6)
Cl(2)–Mo(1)–Cl(3)	150.226(17)	Cl(4)–Mo(1)–Cl(5)	148.82(2)
C(2)–C(1)–C(8)	119.34(15)	C(2)–C(1)–C(14)	121.35(15)
C(8)–C(1)–C(14)	119.31(15)		

Instead, while the isolation of well-defined products from the WOCl$_4$/Ph$_3$CCOOH reaction (pathway **b**, Figure 88) was unsuccessful, ^{13}C NMR analysis of the reaction mixture allowed for the identification of the [Ph$_3$C]$^+$ cation, due to a diagnostic resonance at around 210 ppm.

The interaction of Ph$_3$CCOOH with niobium pentahalides, NbX$_5$ (X = F, Cl), yielded trityl salts **22-23**, together with the corresponding niobium oxido-halides, NbOX$_3$ (pathways **c-d**, Figure 88). These reactions appear to proceed with a 2:1 NbX$_5$/Ph$_3$CCOOH stoichiometry (Equation 3): presumably, one equivalent of the metal halide is consumed during the X/O exchange, while the other equivalent is entrapped in the anion.

128

$$2\ NbX_5\ +\ Ph_3CCOOH\ \longrightarrow\ [Ph_3C][NbX_6]\ +\ NbOX_3\ +\ HX\ +\ CO$$

Equation 3. NbX_5-promoted decarbonylation of Ph_3CCOOH (X = F, Cl).

After the NbF_5/Ph_3CCOOH reaction (pathway **c**, Figure 88), the separation of $NbOF_3$ (which was characterized by IR spectroscopy, ν = 995 cm^{-1}, Nb=O),[355,436] yielded $[Ph_3C][NbF_6]$, **22**. The latter was characterized by analytical and spectroscopic techniques, multinuclear NMR being crucial for the identification of the anion: a decet at 102 ppm in the ^{19}F spectrum confirmed the presence of $[NbF_6]^-$.[351,377,378,437] Furthermore, the solid-state structure of **22** was elucidated by single crystal X-ray diffraction, and found to consist of an ionic packing of previously described $[Ph_3C]^+$ cations and $[NbF_6]^-$ anions.[43,58,352] A view of the structure is shown in Figure 104, with selected bond lengths and angles reported in Table 27, in Section 5.10 (p. 202).

In the $NbCl_5/Ph_3CCOOH$ reaction (pathway **d**, Figure 88), ^{93}Nb NMR spectroscopy allowed for the detection of two different Nb(V) anions, $[NbCl_6]^-$ (δ = 8.8 ppm)[59,64,85,170,352] and $[NbOCl_4]^-$ (δ = −358 ppm, consistently with freshly prepared $[Bu_4N][NbOCl_4]$, see Section 5.8 for details). However, isolation of the corresponding trityl salts was not possible in this case. The IR spectrum of the solid residue suggested the presence of $NbOCl_3$ (ν = 780 cm^{-1}, Nb=O).[353] In order to cleanly obtain **23**, Ph_3CCOCl was prepared beforehand (from Ph_3CCOOH and PCl_5), and then allowed to react with $NbCl_5$ (pathway **e**, Figure 88).

Interestingly, the formation of the trityl cation $[Ph_3C]^+$ also occurred from the reactions of Ph_3CCOOH with titanium tetrahalides, TiX_4 (X =

F, Cl). While the ^{19}F NMR spectrum of TiF$_4$/Ph$_3$CCOOH displayed a complicated set of signals, the presence of the [Ph$_3$C]$^+$ cation was verified by the ^{13}C NMR spectrum, which featured the diagnostic carbocation signal (*ca.* 210 ppm). Instead, the crystalline salt [Ph$_3$C][Ti$_2$Cl$_8$(O$_2$CCPh$_3$)], **24**, was obtained in low yield from TiCl$_4$/Ph$_3$CCOOH. This outcome suggests a hybrid behaviour of TiCl$_4$ towards Ph$_3$CCOOH, the latter being partially converted into carboxylate and partially decarbonylated, in a non-selective reaction. Compound **24** was characterized by analytical and spectroscopic techniques, and single crystal X-ray diffraction. For a view of the structure (Figure 105) and relevant bonding parameters (Table 28), see Section 5.10 (p. 203).

Beside Ph$_3$CCOOH, several different tertiary α-phenyl carboxylic acids were investigated for their reactivity with HVMH. After room temperature interaction with WCl$_6$, CO evolution was detected (GC analysis) from EtPh$_2$CCOOH, MePh$_2$CCOOH, Me$_2$PhCCOOH, and Ph$_2$(BrCH$_2$CH$_2$)CCOOH, in variable amounts. Instead, no carbon monoxide was produced from Me$_3$CCOOH, even after prolonged thermal treatment.[75] In some of the above-mentioned cases, the isolation of organic derivatives was possible, after hydrolytic treatment and chromatographic purification.

From the interaction of WCl$_6$ with RMePhCCOOH, indanes (R = Ph, **25a**; R = Me = **25b**) were obtained in good yields (Figure 90). The organic products were characterized by means of analytical and spectroscopic techniques, and a crystal structure was obtained for **25a** (shown in Figure 106, Section 5.10, p. 206; relevant bonding parameters in Table 30)

130
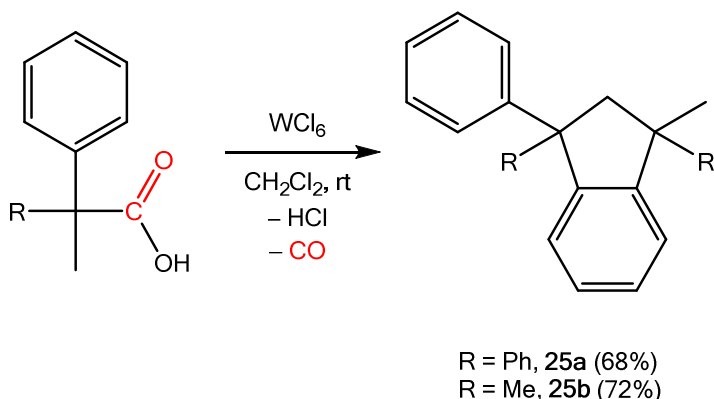
Figure 90. Synthesis of indanes **25a-b** from MePh$_2$CCOOH and Me$_2$PhCCOOH.

Analogously to the reactions involving Ph$_3$CCOOH, the generation of **25a-b** occurs after the preliminary formation of the acyl chlorides RMePhCCOCl, which was observed *via* NMR. Indeed, **25a** and **25b** could also be obtained by preparing the acyl chlorides with PCl$_5$, and then adding NbCl$_5$ *in situ*: this allowed for the isolation of the products in 88-97% yield. Oxido-chlorides WOCl$_4$ and NbOCl$_3$ instead were found to be less efficient in the generation of **25a-b** (see Section 5.8). Indanes were previously reported to be accessible from styrenes through acid catalysis in harsh conditions,[438] or as dimerization products of cyclobutenes (in turn obtained *via* Au(I)-catalysed cycloadditions).[439]

Moreover, 1,1-diphenylpropene, **26**, was obtained in 62% yield from the WCl$_6$/EtPh$_2$CCOOH reaction system (Figure 91), and characterized by elemental analysis and IR/NMR spectroscopy. As for the previous cases, NMR analysis of the reaction mixture indicated the presence of EtPh$_2$CCOCl.
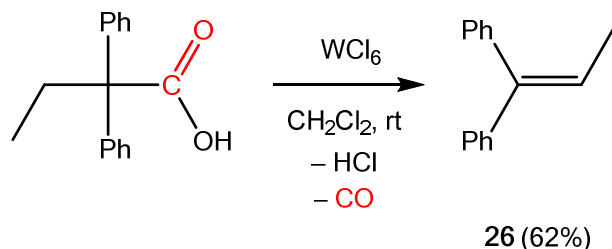
Figure 91. Room temperature decarbonylation of EtPh$_2$CCOOH mediated by WCl$_6$, yielding 1,1-diphenylpropene, **26**.

Given the involvement of acyl chloride intermediates, the formation of **25a-b** and **26** is likely to occur *via* tertiary carbocation intermediates, [RR'PhC]$^+$, generated after decarbonylation of RR'PhCCOCl (R = Me, R' = Ph, for **25a**; R = R' = Me, **25b**; R = Ph; R' = Et, **26**). Unlike the stable trityl cation [Ph$_3$C]$^+$, these reactive tertiary carbocations are prone to intra- and intermolecular rearrangements: [Me$_2$PhC]$^+$ was found to undergo dimerization to **25b** at T > − 40 °C;[440] moreover, the equilibrium of [EtPh$_2$C]$^+$ with its deprotonated form **26** was previously documented.[441]

Tertiary carbocations [RR'PhC]$^+$, (R, R' = Me, Et, Ph) were generated in the past by various synthetic strategies: protonation of alkenes or alcohols in strongly acidic media;[442–446] photolysis of alkenes[447] or alcohols/ethers;[448,449] photoinduced C–C homolysis of dimeric precursors[450] or N$_2$ elimination from indazoles;[451] hydrogen[452] or chloride[453] abstraction from quaternary hydrocarbons. However, their generation from the room temperature decarbonylation of carboxylic acids is an unprecedented reaction pathway.

Presumably, the greater instability of primary/secondary carbocations is the explanation to why the decarbonylation reaction is only observed with tertiary carboxylic acids: in fact, when diphenylacetic

132

acid, Ph$_2$CHCOOH, was treated with NbCl$_5$ and WCl$_6$, the typical reactivity of metal chlorides with carboxylic acids was observed (*vide supra*), instead of the decarbonylation product. Thus, the Nb(V) carboxylate NbCl$_4$(O$_2$CCHPh$_2$), **27**, was isolated and characterized from the NbCl$_5$/Ph$_2$CHCOOH reaction system, following HCl release. Instead, the WCl$_6$/Ph$_2$CHCOOH combination led to the identification of Ph$_2$CHCOCl by NMR spectroscopy.

Finally, the presence of a leaving group on the carboxylic acid backbone inhibited the decarbonylation pathway, in favour of a different pathway: more precisely, the interaction between WCl$_6$ and 4-bromo-2,2-diphenylbutyric acid, Ph$_2$(BrCH$_2$CH$_2$)CCOOH, proceeded with release of HBr, and finally afforded the cyclization product **28** (Figure 92).
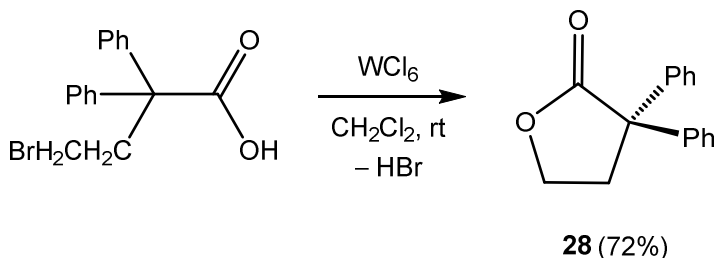
Figure 92. WCl$_6$-mediated synthesis of lactone **28** *via* HBr elimination from Ph$_2$(BrCH$_2$CH$_2$)CCOOH.

Lactone **28** was isolated in good yield after work-up, and characterized by IR (ν = 1762 cm^{-1}, C=O) and NMR spectroscopy (diagnostic ^{13}C NMR resonance at 177.8 ppm), as well as X-ray diffraction (molecular structure shown in Figure 107, with selected bond lengths and angles featured in Table 31, Section 5.10, p. 207).

4. Concluding Remarks

During this thesis work, the reactivity of high valent metal halides was evaluated with a selection of organic substrates bearing unsaturated C–N or C–O bonds.

The unexplored, direct interaction of high valent metal chlorides with N-aryl α-diimines (i.e. versatile and robust ligands, widely employed in coordination chemistry) has provided the unprecedented, intramolecular cyclization to quinoxalinium species, and a rare intermolecular rearrangement leading to imidazolium salts. Based on computational studies and experimental observations, these reactions appear to be promoted by the multitasking nature of high valent metal chlorides, exploiting both their chlorinating and their oxidizing behaviour. Indeed, stable coordination compounds can be obtained by quenching the activating power of high valent metal chlorides, either by introducing an oxido ligand (as in $NbOCl_3$), or replacing the chloride ligands with fluorides or bromides: these strategies inhibit activation routes, and provide unusual examples of structurally characterized coordination compounds of α-diimines with high valent metal halides. In particular, the stability of NbF_5 coordination compounds is presumably due to the presence of strong Nb–F bonds, disfavouring fluorine transfer, while the stabilization of MBr_5 (M = Nb, Ta) coordination compounds may be related to the relatively low oxidative power of these metal halides.

The synthesis and the structural characterization of the first examples of coordination complexes of niobium pentahalides with an isocyanide ligand have been described: the $NbX_5(CNXyl)$ complexes (X = Cl, Br)

feature a shorter C–N triple bond with respect to the non-coordinated CNXyl, as demonstrated by IR spectra and X-ray diffraction studies. Moreover, intramolecular contacts have been observed between the isocyanide carbon and the *cis* halide ligands. The two complexes have been also theoretically investigated by the NOCV-CD approach and the NBO analysis, in order to elucidate the nature of the Nb–C bond: while the shortening of the C–N triple bond is presumably related to the polarization effect by the metal fragment, the isocyanide ligand still appears to accept some back-donation, in the form of standard metal-to-ligand back-bonding, and also halide-to-ligand (interligand) direct interaction.

Carboxylic acids with additional, adjacent functionalities are shown to undergo unusual activation pathways when allowed to interact with high valent metal halides: α-phenylcinnamic acid (i.e. an α,β-unsaturated carboxylic acid) is converted into polycyclic derivatives as a result of a one-pot, domino reaction promoted by high valent metal halides. Local structural diversity was achieved by using different metal halide systems: in particular, WCl_6 appears to be able to exploit its variety of behaviours, by acting as a chlorinating agent towards the carboxylic acid moiety, and by enabling the subsequent transformations, including a final Baeyer Villiger lactonization, notably achieved exploiting air as oxygen source, in aqueous environment at room temperature.

Although the reactivity displayed by α-phenylcinnamic acid appeared to be rather unique among α,β-unsaturated carboxylic acid, the presence of a phenyl substituent in the α-position to the carboxyl

group is found to be crucial to the manifestation of unprecedented reactivity in a series of tertiary carboxylic acids: variably substituted α-phenylacetic acids underwent release of carbon monoxide at room temperature, as a consequence of a one-pot conversion into tertiary carbocations, *via* preliminary formation of the corresponding acyl halides. Tertiary carbocations may in turn be converted into stable hydrocarbons, according to their relative stability and characteristics: hence, Ph_3CCOOH was converted into the stable trityl carbocation, which formed isolable salts, while tertiary carboxylic acids with a lower number of α-phenyl substituents, generated less stable carbocations, which underwent further intra-/intermolecular rearrangements. Furthermore, the results suggest that secondary/primary carboxylic acids do not undergo CO release under the same conditions, possibly hinting that these substrates are unable to generate sufficiently stable carbocations. Moreover, some general character for this unusual reaction pathway was demonstrated, by extending the study to a series of homoleptic high valent halides: a minimum oxidation state of +5 for the metal centre seemed to be necessary in order to attain selective transformations.

In summary, the viability of all the transformations herein described appears to be related to the many peculiar features of high valent transition metal halides, being able to exploit their high Lewis acidity, halogenating power, oxidation potential, and ability to generate stabilizing counterions. It is noteworthy that different metal halides enable different reactivity patterns, with the nature of the M–X bond often playing a pivotal role in the determination of the outcome of the transformations.

5. Experimental Section

5.1. Materials and Methods
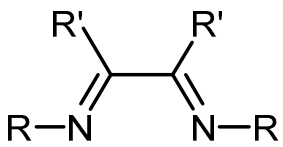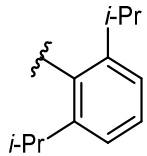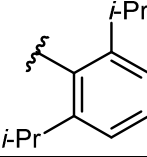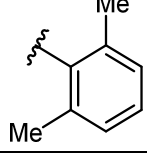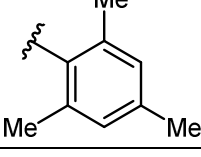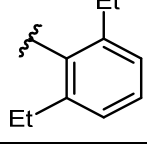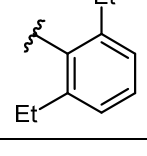
Warning! The metal reactants used in this work are highly moisture-sensitive; thus, rigorous anhydrous conditions were required for the reaction and isolation procedures. The reaction vessels were oven dried at 150 °C prior to use, evacuated (10^{-2} mmHg) and then filled with inert gas (Ar or N_2); standard Schlenk techniques were employed. NbF_5 (99.5%) was purchased from Apollo Sci., sublimed and stored under an argon atmosphere in sealed glass tubes. $NbCl_5$ (99+%), TaF_5 (99.5%), $TaCl_5$ (99.9%), WCl_6 (99.9%), $MoCl_5$ (99.9%), PCl_5 (98%), and $NOBF_4$ (97%) were purchased from Strem and stored under an argon atmosphere in sealed glass tubes. $NbOCl_3$ (from $NbCl_5$),[353] $WOCl_4$,[397] $NbBr_5$ and $TaBr_5$ (from MBr_5, M = Nb or Ta)[423] were prepared according to the literature. DAD_{Dipp}, $_{Me}DAD_{Dipp}$, DAD_{Xyl}, DAD_{Mes}, DAD_{tBu} and $_{Me}DAD_{Dep}$ were synthesized according to published procedures;[454–456] DAD_{Dep} was prepared by a slightly modified literature procedure.[457]

Other organic reactants were commercial products (Sigma Aldrich, TCI Europe) of the highest purity available, which were stored under a nitrogen atmosphere as received. Once isolated, all the metal products were stored under an inert atmosphere (Ar or N_2) in sealed glass tubes. Solvents (Sigma Aldrich) were distilled from appropriate drying agents before use. Deuterated solvents (98+%) were purchased from Cortecnet and stored under argon atmosphere as received. Infrared spectra were recorded at 298 K on a FT-IR Perkin Elmer spectrometer, equipped with an UATR sampling accessory.

NMR spectra were recorded at 298 K on a Bruker Avance II DRX400 instrument equipped with a BBFO broadband probe. The chemical shifts for ^{1}H and ^{13}C were referenced to TMS as an external reference; the chemical shifts for [93]Nb were referenced to external [NEt$_4$][NbCl$_6$]; the chemical shifts for ^{19}F were referenced to external CFCl$_3$. The NMR signals were assigned with the assistance of DEPT experiments and of ^{1}H, ^{13}C correlation measured through gs-HSQC and gs-HMBC experiments.[458] NMR signals due to a second isomeric form (where it has been possible to detect them) are italicized. EPR spectra were recorded at 298 K on a Varian (Palo Alto, CA, USA) E112 spectrometer operating at the X band, equipped with a Varian E257 temperature control unit and interfaced to an IPC 610/P566C industrial grade Advantech computer, using an acquisition board[459] and software package especially designed for EPR experiments.[460] Experimental EPR spectra were simulated by using the WINSIM 32 program.[461] Magnetic susceptibilities (reported per Mo atom) were measured at 298 K on solid samples using a Magway MSB Mk1 magnetic susceptibility balance (Sherwood Scientific Ltd). Diamagnetic corrections were introduced according to König.[462] Carbon, hydrogen and nitrogen analyses were performed on a Vario MICRO cube instrument (Elementar). Chloride and bromide were determined by the Mohr method[463] on solutions prepared by dissolution of the solid in aqueous KOH at boiling temperature, followed by cooling to room temperature and addition of HNO$_3$ up to neutralization. GC-MS analyses were performed on a HP6890 instrument, interfaced with an MSD-HP5973 detector and equipped with a Phenonex Zebron column. Mass spectra were obtained in positive ion scan mode on API 4000 instrument (SCIEX), equipped

with an Ionspray/APCI source. Gas chromatographic analyses were carried out on a Dani 3200 instrument, equipped with capillary column with molecular sieves (2m; 0.25in ID), using Ar at p = 1.5 atm as a gas carrier, at 50 °C.

Table 12. α-Diimines employed in the present work.

Name	R	R'
	R'—C(=N—R)—C(R')(=N—R)	
DADDipp	(*i*-Pr, *i*-Pr substituted phenyl)	H
Me**DAD**Dipp	(*i*-Pr, *i*-Pr substituted phenyl)	Me
DADXyl	(Me, Me substituted phenyl)	H
DADMes	(Me, Me, Me substituted phenyl)	H
DADDep	(Et, Et substituted phenyl)	H
Me**DAD**Dep	(Et, Et substituted phenyl)	Me
DADtBu	(*t*-Bu)	H

142

5.2. Reactions of WCl₆ with α-diimines.

Reactions of WCl₆ with DAD_Dipp and _Me_DAD_Dipp in dichloromethane. Synthesis and characterization of [{2,6-C₆H₃(CHMe₂)₂}N(CR')₂NCC(CHMe₂)(CH)₃C][WCl₆] (R' = H, 1a; R' = Me, 1b).

[{2,6-C₆H₃(CHMe₂)₂}N(CH)₂NCC(CHMe₂)(CH)₃C][WCl₆], 1a. WCl₆ (250 mg, 0.623 mmol) was added to a solution of DAD_Dipp (235 mg, 0.623 mmol) in CH₂Cl₂ (5 mL), and the resulting mixture was stirred at room temperature for 18 h. The final red solution was dried under vacuum. The dark red residue was washed with diethyl ether (2x20 mL), thus a dark red solution was separated from a brown/green solid. Elimination of the solvent from the solution gave a solid whose NMR analysis (in CDCl₃ solution) revealed the presence of **2a** (*vide infra*) as the prevalent species. The brown/green solid was washed with pentane (2x10 mL) and then dried under vacuum. Yield 273 mg, 60%. Dark red crystals suitable for X-ray analysis were collected by slow diffusion of hexane into a CH₂Cl₂ solution of **1a** stored at –30 °C. IR (solid state): ν = 3114w, 3091w, 3061w, 2965s, 2927m, 2868m, 1621m-s (C=N), 1590m (C=N), 1544w-m, 1507w-m, 1463vs, 1406w-m, 1387m-s, 1362s, 1319m-s-sh, 1261w-m, 1245w, 1214m-s, 1201m, 1182m-s, 1149m-s, 1093s-sh, 1059m-s-sh, 1041m, 990m-s, 967m, 935m, 867m, 799vs, 755vs, 737s, 700m-s, 668w-m, 656w-m cm⁻¹. ¹H NMR (CD₂Cl₂): δ = 10.09, 8.90 (br, 2 H, C1-H + C2-H); 8.28, 7.50 (m, 3 H, C4-H, C5-H, C6-H); 7.87 (t, 1 H, $^3J_{HH}$ = 7.6 Hz, C12-H); 7.63 (d, 2 H, $^3J_{HH}$ = 7.8 Hz, C11-H); 4.55, 4.31 (hept, 3 H, $^3J_{HH}$ = 6.7 Hz, C*H*Me₂); 1.61, 1.28, 1.11 ppm (d,18 H, $^3J_{HH}$ = 5.9 Hz, CH*Me*₂). ¹³C NMR (CD₂Cl₂): δ = 152.6, 151.1 (C3 + C8); 151.9, 151.4 (C1 + C2);

146.0, 143.6, 134.3, 117.3 (C7 + C9 + C10); 140.2, 133.9, 132.4, 126.4, 125.2 (*arom* CH); 29.7 (*C*HMe$_2$); 26.2, 24.3, 23.9 ppm (CH*Me$_2$*). NMR assignments refer to atom numbering in Chart 1.

[{2,6-C$_6$H$_3$(CHMe$_2$)$_2$}N(CMe)$_2$NCC(CHMe$_2$)(CH)$_3$C][WCl$_6$], 1b. This compound was obtained using a procedure analogous to that described for **1a**, from WCl$_6$ (240 mg, 0.605 mmol) and $_{Me}$DAD$_{Dipp}$ (246 mg, 0.608 mmol). Dark brown solid, yield 206 mg (45%). IR (solid state): ν = 2967m-s, 2929m, 2871w-m, 1673w, 1607m-sh (C=N), 1463m-s, 1442m-s, 1384m-s, 1367m-s, 1330m, 1260m-s, 1219w-m, 1199w-m, 1180m, 1144w-m, 1095m-s, 1057s, 985s-sh, 935m-br, 864m-br, 806vs-sh, 769s, 747s, 731m-s, 707m, 674m cm^{-1}.
^{1}H NMR (CDCl$_3$): δ = 8.03, 7.93, 7.85 (m, 3 H, C4-H, C5-H, C6-H); 7.61 (m, 3 H, C12-H, C11-H); 4.73, 4.52 (m, 3 H, C*H*Me$_2$); 3.34, 3.24 (m, 6 H, C1-*Me*, C2-Me); 1.54, 1.20, 1.11 ppm (m,18 H, CH*Me$_2$*). ^{13}C NMR (CDCl$_3$): δ = 176.1, 171.0 (C2 + C1); 143.0, 141.5 (C3 + C8); 138.8, 133.3, 129.4 (C4 + C5 + C6); 126.7, 124.9 (C11 + C12); 135.1, 131.7, 130.6, 127.8 (C7 + C9 + C10); 28.7, 28.1 (C1-Me + C2-Me); 27.4 (*C*HMe$_2$); 25.0, 24.1, 24.0 ppm (CH*Me$_2$*). NMR assignments refer to atom numbering in Chart 1.
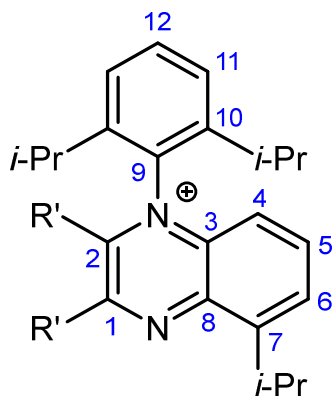
Chart 1. Structures of quinoxalinium cations **1a** (R' = H) and **1b** (R' = Me).

Reactions of WCl$_6$ with α-diimines: identification of organic products. *General procedure*: a mixture of WCl$_6$ (0.40 mmol) and α-diimine (0.40 mmol) was allowed to react in CD$_2$Cl$_2$ (1.5 mL) at room temperature for 36 h. Then the volatiles were distilled *in vacuo* and collected in a Schlenk tube frozen with liquid nitrogen. Benzene (0.40 mmol) was added to the colourless solution. An aliquot of the solution was analysed by NMR spectroscopy and GC-MS. Yields were determined by ^{1}H NMR using C$_6$H$_6$ as reference. From WCl$_6$ and DAD$_{Dipp}$: ClCH(Me)$_2$ (34.3%); from WCl$_6$ and $_{Me}$DAD$_{Dipp}$: ClCH(Me)$_2$ (24.7%); from WCl$_6$ and DAD$_{Xyl}$: ClCH$_3$ (1.0%); from WCl$_6$ and DAD$_{Mes}$: ClCH$_3$ (1.4%); from WCl$_6$ and DAD$_{Dep}$: ClCH$_2$CH$_3$ (4.8%).

Reactions of WCl$_6$ with DAD$_{Dipp}$ and DAD$_{Dep}$ in toluene: synthesis and characterization of WCl$_4$(DAD) (DAD = DAD$_{Dipp}$, 2a; DAD$_{Dep}$, 2b).

WCl$_4$(DAD$_{Dipp}$), 2a.[5] A solution of DAD$_{Dipp}$ (353 mg, 0.937 mmol) in toluene (10 mL) was added to WCl$_6$ (373 mg, 0.941 mmol), and the resulting mixture was allowed to stir at room temperature for 18 h. The volatiles from the final dark red solution were eliminated *in vacuo*. The residue was washed with pentane (10 mL), extracted with diethyl ether (2 x 25 mL) and dried *in vacuo*, thus affording a brown powder. Yield 383 mg, 60%. IR (solid state): ν = 3067w-br, 2966m-s, 2928m, 2870m, 1596br-m (C=N), 1508m, 1461s-sh, 1388m, 1358m-s-sh, 1330m, 1290w-m, 1257w-m, 1225w-m, 1213m, 1180m, 1165w-m, 1142w-m, 1094m-br, 1059m-s-sh, 1026w, 994w-m, 932s, 866m-s, 806vs-sh, 764s, 734s, 703w-m, 681w cm^{-1}. ^{1}H NMR (CDCl$_3$): δ = 7.44 (m, 4 H, *meta*-Ar-*H*); 7.20 (m, 2 H, *para*-Ar-*H*); 4.29 (m, 4 H, C*H*Me$_2$); 1.29 (m, 24 H, CH*Me$_2$*); 0.49 ppm (s, 2 H, C*H*=N). ^{13}C{^{1}H} NMR

145

(CDCl$_3$): δ = 152.4 (*ipso*-Ar); 150.5 (*ortho*-Ar); 149.6 (C=N); 129.4 (*para*-Ar); 124.7 (*meta*-Ar); 27.0 (*C*HMe$_2$), 23.0 ppm (CH*Me$_2$*).

WCl$_4$(DAD$_{Dep}$), 2b. The reaction of WCl$_6$ (255 mg, 0.643 mmol) with DAD$_{Dep}$ (207 mg, 0.646 mmol) was carried out by a procedure similar to that described for WCl$_6$/DAD$_{Dipp}$. Several X-ray quality crystals of **2b** were collected after slow diffusion of pentane into a toluene solution stored at –30 °C. Dark red solid. Yield 291 mg, 40%. IR (solid state): ν = 3084w-m, 2966m-s-br, 2933m, 2873m, 2854w-m, 1625w-m (*asymm* C=N), 1583w-m (*symm* C=N), 1483vs, 1457s, 1439m-s, 1413w-m, 1372m, 1326w-m-sh, 1263w-m, 1242w, 1221m, 1201m, 1172w-m, 1150m-s, 1108m, 1056w-m, 1034w-m, 991m, 973w-m, 940w-m, 901w-m, 868w-m, 813m-s, 802vs, 770vs, 754s, 695m cm^{-1}.
^{1}H NMR (CDCl$_3$): δ = 7.45 (m, 4 H, *meta*-Ar-*H*); 7.12 (m, 2 H, *para*-Ar-*H*); 2.48 (m, 8 H, CH$_2$); 1.30 (m, 12 H, CH$_3$); 0.2 ppm (s, 2 H, C*H*=N).

Reaction of DAD$_{Dipp}$ with PCl$_5$: synthesis of [2,6-C$_6$H$_3$(CHMe$_2$)$_2$]NCHC(Cl)N[2,6-C$_6$H$_3$(CHMe$_2$)$_2$].

A solution of DAD$_{Dipp}$ (180 mg, 0.48 mmol) in CD$_2$Cl$_2$ (3 mL) was treated with PCl$_5$ (100 mg, 0.48 mmol), and the resulting mixture was allowed to stir at room temperature for 18 h. An aliquot of the final red solution was analysed by NMR. The volatiles were removed from the solution under vacuum, affording an orange-red oil. IR (solid state): ν = 3065w, 2962s, 2929w-m, 2870w-m, 1641m-s (C=N), 1589w, 1521w, 1460m-s, 1436m, 1384m, 1363m, 1348w, 1328w-m, 1306w, 1257m-s, 1175m, 1148w-m, 1097m, 1060m-s, 1044m, 1019m, 968w-m, 931m, 909m, 885w, 819s, 796vs, 764vs, 732s, 702m, 687m cm^{-1}.
^{1}H NMR (CDCl$_3$): δ = 8.24 (s, 1 H, C*H*=N); 7.35, 7.32 (m, 6 H, Ar-*H*); 3.12, 2.95 (hept, 4 H, $^3J_{HH}$ = 6.7 Hz, C*H*Me$_2$); 1.38 ppm (m, 24 H,

Me). $^{13}C\{^1H\}$ NMR (CDCl$_3$): δ = 157.3 (H*C*=N); 147.0 (Cl*C*=N); 144.5, 143.2 (*ipso*-Ar); 136.7, 135.8 (*ortho*-Ar); 125.9, 125.6 (*para*-Ar); 123.4 (*meta*-Ar); 29.0, 28.4 (CH); 23.5, 23.2 ppm (Me). $^{31}P\{^1H\}$ NMR (CDCl$_3$): δ = 219.3 ppm (PCl$_3$).

Reaction of DAD$_{Dipp}$ with NOBF$_4$.

A solution of DAD$_{Dipp}$ (314 mg, 0.834 mmol) in CH$_2$Cl$_2$ (10 mL) was treated with NOBF$_4$ (95 mg, 0.813 mmol), and the resulting mixture was stirred at room temperature for 18 h. The final brown solution was dried under vacuum. NMR analysis of an aliquot of the residue (in CDCl$_3$ solution) indicated the formation of a complicated mixture of products. The resonances typical of the quinoxalinium cation contained in **1a** were not detected.

Reaction of WCl$_6$ with DAD$_{Xyl}$: synthesis of [(2,6-C$_6$H$_3$Me$_2$)NCHCHN(2,6-C$_6$H$_3$Me$_2$)CCHN(2,6-C$_6$H$_3$Me$_2$)][WCl$_6$], 3.

A solution of DAD$_{Xyl}$ (235 mg, 0.889 mmol) in CH$_2$Cl$_2$ (10 mL) was treated with WCl$_6$ (350 mg, 0.883 mmol), and the mixture was stirred at room temperature for 24 h. The resulting red solution was concentrated to ca. 2 mL, layered with hexane and stored at –30 °C. Thus, **3** was recovered as a microcrystalline solid after one week. Yield 334 mg, 47%. IR (solid state): ν = 2919w-br, 2864w, 1634w-sh, 1605m, 1580m, 1558w-m, 1536w-m, 1497m-s, 1470s, 1453m-s, 1379m, 1319w, 1222m, 1189m, 1168m-s, 1089vs, 1031s, 953w-m, 902w-m-sh, 797s, 772vs, 732s, 701m, 661w-m cm^{-1}. ^1H NMR (CD$_2$Cl$_2$): δ = 8.66 (s, 1 H, C13-H); 7.40 (s, 2 H, C2-H); 7.43, 7.13 (m, 3 H, C9-H + C10-H); 7.30, 6.92 (m, 6 H, C5-H + C6-H); 2.18 (s, 12 H, C11-H); 1.69 ppm (s, 6 H, C12-H). $^{13}C\{^1H\}$ NMR (CD$_2$Cl$_2$): δ = 147.7

(C7); 143.1 (C13); 137.4 (C1); 134.3, 129.1 (C5 + C6); 132.5, 132.3 (C3 + C4); 131.4, 128.3 (C9 + C10); 126.6, 126.2 (C8); 125.3 (C2); 19.7, 17.4 ppm (C11 + C12), see Chart 2 for atom numbering. Analogous reaction of DAD_{Xyl} with WCl_6 in CD_2Cl_2 gave a red solution which was analysed by NMR. Additional signals, except those of **3**, were clearly detected. ^1H NMR (CD_2Cl_2): δ = 3.43 ppm (s, 6 H). $^{13}C\{^1H\}$ NMR (CD_2Cl_2): δ = 144.6, 124.5, 16.3 ppm.
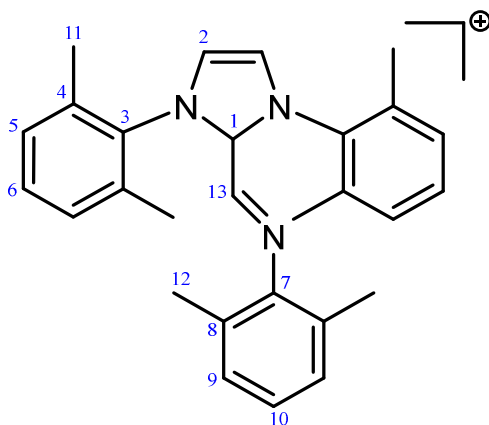
Chart 2. Structure of the imidazolium cation **3**.

Reaction of WCl_6 with $_{Me}DAD_{Dep}$: formation of [(2,6-$C_6H_3Et_2$)NH=CMeCMe=N($C_6H_2Et_2$Me)][WCl_6], 4. WCl_6 (108 mg, 0.271 mmol) was added to a solution of $_{Me}DAD_{Dep}$ (94 mg, 0.268 mmol) in CH_2Cl_2 (5 mL), and the resulting mixture was stirred at room temperature for 24 h. The final solution was layered with pentane and stored at −30 °C. A few violet, X-ray quality crystals of **4** were collected after 72 h.

148

5.3. Reactions of MCl₅ (M = Mo, Nb, Ta) with α-diimines.

Reactions of MoCl₅ with α-diimines: synthesis of [DAD(H)]₂[Mo₂Cl₁₀] (DAD = DAD_Dep, 5a; DAD_tBu, 5b)

[DAD_Dep(H)]₂[Mo₂Cl₁₀], 5a. MoCl₅ (332 mg, 1.22 mmol) and DAD_Dep (391 mg, 1.22 mmol) were added to CH₂Cl₂ (15 mL), and the resulting mixture was stirred for 18 h at room temperature. The final mixture was dried under reduced pressure, and the residue was washed with hexane (30 mL). A dark green solid was isolated. Yield 492 mg, 68%. Anal. Calcd. for $C_{22}H_{29}Cl_5MoN_2$: C, 44.43; H, 4.92; N, 4.71; Cl, 29.81. Found: C, 44.27; H, 4.78; N, 4.58; Cl, 29.70. IR (solid state): ν = 3251w (NH), 2936w, 2877w, 1586w-br (*symm* C=N), 1455w-m-sh, 1376w, 1165m-br, 1028s-br, 990s-br, 802m-sh cm⁻¹. Magnetic measurement: $\chi_M^{corr} = 2.23 \times 10^{-3}$ cgsu, μ_{eff} = 2.32 BM.

[DAD_tBu(H)]₂[Mo₂Cl₁₀], 5b. This compound was prepared using a procedure analogous to that described for the synthesis of **5a**, by allowing MoCl₅ (300 mg, 1.10 mmol) to react with DAD_tBu (187 mg, 1.12 mmol). Dark brown solid. Yield 380 mg, 78%. Anal. Calcd. for $C_{10}H_{21}Cl_5MoN_2$: C, 27.14; H, 4.78; N, 6.33; Cl, 40.06. Found: C, 27.23; H, 4.65; N, 6.44; Cl, 39.85. IR (solid state): ν = 3158w-br (NH), 3061w, 2979m, 2846w-m-br, 1667m (*asymm* C=N), 1599w-br (*symm* C=N), 1477m-s, 1429m, 1386m-s-sh, 1373m-s, 1341w, 1315w-sh, 1263m-s, 1237s, 1191s, 1097m-s, 1031vs-sh, 981vs, 930w, 894w-m, 876w, 861w-m, 803s-sh, 758w-m, 733w-m cm⁻¹. Magnetic measurement: $\chi_M^{corr} = 1.87 \times 10^{-3}$ cgsu, μ_{eff} = 2.13 BM.

Reactions of MCl$_5$ (M = Nb, Ta) with DAD$_{Dipp}$: formation and isolation of [{2,6-C$_6$H$_3$(CHMe$_2$)$_2$}N(CH)$_2$NCC(CHMe$_2$)(CH)$_3$C][NbCl$_6$], 6, NbCl$_4$(DAD$_{Dipp}$), 7, and [DAD$_{Dipp}$(H)][MCl$_6$] (M = Nb, 8a; M = Ta, 8b).
A solution of DAD$_{Dipp}$ (358 mg, 0.950 mmol) in CH$_2$Cl$_2$ (15 mL) was treated with NbCl$_5$ (255 mg, 0.925 mmol). A dark red solution formed in a few minutes, and this was allowed to stir for an additional 24 hours. Isopropyl chloride was detected in the mixture by GC-MS. The volatile materials were removed *in vacuo*. ^{93}Nb NMR analysis of the red-brown residue (in CDCl$_3$) suggested the presence of [NbCl$_6$]$^-$ as largely prevalent niobium species (δ = 7.8 ppm, $\Delta\nu\frac{1}{2}$ = 2·10^2 Hz). Crystallization of the residue from CH$_2$Cl$_2$/hexane at –30 °C afforded a mixture of red and yellow crystals, which were mechanically separated. X-ray diffraction on two single crystals allowed identification of **6** and **7** (see Section 5.10, Figure 96 and Figure 97). However, NMR analysis of the crystalline material revealed the presence of several species. When the reaction was performed in CCl$_4$ (10 mL) using analogous quantities of reactants, a red residue was recovered after elimination of the volatiles *in vacuo*. Crystallization of this residue from CH$_2$Cl$_2$/hexane at –30 °C afforded a few crystals of **6** and **8a**. The reaction of TaCl$_5$ (0.80 mmol) with DAD$_{Dipp}$ (0.80 mmol) in CCl$_4$ (10 mL) allowed to isolate a few crystals of **8b** after work up.

EPR analysis of the NbCl$_5$/DAD$_{Dipp}$ system. A suspension of NbCl$_5$ (0.4 mmol) in CH$_2$Cl$_2$ (2 mL) was cooled to –90 °C and then treated with DAD$_{Dipp}$ (0.4 mmol). An aliquot of the resulting mixture was analysed by EPR spectroscopy as a function of temperature and time.
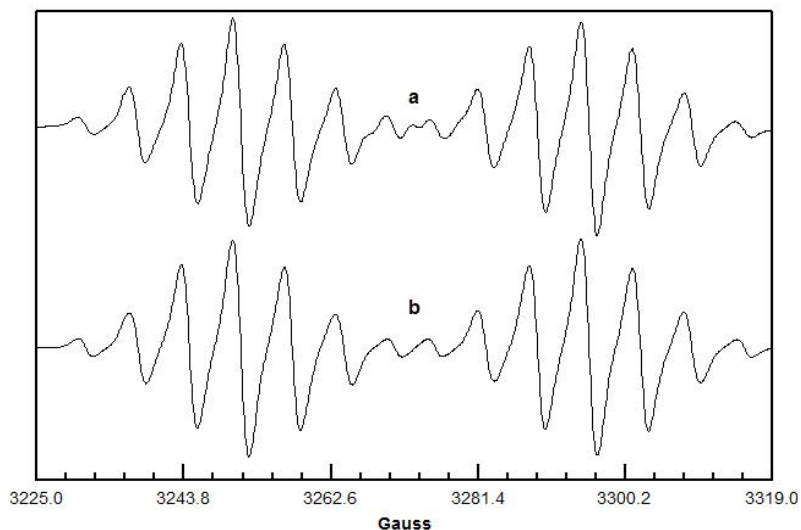
Figure 93. EPR spectrum of the $NbCl_5/DAD_{Dipp}$ mixture. **a**) Experimental spectrum (CH_2Cl_2, –60°C); **b**) calculated spectrum for a $[(CH_3)_2CCH(CH_3)_2]^\bullet$ radical.
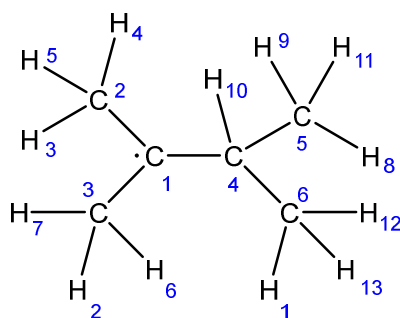
Chart 3. Structure of the $[(CH_3)_2CCH(CH_3)_2]^\bullet$ radical.

Table 13. Experimental and simulated hyperfine coupling constants. Numbering referred to **Chart 3**.

Set	Spin	Number	Coupling (G), exp.	Coupling (G), DFT
1	0.5	1 H	44.500	44.337 (H_{10})
2	0.5	3 H	6.810	7.300 (H_3 H_4 H_5)
3	0.5	3 H	6.360	7.300 (H_2 H_6 H_7)

151
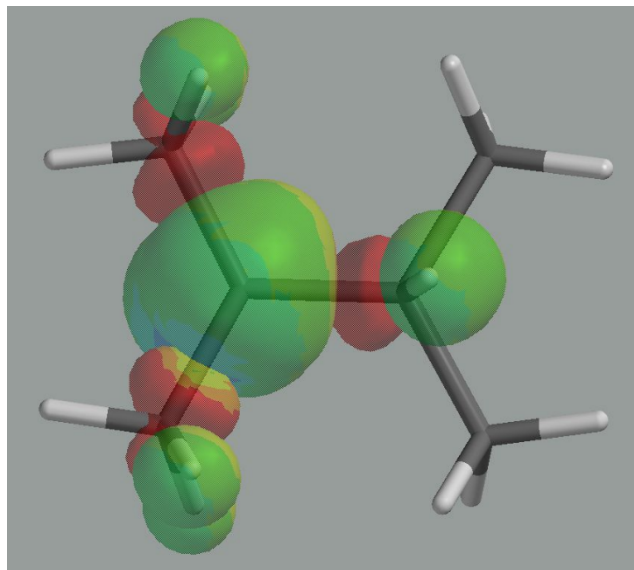
Figure 94. DFT-calculated spin density surface (0.002 electron/au^3) of the [(CH$_3$)$_2$CCH(CH$_3$)$_2$]$^{\bullet}$ radical at −60°C. Red: negative spin density; Green: positive spin density.

Reaction of NbCl$_5$ with DAD$_{Xyl}$: isolation of [(2,6-C$_6$H$_3$Me$_2$)NCHCHN(2,6-C$_6$H$_3$Me$_2$)CCHN(2,6-C$_6$H$_3$Me$_2$)][NbCl$_6$], 9.

A solution of DAD$_{Xyl}$ (148 mg, 0.560 mmol) in CH$_2$Cl$_2$ (15 mL) was treated with NbCl$_5$ (149 mg, 0.552 mmol). The mixture was allowed to react at room temperature for 18 h. The resulting solution was concentrated to ca. 3 mL, layered with hexane and stored at −30 °C. A few crystals of **9** suitable for X-ray analysis were recovered after one week. Yield 40 mg, 8%. IR (solid state): ν = 1631m (C=N) cm^{-1}. The reaction of NbCl$_5$ with DAD$_{Xyl}$ was repeated under analogous conditions but using CD$_2$Cl$_2$ as solvent. Subsequent NMR analysis of the reaction mixture indicated the formation of several products, including methyl chloride.

152

5.4. Synthesis and Characterization of Coordination Complexes with α-Diimines

Reactions of NbF₅ with α-diimines: synthesis of [NbF₄(DAD)₂][NbF₆] (DAD = DAD_Dipp, 10a; DAD_Xyl, 10b; DAD_Mes, 10c). *General procedure*: NbF₅ was added to a solution of the appropriate organic reactant in CH₂Cl₂ (5-10 mL). The mixture was stirred at room temperature for 24 h, then the solvent was removed *in vacuo*. The products were obtained as microcrystalline powders.

[NbF₄(DAD_Dipp)₂][NbF₆], 10a. Yellow-orange solid, 82% yield from NbF₅ (167 mg, 0.889 mmol) and DAD_Dipp (335 mg, 0.890 mmol). IR (solid state): ν = 3063w, 2974m-s, 2971m-s, 2931m, 2870w-m, 1626w (C=N), 1585w-m, 1460m-s-sh, 1386m-s, 1366m-s, 1353w-m, 1331w-m, 1305w, 1266m, 1174m-s, 1110m, 1097m, 1058m-s, 1044m, 942m, 925w, 905s, 839w-m, 799vs, 755vs, 737vs, 704w-m, 677w-m cm⁻¹. ¹H NMR (CD₃CN): δ = 8.34 (s, 2 H, CH=N); 7.31-7.24 (6 H, *arom* CH); 2.97 (m, 4 H, C*H*Me₂); 1.23, 1.06 ppm (d, ³J_HH = 6.85 Hz, 24 H, CH*Me₂*). ¹³C NMR{¹H} (CD₃CN): δ = 164.7 (CH=N), 144.9, 141.8, 128.9, 124.3 (*arom*); 28.2, 27.9 (*C*HMe₂); 24.7, 22.6 ppm (CH*Me₂*). ¹⁹F NMR (CD₃CN): δ = 156.1 (s, Δν½ = 21 Hz, NbF₄); 102.7 ppm (decet, ¹J_NbF = 338 Hz, NbF₆). ⁹³Nb NMR (CD₃CN): δ = 1555 ppm (hept, ¹J_NbF = 337 Hz, NbF₆).

[NbF₄(DAD_Xyl)₂][NbF₆], 10b. Dark-brown solid, 84% yield from NbF₅ (203 mg, 1.08 mmol) and DAD_Xyl (282 mg, 1.07 mmol). IR (solid state): ν = 3050w, 2965w, 2906vw, 1607m-br (C=N), 1539m, 1473s, 1384w, 1372w, 1322w, 1262m, 1179s, 1097m-s, 1030w, 940w, 894w-m, 838w, 810w-m, 776vs, 736w, 684w cm⁻¹. ¹H NMR (CD₃CN): δ = 8.45 (s, 2 H, CH=N); 7.31-7.13 (6 H, *arom* CH); 2.39, 2.06 ppm (s,

12 H, Me). ^{19}F NMR (CD$_3$CN): δ = 145.9 (s, Δν½ = 38 Hz, NbF$_4$); 101.7 ppm (decet, $^1J_{NbF}$ = 337 Hz, NbF$_6$). ^{93}Nb NMR (CD$_3$CN): δ = 1555 ppm (hept, $^1J_{NbF}$ = 337 Hz, NbF$_6$).

[NbF$_4$(DAD$_{Mes}$)$_2$][NbF$_6$], 10c. Orange solid, 91% yield from NbF$_5$ (188 mg, 1.00 mmol) and DAD$_{Mes}$ (294 mg, 1.01 mmol). IR (solid state): ν = 3037w-br, 2964w-m, 2918w-m, 2867w, 1654w, 1607m (C=N), 1475m-s-sh, 1365m-s-sh, 1319w, 1304w, 1262m, 1202s, 1143s, 1098m, 1038m-s, 1022m-s, 963w, 924m, 907w-m, 855vs, 801s, 721w-m, 678w-m cm^{-1}. ^{1}H NMR (CD$_3$CN): δ = 8.43 (s, 2 H, CH=N); 7.01 (4 H, *arom* CH); 2.34, 2.31, 2.02, 1.99 ppm (s, 18 H, Me). ^{19}F NMR (CD$_3$CN): δ = 144.4 (s, Δν½ = 24 Hz, NbF$_4$); 102.5 ppm (decet, $^1J_{NbF}$ = 339 Hz, NbF$_6$). ^{93}Nb NMR (CD$_3$CN): δ = 1555 ppm (hept, $^1J_{NbF}$ = 337 Hz, NbF$_6$).

Reaction of NbOCl$_3$ with DAD$_{Dipp}$: synthesis of NbOCl$_3$(DAD$_{Dipp}$), 11. A solution of DAD$_{Dipp}$ (298 mg, 0.791 mmol) in CH$_2$Cl$_2$ (8 mL) was treated with NbOCl$_3$ (171 mg, 0.794 mmol). The mixture was stirred at room temperature for 18 h. Then, the volatile materials were removed under reduced pressure, and the residue was washed with hexane (2 x 20 mL). Compound **11** was recovered as a light red solid. Yield 290 mg, 62%. Crystals suitable for X-ray analysis were obtained from a CH$_2$Cl$_2$ solution layered with pentane and stored at −30 °C. IR (solid state): ν = 3062w-br, 2965m-s, 2928w-m, 2869w-m, 1626w (C=N), 1586w, 1567w, 1465m-s, 1436w-m, 1384w-m, 1370m-s, 1330w-m, 1300w, 1262w-m, 1184w-m, 1166m, 1097m-s, 1058m-s, 1043m-s, 1014m, 960vs (Nb=O), 930m, 906m-s, 833m, 799s, 752s, 691w-m cm^{-1}. ^{1}H NMR (CD$_2$Cl$_2$): δ = 8.22 (s, 2 H, CH=N); 7.45-7.35 (6 H,

154

arom CH); 2.99 (m, 2 H, CHMe$_2$); 1.37, 1.17 ppm (m, 12 H, CHMe_2). ^{13}C NMR{^{1}H} (CD$_2$Cl$_2$): δ = 162.5 (C=N); 151.8 (*ipso*-CN); 143.0 (*arom* C-*ortho*); 129.5, 124.9 (*arom* CH); 29.1 (*C*HMe$_2$); 26.0, 23.4 ppm (CHMe_2). ^{93}Nb NMR (CD$_2$Cl$_2$): δ = 431 ppm (Δν½ = 2.9·10^3 Hz).

Reactions of MBr$_5$ with DAD$_{Dipp}$: isolation of [MBr$_4$(DAD$_{Dipp}$)][MBr$_6$] (M = Nb, 12a; M = Ta, 12b). *General procedure*: the metal bromide was added to a solution of DAD$_{Dipp}$ in CH$_2$Cl$_2$ (15 mL). The mixture was allowed to react for 18 h at room temperature. Then the volatile materials were removed, and the NMR analysis of the residue indicated the presence of a mixture of products. X-ray quality crystals of **12a-b** were obtained from CH$_2$Cl$_2$ solutions layered with hexane and stored at −30 °C for 48 h.

[NbBr$_4$(DAD$_{Dipp}$)][NbBr$_6$], 12a. Dark red crystals, 31% yield from NbBr$_5$ (273 mg, 0.555 mmol) and DAD$_{Dipp}$ (210 mg, 0.558 mmol). IR (solid state): ν = 3061w-br, 2965s, 2926m, 2867m, 1646w-br (C=N), 1622w-br (C=N), 1587w-m, 1562w-br, 1533w-br, 1507w-m, 1463s, 1426s, 1386m, 1363s, 1320m-sh, 1300w-m, 1263w-m, 1227w, 1214w, 1182w, 1155w-m-sh, 1095m, 1059m, 1044m, 959s, 936m, 904w-m, 867m, 798vs, 751vs, 690m cm^{-1}. ^{1}H NMR (CD$_3$CN): δ = 8.50 (s, 2 H, CH=N); 7.4-7.2 (6 H, *arom* CH); 2.84 (m, 4 H, CHMe$_2$); 1.20, 1.08 ppm (d, 24 H, CHMe_2). ^{93}Nb NMR (CD$_3$CN): δ = 735 (Δν½ = 1·10^2 Hz, NbBr$_6$⁻).

[TaBr$_4$(DAD$_{Dipp}$)][TaBr$_6$], 12b. Red crystals, 24% yield from TaBr$_5$ (350 mg, 0.603 mmol) and DAD$_{Dipp}$ (230 mg, 0.611 mmol). ^{1}H NMR (CD$_3$CN): δ = 8.45 (s, 2 H, CH=N); 7.4-7.2 (6 H, *arom* CH); 2.83 (m, 4 H, CHMe$_2$); 1.20, 1.08 ppm (d, 24 H, CHMe_2).

5.5. Reactions of NbX$_5$ (X = Cl, Br) with isocyanides.

Synthesis and characterization of [NbX$_5$(CNXyl)] (X = Cl, 13a; X = Br, 13b). *General procedure:* In a Schlenk tube, 2,6-dimethylphenylisocyanide (*ca.* 0.5 mmol) was dried under reduced pressure with P$_2$O$_5$ for 1 hour. The tube was then filled with N$_2$, and NbX$_5$ (*ca.* 0.5 mmol) and toluene (10 mL) were added. The yellow/orange mixture was allowed to stir at room temperature for 24 h. Afterwards, the precipitate was separated and washed with heptane (10 mL). The product was collected as a moisture-sensitive solid. Crystals suitable for X-ray diffraction analysis were obtained from a 1,2-dichloroethane (**13a**) or dichloromethane (**13b**) solution layered with hexane and settled aside at –30 °C.

[NbCl$_5$(CNXyl)], 13a. Dark yellow powder. Yield 105 mg (60%), from NbCl$_5$ (143 mg, 0.529 mmol) and CNXyl (70 mg, 0.533 mmol). Anal. Calcd. for C$_9$H$_9$Cl$_5$NNb: C, 26.93; H, 2.26; N, 3.49; Cl, 44.17. Found: C, 25.88; H, 2.22; N, 3.16; Cl, 44.70. IR (solid state): ν = 2958w, 2922w, 2221w-m (C≡N), 1587w-m, 1475w-m, 1383m, 1285w-m, 1264w-m, 1171w-m, 1083w-m, 989w-m, 870m-s, 839s, 806m-s, 787vs, 716m cm^{-1}. ^{1}H NMR (C$_6$D$_6$): δ = 6.60 (t, $^3J_{HH}$ = 7.66 Hz, 1 H, *para*-CH); 6.32 (d, $^3J_{HH}$ = 7.66 Hz, 2 H, *meta*-CH); 1.82 ppm (s,6 H, Me). ^{93}Nb NMR (C$_6$D$_6$): δ = –124 ppm (Δν½ = 426 Hz).

[NbBr$_5$(CNXyl)], 13b. Orange powder. Yield 309 mg (87%), from NbBr$_5$ (280 mg, 0.569 mmol) and CNXyl (75 mg, 0.57 mmol). Anal. Calcd. for C$_9$H$_9$Br$_5$NNb: C, 17.33; H, 1.45; N, 2.25; Br, 64.07. Found: C, 17.53; H, 1.51; N, 2.37; Br, 64.50. IR (solid state): ν = 2980w, 2948w, 2918w, 2209m-s (C≡N), 1968w, 1886w-m, 1803w, 1685w, 1587m-sh, 1496w, 1474m-s-sh, 1441w-m, 1380s, 1315w, 1301w-m,

156

1283m, 1263m-s, 1170m, 1082m-br, 986w-m, 806m-s, 784vs, 715w-m cm^{-1}. ^{1}H NMR (C$_6$D$_6$): δ = 6.61 (t, $^3J_{HH}$ = 7.79 Hz, 1 H, *para*-CH); 6.34 (d, $^3J_{HH}$ = 7.79 Hz, 2 H, *meta*-CH); 1.91 ppm (m,6 H, Me). ^{93}Nb NMR (C$_6$D$_6$): δ = 479 (Δν½ = 757 Hz).

Reaction of NbCl$_5$ with CNXyl in dichloromethane. A solution of 2,6-dimethylphenylisocyanide (52 mg, 0.392 mmol) in CD$_2$Cl$_2$ (4 mL) was cooled to ca. −30 °C and then treated with NbCl$_5$ (103 mg, 0.380 mmol). The mixture was stirred at −30 °C for 10 minutes. An aliquot of the resulting yellow solution was readily analysed by NMR at ambient temperature.^{1}H NMR (CD$_2$Cl$_2$): δ = 7.44, *7.39*, 7.27, *7.23* (m, *arom* CH); 2.56, *2.52* ppm (s, Me). ^{13}C NMR{^{1}H} (CD$_2$Cl$_2$): δ = 156.8 (C≡N); 137.5, 132.7, 129.4, 124.1, 122.1, 18.9 ppm (*arom* C). ^{93}Nb NMR (CD$_2$Cl$_2$): δ = 7 (s, Δν½ = 156 Hz, NbCl$_6$$^-$); −60 (s, Δν½ = 426 Hz, NbCl$_4$$^+$); −132 (s, Δν½ = 448 Hz, major).

In a different experiment, CNXyl (0.75 mmol) and NbCl$_5$ (0.75 mmol) were allowed to react in CH$_2$Cl$_2$ (15 mL) at room temperature for 24 hours. The volatiles were removed under vacuum and the residue was washed with hexane (30 mL), giving a green solid that was dried *under vacuum* at room temperature. IR (solid state): ν =3270w-br, 2964w, 2337w, 1652s, 1644vs, 1635vs, 1623vs, 1587m-s, 1521w-m-br, 1472m, 1445w-m, 1404w, 1481m, 1360m-br, 1338m, 1285w, 1261m, 1191w-br, 1170w, 1156w, 1088w-m-br, 1031w-m-br, 1015w-m, 992w, 939m-br, 849s-br, 807vs-br, 786vs, 772vs cm^{-1}. ^{1}H NMR (CD$_2$Cl$_2$): δ =7.41; 7.29-6.75; 3.81-3.74; 2.82; 2.60-1.92 ppm. ^{93}Nb NMR (CD$_2$Cl$_2$): no signals detected.

5.6. Reactions with α-Phenylcinnamic Acid.

Reaction of α-phenylcinnamic acid with PCl₅: synthesis and characterization of α-phenylcinnamoyl chloride, *cis*-PhCH=CPhCOCl (Chart 4).
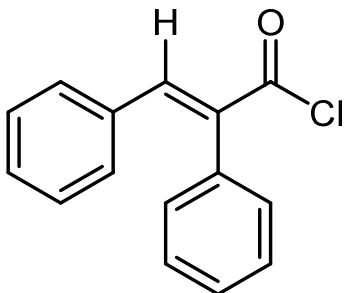
Chart 4. Structure of PhCH=CPhCOCl.

A solution of PhCH=CPhCOOH (113 mg, 0.503 mmol) in CDCl$_3$ (ca. 3 mL) was treated with PCl$_5$ (106 mg, 0.509 mmol) at ambient temperature. After 2 hours stirring, a colourless solution was obtained and analysed via NMR spectroscopy. The volatiles were removed under vacuum, and a colourless solid was recovered, corresponding to PhCH=CPhCOCl. IR (solid state): ν = 3057w, 3025w, 2987w, 2688w, 1737s (C=O), 1613m (C=C), 1592m, 1573w-m, 1492w-m, 1474w, 1445m, 1393w-br, 1314w, 1294w-m, 1215w-m, 1187m, 1159w, 1106w, 1083m, 1063s, 1051m-s, 1025m, 1000w-m, 972w, 935w-m, 916w, 893m, 854w-m, 797m-s, 750s, 708vs, 683vs cm^{-1}. ^{1}H NMR (CDCl$_3$): δ = 8.15 (s, 1H, C*H*=C); 7.45-7.10 ppm (10H, *arom* CH). ^{13}C NMR (CDCl$_3$): δ = 169.2 (C=O); 147.8 (*C*H=C); 136.2, 134.8, 133.5 (*ipso*-C + =*C*Ph–CO$_2$H); 131.4, 130.7, 129.8, 129.2, 128.8, 128.6 ppm (*arom* CH).

158

Synthesis and characterization of 5a-phenyl-14b,14c-dihydrobenzo[a]indeno[2,1-c]fluorene-5,10(5aH,9bH)-dione, 14 (Chart 5).
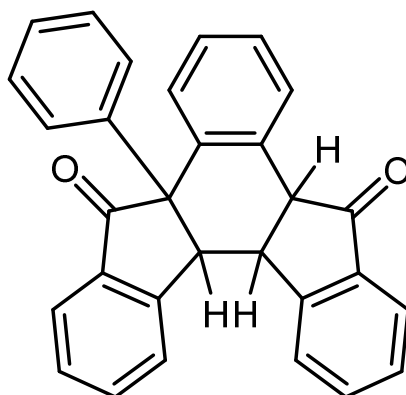
Chart 5. Structure of **14**.

A) From PhCH=CPhCOOH/PCl₅/NbF₅. A solution of PhCH=CPhCOCl in chloroform (10 mL), freshly prepared from PhCH=CPhCOOH (326 mg, 1.45 mmol) and PCl₅ (296 mg, 1.42 mmol), was treated with NbF₅ (267 mg, 1.42 mmol). The resulting mixture was refluxed for 72 hours. After cooling down to ambient temperature, H₂O (ca. 2 mL) was added, and the resulting mixture was stirred for 18 hours. The resulting brown mixture was filtered through alumina using diethyl ether/acetone (1:1 v/v) as eluent. Thus **14** was isolated as an orange solid after removal of the volatiles under vacuum. Yield: 193 mg, 47%. Pale-yellow crystals suitable for X-ray analysis were collected from a dichloromethane solution layered with hexane and stored at −30 °C. Anal. Calcd. for $C_{30}H_{20}O_2$: C, 87.35; H, 4.89. Found: C, 87.61; H, 4.64. IR (solid state): ν = 3058w, 3024w, 2899w, 2833w, 1982w, 1713vs-br (C=O), 1603m-s, 1494m, 1484m,

1468m-s, 1462m-s, 1444m-s, 1353w-m, 1315w-br, 1286m-s, 1269m, 1242w, 1224m-s, 1201m-s, 1180m, 1163w-m, 1154w-m, 1119m, 1110m, 1095w-m, 1084m, 1062w, 1047w, 1024m, 1005m, 974w, 958m, 934w, 917w-m, 898w-m, 883w, 865m, 850w, 837w-m, 822w-m, 793w, 769s, 758s, 751vs, 739m-s, 731m-s, 724m-s, 702vs, 684s cm^{-1}. ^{1}H NMR (CDCl$_3$): δ = 7.97 (d, J = 7.6 Hz, 1H, *arom*); 7.80 (t, J = 7.7 Hz, 1H, *arom*); 7.75 (d, J = 7.1 Hz, 1H, *arom*); 7.71 (d, J = 7.3 Hz, 1H, *arom*); 7.64 (t, J = 7.8 Hz, 2H, *arom*); 7.56 (d, J = 7.9 Hz, 1H, *arom*); 7.43-7.32 (m, 5H, *arom*); 7.22 (t, J = 7.7 Hz, 1H, *arom*); 7.16 (t, J = 7.5 Hz, 1H, *arom*); 7.09 (d, J = 7.0 Hz, 2H, *arom*); 7.02 (t, J = 7.5 Hz, 1H, *arom*); 5.11 (d, J = 7.9 Hz, 1H, C*H*-C=O); 4.20 (m, 1H, CH); 4.01 ppm (d, J = 7.1 Hz, 1H, CH). ^{13}C{^{1}H} NMR (CDCl$_3$): δ = 204.1, 201.6 (C=O); 153.5, 148.9, 143.1, 138.2, 136.6, 132.7, 131.4 (*arom* C); 135.4, 134.5, 130.8, 130.4, 129.5, 129.2, 128.7, 128.3, 127.9, 127.3,126.5, 125.7, 125.1, 124.7 (*arom* CH); 65.1 (*C*Ph-C=O); 53.3 (C*H*-C=O); 49.7, 36.8 ppm (CH).

B) From PhCH=CPhCOOH/WCl$_6$. WCl$_6$ (837 mg, 2.11 mmol) was added to a solution of PhCH=CPhCOCl (947 mg, 4.22 mmol) in chloroform (30 mL), then the mixture was heated at reflux temperature for 18 hours. After cooling down to ambient temperature, H$_2$O (ca. 2 mL) was added, and the resulting mixture was stirred for 18 hours under a nitrogen atmosphere. Then an orange solution was separated by filtration, whence an orange solid residue was obtained after removal of the solvent under reduced pressure. NMR analysis (CDCl$_3$ solution) revealed the presence of **14** in admixture with minor amounts of side products.

Synthesis and characterization of 10b-phenyldibenzo[c,h]indeno[1,2-f]chromene-5,11(10bH,15bH)-dione, 15, and 5a-chloro-9b-phenyl-14b,14c-dihydrobenzo[a]indeno[2,1-c]fluorene-5,10(5aH,9bH)-dione, 16 (Chart 6).
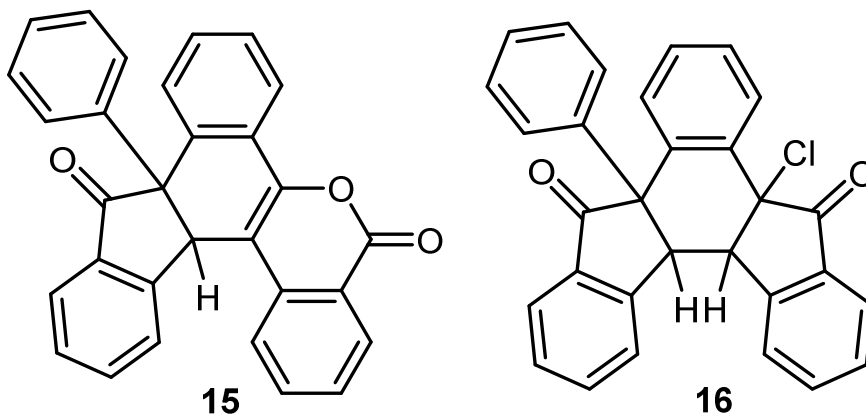
Chart 6. Structures of **15** and **16**.

A mixture of WCl$_6$ (1.59 g, 4.01 mmol) and *cis*-PhCH=CPhC(O)OH (1.797 g, 8.03 mmol) in chloroform (30 mL) was allowed to react at reflux temperature for 18 hours. The resulting dark-green solution was allowed to cool down to ambient temperature, and H$_2$O (ca. 2 mL) was added. The mixture was stirred for 24 hours with air contact. Then, an orange solution was separated from an insoluble material by filtration through a short alumina pad, using diethyl ether/acetone (1:1 v/v) as eluent. The volatiles were removed from the solution under reduced pressure. The obtained residue was washed with petroleum ether (2 x 30 mL) and then dried under vacuum thus affording **15** as an orange powder. The washing liquor was charged on a silica column, and a fraction corresponding to **16** was isolated using

hexane/ethyl acetate (2:3 v/v) as eluent. Crops of orange crystals of **16** and pale-yellow crystals of **16** were obtained by slow evaporation of the solvent from the respective diethyl ether solutions.

15. Yield 867 mg, 51%. Anal. Calcd. for $C_{30}H_{18}O_3$: C, 84.49; H, 4.25. Found: C, 83.81; H, 4.28. IR (solid state): ν = 3072w, 3047w, 1712vs-br (C=O), 1646m (C=C), 1596m-sh, 1562w, 1487m-s-sh, 1460m-sh, 1444w-m, 1374w, 1311m-s, 1282m, 1264w, 1249m, 1221m-s, 1181w-m, 1164w, 1151w-m, 1128w, 1110w-m, 1092m-s, 1066m-s, 1014w-m, 1028m, 961w, 933w-m, 914w, 892w-m, 882w-m, 845w-m, 792w, 764vs, 754vs, 733m-s, 719s, 706s, 693vs, 653vs cm^{-1}. ^{1}H NMR (CDCl$_3$): δ = 8.45 (d, J = 7.9 Hz, 1H, *arom*); 8.09 (d, J = 7.4 Hz, 1H, *arom*); 7.90 (d, J = 7.5 Hz, 1H, *arom*); 7.83 (t, J = 7.5 Hz, 1H, *arom*); 7.74 (d, J = 7.9 Hz, 2H, *arom*); 7.59 (t, J = 7.6 Hz, 1H, *arom*); 7.54 (t, J = 7.3 Hz, 1H, *arom*); 7.44 (t, J = 7.4 Hz, 2H, *arom*); 7.41-7.35 (m, 1H, *arom*); 7.26-7.15 (m, 4H, *arom*); 6.99 (d, J = 7.2 Hz, 2H, *arom*); 4.95 ppm (s, 1H, CH). ^{13}C{^{1}H} NMR (CDCl$_3$): δ = 204.7 (C=O$_{ketone}$); 161.5 (C=O$_{lactone}$); 151.3, 148.0, 142.8, 137.6, 135.9, 135.4, 133.3, 130.8, 130.6, 129.7, 129.0, 128.8, 128.7, 128.5, 128.3, 127.7, 127.5, 125.1, 124.5, 123.8, 122.8 (*arom*); 121.6, 108.0 (O-C=C); 62.8 (*C*Ph-C=O); 48.3 ppm (CH). ESI-MS(+): *m/z* 427 [$C_{30}H_{18}O_3$+H]$^+$.

16. Yield 232 mg, 13%. Anal. Calcd. for $C_{30}H_{19}ClO_2$: C, 80.62; H, 4.29; Cl, 7.93. Found: C, 80.11; H, 4.43; Cl, 8.07. IR (solid state): ν = 3068w, 2981m-sh, 2888w-br, 1732s (C=O), 1713vs (C=O), 1601m-s, 1497w-m, 1487w-m, 1464m-s, 1445m, 1386w, 1354w-m, 1318w, 1289m, 1263w-m, 1242w-m, 1226m, 1203m, 1178w-m, 1154w-m, 1122w-m, 1084m, 1032w-br, 993w-m, 957w-m, 864m-s, 851m, 819w, 769vs, 750vs, 725m, 703vs cm^{-1}. ^{1}H NMR (CDCl$_3$): δ = 8.13, 8.01,

7.73, 7.70, 7.62, 7.51, 7.49-7.10 (18H, *arom* CH); 4.47, 4.36 ppm (d, $^3J_{HH}$ = 6.7 Hz, 2H, CHCH).

Reaction of PhCH=CPhCOCl with NbCl$_5$: formation of 15 and 5a-phenylbenzo[a]indeno[2,1-c]fluorene-5,10(5aH,14cH)-dione, 17 (Chart 7).
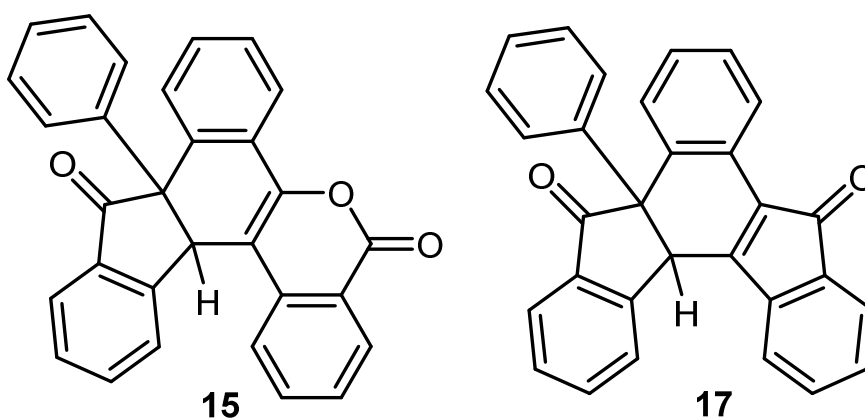
Chart 7. Structures of **15** and **17**.

NbCl$_5$ (605 mg, 2.24 mmol) was added to a solution of PhCH=CPhCOCl in CDCl$_3$ (15 mL), freshly prepared from PhCH=CPhCOOH (1004 mg, 4.48 mmol) and PCl$_5$ (932 mg, 4.47 mmol). The dark-red mixture was heated at reflux temperature for 48 hours, and then allowed to cool to ambient temperature. H$_2$O (ca. 2 mL) was added, and the resulting brown mixture was filtrated through a short alumina pad, using diethyl ether/acetone (1:1 v/v) as eluent. An orange solid residue was obtained upon removal of the volatiles under vacuum. This solid was charged on a silica column, and subsequent chromatography afforded two fractions, corresponding to

15 (eluent: petroleum ether/diethyl ether 4:1) and **17** (eluent: petroleum ether/diethyl ether 2:3).

15. Yield 323 mg, 17%. Anal. Calcd. for $C_{30}H_{18}O_3$: C, 84.49; H, 4.25. Found: C, 84.70; H, 4.36. ESI-MS(+): *m/z* 427 $[C_{30}H_{18}O_3 + H]^+$.

17. Yield 164 mg, 9%. Anal. Calcd. for $C_{30}H_{18}O_2$: C, 87.78; H, 4.42. Found: C, 88.02; H, 4.31. ESI-MS(+): *m/z* 411 $[C_{30}H_{18}O_2 + H]^+$.

5.7. Reactions with α,β-unsaturated carboxylic acids.

Reactions of WCl$_6$ with α,β-alkenyl carboxylic acids: formation of corresponding α,β-alkenyl acyl chlorides. *General procedure*: the appropriate carboxylic acid (ca. 2.0 mmol) and WCl$_6$ (1 eq.) were allowed to react in CHCl$_3$ (ca. 20 mL) at reflux temperature for 18 hours. The resulting mixture was cooled down to ambient temperature, and a residue was obtained after removal of the volatiles under vacuum.

A) From CH$_2$=CMeCOOH (methacrylic acid) and WCl$_6$: formation of CH$_2$=CMeCOCl.[464] Dark green oil. ^{1}H NMR (CDCl$_3$): δ = 6.54 (s, 1H, =CH$_2$); 6.04 (s, 1H, =CH$_2$); 2.08 ppm (s, 3H, Me).

B) From MeCH=CHCOOH (crotonic acid) and WCl$_6$: formation of MeCH=CHCOCl.[464] Brown oil. ^{1}H NMR (CDCl$_3$): δ = 7.49 (dq, $^2J_{HH}$ = 15.0, $^3J_{HH}$ = 6.9 Hz, 1H, MeC*H*=); 6.35 (d, $^3J_{HH}$ = 15.0 Hz, 1H, =C*H*COCl); 2.09 ppm (d, $^3J_{HH}$ = 6.9 Hz, 3H, Me). ^{13}C{^{1}H} NMR (CDCl$_3$): δ = 171.7 (C=O); 156.6 (Me*C*H=); 128.4 (=*C*HCOCl); 18.9 ppm (Me).

C) From Me$_2$C=CHCOOH (methylcrotonic acid) and WCl$_6$: formation of Me$_2$C=CHCOCl.[465] Dark red oil. ^{1}H NMR (CDCl$_3$): δ = 6.33 (s, 1H, =CH); 2.40 (s, 3H, Me); 2.12 ppm (s, 3H, Me). ^{13}C{^{1}H} NMR (CDCl$_3$): δ = 172.0 (C=O); 123.8 (=CH); 116.6 (Me$_2$*C*=); 28.8 (Me); 22.9 ppm (Me).

Reaction of MeC≡CCOOH with WCl$_6$: synthesis of MeC(Cl)=CHCOOH, 18. MeC≡CCOOH (85 mg, 1.01 mmol) and WCl$_6$ (415 mg, 1.05 mmol) were allowed to react in dichloromethane (30 mL) at room temperature for 7 days. During this period, the progress

of the reaction was evaluated by NMR analysis performed on aliquots of the reaction mixture. The final dark red/brown solution was treated with water. The organic phase was then recovered by filtration, and after removal of the volatiles, **18** was recovered as a dark brown solid. Yield 88 mg, 72%. Anal. Calcd. for $C_4H_5ClO_2$: C, 39.86; H, 4.18; Cl, 29.41; O, 26.55. Found: C, 39.71; H, 4.23; Cl, 29.11; O, 26.38. ^1H NMR (CDCl₃): δ = 9.2 (br); 6.14, 6.09 (s, 1H, CH *cis + trans*); 2.62, 2.33 ppm (s, 3 H, Me *cis + trans*). $^{13}C\{^1H\}$ NMR (CDCl₃): δ = 170.0, 169.2 (C=O *cis + trans*); 155.79, 149.50 (=CCl *cis + trans*); 118.74, 116.35 (=CH *cis + trans*); 28.73, 24.17 ppm (Me *cis + trans*).

X-ray quality crystals of **18** were collected from a concentrated solution of the crude product in hexane, stored at −30°C.

5.8. Reactions with α-Phenylacetic Acids

Spectroscopic data of carboxylic acids.

A) Ph₃CCOOH. IR (solid state): ν = 3056w, 2789w, 2611w, 1693vs (C=O), 1597w, 1488m, 1445m, 1405w, 1282m-sh, 1258m, 1190w-m, 1084w, 1035w, 1002w, 943w-br, 906w, 759m, 733s, 697vs, 667m-s cm⁻¹. ¹H NMR (dmso-d₆): δ = 7.28, 7.15 (m, 15 H, Ph); 3.5 ppm (br, 1 H, OH). ¹³C{¹H} NMR (dmso-d₆): δ = 174.8 (C=O); 143.7 (*ipso*-Ph), 130.4, 128.1, 127.1 (Ph); 67.4 ppm (*C*Ph₃).

B) EtPh₂CCOOH. IR (solid state): ν = 3060w, 2987w, 2967w, 2941w, 2883w, 1695s (C=O), 1597w, 1492m, 1459w, 1444m, 1402w, 1376w, 1316m, 1281w, 1255s, 1196m, 1159w, 1126w, 1093w, 1032w, 1002vw, 917m, 898w-sh, 802m, 760s, 729s, 700vs cm⁻¹. ¹H NMR (CDCl₃): δ = 7.36-7.27 (m, 10 H, Ph); 2.45 (q, ³J$_{HH}$ = 7.34 Hz, 2 H, CH₂); 0.79 ppm (t, ³J$_{HH}$ = 7.34 Hz, 3 H, Me). ¹³C{¹H} NMR (CDCl₃): δ = 179.8 (C=O); 142.3 (*ipso*-Ph); 129.1, 127.9, 126.9 (Ph); 60.7 (*C*Ph₂); 30.8 (CH₂); 9.8 ppm (Me).

C) MePh₂CCOOH. IR (solid state): ν = 3088w, 3063w, 3024w, 3003w, 2985w, 2945w, 2825w, 1697s (C=O), 1598w, 1581w, 1494m, 1462w-m, 1445m, 1409w-m, 1379w, 1293m, 1275m-s, 1213w-m, 1200w-m, 1125w-m, 1070w-m-sh, 1052w, 1030w-m, 937m-br, 922m, 882w, 838w, 773w, 757m-s, 734m-s, 697vs, 657m-s cm⁻¹. ¹H NMR (CDCl₃): δ = 7.36-7.25 (10 H, Ph); 1.95 ppm (s, 3 H, Me). ¹³C{¹H} NMR (CDCl₃): δ = 180.9 (OCO); 144.4 (*ipso*-Ph); 128.7, 128.6, 127.6 (Ph); 56.9 (*C*Ph₂); 27.2 ppm (Me).

D) Me₂PhCCOOH. IR (solid state): ν = 2974w, 2115w, 1694vs (C=O), 1497w, 1471w, 1446w, 1438w, 1404w, 1365w, 1293m, 1176w,

1160w-m, 1102w, 1078w, 1030w, 1013w, 938m, 840w, 776w, 756w, 731m, 697s cm^{-1}. ^{1}H NMR (CDCl$_3$): δ = 7.43 (d, $^3J_{HH}$ = 7.6 Hz, 2 H, *ortho* H); 7.37 (t, $^3J_{HH}$ = 7.6 Hz, 2 H, *meta* H); 7.29 (d, $^3J_{HH}$ = 7.2 Hz, 1 H, *para* H); 1.63 (s, 3H).; 1.63 ppm (s, 6 H, Me). ^{13}C{^{1}H} NMR (CDCl$_3$): δ = 182.9 (C=O); 143.8 (*ipso*-Ph); 128.5, 127.0, 125.8 (Ph); 46.3 (*C*Me$_2$); 26.2 ppm (Me).

E) Ph$_2$(BrCH$_2$CH$_2$)CCOOH. IR (solid state): ν = 3058w, 2983w, 2932w, 2815w, 2684w, 2639w, 2516w, 1958w, 1900w, 1815w, 1771w, 1702vs, 1599w-m, 1494m-s, 1440m-sh, 1402m, 1335w, 1306w-m, 1270s, 1229w, 1209w, 1178w, 1162w, 1147w-m, 1088w, 1066w, 1034w, 1015w-m, 915m-br, 841w, 785w-m, 756s, 740m, 726m-s, 687vs cm^{-1}. ^{1}H NMR (CDCl$_3$): δ = 10.58 (br, 1 H, OH); 7.40-7.31 (m, 10 H, Ph); 3.15-3.11 (m, 2 H, BrCH$_2$); 3.01-2.97 ppm (m, 2 H, CH$_2$). ^{13}C{^{1}H} NMR (CDCl$_3$): δ = 179.9 (C=O); 141.0 (*ipso*-Ph); 128.7, 128.4, 127.6 (Ph); 60.6 (*C*Ph$_2$); 41.6 (CH$_2$); 28.8 ppm (BrCH$_2$).

F) Ph$_2$CHCOOH. IR (solid state): ν = 3025w, 2903w, 2703w, 2604w, 1956w, 1699s (C=O), 1600w-m, 1581w, 1497m, 1449m-sh, 1410m, 1314m-sh, 1282w, 1222s, 1183w-br, 1080w, 1033w-m, 1003w, 933m-s-br, 886w, 768w, 749m-s, 731s, 695vs, 666m-s cm^{-1}. ^{1}H NMR (CDCl$_3$): δ =11.2 (s, br, 1 H, OH); 7.74 − 6.98 (m, 10 H, Ph); 5.11 ppm (s, 1 H, CH). ^{13}C{^{1}H} NMR (CDCl$_3$): δ =179.0 (C=O); 137.9, 128.7, 127.6 (Ph); 57.1 ppm (CH).

Synthesis and characterization of carboxylic acid chlorides.

General procedure. In a Schlenk tube, a solution of the carboxylic acid reactant (ca. 0.50 mmol) in CDCl$_3$ (ca. 4 mL) was treated with PCl$_5$ (1.0 eq.). The mixture was stirred at room temperature for 2 h.

An aliquot (0.5 mL) of the resulting solution was analysed by NMR spectroscopy. The ^{31}P spectrum clearly showed the presence of $POCl_3$ (δ = 4-5 ppm) as a unique phosphorus species.[52] The resulting solution was unchanged after stirring for 24-48 hours at room temperature. The solution was dried under vacuum, and the colourless residue characterized by IR spectroscopy.

A) Ph₃CCOCl. IR (solid state): ν = 3059w, 3034w, 1804m, 1790m-s, 1770s (C=O), 1594w, 1494s, 1443s, 1322w, 1186w, 1157w, 1087m, 1034m, 1009m-s, 994m-s, 941w, 917w, 901w, 790s, 753s, 729vs, 697vs, 666vs cm^{-1}. ^{1}H NMR (CDCl₃): δ = 7.43-7.31 ppm (Ph). ^{13}C{^{1}H} NMR (CDCl₃): δ = 175.6 (C=O), 141.0 (*ipso*-Ph), 130.4, 128.3, 127.6 (Ph), 76.3 ppm (*C*Ph₃).

B) EtPh₂CCOCl. IR (solid state): ν = 3061vw, 2981w, 2940vw, 2882vw, 1796s, 1770s-sh (C=O), 1495m, 1445m, 1383w, 1297vs, 1094w, 1033w, 1014w, 967m, 912w, 807s, 756w, 731vs, 699vs cm^{-1}. ^{1}H NMR (CDCl₃): δ = 7.40-7.33 (10 H, Ph); 2.57 (q, $^3J_{HH}$ = 7.34 Hz, 2 H, CH₂); 0.86 ppm (t, $^3J_{HH}$ = 7.34 Hz, 3 H, Me). ^{13}C{^{1}H} NMR (CDCl₃): δ = 176.3 (C=O); 139.9 (*ipso*-Ph); 129.4, 128.3, 127.7 (Ph); 70.3 (*C*Ph₂); 32.0 (CH₂); 9.6 ppm (CH₃).

C) MePh₂CCOCl. IR (solid state): ν = 3061w, 3027w, 2999w, 1775vs (C=O), 1599w, 1495m, 1460w-m, 1444m, 1377m, 1336w, 1297w, 1223w, 1189w, 1159w, 1127w, 1082w, 1027w-m, 929s, 903s, 779m-s, 759m, 746m, 729vs, 695vs, 654vs cm^{-1}. ^{1}H NMR (CDCl₃): δ = 7.39, 7.29 (m, 10 H, Ph), 2.13 ppm (s, 3 H, Me). ^{13}C{^{1}H} NMR (CDCl₃): δ = 177.6 (CO), 141.5 (*ipso*-Ph), 128.5, 128.3, 127.8 (Ph), 66.0 (*C*Ph₃), 27.9 ppm (Me).

D) Me₂PhCCOCl. IR (solid state): ν = 3062w, 2982w, 2939vw, 1820w-sh, 1780s (C=O), 1753w-sh, 1601w, 1584w, 1496m, 1461w, 1448m, 1388w, 1368w, 1238w, 1191w, 1157w, 1105w, 1077w, 1031w, 1015w, 944s, 909w, 874vs, 755s, 696vs cm⁻¹. ^{1}H NMR (CDCl₃): δ = 7.44-7.33 (5 H, Ph); 1.73 ppm (s, 6 H, Me). ^{13}C{^{1}H} NMR (CDCl₃): δ = 178.9 (C=O); 141.5 (*ipso*-Ph); 128.9, 127.8, 126.1 (Ph); 56.8 (*C*Me₂); 26.5 ppm (Me).

Reaction of WCl₆ with triphenylacetic acid.

A) NMR study: detection of Ph₃CCl, 20, and [Ph₃C]⁺. A suspension of WCl₆ (108 mg, 0.272 mmol) in CD₂Cl₂ (5 mL) was treated with Ph₃CCOOH (81 mg, 0.281 mmol), and the mixture was stirred at ambient temperature for 72 hours. During this period of time, the system was purged with nitrogen in order to dynamically remove the released gas. Aliquots of the reaction solution were analysed by NMR spectroscopy at different times. The ^{1}H spectrum after ca. 20 minutes showed the prevalent presence of Ph₃CCOCl. ^{1}H and ^{13}C spectra after 72 hours were as follows. ^{1}H NMR (CD₂Cl₂): δ = 8.31 (d, $^{3}J_{HH}$ = 6.8 Hz, 1 H, *para* H); 7.96 (t, $^{3}J_{HH}$ = 6.8 Hz, 2 H, *meta* H); 7.75 ppm (d, $^{3}J_{HH}$ = 7.0 Hz, 2 H, *ortho* H). Ph₃CCl/[Ph₃C]⁺ ratio = 2:1. ^{13}C{^{1}H} NMR (CD₂Cl₂): δ = 210.0 (br, *C*Ph₃), 143.5, 142.9, 140.0, 130.7 ppm (Ph).

B) Isolation of [Ph₃C][WOCl₅], 19. A suspension of Ph₃CCOOH (367 mg, 1.262 mmol) in CH₂Cl₂ (30 mL) was treated with WCl₆ (505 mg, 1.273 mmol), and the mixture was stirred at ambient temperature for 18 hours. During this period of time, the system was purged with nitrogen in order to dynamically remove the released gas: a silver

170

chloride precipitation test evidenced the formation of HCl, while GC analysis (see Section 5.9) allowed to detect carbon monoxide. Removal of the volatiles gave a red-orange solid residue, which was washed with hexane (50 mL) and dried under vacuum. Thus **19** was isolated as an orange solid. Yield 252 mg, 32%. IR (solid state): ν = 3060w, 1577vs, 1558w-m, 1480m, 1447s, 1352vs, 1292vs, 1183m-s, 1163w-m, 1125w, 1110w, 1085w, 993m-s (W=O), 977m, 965m-s, 914w-m, 841m, 807w-m, 767m-s, 740w-m, 696vs cm^{-1}. ^{1}H NMR (CD$_2$Cl$_2$): δ = 8.16, 7.85, 7.67 ppm (m, 15 H, Ph). ^{13}C{^{1}H} NMR (CD$_2$Cl$_2$): δ = 210.0 (br, *C*Ph$_3$), 143.4, 143.0, 140.4, 131.1 ppm (Ph). Crystals of **19** suitable for X-ray analysis were collected from a dichloromethane reaction solution layered with hexane and stored at −30°C for one week.

C) Reaction of Ph$_3$CCOCl with WOCl$_4$. A solution of Ph$_3$CCOCl (obtained from Ph$_3$CCOOH, 153 mg, 0.531 mmol, and PCl$_5$, 119 mg, 0.571 mmol, *vide supra*) in CD$_2$Cl$_2$ (5 mL) was treated with WOCl$_4$ (182 mg, 0.533 mmol). The resulting orange-brown mixture was stirred at room temperature for 5 days. NMR analysis on the final orange-red solution allowed for the identification of **19** and **20**. **19**/**20** ratio = 1:1.

D) Reaction of Ph$_3$CCOOH with WOCl$_4$. The reaction of WOCl$_4$ (302 mg, 0.884 mmol) with Ph$_3$CCOOH (255 mg, 0.884mmol) was carried out with a procedure analogous to that described for WCl$_6$/Ph$_3$CCOOH. Evolution of CO was detected by GC (see Section 5.9).

Reaction of MoCl₅ with triphenylacetic acid: synthesis of [Ph₃C][MoOCl₄], 21. A suspension of $MoCl_5$ (0.250 g, 0.915 mmol) in CH_2Cl_2 (15 mL) was treated with Ph_3CCOOH (0.270 g, 0.936 mmol). The mixture was stirred at ambient temperature for 18 hours, then the final brown solution was concentrated to *ca.* 3 mL and hexane (30 mL) was added. The resulting precipitate was washed with pentane (20 mL) and dried under vacuum: compound **21** was isolated as a dark-red powder. Yield 0.359 g, 79%. IR (solid state): ν = 3062vw, 1579vs, 1479m, 1446s, 1385w, 1352vs, 1292s, 1180m, 1169m, 1098w, 1029w, 993vs (Mo=O), 976w, 949w, 913w, 841w-m, 803m, 768m-sh, 762m, 697vs, 684s cm^{-1}. ^{1}H NMR (CD_2Cl_2): δ = 8.5-8.1 ppm (br, Ph). ^{13}C{^{1}H} NMR (CD_2Cl_2): δ = 211.6 (*C*Ph₃), 148.3, 147.5, 141.3, 135.1 ppm (Ph). Crystals of **21** suitable for X-ray analysis were collected from a dichloromethane reaction solution layered with hexane and settled aside at –30°C for one week.

Reaction of NbF₅ with triphenylacetic acid: synthesis of [Ph₃C][NbF₆], 22, and NbOF₃. The reaction of NbF_5 (0.200 g, 1.06 mmol) with Ph_3CCOOH (0.154 g, 0.534 mmol) was carried out with a procedure analogous to that described for $MoCl_5/Ph_3CCOOH$. The final yellow solution was separated from a pale-yellow precipitate by filtration. IR analysis on the precipitate clearly showed the presence of a strong band at 995 cm^{-1} (Nb=O, NbOF₃). Compound **22** was recovered from the solution as a yellow solid after work-up. Yield 0.167 g, 70%. IR (solid state): ν = 2958w, 2925w, 1581vs, 1483m, 1449s, 1355vs, 1294s, 1186m, 1169w-m, 1030w, 995w-m, 982w-br, 914w, 846m, 837m, 806m, 765m, 733w, 699vs cm^{-1}. ^{1}H NMR

172

(CD$_3$CN): δ = 8.30, 7.88, 7.76 ppm (m, CPh$_3$). ^{13}C{^{1}H} NMR (CD$_3$CN): δ = 212.0 (CPh$_3$), 143.1, 140.2, 130.1 ppm (Ph). ^{19}F NMR (CD$_3$CN): δ = 102 (decet, ^{1}J$_{NbF}$ = 3.4·10^2 Hz, NbF$_6^-$). ^{93}Nb NMR (CD$_3$CN): δ = −1556 (hept, ^{1}J$_{NbF}$ = 3.4·10^2 Hz, NbF$_6^-$). Crystals of **22** suitable for X-ray analysis were collected from a dichloromethane reaction solution layered with hexane and stored at −30°C for one week.

Reaction of NbCl$_5$ with triphenylacetic acid.

A) Identification of [Ph$_3$C]$^+$, [NbCl$_6$]$^-$, [NbOCl$_4$]$^-$ and NbOCl$_3$. The reaction of NbCl$_5$ (0.110 g, 0.407 mmol) with Ph$_3$CCOOH (0.125 g, 0.433 mmol) was carried out with in CD$_2$Cl$_2$ (5 mL). The reaction solution was analysed by NMR spectroscopy after 72 hours. ^{1}H NMR (CD$_2$Cl$_2$): δ = 8.31 (t, J = 7.4 Hz, 3 H, [CPh$_3$]$^+_{para}$); 7.94 (t, J = 7.6 Hz, 6 H, [CPh$_3$]$^+_{meta}$); 7.73 (d, J = 7.5 Hz, 6 H, [CPh$_3$]$^+_{ortho}$); 7.32-7.27 ppm (m, CPh$_3$Cl). ^{13}C{^{1}H} NMR (CD$_2$Cl$_2$): δ = 210.7 (CPh$_3$), 143.5, 142.8, 140.0, 130.7 ppm (Ph). ^{93}Nb NMR (CD$_2$Cl$_2$): δ = 6.6 (Δν½ = 138 Hz, NbCl$_6^-$); −107.2 (Δν½ = 142 Hz, minor); −358 (Δν½ = 2·10^3 Hz, NbOCl$_4^-$); −588 (Δν½ = 6·10^4 Hz, minor). Ratio NbCl$_6^-$/NbOCl$_4^-$ ≅ 2:5. The IR spectrum of the solid residue obtained by elimination of volatile materials appeared as follows. IR (solid state): ν = 3059vw, 1579vs, 1481s, 1447m-s, 1353vs, 1293s, 1183m, 1165w, 1083w, 994m, 835m-sh, 804m, 780br (Nb=O, NbOCl$_3$), 763s, 696vs cm^{-1}.

B) NMR analysis of [Bu$_4$N][NbOCl$_4$]. The solid obtained by reacting NbOCl$_3$ (0.130 g, 0.604 mmol) with [Bu$_4$N]Cl (0.167 g, 0.601 mmol) for 18 h in CH$_2$Cl$_2$ (10 mL), after solvent elimination, was analysed by ^{93}Nb NMR in CD$_2$Cl$_2$. The spectrum consisted of a single resonance at δ = −350 ppm (Δν½ = 10^3 Hz, NbOCl$_4^-$).

C) Reaction of NbCl$_5$ with Ph$_3$CCOCl: synthesis of [Ph$_3$C][NbCl$_6$], 23. A solution of Ph$_3$CCOCl (obtained from Ph$_3$CCOOH, 172 mg, 0.60 mmol, and PCl$_5$, 123 mg, 0.59 mmol, *vide supra*) in CD$_2$Cl$_2$ (5 mL) was treated with NbCl$_5$ (155 mg, 0.57 mmol), and the resulting mixture was stirred at ambient temperature for 48 hours. The volatiles were removed under vacuum, the residue was repeatedly washed with hexane (3 x 20 mL) and then dried under vacuum. ^{1}H NMR (CD$_2$Cl$_2$): δ = 8.27, 7.90, 7.71, *7.29* ppm (m, Ph). ^{13}C{^{1}H} NMR (CD$_2$Cl$_2$): δ = 211.5 (*C*Ph$_3$), 143.6, 140.8, 131.4, 128.5 ppm (Ph). ^{93}Nb NMR (CD$_2$Cl$_2$): δ = 7.0 (NbCl$_6^-$).

Reactions of TiF$_4$ with triphenylacetic acid: identification of [Ph$_3$C]$^+$. The reaction of TiF$_4$ (126 mg, 1.017 mmol) with Ph$_3$CCOOH (146 mg, 0.506 mmol) was carried out with a procedure analogous to that described for MoCl$_5$/Ph3CCOOH. The final mixture was eliminated of the volatile materials, then the resulting residue was dried under vacuum. IR (yellow solid): ν = 3061vw, 1581s, 1485m, 1446m, 1357s, 1295w, 1187w, 866m, 796vs, 758s, 731s, 694vs cm^{-1}. ^{1}H NMR (CD$_3$CN): δ = 8.30, 7.89, 7.72 ppm (m, CPh$_3$).

Reaction of TiCl$_4$ with triphenylacetic acid: isolation of [Ph$_3$C][Ti$_2$Cl$_8$(μ-κ^2-O$_2$CCPh$_3$)], 24. The reaction of Ph$_3$CCOOH (0.280 g, 0.971 mmol) with TiCl$_4$ (1.0 M solution in heptane, 0.97 mL) was carried out with a procedure analogous to that described for MoCl$_5$/Ph$_3$CCOOH. IR and NMR analyses on the obtained orange solid residue suggested the formation of a complicated mixture of products. Yield 0.080 g, 18%. IR (solid state): ν = 3059w, 3023w,

174

1644s (C=O), 1580w, 1537s, 1493s, 1446m, 1365s, 1334m, 1264w, 1191w, 1160w, 1085w, 1034w, 1002w, 986w, 940w, 904w, 753s-sh, 740vs, 697vs, 669s, 658s cm^{-1}. Yellow crystals of **24** suitable for X-ray analysis were isolated from a CH_2Cl_2 reaction mixture layered with hexane and settled aside at -30 °C for 72 h.

Synthesis of indanes.

General procedure. In a Schlenk tube, the appropriate metal halide was added to a solution of the carboxylic acid or acyl chloride reactant in CH_2Cl_2 (ca. 20 mL). The obtained mixture was stirred at ambient temperature for the appropriate time, which was determined by monitoring the reaction evolution by NMR. Evolution of HCl was observed by means of silver chloride precipitation test. At the end, the mixture was treated with H_2O (ca. 2 mL), and the resulting mixture was allowed to stir at room temperature for 24 hours. The solution was separated from the precipitate by filtration. The precipitate was then dissolved in a saturated $NaHCO_3$ solution, and, after liquid/liquid extraction with diethyl ether, the organic phase was added to the filtrated solution. After drying under vacuum, the residue was dissolved in diethyl ether and filtrated on an alumina column using diethyl ether/CH_2Cl_2 mixture (ca. 1:1) as eluent. The eluted solution was dried under vacuum thus affording a colourless residue.

A) Synthesis of 1-methyl-1,3,3-triphenyl-2,3-dihydro-1*H*-indene, 25a (Chart 8).[466]
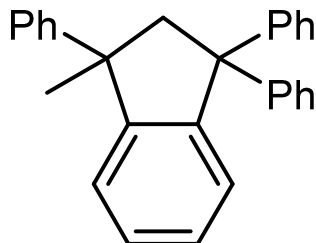
Chart 8. Structure of **25a**.

From WCl$_6$ (190 mg, 0.479 mmol) and MePh$_2$CCOOH (210 mg, 0.928 mmol), reaction time = 7 days. Colourless solid, yield 106 mg (63%).

From NbCl$_5$ (91 mg, 0.34 mmol) and MePh$_2$CCOCl (obtained from MePh$_2$CCOOH, 229 mg, 1.01 mmol, and PCl$_5$, 209 mg, 1.00 mmol), reaction time = 48 hours. Colourless solid, 176 mg (97%).

IR (solid state): ν = 3057w, 3028w, 2970w, 2868w, 1594m, 1488m, 1475w-sh, 1444m, 1373w, 1306w, 1250w, 1223w, 1154w, 1119w, 1071w, 1054w, 1028m, 945w, 910w, 765w, 749s, 698vs cm^{-1}. ^{1}H NMR (CDCl$_3$): δ = 7.49-7.14 (19 H, *arom* CH); 3.60, 3.28 (d, 2 H, J = 13.52 Hz, CH$_2$); 1.71 ppm (s, 3 H, Me). ^{13}C{^{1}H} NMR (CDCl$_3$): d = 150.6, 149.4, 148.9, 148.6, 147.5 (*arom* + *C*Ph$_2$); 128.8, 128.7, 128.0, 127.9, 127.6, 127.4, 126.9, 126.0, 125.7, 125.6, 125.1 (*arom*); 61.4 (CH$_2$); 51.2 (*C*MePh); 28.9 ppm (Me). Crystals of **25a** suitable for X-ray analysis were obtained from a concentrated diethyl ether solution, at –30 °C. When the same reaction was repeated in CD$_2$Cl$_2$, NMR analysis of an aliquot of the reaction mixture after ca. 20 minutes showed that mainly MePh$_2$CCOCl was present.

176

B) Synthesis of 1,1,3-trimethyl-3-phenyl-2,3-dihydro-1_H_-indene, 25b (Chart 9).[439]
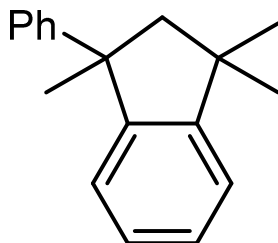
Chart 9. Structure of **25b**.

From WCl_6 (133 mg, 0.335 mmol) and $Me_2PhCCOOH$ (110 mg, 0.670 mmol), reaction time = 7 days. Light yellow solid, yield 70 mg (88%).

From $NbCl_5$ (85 mg, 0.315 mmol) and $Me_2PhCCOCl$ (obtained from $Me_2PhCCOOH$, 154 mg, 0.938 mmol, and PCl_5, 200 mg, 0.960 mmol), reaction time = 48 hours. Colourless solid, yield 88 mg (79%).

From $NbOCl_3$ (207 mg, 0.962 mmol) and $Me_2PhCCOCl$ (obtained from $Me_2PhCCOOH$, 161 mg, 0.981 mmol, and PCl_5, 212 mg, 1.018 mmol), reaction time = 5 days. Colourless solid, yield 165 mg (70%).

IR (solid state): ν = 3029w, 3025w, 2929w, 1598w-m, 1493s, 1441s, 1378w, 1354w, 1181w, 1107w, 1073w, 1031w, 964w, 9113w, 891w, 840w, 769s, 755vs, 694vs cm^{-1}. ^1H NMR (CDCl$_3$): δ = 7.38-7.19 (9 H, _arom_ CH); 2.50, 2.27 (d, J = 13.20 Hz, 2 H, CH$_2$); 1.77, 1.42, 1.11 ppm (s, 9 H, Me). $^{13}C\{^1H\}$ NMR (CDCl$_3$): δ = 152.3, 151.1, 148.9 (_arom_ C); 128.0, 127.3, 126.7, 125.5, 125.1, 122.6 (_arom_ CH); 59.3 (CH$_2$); 50.9, 42.9 (_C_Me); 31.0, 30.7, 30.4 ppm (Me).

When the same reaction was repeated in CD$_2$Cl$_2$, NMR analysis of an aliquot of the reaction mixture after ca. 20 minutes showed that mainly PhMe$_2$CCOCl was present.

C) Isolation and characterization of WO₂Cl₂.

The reaction of WCl_6 (283 mg, 0.714 mmol) with $Me_2PhCCOOH$ (243 mg, 1.48 mmol) was carried out in CH_2Cl_2 (15 mL), and the mixture was stirred at ambient temperature for 6 hours. A dark red solution over a dark precipitate was obtained. The precipitate, WO_2Cl_2, was separated from the solution and washed with $CHCl_3$ (ca. 30 mL), thus affording a microcrystalline grey-green solid. Yield 152 mg, 74%. IR: 797vs, 699m cm^{-1}.[397] Anal. Calcd for Cl_2O_2W: Cl, 24.73. Found: Cl, 24.39. A similar outcome was achieved starting from WCl_6 (ca. 0.70 mmol) and $MePh_2CCOOH$ (2 eq.).

Reaction of WCl$_6$ with 2,2-diphenylbutyric acid: formation of 1,1-diphenylpropene, 26 (Chart 10).
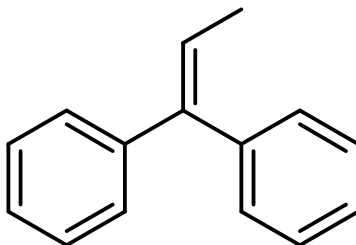
Chart 10. Structure of **26**.

A solution of EtPh$_2$CCOOH (295 mg, 1.23 mmol) in CH$_2$Cl$_2$ (15 mL) was treated with WCl$_6$ (162 mg, 0.409 mmol), and the mixture was allowed to stir at ambient temperature for 22 hours. The resulting dark-red solution was added to H$_2$O (ca. 3 mL). A yellow solid (**26**) was obtained after filtration through an alumina column, using dichloromethane as eluent. Yield 148 mg, 62%. IR (solid state): ν = 3080vw, 3056w, 3025w, 2911w, 1598w, 1494m, 1441m, 1355w, 1073w, 1031w, 964w, 914w, 891w, 840w, 756s, 695vs cm^{-1}. ^{1}H NMR (CDCl$_3$): δ = 7.51-7.31 (10H, Ph); 6.31 (q, J = 6.85 Hz, 1 H, CH); 1.89 ppm (d, J = 6.85 Hz, 3 H, Me). ^{13}C{^{1}H} NMR (CDCl$_3$): δ = 143.1, 142.6, 140.1 (*arom* C + *C*Ph$_2$); 130.2, 128.5, 128.2, 127.3, 127.0, 126.9 (Ph); 124.2 (CH); 15.8 ppm (Me). When the same reaction was repeated in CD$_2$Cl$_2$, NMR analysis of an aliquot of the reaction mixture after ca. 20 minutes showed the presence of mainly EtPh$_2$CCOCl.

Reactions with diphenylacetic acid.

A) Synthesis of NbCl$_4$(O$_2$CCHPh$_2$), 27. A solution of Ph$_2$CHCOOH (230 mg, 1.08 mmol) in CH$_2$Cl$_2$ (10 mL) was added to NbCl$_5$ (292 mg, 1.08 mmol). The mixture was stirred at room temperature for 18 hours. The resulting red solution was eliminated of the volatiles, then the residue was washed with hexane (2 x 10 mL) and dried under vacuum. A red solid was obtained. Yield 338 mg, 70%. IR (solid state): ν = 3060w, 3027w, 1579s, 1481m, 1447m, 1416m, 1354s, 1295m, 1261w-m, 1180m, 1079w, 1000w, 995w, 978w, 920w, 800vs-br, 733vs, 694vs cm^{-1}. ^{1}H NMR (CDCl$_3$): δ = 7.44-7.12 (10 H, Ph); 5.37 ppm (s, 1 H, CH). ^{13}C{^{1}H} NMR (CDCl$_3$): δ = 167.2 (OCO); 143.5-126.1 (Ph); 59.1 ppm (CH). ^{93}Nb NMR (CDCl$_3$): δ = −234 ($\Delta\nu\frac{1}{2}$ = 2.7·10^3 Hz).

B) Formation of Ph$_2$CHCOCl. A solution of Ph$_2$CHCOOH (269 mg, 1.27 mmol) in CD$_2$Cl$_2$ (2 mL) was added of WCl$_6$ (251 mg, 0.633 mmol). A light red solution formed after 18 hours, which was analysed by NMR spectroscopy. The analysis clearly evidenced the formation of Ph$_2$CHCOCl,[467] in admixture with a secondary, non-identified species. ^{1}H NMR (CD$_2$Cl$_2$): δ = 7.50-7.38 (Ph), 5.40 ppm (CH); ^{13}C{^{1}H} NMR (CD$_2$Cl$_2$): δ = 182.3 (C=O), 136.4 (*ipso*-Ph), 129.1, 128.8, 128.2 (Ph), 57.2 ppm (CH). The solution was dried under vacuum, then the residue was characterized by IR spectroscopy. IR (solid state): ν = 1702s, 1659s, 1599s, 1581s cm^{-1}.

Reactions of WCl₆ with 4-bromo-2,2-diphenylbutyric acid: synthesis of 3,3-diphenyldihydrofuran-2(3H)-one, 28, (Chart 11).[468]
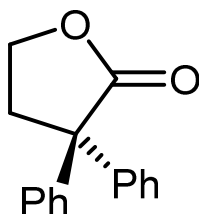
Chart 11. Structure of **28**.

The title compound was obtained by a procedure similar to that described for **25a**, from WCl₆ (188 mg, 0.474 mmol) and Ph₂(BrCH₂CH₂)CCOOH (303 mg, 0.949 mmol), reaction time: 26 h. The product was isolated as colourless crystals upon crystallization from a diethyl ether/pentane mixture, at –30 °C. Yield 197 mg, 72%. IR (solid state): ν = 3056w, 2988w, 2912w, 1762vs (C=O), 1596w, 1493m, 1446m, 1369m, 1340w, 1322w, 1226w, 1207w, 1160s, 1090w-m, 1021s, 1000w-m, 954m, 916w, 897w, 834w, 772m, 753s, 725w, 698vs, 675m cm^{-1}. ^{1}H NMR (CDCl₃): δ = 7.44-7.29 (10 H, Ph); 4.25 (t, 2 H, J = 6.36 Hz, Ph₂CC*H*₂); 2.98 ppm (t, 2 H, J = 6.36, 6.85 Hz, CH₂Br). ^{13}C{^{1}H} NMR (CDCl₃): δ = 177.8 (C=O); 140.8 (*ipso*-Ph); 128.8, 127.7, 127.6 (Ph); 65.3 (Ph₂C*C*H₂); 56.5 (*C*Ph₂); 37.5 ppm (CH₂Br).

5.9. Gas-chromatographic analyses

A mixture of metal compound (ca. 1 mmol) and the appropriate carboxylic acid (1 eq.) in CH_2Cl_2 (10 mL) was stirred at ambient temperature for 72 hours in a Schlenk tube capped with a silicon stopper. Then an aliquot of the reaction atmosphere was withdrawn by a 1 mL syringe through the stopper, and injected into the GC instrument. The yields of CO formation were estimated based on analyses of gaseous standard mixtures containing known amounts of CO. From WCl_6/Ph_3CCOOH: 47%; from $WOCl_4$/Ph_3CCOOH: 28%; from WCl_6/$MePh_2CCOOH$: 52%; from WCl_6/$Me_2PhCCOOH$: 54%; from $MoCl_5$/Ph_3CCOOH: 45%; from NbF_5/Ph_3CCOOH: 38%; from $NbCl_5$/Ph_3CCOOH: 39%; from TiF_4/Ph_3CCOOH: 9.4%; WCl_6/$Ph_2(BrCH_2CH_2)CCOOH$: 3.1%; from WCl_6/$Ph_2CHCOOH$: 0%.

5.10. X-ray Crystallographic studies.

All the crystallographic studies were performed by Prof. Stefano Zacchini (University of Bologna). Crystal data and collection details are herein reported. The diffraction experiments were carried out on a Bruker APEX II diffractometer equipped with a CCD detector (**1a·CH₂Cl₂, 2b, 3, 4, 6, 7, 8a·CH₂Cl₂, 8b·CH₂Cl₂, 9·0.5CH₂Cl₂, 11, 12a, 12b, 19, 21, 22, 24·2CH₂Cl₂, 25a**) or a PHOTON100 detector (**13a, 13b, 14, 16, 18**, **28**), and using *Mo-Kα* radiation (λ = 0.71073 Å). Data were corrected for Lorentz polarization and absorption effects (empirical absorption correction SADABS).[469] Structures were solved by direct methods and refined by full-matrix least-squares based on all data using F^2.[470] All non-hydrogen atoms were refined with anisotropic displacement parameters. Hydrogen atoms were fixed at calculated positions and refined by a riding model. H-atoms were treated isotropically using the 1.2-fold U_{iso} value of the parent atom except methyl protons, which were assigned the 1.5-fold U_{iso} value of the parent C-atom.

Two independent molecules are present within the unit cell of **1a·CH₂Cl₂** displaying similar geometries and bonding parameters; the CH₂Cl₂ molecules have been refined isotropically and restrained to have similar *U* parameters (s.u. 0.02).

The crystals of **2b** are non-merohedrally twinned. The TwinRotMat routine of PLATON was used to determine the twinning matrix and to write the reflection data file (.hkl) containing two twin components.[471] Refinement was performed using the instruction HKLF 5 in SHELXL and one BASF parameter.

Crystals of **3** contain some voids that are likely to be occupied by one disordered CH_2Cl_2 molecule per formula unit. It has not been possible to refine the CH_2Cl_2 molecule associated to **3** satisfactorily. Thus, the SQUEEZE routine of PLATON has been applied.[471–473]

The $[WCl_6]^-$ anion, two ethyl groups and one methyl group on the cation of **4** are disordered. Disordered atomic positions were split and refined using one occupancy parameter per disordered group.

The N-bonded hydrogen atom of **8a·CH_2Cl_2** has been located in the Fourier map and refined isotropically. The Nb atom of **9** is located on a mirror plane and, thus, only half of the molecule is present within the asymmetric unit of the unit cell. The CH_2Cl_2 molecule of **9·0.5CH_2Cl_2** is disordered over four positions (two by two related by an inversion centre). The Nb atom in **11** is located on a mirror plane and, consequently, Cl(1) and O(1) are disordered over two equally populated positions related by *m*. The crystals of **12a** are racemically twinned with refined Flack parameter 0.14(3).[474]

One CH_2Cl_2 molecule of **24·2CH_2Cl_2** is disordered and, thus, it has been split into two positions and refined isotropically using one occupancy factor per disordered group. The CH_2Cl_2 molecules of **24·2CH_2Cl_2** have been restrained to have similar geometries (SAME line in SHELXL; s.u. 0.02) and their C–Cl distances have been restrained to 1.75 Å (s.u. 0.02).

The structure of **25a** contains a centrosymmetric chiral carbon, and the crystallographic cell comprises two enantiomers in 1:1 ratio.
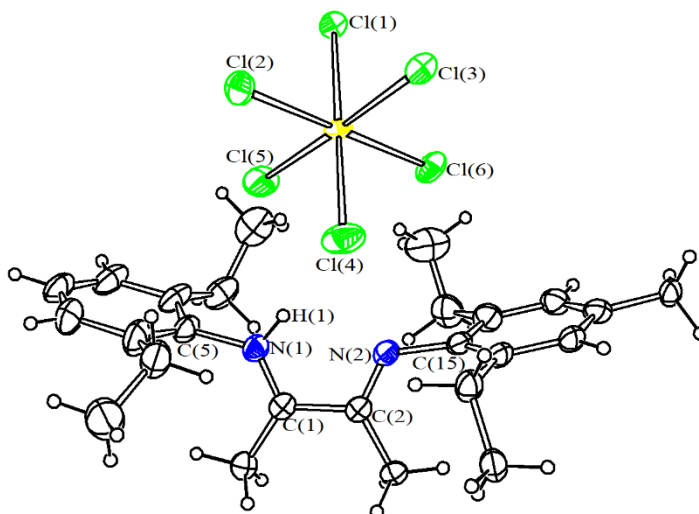
Figure 95. ORTEP drawing of **4**. Displacement ellipsoids are at the 50% probability level. Only the main images of the disordered groups are represented.

Table 14. Selected bond distances (Å) and angles (deg) for **4**.

Bond Distances (Å)			
W(1)–Cl(1)	2.333(5)	W(1)–Cl(2)	2.295(5)
W(1)–Cl(3)	2.340(4)	W(1)–Cl(4)	2.310(5)
W(1)–Cl(5)	2.313(4)	W(1)–Cl(6)	2.294(3)
C(1)–C(2)	1.508(10)		
C(1)–N(1)	1.277(9)	C(2)–N(2)	1.266(10)
C(5)–N(1)	1.441(10)	C(15)–N(2)	1.437(10)
Angles (deg)			
Cl(1)–W(1)–Cl(4)	179.4(3)	Cl(2)–W(1)–Cl(6)	176.1(7)
Cl(3)–W(1)–Cl(5)	178.5(2)		
C(5)–N(1)–C(1)	127.2(7)	N(1)–C(1)–C(2)	115.0(7)
C(1)–C(2)–N(2)	114.2(7)	C(2)–N(2)–C(15)	122.9(6)

Table 15. Crystal data and experimental details for **1a·CH₂Cl₂**, **2b**, **3** and **4**.

	1a·CH₂Cl₂	2b	3	4
Formula	C$_{24}$H$_{31}$Cl$_8$N$_2$W	C$_{22}$H$_{28}$Cl$_4$N$_2$W	C$_{28}$H$_{30}$Cl$_6$N$_3$W	C$_{25}$H$_{35}$Cl$_6$N$_2$W
Fw	814.96	646.11	*805.10*	760.10
T, K	100(2)	100(2)	0.71073	100(2)
λ, Å	0.71073	0.71073	100(2)	0.71073
Crystal system	Triclinic	Monoclinic	Monoclinic	Monoclinic
Space group	*P*-1	*P*2$_1$/*n*	P2$_1$/*n*	*P*2$_1$/*n*
a, Å	9.9556(3)	11.3214(13)	8.3116(4)	9.5610(5)
b, Å	13.4893(4)	12.5342(15)	18.5141(9)	15.4452(8)
c, Å	23.5871(7)	17.149(2)	22.4919(11)	19.6813(11)
α, °	80.107(2)	90	90	90
β, °	77.8480(10)	104.770(3)	97.532(3)	97.790(2)
γ, °	89.233(2)	90	90	90
Cell Volume, Å³	3049.73(16)	2353.1(5)	3431.2(3)	2879.5(3)
Z	4	4	*4*	4
D$_c$, g cm⁻³	1.775	1.824	1.559	1.753
μ, mm⁻¹	4.506	5.375	3.855	4.586
F(000)	1596	1264	1580	1500
Crystal size, mm	0.15×0.13×0.12	0.16×0.13×0.12		0.16×0.12×0.10
θ limits, °	1.53–28.00	1.95–26.00	1.43–28.00	1.68–25.05
Reflections collected	54541	25047	60561	34360
Independent reflections	14465 [R$_{int}$ = 0.0390]	4578 [R$_{int}$ = 0.0668]	8263 [*R*$_{int}$ = 0.0676]	5108 [R$_{int}$ = 0.0416]
Data / restraints /parameters	14465 / 7 /601	4578 / 0 / 267	8263 / 0 /349	5108 / 317 / 385
Goodness on fit on F²	1.084	1.045	1.020	1.151
R$_1$ (*I*> 2σ(*I*))	0.0483	0.0585	0.0304	0.0528
wR$_2$ (all data)	0.1197	0.1562	0.0746	0.1132
Largest diff. peak and hole, e Å⁻³	3.059 / -2.923	2.945 / -3.493	1.773 / -0.780	1.416 / -1.482

186
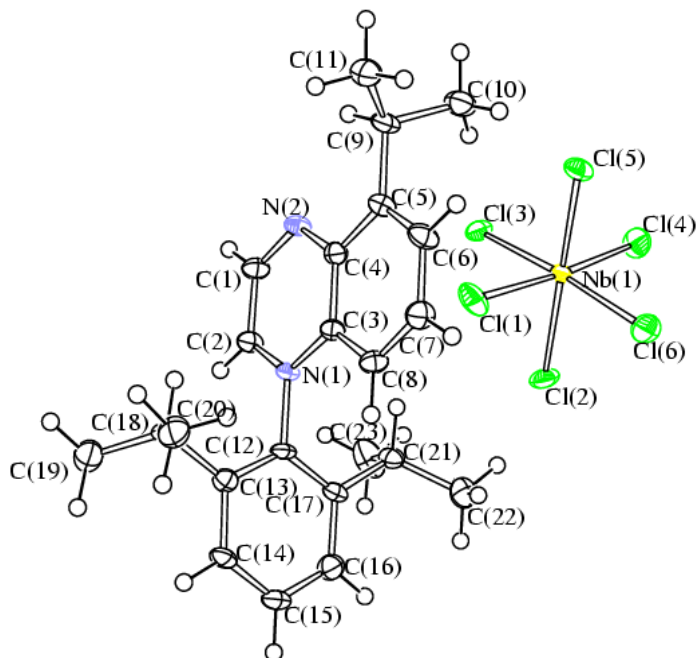
Figure 96. ORTEP drawing of [{2,6-
$C_6H_3(CHMe_2)_2$}N(CH)$_2$NCC(CHMe$_2$)(CH)$_3$C][NbCl$_6$], **6**. Displacement
ellipsoids are at the 50% probability level.

Table 16. Selected bond distances (Å) and angles (deg) for **6**.

Bond Distances (Å)			
Nb(1)-Cl(1)	2.3676(11)	Nb(1)-Cl(2)	2.3814(11)
Nb(1)-Cl(3)	2.3598(10)	Nb(1)-Cl(4)	2.3096(11)
Nb(1)-Cl(5)	2.3284(10)	Nb(1)-Cl(6)	2.3270(11)
C(1)-C(2)	1.406(5)	C(3)-C(4)	1.427(5)
C(1)-N(2)	1.316(4)	C(4)-N(2)	1.354(4)
C(2)-N(1)	1.323(4)	C(3)-N(1)	1.383(4)
C(4)-C(5)	1.425(5)	C(5)-C(6)	1.366(5)
C(6)-C(7)	1.412(5)	C(7)-C(8)	1.371(5)
C(8)-C(3)	1.390(5)	N(1)-C(12)	1.475(4)

Angles (deg)			
Cl(1)-Nb(1)-Cl(4)	174.99(4)	Cl(2)-Nb(1)-Cl(5)	177.89(4)
Cl(3)-Nb(1)-Cl(6)	174.67(4)	C(2)-C(1)-N(2)	122.7(3)
C(1)-N(2)-C(4)	118.3(3)	N(2)-C(4)-C(3)	121.6(3)
C(4)-C(3)-N(1)	116.9(3)	C(3)-N(1)-C(2)	121.2(3)
N(1)-C(2)-C(1)	119.2(3)	C(3)-C(4)-C(5)	119.1(3)
C(4)-C(5)-C(6)	117.3(3)	C(5)-C(6)-C(7)	122.7(3)
C(6)-C(7)-C(8)	121.2(3)	C(7)-C(8)-C(3)	117.7(3)
C(8)-C(3)-C(4)	122.0(3)		
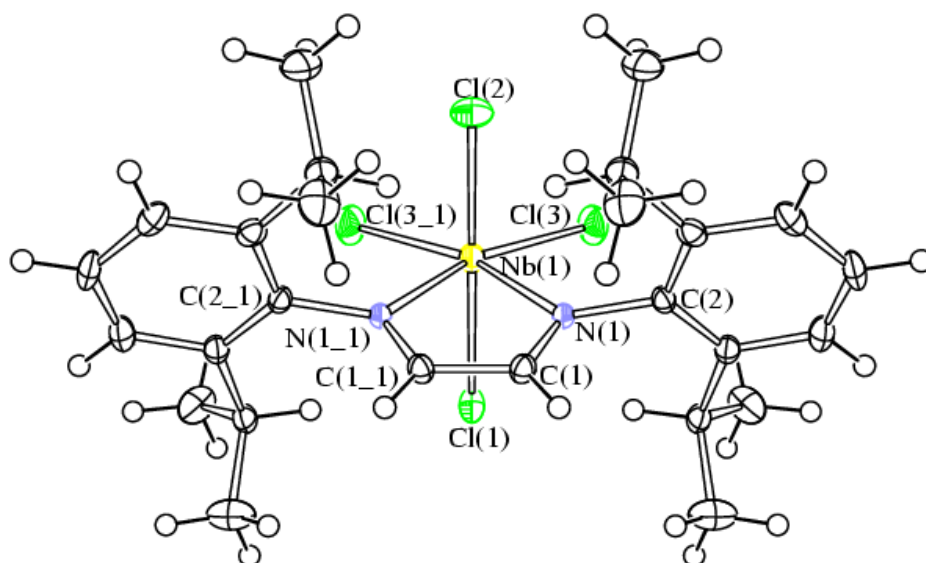
Figure 97. ORTEP drawing of NbCl$_4$(DAD$_{Dipp}$), **7**. Displacement ellipsoids are at the 50% probability level.

Table 17. Selected bond lengths (Å) and angles (deg) for **7**.

Bond Distances (Å)			
Nb(1)-Cl(1)	2.4194(8)	Nb(1)-Cl(2)	2.3306(9)
Nb(1)-Cl(3)	2.3088(6)	Nb(1)-N(1)	2.2211(17)
N(1)-C(1)	1.296(3)	C(1)-C(1_1)	1.444(4)
Angles (deg)			
Cl(1)-Nb(1)-Cl(2)	178.28(3)	Cl(3)-Nb(1)-N(1_1)	162.51(5)
N(1)-Nb(1)-N(1_1)	73.01(9)	Cl(3)-Nb(1)-Cl(3_1)	106.93(3)
Nb(1)-N(1)-C(1)	114.99(14)	Nb(1)-N(1)-C(2)	129.27(13)
C(1)-N(1)-C(2)	115.59(17)	N(1)-C(1)-C(1_1)	117.54(12)
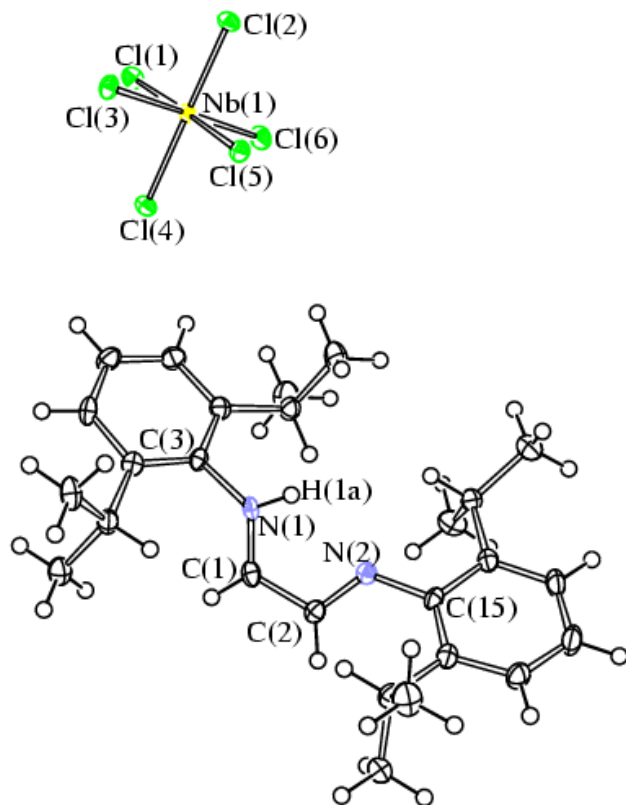
Figure 98. ORTEP drawing of [DAD$_{\text{Dipp}}$(H)][NbCl$_6$], **8a**. Displacement ellipsoids are at the 50% probability level.

Table 18. Selected bond lengths (Å) and angles (deg) for **8a**.

Bond Distances (Å)			
Nb(1)-Cl(1)	2.3319(9)	Nb(1)-Cl(2)	2.3380(9)
Nb(1)-Cl(3)	2.3779(9)	Nb(1)-Cl(4)	2.3684(9)
Nb(1)-Cl(5)	2.3769(9)	Nb(1)-Cl(6)	2.3125(9)
N(1)-C(1)	1.275(4)	N(2)-C(2)	1.274(4)
C(1)-C(2)	1.473(5)	N(1)-C(3)	1.441(4)
N(2)-C(15)	1.414(4)		

Angles (deg)			
Cl(1)-Nb(1)-Cl(5)	176.71(3)	Cl(2)-Nb(1)-Cl(4)	177.67(3)
Cl(3)-Nb(1)-Cl(6)	179.66(4)	N(1)-C(1)-C(2)	117.9(3)
C(1)-C(2)-N(2)	114.8(3)	C(2)-N(2)-C(15)	124.4(3)
C(1)-N(1)-C(3)	130.1(3)		
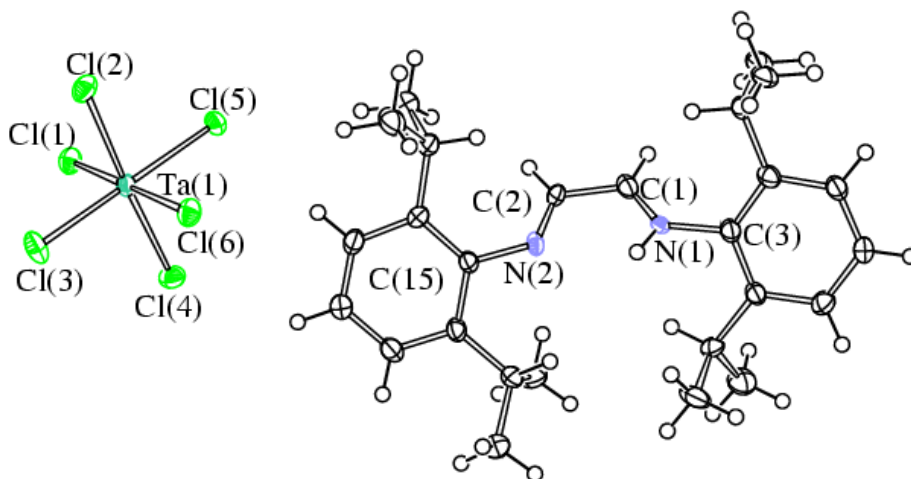
Figure 99. ORTEP drawing of [DAD$_{Dipp}$(H)][TaCl$_6$], **8b**. Displacement ellipsoids are at the 50% probability level.

Table 19. Selected bond lengths (Å) and angles (deg) for **8b**.

Bond Distances (Å)			
Ta(1)-Cl(1)	2.345(2)	Ta(1)-Cl(2)	2.3446(19)
Ta(1)-Cl(3)	2.324(2)	Ta(1)-Cl(4)	2.3832(19)
Ta(1)-Cl(5)	2.3802(19)	Ta(1)-Cl(6)	2.371(2)
N(1)-C(1)	1.275(10)	N(2)-C(2)	1.267(9)
C(1)-C(2)	1.496(10)	N(1)-C(3)	1.448(9)
N(2)-C(15)	1.428(8)		
Angles (deg)			
Cl(1)-Ta(1)-Cl(6)	177.92(6)	Cl(2)-Ta(1)-Cl(4)	177.09(7)
Cl(3)-Ta(1)-Cl(5)	179.83(7)	N(1)-C(1)-C(2)	117.9(7)
C(1)-C(2)-N(2)	113.7(7)	C(2)-N(2)-C(15)	123.9(6)
C(1)-N(1)-C(3)	129.6(6)		

192
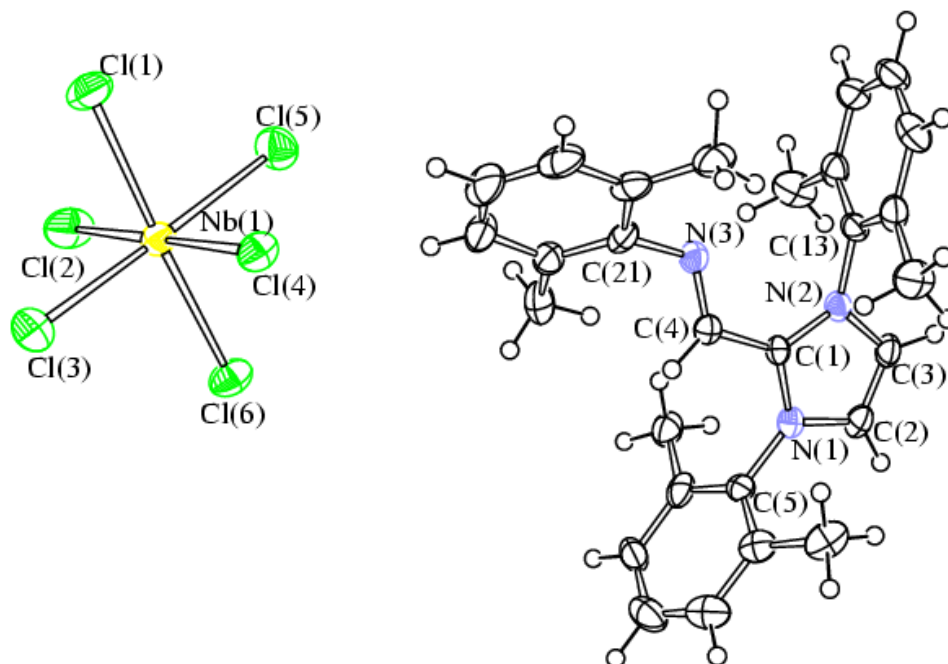
Figure 100. ORTEP drawing of [(2,6-$C_6H_3Me_2$)NCHCHN(2,6-$C_6H_3Me_2$)CCHN(2,6-$C_6H_3Me_2$)][NbCl$_6$], **9**. Displacement ellipsoids are at the 50% probability level.

Table 20. Selected bond lengths (Å) and angles (deg) for **9**.

Bond Distances (Å)			
Nb(1)-Cl(1)	2.3547(17)	Nb(1)-Cl(2)	2.3470(18)
Nb(1)-Cl(3)	2.3247(19)	Nb(1)-Cl(4)	2.3634(17)
Nb(1)-Cl(5)	2.3500(18)	Nb(1)-Cl(6)	2.3483(17)
C(1)-N(1)	1.360(8)	N(1)-C(2)	1.379(8)
C(2)-C(3)	1.349(10)	C(3)-N(2)	1.370(9)
N(2)-C(1)	1.348(8)	C(1)-C(4)	1.462(9)
C(4)-N(3)	1.270(8)	N(3)-C(21)	1.429(9)
N(1)-C(5)	1.441(8)	N(2)-C(13)	1.445(8)

Angles (deg)			
Cl(1)-Nb(1)-Cl(6)	177.41(7)	Cl(2)-Nb(1)-Cl(4)	178.95(7)
Cl(3)-Nb(1)-Cl(5)	178.51(7)	C(1)-N(1)-C(2)	108.6(5)
N(1)-C(2)-C(3)	107.2(6)	C(2)-C(3)-N(2)	108.0(6)
C(3)-N(2)-C(1)	109.0(5)	N(2)-C(1)-N(1)	107.2(5)
N(1)-C(1)-C(4)	123.1(5)	N(2)-C(1)-C(4)	129.6(6)
C(1)-C(4)-N(3)	119.9(6)	C(4)-N(3)-C(21)	118.5(6)

Table 21. Crystal data and experimental details for **6**, **7**, **8a·CH$_2$Cl$_2$**, **8b·CH$_2$Cl$_2$**, and **9·0.5CH$_2$Cl$_2$**.

	6	**7**	**8a·CH$_2$Cl$_2$**	**8b·CH$_2$Cl$_2$**	**9·0.5CH$_2$Cl$_2$**
Formula	C$_{23}$H$_{29}$Cl$_6$N$_2$Nb	C$_{26}$H$_{36}$Cl$_4$N$_2$Nb	C$_{27}$H$_{39}$Cl$_8$N$_2$Nb	C$_{27}$H$_{39}$Cl$_8$N$_2$Ta	C$_{28.5}$H$_{31}$Cl$_7$N$_3$Nb
Fw	639.09	611.28	768.11	856.15	756.62
λ, Å	0.71073	0.71073	0.71073	0.71073	0.71073
Temperature, K	100(2)	100(2)	100(2)	100(2)	100(2)
Crystal system	Triclinic	Orthorhombic	Monoclinic	Monoclinic	Monoclinic
Space group	P-1	$Pnma$	$P2_1/c$	$P2_1/n$	$P2_1/n$
a, Å	10.004(2)	12.8295(9)	16.0202(4)	16.105(7)	8.3272(6)
b, Å	10.785(3)	21.6973(15)	13.0226(3)	13.078(5)	18.4834(12)
c, Å	12.934(3)	10.3071(7)	17.8448(4)	17.933(8)	22.5408(15)
α °	85.466(3)	90	90	90	90
β, °	88.650(3)	90	113.1630(10)	113.164(5)	97.617(4)
γ, °	83.733(3)	90	90	90	90
Cell volume, Å^3	1382.7(6)	2869.1(3)	3422.76(14)	3473(3)	3438.8(4)
Z	2	4	4	4	4
D_c, g cm^{-3}	1.535	1.415	1.491	1.638	1.461
μ, mm^{-1}	1.030	0.809	0.997	3.801	0.917
F(000)	648	1260	1568	1696	1532
θ limits, °	0.22×0.20×0.16	0.21×0.16×0.14	1.45 – 25.03	1.44 – 26.00	1.82–25.02
Reflections collected	13141	24389	36558	28556	49289
Independent reflections	5167 [R$_{int}$ = 0.0405]	3209 [R$_{int}$ = 0.0351]	6047 [R$_{int}$ = 0.0666]	6772 [R$_{int}$ = 0.0973]	6041 [R_{int} = 0.0872]
Data / restraints /parameters	5167 / 0 / 295	3209 / 0 / 154	6047 / 1 / 346	6772 / 0 / 343	6041 / 9 / 366
Goodness of fit on F^2	1.014	1.077	1.041	1.045	1.034
$R1$ ($I > 2\sigma(I)$)	0.0399	0.0321	0.0370	0.0464	0.0670
$wR2$ (all data)	0.0955	0.0842	0.0903	0.1174	0.2200
Largest diff. peak and hole, e.Å^{-3}	0.530 / -0.699	0.751/ -0.777	0.717 / -0.492	2.402/ -1.942	2.335 / -1.134

Figure 101. Molecular structure of **12b**, with key atoms labelled.
Displacement ellipsoids are at the 50% probability level.

Table 22. Selected bond lengths (Å) and angles (deg) for **12b**.

Bond Distances (Å)			
Ta(2)-Br(5)	2.5637(11)	Ta(2)-Br(6)	2.5414(11)
Ta(2)-Br(7)	2.5051(11)	Ta(2)-Br(8)	2.4759(11)
Ta(2)-Br(9)	2.4593(12)	Ta(2)-Br(10)	2.4931(11)
Ta(1)-Br(1)	2.4508(11)	Ta(1)-Br(2)	2.4476(11)
Ta(1)-Br(3)	2.4103(10)	Ta(1)-Br(4)	2.3890(11)
Ta(1)-N(1)	2.320(8)	Ta(1)-N(2)	2.302(8)
N(1)-C(1)	1.276(12)	N(2)-C(2)	1.270(12)
C(1)-C(2)	1.446(13)		

Angles (deg)			
Br(5)-Ta(2)-Br(10)	177.50(4)	Br(6)-Ta(2)-Br(8)	172.92(4)
Br(7)-Ta(2)-Br(9)	179.01(4)	Br(1)-Ta(1)-Br(2)	166.52(4)
Br(4)-Ta(1)-N(1)	166.27(19)	Br(3)-Ta(1)-N(2)	161.4(2)
N(1)-Ta(1)-N(2)	71.3(3)	Ta(1)-N(1)-C(1)	115.3(6)
Ta(1)-N(1)-C(3)	124.5(6)	C(1)-N(1)-C(3)	118.9(8)
Ta(1)-N(2)-C(2)	113.1(6)	Ta(1)-N(2)-C(15)	129.9(6)
C(2)-N(2)-C(15)	116.4(9)	N(1)-C(1)-C(2)	120.7(10)
N(2)-C(2)-C(1)	117.9(9)		

Table 23. Crystal data and experimental details for **11**, **12a**, **12b**, **13a** and **13b**.

	11	**12a**	**12b**	**13b**	**13b**
Formula	$C_{26}H_{36}Cl_3N_2NbO$	$C_{26}H_{36}Br_{10}N_2Nb_2$	$C_{26}H_{36}Br_{10}N_2Ta_2$	$C_9H_9Cl_5NNb$	$C_9H_9Br_5NNb$
Fw	591.83	1361.49	1537.57	*401.33*	*623.63*
λ, Å	0.71073	0.71073	0.71073	*100(2)*	*100(2)*
Temperature, K	100(2)	100(2)	100(2)	*0.71073*	*0.71073*
Crystal system	Orthorhombic	Monoclinic	Monoclinic	Orthorhombic	Orthorhombic
Space group	*Pnma*	*P2₁*	*P2₁/n*	*Cmcm*	*Cmcm*
a, Å	12.5172(8)	10.805(4)	11.6799(4)	12.7342(12)	13.0763(12)
b, Å	21.3437(14)	13.497(4)	12.2717(5)	15.3656(14)	15.5844(15)
c, Å	10.4112(6)	13.691(5)	27.3280(10)	7.0711(7)	7.2456(7)
α °	90	90	90		
β, °	90	109.104(4)	98.414(2)		
γ, °	90	90	90		
Cell volume, Å³	2781.5(3)	1886.7(11)	3875.2(3)	1383.6(2)	1476.6(2)
Z	4	2	4	*4*	*4*
D_c, g cm⁻³	1.413	2.397	2.635	1.927	2.805
μ, mm⁻¹	0.742	11.217	15.975	1.807	14.319
$F(000)$	1224	1276	2808	784	1144
θ limits, °	1.91 – 25.00	1.57–25.03	1.51 ☐ 25.00	2.077-25.974	2.033-26.989
Reflections collected	37999	15974	54924	8776	7110
Independent reflections	2528 [R_{int} = 0.0903]	6558 [R_{int} = 0.1192]	6811 [R_{int} = 0.1469]	772 [R_{int} = 0.0279]	901 [R_{int} = 0.0373]
Data / restraints /parameters	2528 / 1 / 164	6558 / 465 / 338	6811 / 228 / 369	772 / 0 / 53	901 / 0 / 52
Goodness of fit on F^2	1.093	1.040	1.038	1.251	1.116
$R1$ ($I > 2\sigma(I)$)	0.0475	0.0931	0.0448	0.0210	0.0447
$wR2$ (all data)	0.1250	0.2441	0.1092	0.0470	0.1255
Largest diff. peak and hole, e.Å⁻³	0896 / -1.294	2.690 / -1.928	2.694 / -2.486	0.371 / −0.984	1.638 / −3.036

198

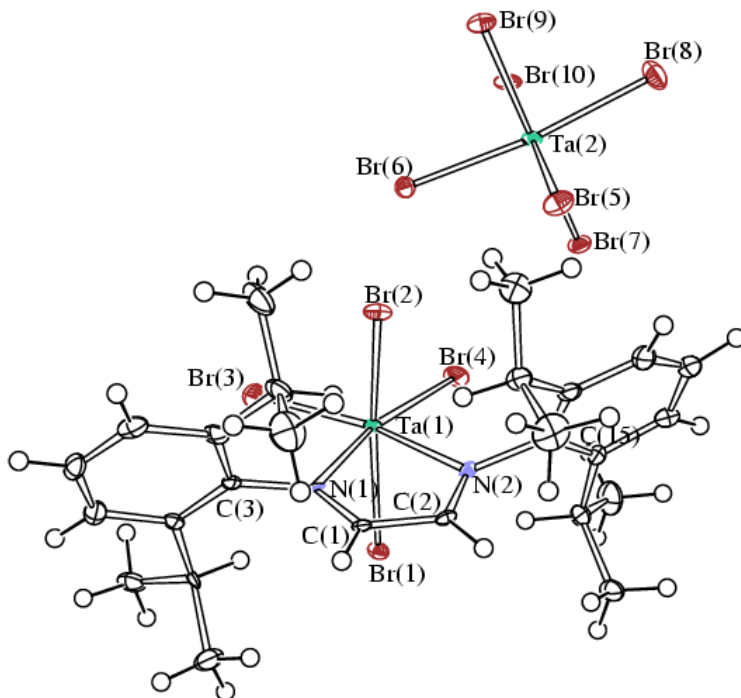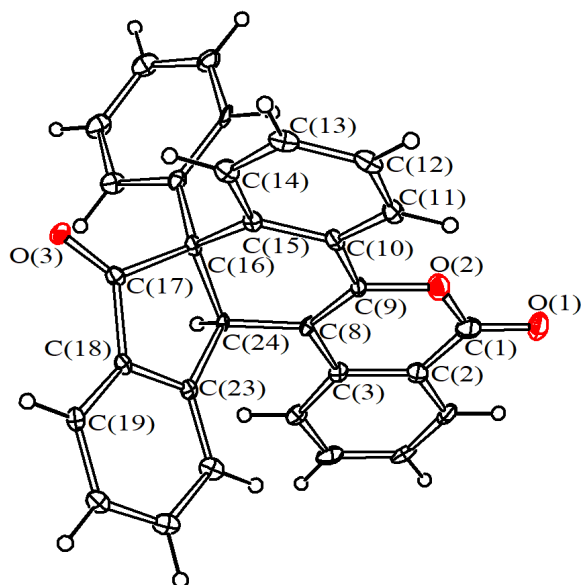**Figure 102.** X-Ray molecular structure of **15** with key atoms labelled.
Displacement ellipsoids are at the 30% probability level.

Table 24. Selected bond lengths (Å) and angles (deg) for **15**.

Bond Distances (Å)			
C(1)-O(1)	1.223(13)	C(1)-O(2)	1.330(13)
C(17)-O(3)	1.194(11)	C(1)-C(2)	1.452(15)
C(8)-C(9)	1.348(13)	C(15)-C(16)	1.516(12)
C(16)-C(17)	1.567(12)	C(16)-C(24)	1.587(12)
Angles (deg)			
C(15)-C(16)-C(17)	106.5(7)	C(15)-C(16)-C(24)	109.9(7)
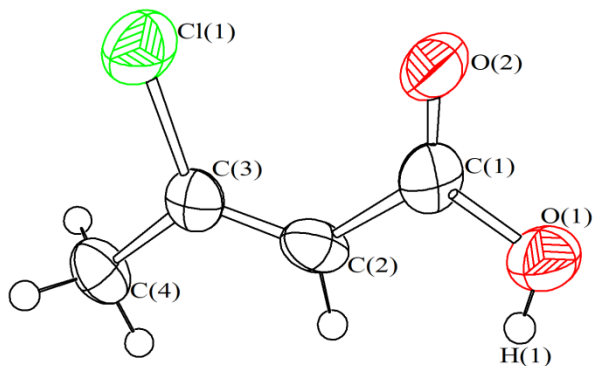
Figure 103. ORTEP drawing of the structure of MeC(Cl)=CHCOOH, **18**. Displacement ellipsoids are at the 50% probability level.

Table 25. Selected bond lengths (Å) and angles (deg) for **18**.

Bond Distances (Å)			
C(1)-O(1)	1.351(13)	C(1)-O(2)	1.179(13)
C(1)-C(2)	1.507(15)	C(2)-C(3)	1.331(14)
C(3)-C(4)	1.496(14)	C(3)-Cl(1)	1.709(12)
Angles (deg)			
O(1)-C(1)-O(2)	122.5(10)	O(1)-C(1)-C(2)	109.2(11)
O(2)-C(1)-C(2)	128.3(10)	C(1)-C(2)-C(3)	126.8(11)
C(2)-C(3)-C(4)	122.9(11)	C(2)-C(3)-Cl(1)	122.6(9)
C(4)-C(3)-Cl(1)	114.5(8)		

200

Table 26. Crystal data and experimental details for **14**, **16**, and **18**.

|	14	16	18
Formula	$C_{30}H_{20}O_2$	$C_{30}H_{19}ClO_2$	$C_4H_5ClO_2$
Fw	412.46	446.90	120.53
T, K	100(2)	100(2)	0.71073
λ, Å	0.71073	0.71073	292(2)
Crystal system	Monoclinic	Monoclinic	Monoclinic
Space group	$P2_1/c$	$P2_1/n$	$P2_1/n$
a, Å	11.0410(6)	11.1693(19)	5.387(15)
b, Å	11.1879(6)	10.7604(19)	9.02(3)
c, Å	16.9592(10)	17.788(3)	11.16(3)
β, °	107.115(2)	103.215(5)	101.87(5)
Cell Volume, Å³	2002.12(19)	2081.2(6)	531(3)
Z	4	4	4
D_c, g cm⁻³	1.368	1.426	1.509
μ, mm⁻¹	0.084	0.211	0.597
F(000)	864	928	248
Crystal size, mm	0.18×0.16×0.14	0.18×0.15×0.10	
θ limits, °	1.930–25.493	1.971–25.099	2.929 - 24.999
Reflections collected	24951	25632	3721
Independent reflections	3729 [R_{int}=0.0705]	3711 [R_{int}=0.1038]	925 [R_{int} = 0.2230]
Data / restraints /parameters	3729 / 0 / 289	3711 / 12 / 298	925 / 0 / 66
Goodness on fit on F^2	1.138	1.181	1.081
R_1 (*I*> 2σ(*I*))	0.0664	0.0789	0.1338
wR_2 (all data)	0.1422	0.1544	0.3275
Largest diff. peak and hole, e Å⁻³	0.338/–0.362	0.368/–0.567	0.550 / -0.511
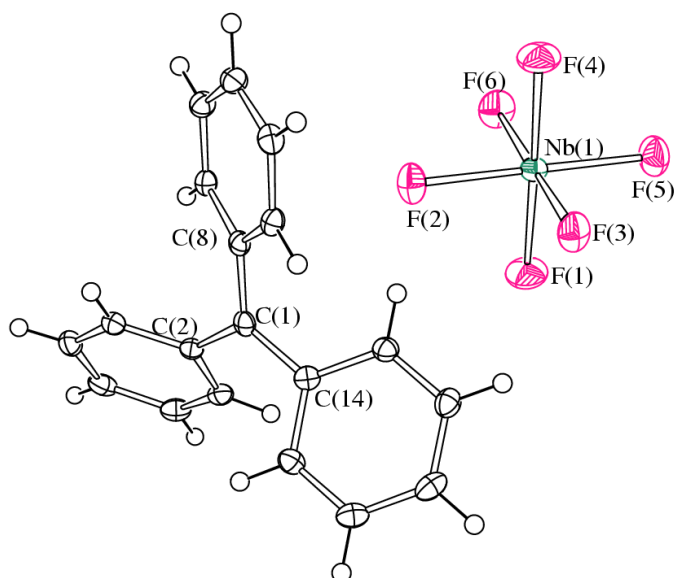
Figure 104. Molecular structure of [Ph₃C][NbF₆], **22**, with key atoms labelled. Thermal ellipsoids are at the 50% probability level.

Table 27. Selected bond lengths (Å) and angles (deg) for **22**.

Bond Distances (Å)			
Nb(1)–F(1)	1.8698(13)	Nb(1)–F(2)	1.8963(13)
Nb(1)–F(3)	1.8885(13)	Nb(1)–F(4)	1.8774(13)
Nb(1)–F(5)	1.8919(14)	Nb(1)–F(6)	1.8892(13)
C(1)–C(2)	1.447(3)	C(1)–C(8)	1.440(3)
C(1)–C(14)	1.452(3)		
Angles (deg)			
F(1)–Nb(1)–F(4)	178.25(6)	F(2)–Nb(1)-F(5)	179.20(5)
F(3)–Nb(1)–F(6)	178.39(6)	C(2)–C(1)–C(8)	120.79(18)
C(2)–C(1)–C(14)	118.87(18)	C(8)–C(1)–C(14)	120.29(18)
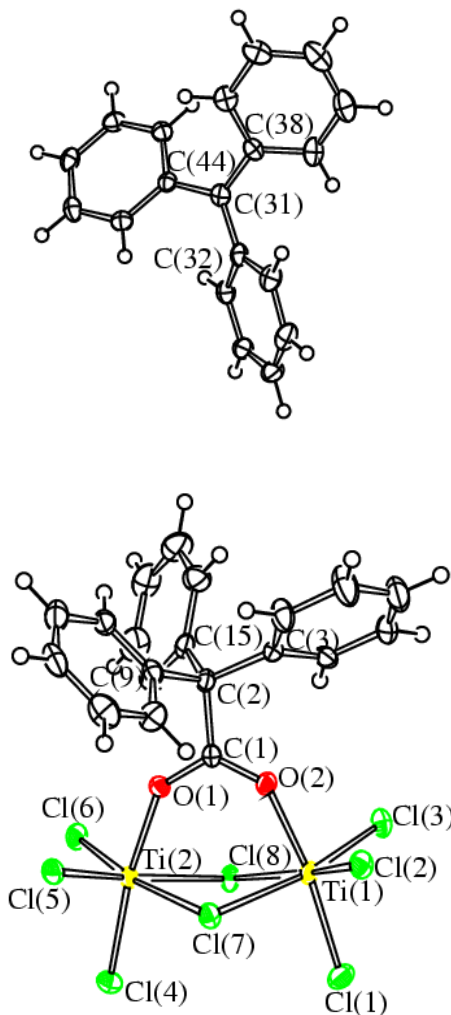
Figure 105. Molecular structure of [Ph₃C][Ti₂Cl₈(OOCCPh₃)], **24**, with key atoms labelled. Thermal ellipsoids are at the 50% probability level.

Table 28. Selected bond lengths (Å) and angles (deg) for **24**.

Bond Distances (Å)			
Ti(1)–O(2)	2.008(4)	Ti(2)–O(1)	2.000(3)
Ti(1)–Cl(1)	2.2406(16)	Ti(2)–Cl(4)	2.2402(16)
Ti(1)–Cl(2)	2.2165(16)	Ti(2)–Cl(5)	2.2205(16)

Ti(1)–Cl(3)	2.2368(16)	Ti(2)–Cl(6)	2.2272(16)
Ti(1)–Cl(7)	2.4790(15)	Ti(2)–Cl(7)	2.4835(15)
Ti(1)–Cl(8)	2.5054(15)	Ti(2)–Cl(8)	2.5051(15)
C(1)–O(1)	1.262(6)	C(1)–O(2)	1.249(6)
C(1)–C(2)	1.534(7)	C(2)–C(3)	1.550(7)
C(2)–C(9)	1.536(7)	C(2)–C(15)	1.560(7)
C(31)–C(32)	1.447(7)	C(31)–C(38)	1.433(7)
C(31)–C(44)	1.454(7)		

Angles (deg)

O(2)–Ti(1)–Cl(1)	170.42(11)	O(1)–Ti(2)–Cl(4)	171.96(11)
Cl(2)–Ti(1)–Cl(8)	166.45(6)	Cl(5)–Ti(2)–Cl(8))	165.76(6)
Cl(3)–Ti(1)–Cl(7)	168.12(6)	Cl(6)–Ti(2)–Cl(7)	168.41(6)
Cl(2)–Ti(1)–Cl(3))	99.84(6)	Cl(5)–Ti(2)–Cl(6)	101.52(6)
Cl(7)–Ti(1)–Cl(8)	79.15(5)	Cl(7)–Ti(2)–Cl(8)	79.07(5)
Ti(1)–Cl(7)–Ti(2)	97.73(5)	Ti(1)–Cl(8)–Ti(2)	96.48(5)
Ti(1)–O(2)–C(1)	141.4(3)	Ti(2)–O(1)–C(1)	140.1(3)
O(1)–C(1)–O(2)	123.2(5)	O(1)–C(1)–C(2)	116.7(4)
O(2)–C(1)–C(2)	120.1(4)	C(1)–C(2)–C(3)	109.8(4)
C(1)–C(2)–C(9)	105.4(4)	C(1)–C(2)–C(15)	110.3(4)
C(32)–C(31)–C(38)	119.8(5)	C(32)–C(31)–C(44)	118.7(5)
C(38)–C(31)–C(44)	119.8(5)		

204

Table 29. Crystal data and experimental details for **19**, **21**, **22** and **24·2CH$_2$Cl$_2$**

|	19	21	22	24·2CH$_2$Cl$_2$
Formula	C$_{19}$H$_{15}$Cl$_5$OW	C$_{19}$H$_{15}$Cl$_4$MoO	C$_{19}$H$_{15}$F$_6$Nb	C$_{41}$H$_{34}$Cl$_{12}$O$_2$Ti$_2$
Fw	620.41	497.05	450.22	1079.88
λ, Å	0.71073	0.71073	0.71073	0.71073
Temperature, *K*	100(2)	100(2)	100(2)	100(2)
Crystal system	Monoclinic	Monoclinic	Monoclinic	Monoclinic
Space group	P2$_1$/c	P2$_1$/n	P2$_1$/c	P2$_1$/n
a, Å	14.275(2)	8.9934(15)	8.5095(15)	17.897(3)
b, Å	7.9205(11)	19.335(3)	12.681(2)	10.5524(18)
c, Å	18.698(3)	11.3379(19)	16.036(3)	25.825(5)
β, °	103.080(2)	98.547(2)	94.183(2)	106.889(2)
Cell volume, Å^3	2059.2(5)	1949.6(6)	1725.9(5)	4666.8(14)
Z	4	4	4	4
D$_c$, g cm^{-3}	2.001	1.693	1.733	1.537
μ, mm^{-1}	6.265	1.225	0.757	1.064
F(000)	1184	988	896	2176
θ limits, °	1.465 - 25.049	2.100 - 26.996	2.050 - 27.000	1.234 - 25.026
Reflections collected	16758	21352	18372	43028
Independent reflections	3654 [R$_{int}$ = 0.0568]	4254 [R$_{int}$ = 0.0254]	3763 [R$_{int}$ = 0.0335]	8248 [R$_{int}$ = 0.0717]
Data / restraints / parameters	3654 / 1 / 235	4254 / 0 /226	3763 / 0 / 235	8248 / 27 / 512
Goodness on fit on *F*^{2}	1.076	1.104	1.044	1.045
*R*1 (*I*> 2σ(*I*))	0.0374	0.0227	0.0266	0.0617
*wR*2 (all data)	0.0875	0.0560	0.0647	0.1896
Largest diff. peak and hole, e.Å^{-3}	2.845 / -1.399	0.528 / -0.587	0.365 / -0.458	2.805 / -1.361
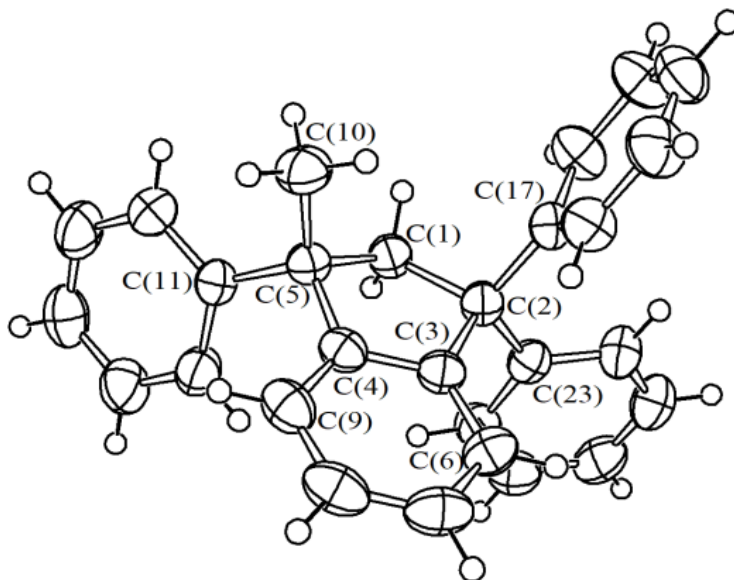
Figure 106. Molecular structure of **25a** with key atoms labelled. Thermal ellipsoids are at the 50% probability level.

Table 30. Selected bond lengths (Å) and angles (deg) for **25a**.

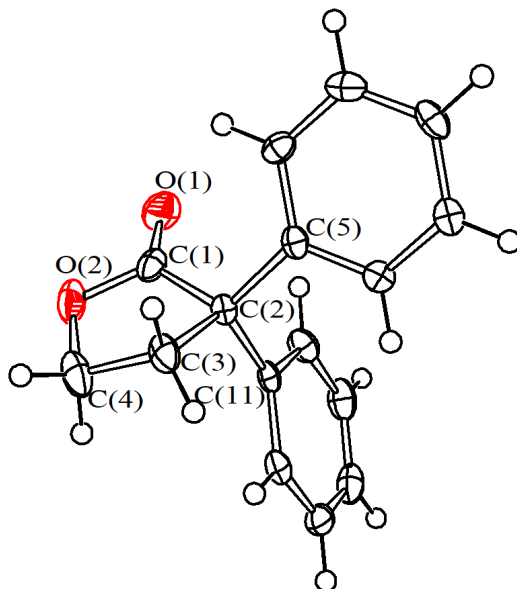| Bond Distances (Å)			
C(1)-C(2)	1.5662(17)	C(2)-C(3)	1.5270(17)
C(3)-C(4)	1.3868(18)	C(4)-C(5)	1.5191(18)
C(1)-C(5)	1.5599(17)		
Angles (deg)			
C(5)-C(1)-C(2)	107.99(10)	C(1)-C(2)-C(3)	101.16(10)
C(2)-C(3)-C(4)	111.91(11)	C(3)-C(4)-C(5)	112.14(11)
C(4)-C(5)-C(1)	113.65(10)		

Figure 107. ORTEP drawing of the structure of **28**. Displacement ellipsoids are at the 50% probability level.

Table 31. Selected bond lengths (Å) and angles (deg) for **28**.

Bond Distances (Å)			
C(1)-O(1)	1.187(4)	C(1)-O(2)	1.341(4)
C(1)-C(2)	1.538(5)	C(2)-C(3)	1.541(4)
C(3)-C(4)	1.510(5)	C(4)-O(2)	1.454(5)
C(2)-C(5)	1.532(4)	C(2)-C(11)	1.540(5)
Angles (deg)			
O(2)-C(1)-C(2)	128.5(3)	O(2)-C(1)-O(1)	121.9(3)
O(1)-C(1)-C(2)	109.6(3)	C(1)-C(2)-C(3)	100.9(3)
C(2)-C(3)-C(4)	102.3(3)	C(3)-C(4)-O(2)	104.3(3)
C(4)-O(2)-C(1)	110.9(3)	C(5)-C(2)-C(11)	110.5(3)

Table 32. Crystal data and experimental details for **25a** and **28**.

	25a	28
Formula	$C_{28}H_{24}$	$C_{16}H_{14}O_2$
Fw	360.47	238.27
λ, Å	0.71073	0.71073
Temperature, *K*	293(2)	100(2)
Crystal system	Monoclinic	Monoclinic
Space group	$P2_1/n$	Pc
a, Å	11.0309(3)	7.3476(6)
b, Å	17.4337(5)	15.2022(11)
c, Å	11.3811(3)	10.9707(9)
β, °	111.847(2)	91.960(3)
Cell volume, Å^3	2031.50(10)	1224.71(17)
Z	4	4
D_c, g cm^{-3}	1.179	1.292
μ, mm^{-1}	0.066	0.084
F(000)	768	504
θ limits, °	2.195 - 26.999	1.339 - 25.998
Reflections collected	34185	14249
Independent reflections	4436 [R_{int} = 0.0409]	4780 [R_{int} = 0.0446]
Data / restraints / parameters	4436 / 0 / 254	4780 / 2 / 325
Goodness on fit on F^2	1.024	1.070
*R*1 ($I > 2\sigma(I)$)	0.0406	0.0489
*wR*2 (all data)	0.1099	0.0995
Largest diff. peak and hole, e.Å^{-3}	0.185 / -0.146	0.192 / -0.272

5.11. Computational Details.

All the computational studies were performed by Dr. Marco Bortoluzzi (University of Venice), with the exception of calculations related to compounds **13a** and **13b**, which were performed by Dr. Gianluca Ciancaleoni (University of Pisa). The electronic structures of the compounds were optimized using the range-separated ωB97X DFT functional[475–477] in combination with Ahlrichs' split-valence polarized basis set, with ECP on the metal centres.[478,479] The "unrestricted" formalism was applied to compounds with unpaired electrons, and the lack of spin contamination was verified by comparing the computed $<S^2>$ values with the theoretical ones. The C-PCM implicit solvation model (ε = 9.08) was added to the ωB97X calculations.[480,481] The stationary points were characterized by IR simulations (harmonic approximation), from which zero-point vibrational energies and thermal corrections (T = 298.15K) were obtained.[482] The software used was Gaussian 09.[483]

For compounds **13a** and **13b**, the geometry optimizations and bond analysis have been computed with the ADF package (version 2014.09)[484] at the density functional theory (DFT) level using TZ2P Slater-type basis sets, Becke's exchange functional[485] in combination with the Lee-Yang-Parr correlation functional,[486] frozen-core approximation and ZORA Hamiltonian to account for scalar relativistic effects.[487–489] The numerical integration grid was employed with precision 6.0.
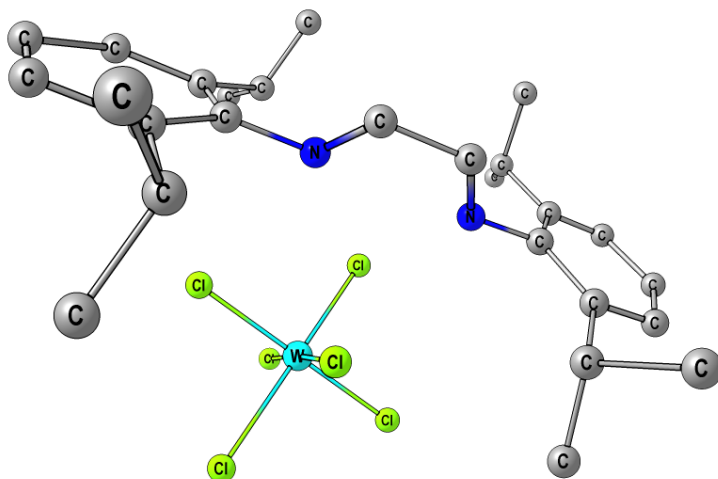
Figure 108. DFT-optimized structure of WCl_6---DAD_{Dipp}. C-PCM/ωB97X, dichloromethane as continuous solvent. Hydrogen atoms are omitted for clarity. Selected computed distances (Å): W-Cl 2.268, 2.275, 2.291, 2.312, 2.317, 2.320; C=N 1.265, 1.267; W---N 4.183, 4.330.
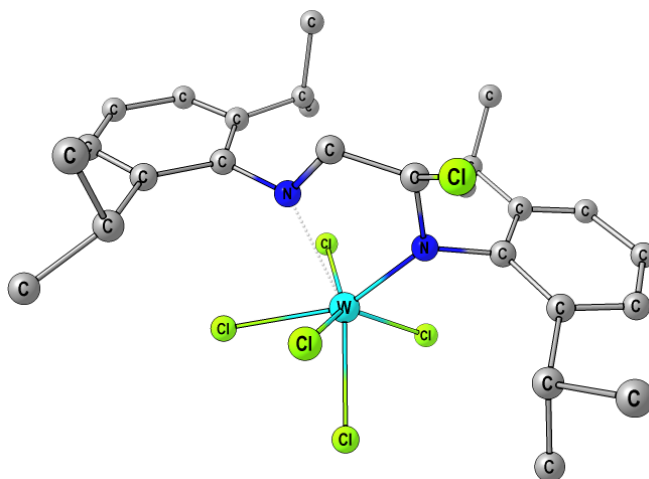

Figure 109. DFT-optimized structure of $W^{VI}Cl_5(N\{2,6$-$C_6H_3(CHMe_2)_2\}CHClCHN\{2,6$-$C_6H_3(CHMe_2)_2\})$ (**Figure 57**, intermediate **A**). C-PCM/ωB97X, dichloromethane as continuous solvent. Hydrogen atoms are omitted for clarity. Selected computed distances (Å): W-Cl 2.363, 2.363, 2.379, 2.379, 2.430; W-N 1.983, 2.431; C=N 1.268; C(Cl)-N 1.450; C-Cl 1.793.
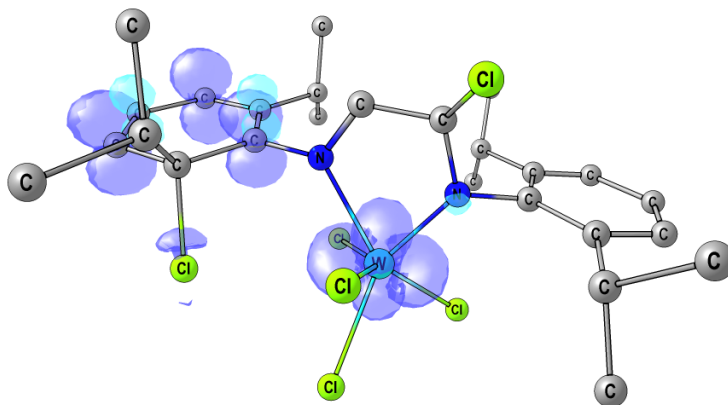
Figure 110. DFT-optimized structure of $W^VCl_4(N\{2$-Cl-2,6-$C_6H_3(CHMe_2)\}CHClCHN\{2,6$-$C_6H_3(CHMe_2)_2\})$ (**Figure 57**, intermediate **B**) and spin density surface (isovalue = 0.01 a.u.). C-PCM/ωB97X, dichloromethane as continuous solvent. Hydrogen atoms are omitted for clarity. Selected computed distances (Å): W-Cl 2.333, 2.364, 2.370, 2.389; W-N 1.981, 2.288; C=N 1.275; C(Cl)-N 1.439; C(N)-Cl 1.807; C(^{i}Pr)-Cl 1.863.
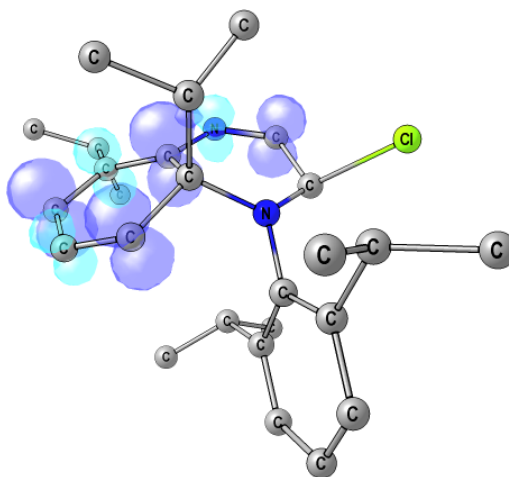

Figure 111. DFT-optimized structure of $\{2,6$-$C_6H_3(CHMe_2)_2\}N(CHCl)(CH)NCC(CHMe_2)(CH)_3C(CHMe_2)$ (**Figure 57**, intermediate **C**) and spin density surface (isovalue = 0.01 a.u.). C-PCM/ωB97X, dichloromethane as continuous solvent. Hydrogen atoms are omitted for clarity. Selected computed distances (Å): N-C(Cl) 1.385; C-Cl 1.926; C(Cl)-C 1.497; C=N 1.281.
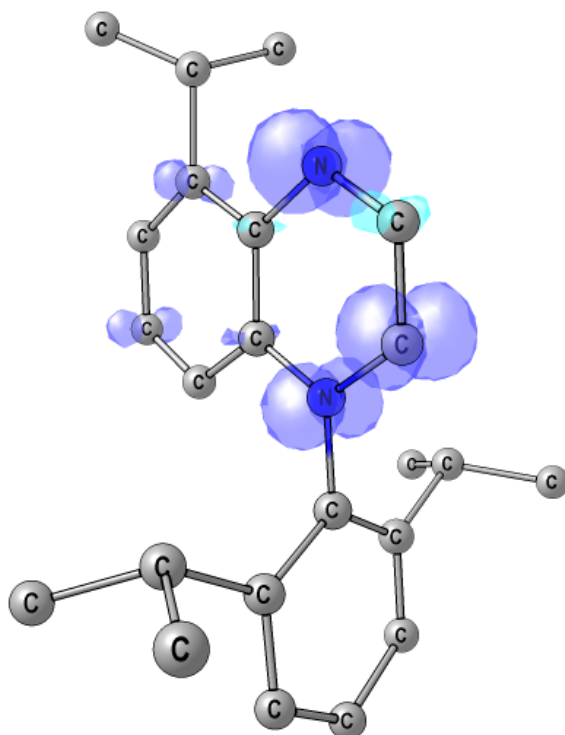
Figure 112. DFT-optimized structure of {2,6-$C_6H_3(CHMe_2)_2$}$N(CH)_2NCC(CHMe_2)(CH)_3C$ (**Figure 57**, intermediate **D**) and spin density surface (isovalue = 0.01 a.u.). C-PCM/ωB97X, dichloromethane as continuous solvent. Hydrogen atoms are omitted for clarity. Selected computed distances (Å): N-C(H) 1.338, 1.378; C(N)-C(N) 1.375, 1.425.
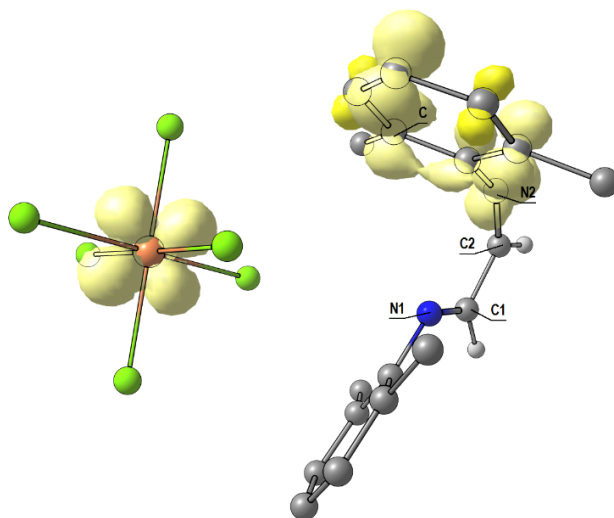
Figure 113. DFT-optimized geometry of [DAD$_{Xyl}$][WCl$_6$] (C-PCM/ωB97X calculations) and spin density surface (isovalue = 0.01 a.u.). Hydrogen atoms on the Xyl moieties are omitted for clarity. Selected computed lengths (Å): C1-N1 1.265, C2-N2 1.258, C1-C2 1.494, W-Cl (average) 2.348, W---N1 5.302, W---N2 6.687.
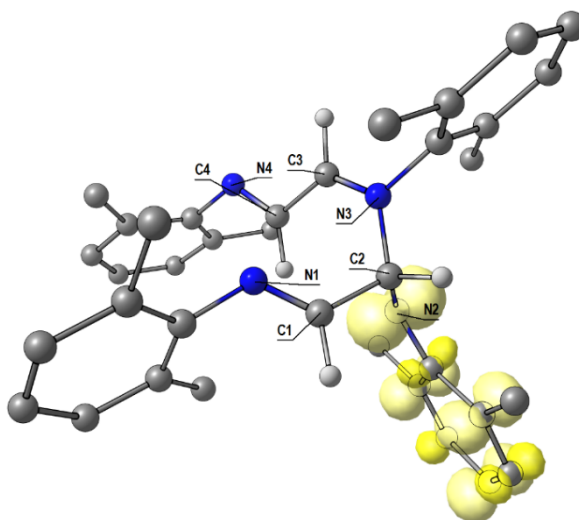
Figure 114. DFT-optimized geometry of [XylNCHCHN(Xyl)CH(NXyl)CHNXyl]$^{+•}$ (C-PCM/ωB97X calculations) and spin density surface (isovalue = 0.01 a.u.). Hydrogen atoms on the Xyl moieties are omitted for clarity. Selected computed lengths (Å): C1-N1 1.258, C2-N2 1.425, C2-N3 1.492, C3-N3 1.288, C4-N4 1.268, C1-C2 1.529, C3-C4 1.471.

Figure 115. DFT-optimized geometry of [XylNCHCHN(Xyl)CH(NXyl)CHNXyl]²⁺ (C-PCM/ωB97X calculations). Hydrogen atoms on the Xyl moieties are omitted for clarity. Selected computed lengths (Å): C1-N1 1.253, C2-N2 1.429, C2-N3 1.481, C3-N3 1.293, C4-N4 1.269, C1-C2 1.541, C3-C4 1.467.
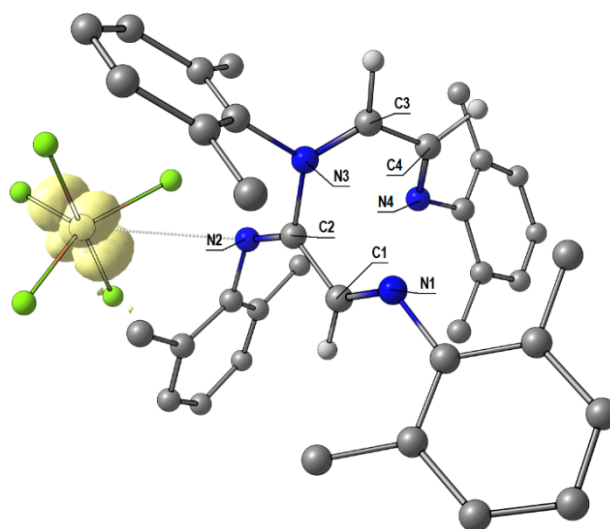
Figure 116. DFT-optimized geometry of [WCl₅{N(Ar)C(CHNXyl)NXylCHCHNXyl}]⁺ (C-PCM/ωB97X calculations) and spin density surface (isovalue = 0.01 a.u.). Hydrogen atoms on the Xyl moieties are omitted for clarity. Selected computed lengths (Å): C1-N1 1.265, C2-N2 1.256, C2-N3 1.464, C3-N3 1.291, C4-N4 1.271, C1-C2 1.491, C3-C4 1.471, W-Cl (average) 2.294, W---N2 4.307.
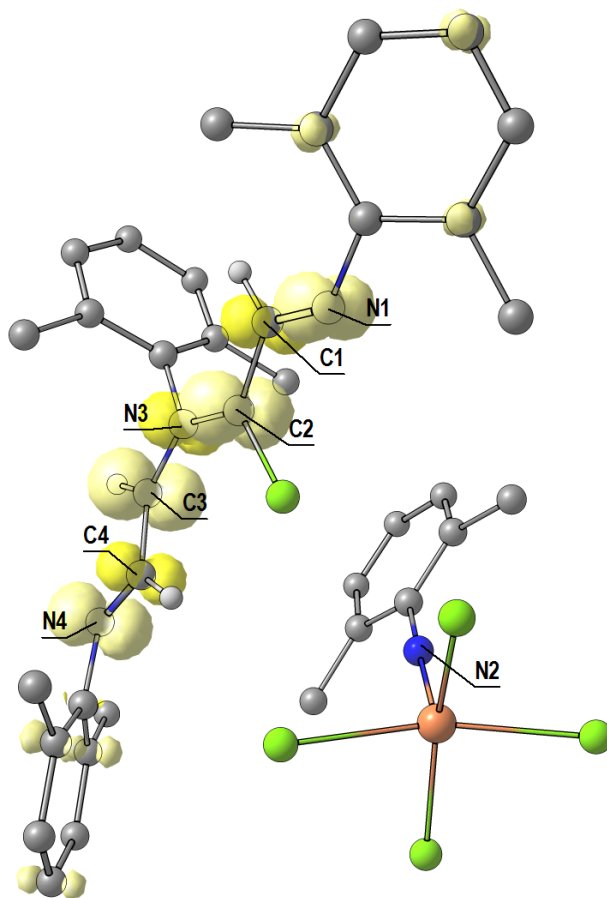
Figure 117. DFT-optimized geometry of WCl₄(NClXyl) and

[XylNCHCHN(Xyl)C(Cl)CHNXyl]⁺˙ (C-PCM/ωB97X calculations) and spin density

surface (isovalue = 0.01 a.u.). Hydrogen atoms on the Xyl moieties are omitted for

clarity. Selected computed lengths (Å): C1-N1 1.284, C2-Cl 1.689, C2-N3 1.355,

C3-N3 1.354, C4-N4 1.296, C1-C2 1.449, C3-C4 1.430, W-Cl (average) 2.341, W-
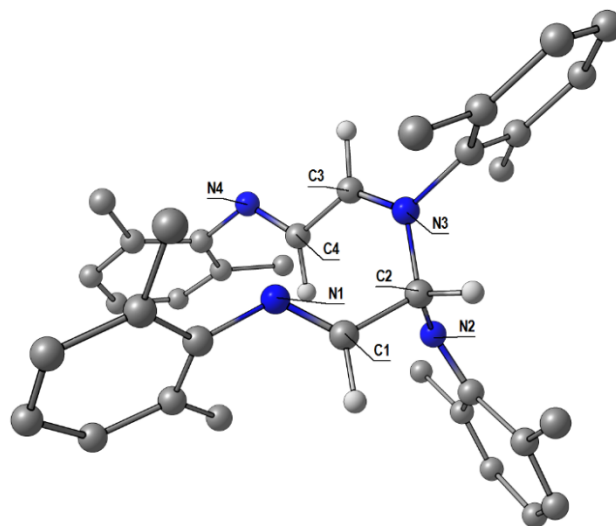
N2 1.693.
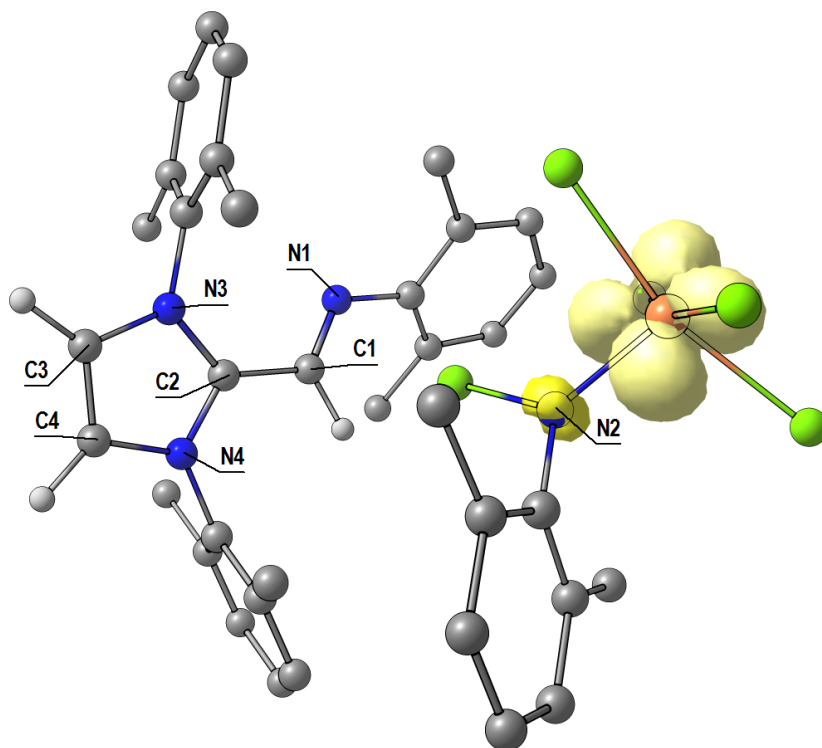
Figure 118. DFT-optimized geometry of WCl$_4$(NClXyl) and of the cation in **1** (C-PCM/ωB97X calculations) and spin density surface (isovalue = 0.01 a.u.). Hydrogen atoms on the Xyl moieties are omitted for clarity. Selected computed lengths (Å): C1-N1 1.267, C2-N3 1.343, C2-N4 1.344, C3-N3 1.379, C4-N4 1.376, C1-C2 1.471, C3-C4 1.360, W-Cl (average) 2.335, W-N2 1.881, N2-Cl 1.746.
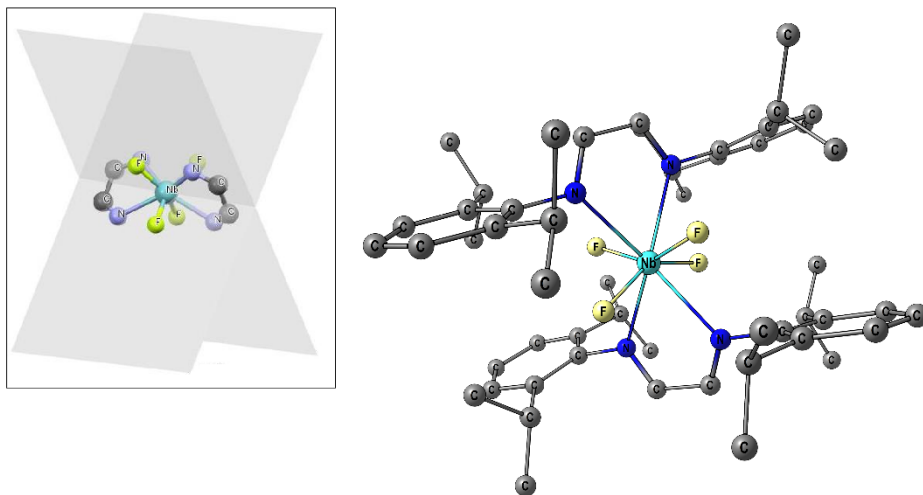
Figure 119. DFT-optimized geometry for the [NbF$_4$(DAD$_{Dipp}$)$_2$]$^+$ cation in **10a** (C-PCM/ωB97X, dichloromethane as continuous medium). Hydrogen atoms are omitted for clarity. Selected bond lengths (Å): Nb-F 1.885, 1.885, 1.886, 1.886; Nb-N 2.434, 2.434, 2.438, 2.438; C=N 1.272, 1.272, 1.272, 1.272. Selected angles (°): N-Nb-N (chelate) 67.0, 67.0; F-Nb-F (trans) 146.1, 146.1. Inset: planes crossing the DAD$_{Dipp}$ donor moieties.
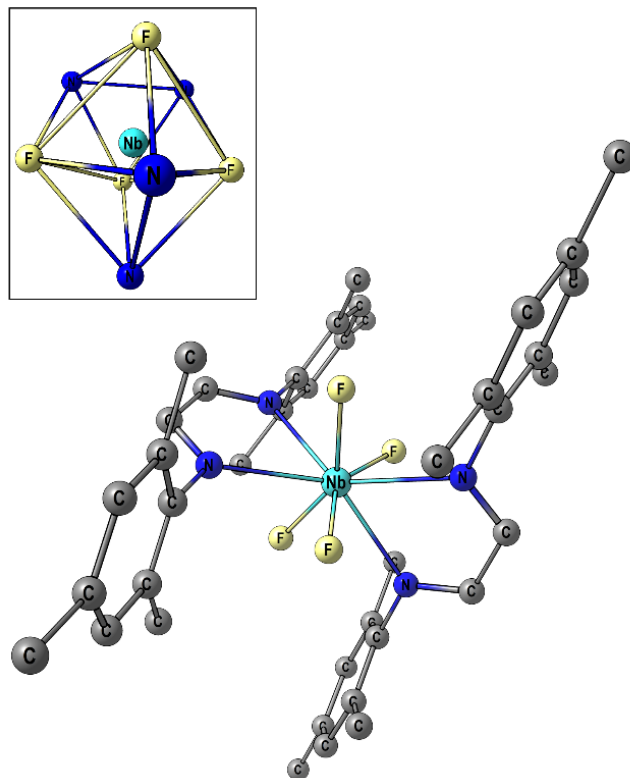
Figure 120. DFT-optimized geometry for the [NbF$_4$(DAD$_{Mes}$)$_2$]$^+$ cation in **10c** (C-PCM/ωB97X, dichloromethane as continuous medium). Hydrogen atoms are omitted for clarity. Selected bond lengths (Å): Nb-F 1.889, 1.889, 1.889, 1.889; Nb-N 2.401, 2.401, 2.401, 2.401; C=N 1.271, 1.271, 1.271, 1.271. Selected angles (°): N-Nb-N (chelate) 67.6, 67.6; F-Nb-F (trans) 145.2, 145.2.

Inset: polyhedron around the metal centre.
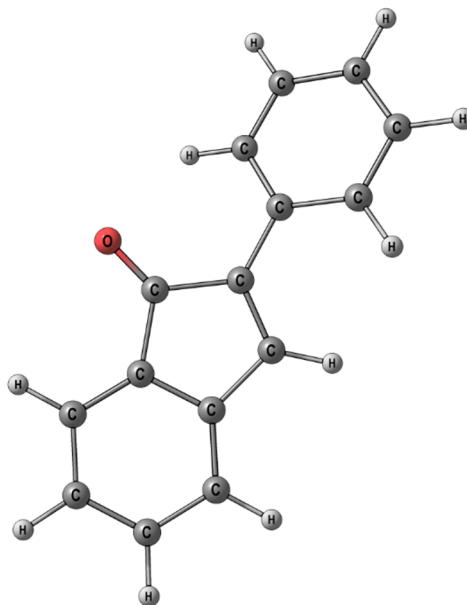
Figure 121. DFT-optimized structure for 2-phenylindenone (intermediate **B**) in the mechanistic pathway to **14** (**Figure 80**). C-PCM/ωB97X calculations, chloroform as continuous medium.
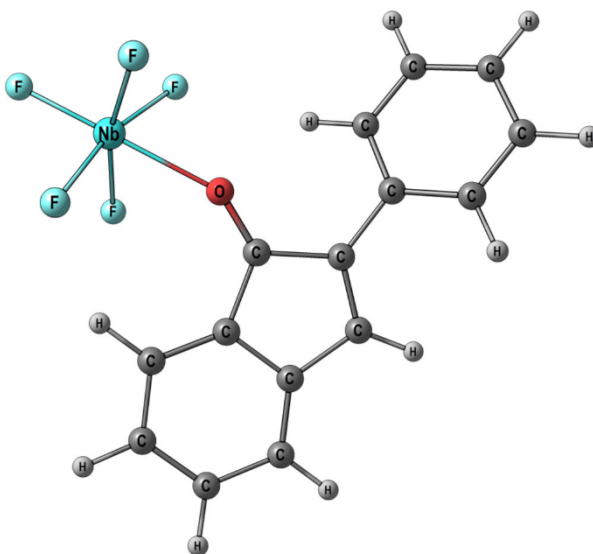
Figure 122. DFT-optimized structure for intermediate **B-NbF₅** in the mechanistic pathway to **14** (**Figure 80**). C-PCM/ωB97X calculations, chloroform as continuous medium.
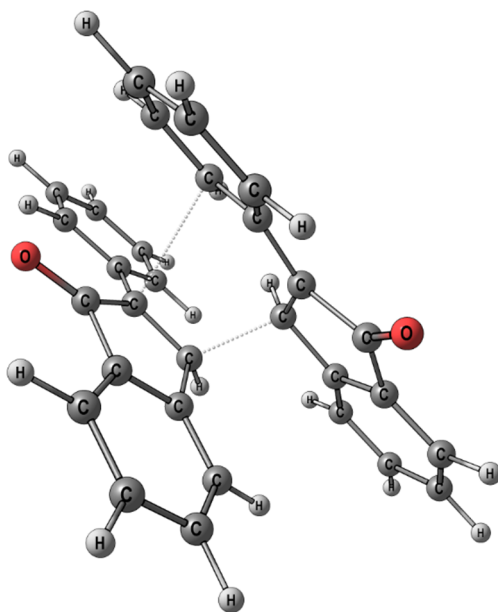
Figure 123. DFT-optimized structure for transition state **TS** in the mechanistic pathway to **14** (**Figure 80**). C-PCM/ωB97X calculations, chloroform as continuous medium.
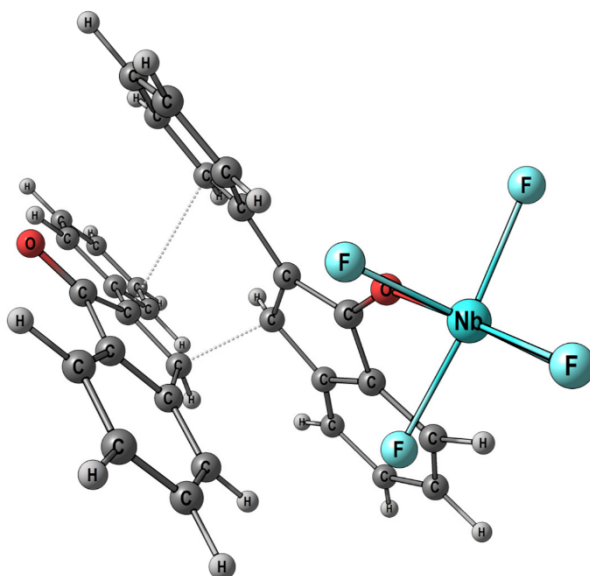
Figure 124. DFT-optimized structure for transition state **TS-NbF₅-diene** in the mechanistic pathway to **14** (**Figure 80**). C-PCM/ωB97X calculations, chloroform as continuous medium.
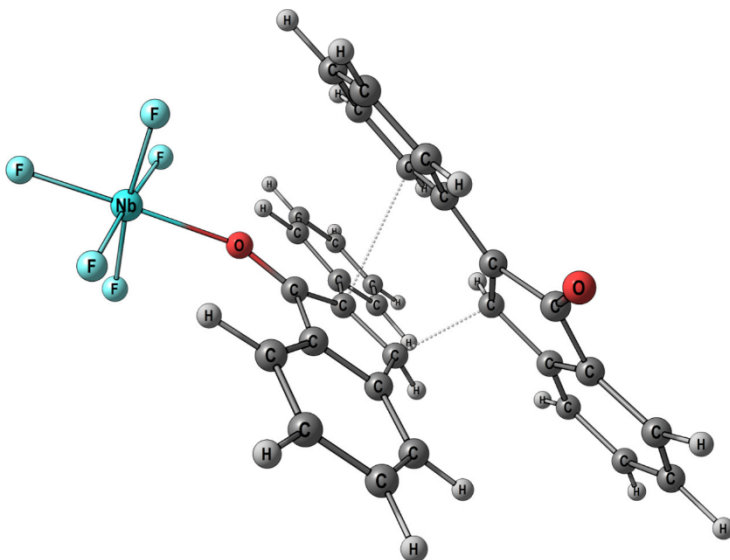
Figure 125. DFT-optimized structure for transition state **TS-NbF$_5$-dienophile** in the mechanistic pathway to **14** (**Figure 80**). C-PCM/ωB97X calculations, chloroform as continuous medium.
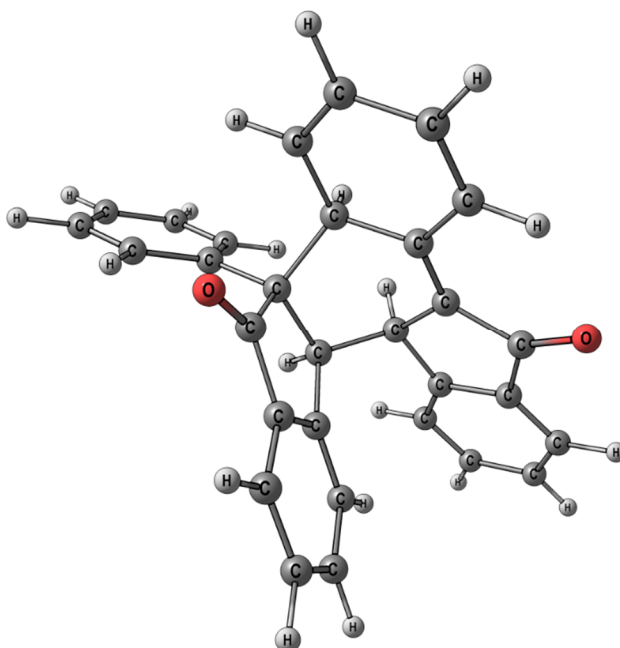
Figure 126. DFT-optimized structure for intermediate **C** in the mechanistic pathway to **14** (**Figure 80**). C-PCM/ωB97X calculations, chloroform as continuous medium.
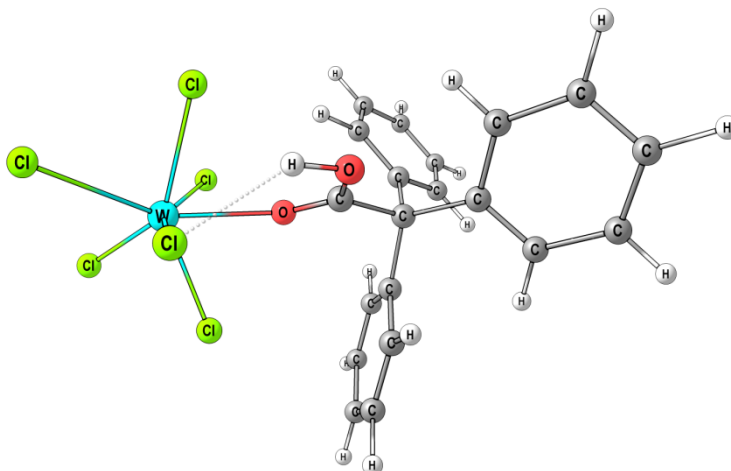
Figure 127. DFT-optimized geometry of [WCl$_6${OC(OH)CPh$_3$}] (intermediate **a**, **Figure 87**) (C-PCM-ωB97X calculations, dichloromethane as continuous medium). Selected computed bond lengths (Å): W-Cl 2.302, 2.324, 2.331, 2.354, 2.418, 2.432; W-O 2.208; C=O 1.240; C-O(H) 1.289; C-CPh$_3$ 1.531; O-H 0.983; H---Cl 2.112. Selected computed angles (°): O-W-Cl 72.6, 72.8, 74.7, 78.9, 137.0, 144.6; W-O-C 144.3; O-C-O 124.5; C-O-H 110.8; O-H-Cl 141.5.
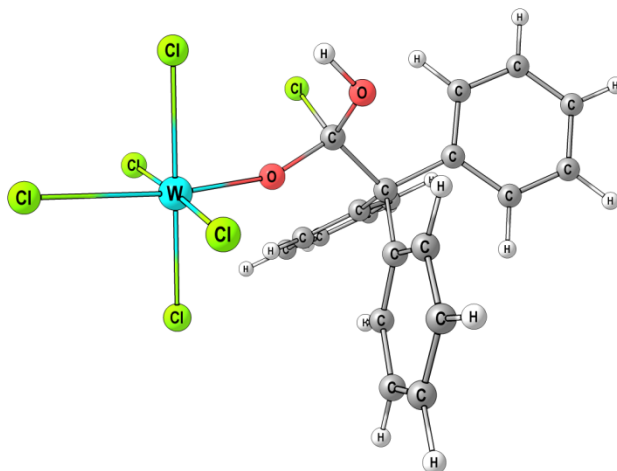
Figure 128. DFT-optimized geometry of [WCl$_5${OCCl(OH)CPh$_3$}] (intermediate **b**, **Figure 87**) (C-PCM-ωB97X calculations, dichloromethane as continuous medium). Selected computed bond lengths (Å): W-Cl 2.293, 2.302, 2.309, 2.312, 2.364; W-O 1.821; C-O 1.433; C-O(H) 1.344; C-CPh$_3$ 1.581; C-Cl 1.810; O-H 0.972. Selected computed angles (°): O-W-Cl 85.7, 94.6, 90.5, 92.8, 172.0; W-O-C 157.0; O-C-O 108.8; O-C-Cl 103.5, 110.5.

222
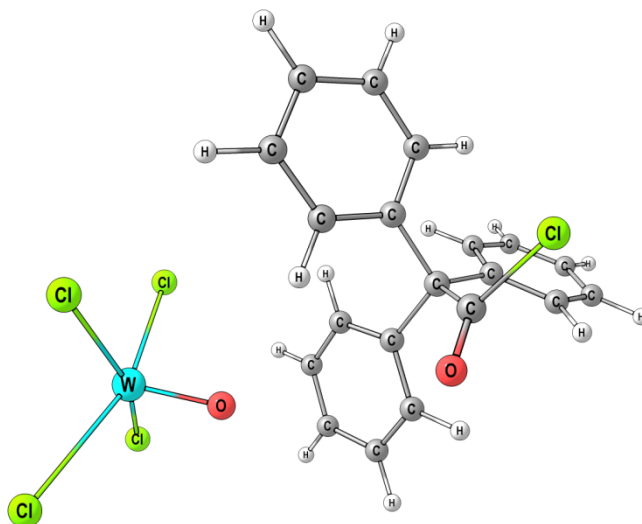
Figure 129. DFT-optimized geometry of WOCl$_4$ + Ph$_3$CCOCl (intermediate **c**, **Figure 87**) (C-PCM-ωB97X calculations, dichloromethane as continuous medium). Selected computed bond lengths (Å): W-Cl 2.315, 2.316, 2.320, 2.327; W=O 1.654; C=O 1.184; C-CPh$_3$ 1.544; C-Cl 1.787. Selected computed angles (°): O=W-Cl 99.5, 99.9, 100.7, 100.7; O-C-Cl 118.8.
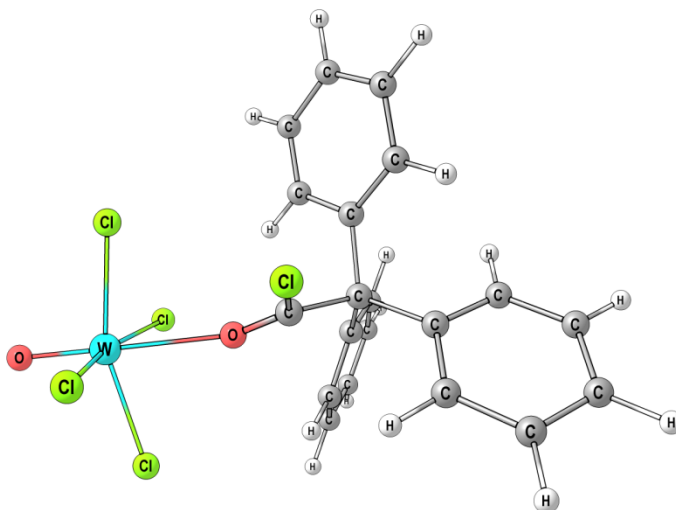
Figure 130. DFT-optimized geometry of [WOCl$_4$(OCClCPh$_3$)] (intermediate **d**, **Figure 87**) (C-PCM-ωB97X calculations, dichloromethane as continuous medium). Selected computed bond lengths (Å): W-Cl 2.316, 2.318, 2.321, 2.328; W=O 1.660; W-O 2.389; C=O 1.203; C-CPh$_3$ 1.534; C-Cl 1.737. Selected computed angles (°): O=W-Cl 98.7, 98.8, 100.1, 100.3; O=W-O 178.8; O-C-Cl 119.2.

223
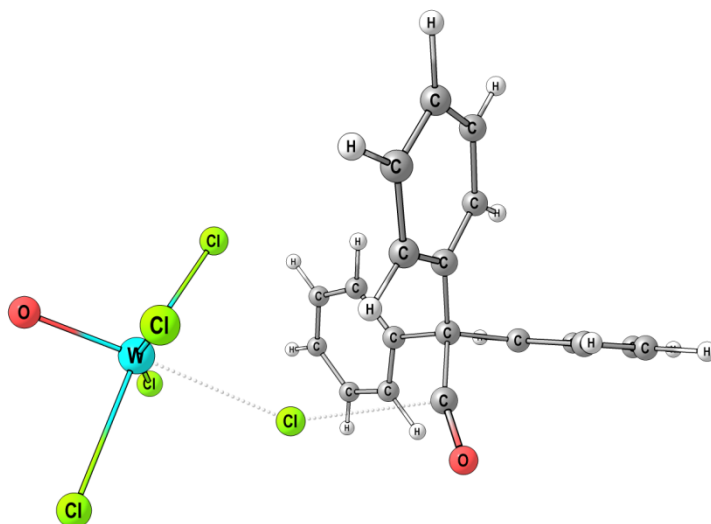
Figure 131. DFT-optimized geometry of [WOCl4---Cl---C(O)CPh3)] (transition state **ts1**, **Figure 87**) (C-PCM-ωB97X calculations, dichloromethane as continuous medium). Selected computed bond lengths (Å): W-Cl 2.328, 2.330, 2.332, 2.344; W=O 1.668; W---Cl 2.660; C=O 1.123; C-CPh3 1.488; C---Cl 2.670. Selected computed angles (°): O=W-Cl 95.5, 96.1, 96.3, 96.7; O=W---Cl 177.9; O-C---Cl 94.6. Imaginary frequency i76.2 cm^{-1}.
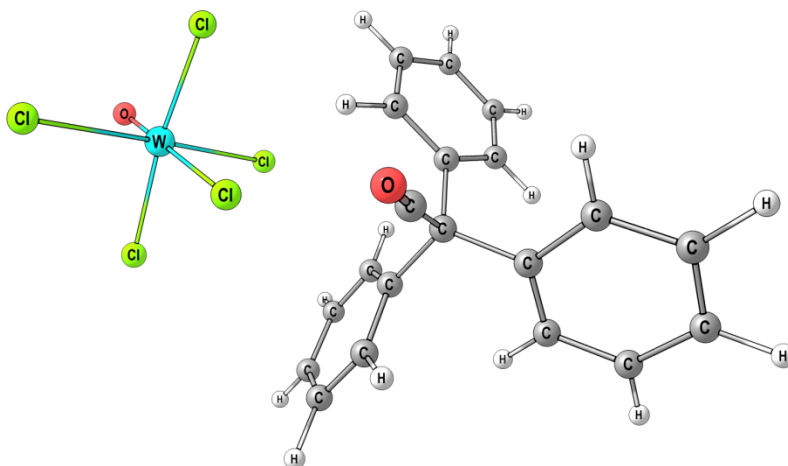
Figure 132. DFT-optimized geometry of [Ph3CCO][WOCl5] (intermediate **e**, **Figure 87**) (C-PCM-ωB97X calculations, dichloromethane as continuous medium). Selected computed bond lengths (Å): W-Cl 2.333, 2.335, 2.341, 2.353, 2.583; W=O 1.673; C=O 1.118; C-CPh3 1.469. Selected computed angles (°): O=W-Cl 94.3, 95.0, 95.3, 95.8, 178.4; O-C-C 172.2.
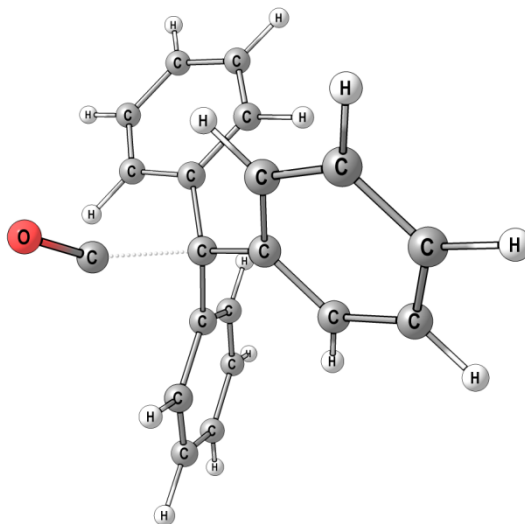
Figure 133. DFT-optimized geometry of [CPh₃---CO]⁺ (transition state **ts2**, **Figure 87**) (C-PCM-ωB97X calculations, dichloromethane as continuous medium). Selected computed bond lengths (Å): C---C(CO) 1.867; C=O 1.132; C-C(Ph) 1.503, 1.504, 1.506. Selected computed angles (°): C(CO)-C-C(Ph) 99.3, 99.5, 103.5. Imaginary frequency i424.4 cm⁻¹.
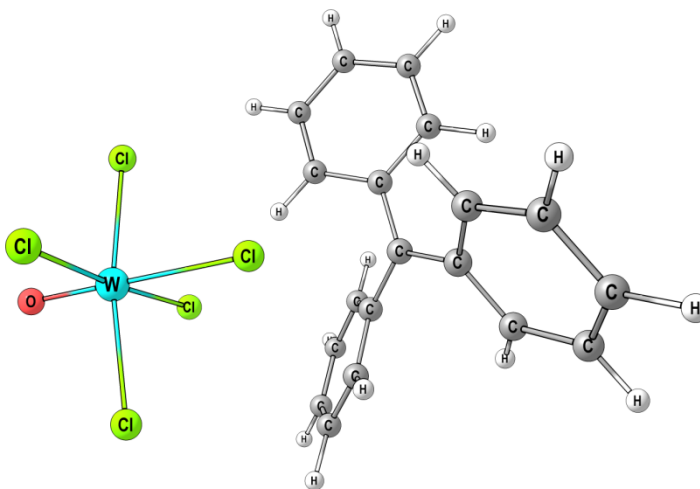
Figure 134. DFT-optimized geometry of [Ph₃C][WOCl₅] (intermediate **f**, **Figure 87**) (C-PCM-ωB97X calculations, dichloromethane as continuous medium). Selected computed bond lengths (Å): W-Cl 2.335, 2.341, 2.345, 2.359, 2.545; W=O 1.676; C-C(Ph) 1.446, 1.448, 1.451. Selected computed angles (°): O=W-Cl 94.2, 94.3, 94.7, 95.0, 179.2; C(Ph)-C-C(Ph) 119.8, 119.8, 120.4.

Figure 135. DFT-optimized geometry of WOCl₄ + Ph₃CCl (intermediate **g**, **Figure 87**) (C-PCM-ωB97X calculations, dichloromethane as continuous medium). Selected computed bond lengths (Å): W-Cl 2.310, 2.311, 2.315, 2.335; W=O 1.655; C-Cl 1.839. Selected computed angles (°): O=W-Cl 98.5, 98.6, 103.1, 103.2.

226

6. References

[1]   S. M. Coman, M. Verziu, A. Tirsoaga, B. Jurca, C. Teodorescu, V. Kuncser, V. I. Parvulescu, G. Scholz, E. Kemnitz, *ACS Catal.* **2015**, *5*, 3013–3026.

[2]   S. Afewerki, A. Córdova, *Chem. Rev.* **2016**, *116*, 13512–13570.

[3]   M. M. Rahman, M. D. Smith, J. A. Amaya, T. M. Makris, D. V. Peryshkov, *Inorg. Chem.* **2017**, *56*, 11798–11803.

[4]   M. Bortoluzzi, E. Ferretti, M. Hayatifar, F. Marchetti, G. Pampaloni, S. Zacchini, *Eur. J. Inorg. Chem.* **2016**, *2016*, 3838–3845.

[5]   H. Tsurugi, H. Tanahashi, H. Nishiyama, W. Fegler, T. Saito, A. Sauer, J. Okuda, K. Mashima, *J. Am. Chem. Soc.* **2013**, *135*, 5986–5989.

[6]   N. G. Connelly, W. E. Geiger, *Chem. Rev.* **1996**, *96*, 877–910.

[7]   F. Marchetti, G. Pampaloni, C. Pinzino, *Chem. - Eur. J.* **2013**, *19*, 13962–13969.

[8]   O. B. Babushkina, S. Ekres, *Electrochim. Acta* **2010**, *56*, 867–877.

[9]   M. Schubert, S. R. Waldvogel, *European J. Org. Chem.* **2016**, *2016*, 1921–1936.

[10]   S. R. Waldvogel, S. Trosien, *Chem. Commun.* **2012**, *48*, 9109–9119.

[11]   V. Lacerda, D. Araujo dos Santos, L. C. da Silva-Filho, S. J. Greco, R. Bezerra dos Santos, *Aldrichimica Acta* **2012**, *45*, 19–27.

[12]   M. A. Zolfigol, A. R. Moosavi-Zare, P. Arghavani-Hadi, A. Zare, V. Khakyzadeh, G. Darvishi, *RSC Adv.* **2012**, *2*, 3618.

[13]   L. Ferrand, Y. Tang, C. Aubert, L. Fensterbank, V. Mouriès-Mansuy, M. Petit, M. Amatore, *Org. Lett.* **2017**, *19*, 2062–2065.

[14]   P. M. Edwards, L. L. Schafer, *Chem. Commun.* **2018**, *54*, 12543–12560.

[15]   D. J. Gilmour, J. M. P. Lauzon, E. Clot, L. L. Schafer, *Organometallics* **2018**, *37*, 4387–4394.

[16]   I. V. Tatarinova, O. A. Tarasova, M. V. Markova, L. V. Morozova, A. I. Mikhaleva, B. A. Trofimov, *J. Organomet. Chem.* **2012**, *706–707*, 124–127.

[17]   A. Kanazawa, S. Kanaoka, S. Aoshima, *Macromolecules* **2009**, *42*, 3965–3972.

[18]   Y. Satoh, Y. Obora, *European J. Org. Chem.* **2015**, *2015*, 5041–5054.

[19]   F. Marchetti, G. Pampaloni, *Chem. Commun.* **2012**, *48*, 635–653.

[20]   S. Chandrasekhar, T. Ramachandar, T. Shyamsunder, *Indian J. Chem. - Sect. B Org. Med. Chem.* **2004**, *43*, 813–838.

[21]   C. Z. Andrade, *Curr. Org. Synth.* **2004**, *1*, 333–353.

[22]   C. Kleber Z. Andrade, R. Rocha, *Mini. Rev. Org. Chem.* **2006**, *3*, 271–280.

[23]   A. Spannenberg, H. Fuhrmann, P. Arndt, W. Baumann, R. Kempe, *Angew. Chem., Int. Ed.* **1998**, *37*, 3363–3365.

[24]   R. R. Langeslay, D. M. Kaphan, C. L. Marshall, P. C. Stair, A. P. Sattelberger, M. Delferro, *Chem. Rev.* **2019**, *119*, 2128–2191.

[25]   C. S. Digwal, U. Yadav, P. V. S. Ramya, S. Sana, B. Swain, A. Kamal, *J. Org. Chem.* **2017**, *82*, 7332–7345.

[26] C. Redshaw, *Dalton Trans.* **2010**, *39*, 5595–5604.

[27] V. C. Gibson, S. K. Spitzmesser, *Chem. Rev.* **2003**, *103*, 283–316.

[28] H. Hagen, J. Boersma, G. van Koten, *Chem. Soc. Rev.* **2002**, *31*, 357–364.

[29] D. Zhao, K. Chang, T. Ebel, M. Qian, R. Willumeit, M. Yan, F. Pyczak, *J. Mech. Behav. Biomed. Mater.* **2013**, *28*, 171–182.

[30] I. Jirka, M. Vandrovcová, O. Frank, Z. Tolde, J. Plšek, T. Luxbacher, L. Bačáková, V. Starý, *Mater. Sci. Eng. C* **2013**, *33*, 1636–1645.

[31] S. A. Cotton, F. A. Hart, in *The Heavy Transition Elements*, Macmillan Education UK, London, **1975**, pp. 15–26.

[32] L. G. Hubert-Pfalzgraf, in *Encyclopedia of Inorganic Chemistry*, John Wiley & Sons, Ltd, Chichester, UK, **2006**.

[33] J. M. Brink, F. D. Stevenson, *J. Chem. Eng. Data* **1972**, *17*, 143–145.

[34] D. R. Sadoway, S. N. Flengas, *Can. J. Chem.* **1976**, *54*, 1692–1699.

[35] A. J. Edwards, *J. Chem. Soc.* **1964**, 3714.

[36] W. Hönle, H. G. von Schnering, *Zeitschrift für Krist. - Cryst. Mater.* **1990**, *191*, 139–140.

[37] L. G. Hubert-Pfalzgraf, M. Postel, J. G. Riess, in *Comprehensive Coordination Chemistry* (Eds.: G. Wilkinson, R.D. Gillard, J.A. McCleverty), Pergamon Press, Oxford, **1987**, pp. 586–697.

[38] T. Waters, A. G. Wedd, M. Ziolek, I. Nowak, in *Comprehensive Coordination Chemistry II* (Eds.: J.A. McCleverty, T.J. Meyer, E. Constable), Elsevier, Oxford, **2003**, pp. 241–312.

[39] R. G. Kidd, H. G. Spinney, *Inorg. Chem.* **1973**, *12*, 1967–1971.

[40] C. M. P. Favez, H. Rollier, A. E. Merbach, *Helv. Chim. Acta* **1976**, *59*, 2383–2392.

[41] G. R. Willey, T. J. Woodman, M. G. B. Drew, *Polyhedron* **1997**, *16*, 351–353.

[42] F. Marchetti, G. Pampaloni, S. Zacchini, *Inorg. Chem.* **2008**, *47*, 365–372.

[43] R. Haiges, P. Deokar, K. O. Christe, *Z. Anorg. Allg. Chem.* **2014**, *640*, 1568–1575.

[44] S. Elbel, M. Grodzicki, L. Pille, G. Rünger, *J. Mol. Struct.* **1988**, *175*, 441–446.

[45] B. N. Meyer, J. N. Ishley, A. V. Fratini, H. C. Knachel, *Inorg. Chem.* **1980**, *19*, 2324–2327.

[46] F. A. Cotton, G. Wilkinson, C. A. Murillo, M. Bochmann, *Advanced Inorganic Chemistry*, John Wiley & Sons, Inc., New York, NY, **1999**.

[47] T. J. Richardson, F. L. Tanzella, N. Bartlett, *J. Am. Chem. Soc.* **1986**, *108*, 4937–4943.

[48] F. Marchetti, C. Pinzino, S. Zacchini, G. Pampaloni, *Angew. Chem., Int. Ed.* **2010**, *49*, 5268–5272.

[49] J. E. Burks, in *Encycl. Reagents Org. Synth.*, John Wiley & Sons, Ltd, Chichester, UK, **2001**, pp. 1–4.

[50] A. M. Gregson, S. M. Wales, S. J. Bailey, P. A. Keller, *J. Organomet. Chem.* **2015**, *785*, 77–83.

[51] A. Kędzia, K. Jasiak, A. Kudelko, *Synlett* **2018**, *29*, 1745–1748.

[52]   M. Bortoluzzi, F. Marchetti, M. G. Murrali, G. Pampaloni, *Inorganica Chim. Acta* **2015**, *427*, 150–154.

[53]   D. V. Drobot, E. A. Pisarev, *Zh. Neorg. Khim.* **1981**, *26*, 3–16.

[54]   V. Pershina, B. Fricke, *J. Phys. Chem.* **1994**, *98*, 6468–6473.

[55]   H. D. B. Jenkins, L. Sharman, A. Finch, P. N. Gates, *Inorg. Chem.* **1996**, *35*, 6316–6326.

[56]   M. Jan-Khan, R. Samuel, *Proc. Phys. Soc.* **1936**, *48*, 626–641.

[57]   F. Marchetti, G. Pampaloni, S. Zacchini, *Dalton Trans.* **2007**, 4343.

[58]   R. Bini, C. Chiappe, F. Marchetti, G. Pampaloni, S. Zacchini, *Inorg. Chem.* **2010**, *49*, 339–351.

[59]   F. Marchetti, G. Pampaloni, S. Zacchini, *RSC Adv.* **2014**, *4*, 60878–60882.

[60]   B. P. Mundy, C. A. Stewart, in *Encycl. Reagents Org. Synth.*, John Wiley & Sons, Ltd, Chichester, UK, **2008**, pp. 5–6.

[61]   B. Schimmelpfennig, U. Wahlgren, O. Gropen, A. Haaland, *J. Chem. Soc. Dalt. Trans.* **2001**, 1616–1620.

[62]   F. Tamadon, K. Seppelt, *Angew. Chem., Int. Ed.* **2013**, *52*, 767–769.

[63]   F. Marchetti, G. Pampaloni, L. Biancalana, *Inorganica Chim. Acta* **2012**, *385*, 135–139.

[64]   F. Marchetti, G. Pampaloni, *Inorganica Chim. Acta* **2011**, *376*, 123–128.

[65]   F. Marchetti, G. Pampaloni, S. Zacchini, *J. Fluorine Chem.* **2010**, *131*, 21–28.

[66]   S. L. Benjamin, W. Levason, G. Reid, *Chem. Soc. Rev.* **2013**, *42*, 1460–1499.

[67]   F. Marchetti, G. Pampaloni, S. Zacchini, *Polyhedron* **2015**, *85*, 369–375.

[68]   T. A. Bazhenova, K. A. Lyssenko, D. A. Kuznetsov, N. V. Kovaleva, Y. V. Manakin, T. A. Savinykh, A. F. Shestakov, *Polyhedron* **2014**, *76*, 108–116.

[69]   A. De Palo, L. Biancalana, M. Bortoluzzi, M. Alessandra Martini, F. Marchetti, G. Pampaloni, *Polyhedron* **2018**, *141*, 208–214.

[70]   J. B. Fang, R. Sanghi, J. Kohn, A. S. Goldman, *Inorganica Chim. Acta* **2004**, *357*, 2415–2426.

[71]   J.-T. Hou, H.-L. Chen, Z.-H. Zhang, *Phosphorus. Sulfur. Silicon Relat. Elem.* **2011**, *186*, 88–93.

[72]   E. M. Coe, C. J. Jones, *Polyhedron* **1992**, *11*, 3123–3128.

[73]   M. Constantino, V. Junior, L. Filho, G. Silva, *Lett. Org. Chem.* **2004**, *1*, 360–364.

[74]   M. Bortoluzzi, F. Marchetti, G. Pampaloni, S. Zacchini, *Dalton Trans.* **2014**, *43*, 16416–16423.

[75]   M. Bortoluzzi, F. Guarra, F. Marchetti, G. Pampaloni, S. Zacchini, *Polyhedron* **2015**, *99*, 141–146.

[76]   M. Bortoluzzi, F. Marchetti, M. G. Murrali, G. Pampaloni, S. Zacchini, *Dalton Trans.* **2015**, *44*, 8729–8738.

[77]   J. S. Yadav, D. C. Bhunia, K. Vamshi Krishna, P. Srihari, *Tetrahedron Lett.* **2007**, *48*, 8306–8310.

[78]   C. R. Reddy, P. P. Madhavi, A. S. Reddy, *Tetrahedron Lett.* **2007**, *48*, 7169–

7172.

[79] F. Fleming, P. Ravikumar, L. Yao, *Synlett* **2009**, *2009*, 1077–1080.

[80] P. C. Ravikumar, L. Yao, F. F. Fleming, *J. Org. Chem.* **2009**, *74*, 7294–7299.

[81] F. Marchetti, G. Pampaloni, S. Zacchini, *Dalton Trans.* **2013**, *42*, 15226–15234.

[82] M. Bortoluzzi, F. Marchetti, G. Pampaloni, S. Zacchini, *Eur. J. Inorg. Chem.* **2016**, *2016*, 3169–3177.

[83] S. Arai, Y. Sudo, A. Nishida, *Synlett* **2004**, *5*, 1104–1106.

[84] Y. Sudo, S. Arai, A. Nishida, *European J. Org. Chem.* **2006**, 752–758.

[85] S. L. Benjamin, Y.-P. Chang, C. Gurnani, A. L. Hector, M. Huggon, W. Levason, G. Reid, *Dalt. Trans.* **2014**, *43*, 16640–16648.

[86] Q. Guo, T. Miyaji, G. Gao, R. Hara, T. Takahashi, *Chem. Commun.* **2001**, 1018–1019.

[87] Q. Guo, T. Miyaji, R. Hara, B. Shen, T. Takahashi, *Tetrahedron* **2002**, *58*, 7327–7334.

[88] F. Marchetti, G. Pampaloni, S. Zacchini, *Chem. Commun.* **2008**, *3801*, 3651–3653.

[89] F. Marchetti, G. Pampaloni, S. Zacchini, *Dalton Trans.* **2009**, 8096.

[90] F. Marchetti, G. Pampaloni, T. Repo, *Eur. J. Inorg. Chem.* **2008**, *2008*, 2107–2112.

[91] L. Favero, F. Marchetti, G. Pampaloni, S. Zacchini, *Dalton Trans.* **2014**, *43*, 495–504.

[92] M. G. Constantino, V. Lacerda, P. R. Invernize, L. C. D. S. Filho, G. V. J. Da Silva, *Synth. Commun.* **2007**, *37*, 3529–3539.

[93] F. Marchetti, G. Pampaloni, S. Zacchini, *Polyhedron* **2009**, *28*, 1235–1240.

[94] J. Meinwald, S. S. Labana, M. S. Chadha, *J. Am. Chem. Soc.* **1963**, *85*, 582–585.

[95] S. Chandrasekhar, T. Ramachandar, S. J. Prakash, *Synthesis* **2000**, *13*, 1817–1818.

[96] A. V. Narsaiah, D. Sreenu, K. Nagaiah, *Synth. Commun.* **2006**, *36*, 3183–3189.

[97] J. S. Yadav, B. V. Subba Reddy, B. Eeshwaraiah, P. N. Reddy, *Tetrahedron* **2005**, *61*, 875–878.

[98] J. S. Yadav, D. C. Bhunia, V. K. Singh, P. Srihari, *Tetrahedron Lett.* **2009**, *50*, 2470–2473.

[99] J.-T. Hou, J.-W. Gao, Z.-H. Zhang, *Monatshefte für Chemie - Chem. Mon.* **2011**, *142*, 495–499.

[100] M. Kidwai, N. Bura, N. K. Mishra, *Indian J. Chem. - Sect. B Org. Med. Chem.* **2011**, *50*, 229–232.

[101] R. Wang, B. gang Li, T. kun Huang, L. Shi, X. xia Lu, *Tetrahedron Lett.* **2007**, *48*, 2071–2073.

[102] Y.-H. Liu, P. Wang, G.-T. Cheng, *Monatshefte für Chemie - Chem. Mon.* **2013**, *144*, 191–196.

[103] J. T. Hou, J. W. Gao, Z. H. Zhang, *Appl. Organomet. Chem.* **2011**, *25*, 47–

53.

[104] S. S. Kim, G. Rajagopal, S. C. George, *Appl. Organomet. Chem.* **2007**, *21*, 368–372.

[105] Z. Xue, Y. Zhang, G. Li, J. Wang, W. Zhao, T. Mu, *Catal. Sci. Technol.* **2016**, *6*, 1070–1076.

[106] M. A. Zolfigol, M. Tavasoli, A. R. Moosavi-Zare, P. Arghavani-Hadi, A. Zare, V. Khakyzadeh, *RSC Adv.* **2013**, *3*, 7692.

[107] M. E. Jung, J. I. Wasserman, *Tetrahedron Lett.* **2003**, *44*, 7273–7275.

[108] F. Marchetti, G. Pampaloni, S. Zacchini, *Dalton Trans.* **2013**, *42*, 2477–2487.

[109] S. Dolci, F. Marchetti, G. Pampaloni, S. Zacchini, *Inorg. Chem.* **2011**, *50*, 3846–3848.

[110] M. Hayatifar, F. Marchetti, G. Pampaloni, C. Pinzino, S. Zacchini, *Polyhedron* **2013**, *61*, 188–194.

[111] M. Aresta, A. Dibenedetto, P. Stufano, B. M. Aresta, S. Maggi, I. Pápai, T. A. Rokob, B. Gabriele, *Dalton Trans.* **2010**, *39*, 6985–6992.

[112] P. D. W. Boyd, M. G. Glenny, C. E. F. Rickard, A. J. Nielson, *Polyhedron* **2011**, *30*, 632–637.

[113] S. Chandrasekhar, T. Ramachander, M. Takhi, *Tetrahedron Lett.* **1998**, *39*, 3263–3266.

[114] J. S. Yadav, A. V. Narsaiah, B. V. S. Reddy, A. K. Basak, K. Nagaiah, *J. Mol. Catal. A Chem.* **2005**, *230*, 107–111.

[115] J. S. Yadav, A. V. Narsaiah, A. K. Basak, P. R. Goud, D. Sreenu, K. Nagaiah, *J. Mol. Catal. A Chem.* **2006**, *255*, 78–80.

[116] S. Arai, Y. Sudo, A. Nishida, *Tetrahedron* **2005**, *61*, 4639–4642.

[117] J. da Silva Barbosa, G. V. J. da Silva, M. G. Constantino, *Tetrahedron Lett.* **2015**, *56*, 4649–4652.

[118] Y. Satoh, K. Yasuda, Y. Obora, *Organometallics* **2012**, *31*, 5235–5238.

[119] M. Fuji, Y. Obora, *Org. Lett.* **2017**, *19*, 5569–5572.

[120] Y. Satoh, Y. Obora, *J. Org. Chem.* **2013**, *78*, 7771–7776.

[121] Y. Satoh, Y. Obora, *J. Org. Chem.* **2011**, *76*, 8569–8573.

[122] K. Watanabe, Y. Satoh, M. Kamei, H. Furukawa, M. Fuji, Y. Obora, *Org. Lett.* **2017**, *19*, 5398–5401.

[123] M. Kamei, K. Watanabe, M. Fuji, Y. Obora, *Chem. Lett.* **2016**, *45*, 943–945.

[124] V. A. D'yakonov, G. N. Kadikova, D. I. Kolokol'tsev, L. M. Khalilov, U. M. Dzhemilev, *Russ. Chem. Bull.* **2013**, *62*, 441–443.

[125] M. Aresta, A. Dibenedetto, L. Gianfrate, C. Pastore, *J. Mol. Catal. A Chem.* **2003**, *204–205*, 245–252.

[126] A. Monassier, V. D'Elia, M. Cokoja, H. Dong, J. D. A. Pelletier, J. M. Basset, F. E. Kühn, *ChemCatChem* **2013**, *5*, 1321–1324.

[127] M. E. Wilhelm, M. H. Anthofer, R. M. Reich, V. D'Elia, J.-M. Basset, W. A. Herrmann, M. Cokoja, F. E. Kühn, *Catal. Sci. Technol.* **2014**, *4*, 1638–1643.

[128] X. Wu, M. Wang, Y. Xie, C. Chen, K. Li, M. Yuan, X. Zhao, Z. Hou, *Appl. Catal. A Gen.* **2016**, *519*, 146–154.

[129] V. D'Elia, A. A. Ghani, A. Monassier, J. Sofack-Kreutzer, J. D. A. Pelletier,

M. Drees, S. V. C. Vummaleti, A. Poater, L. Cavallo, M. Cokoja, et al., *Chem. - Eur. J.* **2014**, *20*, 11870–11882.

[130]   S. Arayachukiat, P. Yingcharoen, S. V. C. Vummaleti, L. Cavallo, A. Poater, V. D'Elia, *Mol. Catal.* **2017**, *443*, 280–285.

[131]   N. M. Raju, K. Rajasekhar, J. M. Babu, B. V. Rao, *Asian J. Chem.* **2017**, *29*, 614–616.

[132]   S. Chandrasekhar, B. V. Subba Reddy, *Synlett* **1998**, 851–852.

[133]   J. S. Yadav, B. V. S. Reddy, M. K. Gupta, S. K. Biswas, *Synthesis* **2004**, 2711–2715.

[134]   J. S. Yadav, B. V. S. Reddy, J. J. Naidu, K. Sadashiv, *Chem. Lett.* **2004**, *33*, 926–927.

[135]   M. Adharvana Chari, D. Shobha, S. Parameswari, B. Ramesh, R. R. Pal, *Asian J. Chem.* **2012**, *24*, 15–17.

[136]   W. dos Santos, L. da Silva-Filho, *Synthesis* **2012**, *44*, 3361–3365.

[137]   A. D. A. Bartolomeu, M. L. De Menezes, L. C. Da Silva-Filho, *Synth. Commun.* **2015**, *45*, 1114–1126.

[138]   B. H. S. T. Da Silva, L. M. Martins, L. C. Da Silva-Filho, *Synlett* **2012**, *23*, 1973–1977.

[139]   L. M. Martins, B. H. S. T. da Silva, M. L. de Menezes, L. C. da Silva-Filho, *Heterocycl. Lett.* **2013**, *3*, 307–317.

[140]   P. B. Oshiro, P. S. Da Silva Gomes Lima, M. L. De Menezes, L. C. Da Silva-Filho, *Tetrahedron Lett.* **2015**, *56*, 4476–4479.

[141]   W. H. dos Santos, L. C. da Silva-Filho, *Tetrahedron Lett.* **2017**, *58*, 894–897.

[142]   M. de Souza Siqueira, L. C. da Silva-Filho, *Tetrahedron Lett.* **2016**, *57*, 5050–5052.

[143]   W. dos Santos, E. de Oliveira, F. Lavarda, I. Leonarczyk, M. Ferreira, L. da Silva-Filho, *Synthesis* **2017**, *49*, 2402–2410.

[144]   A. de Andrade, G. C. dos Santos, L. C. da Silva-Filho, *J. Heterocycl. Chem.* **2015**, *52*, 273–277.

[145]   G. C. dos Santos, A. de Andrade Bartolomeu, V. F. Ximenes, L. C. da Silva-Filho, *J. Fluoresc.* **2017**, *27*, 271–280.

[146]   G. C. dos Santos, V. F. Moreno, P. B. Oshiro, L. C. da Silva-Filho, *Tetrahedron* **2018**, *74*, 6144–6149.

[147]   B. H. S. T. da Silva, B. A. Bregadiolli, C. F. de O. Graeff, L. C. da Silva-Filho, *Chempluschem* **2017**, *82*, 261–269.

[148]   R. T. Alarcon, C. Gaglieri, B. H. S. T. da Silva, L. C. da Silva Filho, G. Bannach, *J. Photochem. Photobiol. A Chem.* **2017**, *343*, 112–118.

[149]   L. M. Martins, S. de Faria Vieira, G. B. Baldacim, B. A. Bregadiolli, J. C. Caraschi, A. Batagin-Neto, L. C. da Silva-Filho, *Dye. Pigment.* **2018**, *148*, 81–90.

[150]   V. Veeramani, P. Muthuraja, S. Prakash, M. Senthil Kumar, A. Susaimanickam, P. Manisankar, *ChemistrySelect* **2018**, *3*, 10027–10031.

[151]   N. R. Kamble, V. T. Kamble, *Asian J. Chem.* **2019**, *31*, 1357–1361.

[152]   A. Andrade Bartolomeu, M. Menezes, L. Silva Filho, *Chem. Pap.* **2014**, *68*,

1593–1600.

[153]   W. H. dos Santos, L. C. Da Silva-Filho, *Chem. Pap.* **2016**, *70*, 1658–1664.

[154]   J. Bian, B. Deng, X. Zhang, T. Hu, N. Wang, W. Wang, H. Pei, Y. Xu, H. Chu, X. Li, et al., *Tetrahedron Lett.* **2014**, *55*, 1475–1478.

[155]   J. Bian, X. Qian, J. Fan, X. Li, H. Sun, Q. You, X. Zhang, *Tetrahedron Lett.* **2015**, *56*, 397–400.

[156]   R. R. Schrock, J. S. Murdzek, G. C. Bazan, J. Robbins, M. Dimare, M. O'Regan, *J. Am. Chem. Soc.* **1990**, *112*, 3875–3886.

[157]   A. A. Greish, L. M. Kustov, A. V. Vasnev, *Mendeleev Commun.* **2011**, *21*, 329–330.

[158]   V. I. Bykov, E. M. Khmarin, B. A. Belyaev, T. A. Butenko, E. S. Finkel'shtein, *Kinet. Catal.* **2008**, *49*, 11–17.

[159]   V. I. Bykov, O. B. Chernova, B. A. Belyaev, T. A. Butenko, E. S. Finkelshtein, *Pet. Chem.* **2015**, *55*, 549–551.

[160]   V. I. Bykov, B. A. Belyaev, T. A. Butenko, E. S. Finkel'shtein, *Pet. Chem.* **2016**, *56*, 62–64.

[161]   V. I. Bykov, B. A. Belyaev, T. A. Butenko, *Kinet. Catal.* **2018**, *59*, 688–689.

[162]   M. Fuji, J. Chiwata, M. Ozaki, S. Aratani, Y. Obora, *ACS Omega* **2018**, *3*, 8865–8873.

[163]   K. Yasuda, Y. Obora, *J. Organomet. Chem.* **2015**, *775*, 33–38.

[164]   R. M. Sultanov, U. M. Dzhemilev, E. V. Samoilova, R. R. Ismagilov, L. M. Khalilov, N. R. Popod'Ko, *J. Organomet. Chem.* **2012**, *715*, 5–8.

[165]   R. M. Sultanov, R. R. Ismagilov, N. R. Popod'ko, A. R. Tulyabaev, U. M. Dzhemilev, *J. Organomet. Chem.* **2013**, *724*, 51–56.

[166]   R. M. Sultanov, R. R. Ismagilov, N. R. Popod'Ko, A. R. Tulyabaev, D. S. Sabirov, U. M. Dzhemilev, *J. Organomet. Chem.* **2013**, *745–746*, 120–125.

[167]   R. M. Sultanov, F. S. Khafizov, I. V. Ozden, N. V. Shutov, D. S. Sabirov, U. M. Dzhemilev, *Russ. J. Gen. Chem.* **2019**, *89*, 647–652.

[168]   R. M. Sultanov, E. V. Samoilova, N. R. Popod'Ko, A. R. Tulyabaev, D. S. Sabirov, U. M. Dzhemilev, *Tetrahedron Lett.* **2013**, *54*, 6619–6623.

[169]   R. M. Sultanov, E. V. Samoilova, N. R. Popod'Ko, D. S. Sabirov, U. M. Dzhemilev, *J. Organomet. Chem.* **2015**, *776*, 23–29.

[170]   M. Bortoluzzi, M. Hayatifar, F. Marchetti, G. Pampaloni, S. Zacchini, *Inorg. Chem.* **2015**, *54*, 4047–4055.

[171]   F. Roudesly, J. Oble, G. Poli, *J. Mol. Catal. A Chem.* **2017**, *426*, 275–296.

[172]   T. C. Silva, M. dos S. Pires, A. A. de Castro, L. C. T. Lacerda, M. V. J. Rocha, T. C. Ramalho, *Theor. Chem. Acc.* **2018**, *137*, 146.

[173]   X. Chen, K. M. Engle, D. H. Wang, Y. Jin-Quan, *Angew. Chem., Int. Ed.* **2009**, *48*, 5094–5115.

[174]   H. Li, C. L. Sun, M. Yu, D. G. Yu, B. J. Li, Z. J. Shi, *Chem. - Eur. J.* **2011**, *17*, 3593–3597.

[175]   S. Kumar, M. Manickam, *Chem. Commun.* **1997**, *14*, 1615–1666.

[176]   S. R. Waldvogel, A. R. Wartini, P. H. Rasmussen, J. Rebek, *Tetrahedron Lett.* **1999**, *40*, 3515–3518.

[177] S. R. Waldvogel, R. Fröhlich, C. A. Schalley, *Angew. Chem., Int. Ed.* **2000**, *39*, 2472–2475.

[178] N. M. Boshta, M. Bomkamp, G. Schnakenburg, S. R. Waldvogel, *Chem. - Eur. J.* **2010**, *16*, 3459–3466.

[179] N. M. Boshta, M. Bomkamp, G. Schnakenburg, S. R. Waldvogel, *European J. Org. Chem.* **2011**, 1985–1992.

[180] S. R. Waldvogel, E. Aits, C. Holst, R. Fröhlich, *Chem. Commun.* **2002**, 1278–1279.

[181] B. Kramer, R. Fröhlich, K. Bergander, S. R. Waldvogel, *Synthesis* **2003**, 0091–0096.

[182] S. B. Beil, I. Uecker, P. Franzmann, T. Müller, S. R. Waldvogel, *Org. Lett.* **2018**, *20*, 4107–4110.

[183] S. B. Beil, T. Müller, S. B. Sillart, P. Franzmann, A. Bomm, M. Holtkamp, U. Karst, W. Schade, S. R. Waldvogel, *Angew. Chem., Int. Ed.* **2018**, *57*, 2450–2454.

[184] S. B. Beil, P. Franzmann, T. Müller, M. M. Hielscher, T. Prenzel, D. Pollok, N. Beiser, D. Schollmeyer, S. R. Waldvogel, *Electrochim. Acta* **2019**, *302*, 310–315.

[185] K. Hackeloer, G. Schnakenburg, S. R. Waldvogel, *Org. Lett.* **2011**, *13*, 916–919.

[186] K. Hackelöer, S. R. Waldvogel, *Tetrahedron Lett.* **2012**, *53*, 1579–1581.

[187] B. Kramer, A. Averhoff, S. R. Waldvogel, *Angew. Chem., Int. Ed.* **2002**, *41*, 2981.

[188] P. Franzmann, S. Trosien, M. Schubert, S. R. Waldvogel, *Org. Lett.* **2016**, *18*, 1182–1185.

[189] S. Trosien, S. R. Waldvogel, *Org. Lett.* **2012**, *14*, 2976–2979.

[190] K. Wehming, M. Schubert, G. Schnakenburg, S. R. Waldvogel, *Chem. - Eur. J.* **2014**, *20*, 12463–12469.

[191] S. Trosien, P. Böttger, S. R. Waldvogel, *Org. Lett.* **2014**, *16*, 402–405.

[192] S. Trosien, D. Schollmeyer, S. R. Waldvogel, *Synthesis* **2013**, *45*, 1160–1164.

[193] M. Schubert, K. Wehming, A. Kehl, M. Nieger, G. Schnakenburg, R. Fröhlich, D. Schollmeyer, S. R. Waldvogel, *European J. Org. Chem.* **2016**, *2016*, 60–63.

[194] M. Schubert, S. Trosien, L. Schulz, C. Brscheid, D. Schollmeyer, S. R. Waldvogel, *European J. Org. Chem.* **2014**, *2014*, 7091–7094.

[195] M. Schubert, J. Leppin, K. Wehming, D. Schollmeyer, K. Heinze, S. R. Waldvogel, *Angew. Chem., Int. Ed.* **2014**, *53*, 2494–2497.

[196] B. T. King, J. Kroulík, C. R. Robertson, P. Rempala, C. L. Hilton, J. D. Korinek, L. M. Gortari, *J. Org. Chem.* **2007**, *72*, 2279–2288.

[197] M. Grzybowski, K. Skonieczny, H. Butenschön, D. T. Gryko, *Angew. Chem., Int. Ed.* **2013**, *52*, 9900–9930.

[198] M. Schubert, P. Franzmann, A. Wünsche von Leupoldt, K. Koszinowski, K. Heinze, S. R. Waldvogel, *Angew. Chem., Int. Ed.* **2016**, *55*, 1156–1159.

[199] J. Leppin, M. Schubert, S. R. Waldvogel, K. Heinze, *Chem. - Eur. J.* **2015**, *21*, 4229–4232.

[200] X. Shen, Y. Wu, L. Bai, H. Zhao, X. Ba, *J. Polym. Sci. Part A Polym. Chem.* **2017**, *55*, 1285–1288.

[201] T. Fujikawa, N. Mitoma, A. Wakamiya, A. Saeki, Y. Segawa, K. Itami, *Org. Biomol. Chem.* **2017**, *15*, 4697–4703.

[202] M. Bortoluzzi, F. Marchetti, G. Pampaloni, S. Zacchini, *Inorg. Chem.* **2014**, *53*, 3832–3838.

[203] R. Bondi, F. Marchetti, G. Pampaloni, S. Zacchini, *Polyhedron* **2015**, *100*, 192–198.

[204] M. M. Rahman, M. D. Smith, D. V. Peryshkov, *Inorg. Chem.* **2016**, *55*, 5101–5103.

[205] H. Gandhi, T. P. O'Sullivan, *Tetrahedron Lett.* **2017**, *58*, 3533–3535.

[206] M. Bortoluzzi, F. Marchetti, G. Pampaloni, S. Zacchini, *Chem. Commun.* **2015**, *51*, 1323–1325.

[207] M. Bortoluzzi, F. Marchetti, G. Pampaloni, S. Zacchini, *New J. Chem.* **2016**, *40*, 8271–8281.

[208] L. L. Frolova, A. V Popov, L. V Bezuglaya, I. N. Alekseev, P. A. Slepukhin, A. V Kutchin, *Russ. J. Gen. Chem.* **2016**, *86*, 613–621.

[209] B. Boualy, L. El Firdoussi, M. A. Ali, A. Karim, *J. Braz. Chem. Soc.* **2011**, *22*, 1259–1262.

[210] X.-M. Zhu, Z.-S. Cai, H.-H. Zhang, M.-Z. Sun, *Asian J. Chem.* **2014**, *26*, 110–112.

[211] A. J. Heeger, *Angew. Chem., Int. Ed.* **2001**, *40*, 2591–2611.

[212] T. Masuda, K. Hasegawa, T. Higashimura, *Macromolecules* **1974**, *7*, 728–731.

[213] T. Ohtori, T. Masuda, T. Higashimura, *Polym. J.* **1979**, *11*, 805–811.

[214] T. Masuda, H. Kawai, T. Ohtori, T. Higashimura, *Polym. J.* **1979**, *11*, 813–818.

[215] T. Masuda, Y. Okano, Y. Kuwane, T. Higashimura, *Polym. J.* **1980**, *12*, 907–913.

[216] T. Masuda, M. Kawai, T. Higashimura, *Polymer* **1982**, *23*, 744–747.

[217] T. Masuda, K.-Q. Thieu, N. Sasaki, T. Higashimura, *Macromolecules* **1976**, *9*, 661–664.

[218] B. Z. Tang, X. Kong, X. Wan, H. Peng, W. Y. Lam, X. De Feng, H. S. Kwok, *Macromolecules* **1998**, *31*, 2419–2432.

[219] B. Z. Tang, H. Xu, *Macromolecules* **1999**, *32*, 2569–2576.

[220] C. K. W. Jim, J. W. Y. Lam, C. W. T. Leung, A. Qin, F. Mahtab, B. Z. Tang, *Macromolecules* **2011**, *44*, 2427–2437.

[221] C. Y. K. Chan, J. W. Y. Lam, C. Deng, X. Chen, K. S. Wong, B. Z. Tang, *Macromolecules* **2015**, *48*, 1038–1047.

[222] T. Masuda, E. Isobe, T. Higashimura, K. Takada, *J. Am. Chem. Soc.* **1983**, *105*, 7473–7474.

[223] Y. S. Gal, S. H. Jin, Y. Il Park, J. W. Park, W. S. Lyoo, K. T. Lim, S. Y. Kim,

Fibers Polym. **2011**, *12*, 291–295.

[224]   J. Tak, S. H. Jin, Y. S. Gal, *J. Ind. Eng. Chem.* **2017**, *55*, 74–79.

[225]   Y. S. Gal, S. H. Jin, S. Y. Shim, J. Park, T. K. Son, K. T. Lim, *Mol. Cryst. Liq. Cryst.* **2017**, *659*, 100–107.

[226]   A. C. Pauly, P. Theato, *Polym. Chem.* **2012**, *3*, 1769–1782.

[227]   A. C. Pauly, P. Theato, *J. Polym. Sci. Part A Polym. Chem.* **2011**, *49*, 211–224.

[228]   J. Rodriguez Castanon, N. Sano, M. Shiotsuki, F. Sanda, *J. Polym. Sci. Part A Polym. Chem.* **2017**, *55*, 382–388.

[229]   Y.-J. Jin, H. Kim, D.-Y. Hwang, M. Teraguchi, T. Kaneko, T. Aoki, G. Kwak, *Mol. Cryst. Liq. Cryst.* **2017**, *645*, 50–57.

[230]   Y. Goto, Y. Miyagi, N. Sano, F. Sanda, *J. Polym. Sci. Part A Polym. Chem.* **2017**, *55*, 3011–3016.

[231]   W. E. Lee, D. C. Han, T. Sakaguchi, Y. B. Kim, C. L. Lee, G. Kwak, *Macromol. Chem. Phys.* **2012**, *213*, 2293–2298.

[232]   S. Azuma, T. Sakaguchi, T. Hashimoto, *Polymer* **2016**, *92*, 18–24.

[233]   T. Sakaguchi, S. Azuma, T. Hashimoto, *Synth. Met.* **2016**, *212*, 174–179.

[234]   T. Muroga, T. Sakaguchi, T. Hashimoto, *Polymer* **2012**, *53*, 4380–4387.

[235]   T. Sakaguchi, Y. Hayakawa, R. Ishima, T. Hashimoto, *Synth. Met.* **2012**, *162*, 64–69.

[236]   A. A. Kossov, V. S. Khotimskiy, *Polymer* **2014**, *55*, 989–994.

[237]   V. S. Khotimsky, M. V. Tchirkova, E. G. Litvinova, A. I. Rebrov, G. N. Bondarenko, *J. Polym. Sci. Part A Polym. Chem.* **2003**, *41*, 2133–2155.

[238]   A. A. Kossov, A. V. Rebrov, V. D. Dolzhikova, V. S. Khotimskii, *Polym. Sci., Ser. B* **2013**, *55*, 258–265.

[239]   A. A. Kossov, K. Buhr, S. M. Shishatskii, E. G. Litvinova, V. S. Khotimskii, *Polym. Sci., Ser. B* **2017**, *59*, 452–458.

[240]   A. A. Kossov, E. G. Litvinova, A. A. Ezhov, V. S. Khotimskii, S. M. Shishatskii, K. Buhr, *Pet. Chem.* **2018**, *58*, 1123–1128.

[241]   E. Y. Sultanov, A. A. Ezhov, S. M. Shishatskiy, K. Buhr, V. S. Khotimskiy, *Macromolecules* **2012**, *45*, 1222–1229.

[242]   T. Sakaguchi, S. Nakao, S. Irie, T. Hashimoto, *Polymer* **2018**, *140*, 208–214.

[243]   R. Zheng, H. Dong, H. Peng, J. W. Y. Lam, B. Z. Tang, *Macromolecules* **2004**, *37*, 5196–5210.

[244]   J. Liu, Y. Zhong, J. W. Y. Lam, P. Lu, Y. Hong, Y. Yu, Y. Yue, M. Faisal, H. H. Y. Sung, I. D. Williams, et al., *Macromolecules* **2010**, *43*, 4921–4936.

[245]   R. Hu, J. W. Y. Lam, J. Liu, H. H. Y. Sung, I. D. Williams, Z. Yue, K. S. Wong, M. M. F. Yuen, B. Z. Tang, *Polym. Chem.* **2012**, *3*, 1481–1489.

[246]   S. Kanehashi, M. Onda, R. Shindo, S. Sato, S. Kazama, K. Nagai, *Polym. Eng. Sci.* **2013**, *53*, 1667–1675.

[247]   E. Ceausescu, A. Cornilescu, E. Nicolescu, M. Popescu, S. Coca, M. Cuzmici, C. Oprescu, M. Dimonie, G. Hubca, M. Teodorescu, et al., *J. Mol. Catal.* **1986**, *36*, 163–175.

[248]   M. Dimonie, S. Coca, V. Drăguţan, *J. Mol. Catal.* **1992**, *76*, 79–91.

[249] Y.-R. Zhang, J.-X. Yang, L. Pan, Y.-S. Li, *Chinese J. Polym. Sci.* **2018**, *36*, 214–221.

[250] V. T. Widyaya, H. T. Vo, R. Dhimas Dhewangga Putra, W. S. Hwang, B. S. Ahn, H. Lee, *Eur. Polym. J.* **2013**, *49*, 2680–2688.

[251] A. M. Raspolli Galletti, G. Pampaloni, *Coord. Chem. Rev.* **2010**, *254*, 525–536.

[252] C. Redshaw, M. Walton, L. Clowes, D. L. Hughes, A. M. Fuller, Y. Chao, A. Walton, V. Sumerin, P. Elo, I. Soshnikov, et al., *Chem. - Eur. J.* **2013**, *19*, 8884–8899.

[253] C. Redshaw, D. M. Homden, M. A. Rowan, M. R. J. Elsegood, *Inorganica Chim. Acta* **2005**, *358*, 4067–4074.

[254] M. Hayatifar, F. Marchetti, G. Pampaloni, Y. Patil, A. M. Raspolli Galletti, *Inorganica Chim. Acta* **2013**, *399*, 214–218.

[255] A. Kanazawa, S. Shibutani, N. Yoshinari, T. Konno, S. Kanaoka, S. Aoshima, *Macromolecules* **2012**, *45*, 7749–7757.

[256] M. Hayatifar, F. Marchetti, G. Pampaloni, Y. Patil, A. M. R. Galletti, *Catal. Today* **2012**, *192*, 177–182.

[257] Y. Takegami, T. Ueno, R. Hirai, *Bull. Chem. Soc. Jpn.* **1965**, *38*, 1222–1222.

[258] Y. Takegami, C. Ueno, R. Hirai, *J. Polym. Sci. Part A-1 Polym. Chem.* **1966**, *4*, 973–974.

[259] Q. Wang, Y. Su, L. Li, H. Huang, *Chem. Soc. Rev.* **2016**, *45*, 1257–1272.

[260] S. Chandrasekhar, S. J. Prakash, T. Shyamsunder, T. Ramachandar, *Synth. Commun.* **2004**, *34*, 3865–3873.

[261] C. K. Z. Andrade, G. R. Oliveira, *Tetrahedron Lett.* **2002**, *43*, 1935–1937.

[262] C. K. Z. Andrade, N. R. Azevedo, G. R. Oliveira, *Synthesis* **2002**, 928–936.

[263] F. Marchetti, G. Pampaloni, S. Zacchini, *Polyhedron* **2016**, *115*, 99–104.

[264] M. Bortoluzzi, T. Funaioli, F. Marchetti, G. Pampaloni, C. Pinzino, S. Zacchini, *Chem. Commun.* **2017**, *53*, 364–367.

[265] F. Marchetti, G. Pampaloni, S. Zacchini, *RSC Adv.* **2013**, *3*, 10007–10013.

[266] K. Fuchibe, T. Akiyama, *Synlett* **2004**, 1282–1284.

[267] T. G. Driver, *Angew. Chem., Int. Ed.* **2009**, *48*, 7974–7976.

[268] K. Fuchibe, T. Akiyama, *J. Am. Chem. Soc.* **2006**, *128*, 1434–1435.

[269] K. Fuchibe, T. Kaneko, K. Mori, T. Akiyama, *Angew. Chem., Int. Ed.* **2009**, *48*, 8070–8073.

[270] K. Saito, T. Umi, T. Yamada, T. Suga, T. Akiyama, *Org. Biomol. Chem.* **2017**, *15*, 1767–1770.

[271] F. Marchetti, G. Pampaloni, C. Pinzino, *J. Organomet. Chem.* **2011**, *696*, 1294–1300.

[272] F. Marchetti, G. Pampaloni, C. Pinzino, S. Zacchini, *Eur. J. Inorg. Chem.* **2013**, 5755–5761.

[273] M. Kirihara, A. Harano, H. Tsukiji, R. Takizawa, T. Uchiyama, A. Hatano, *Tetrahedron Lett.* **2005**, *46*, 6377–6380.

[274] M. Kirihara, T. Noguchi, N. Okajima, S. Naito, Y. Ishizuka, A. Harano, H. Tsukiji, R. Takizawa, *Tetrahedron* **2012**, *68*, 1515–1520.

[275] M. Kirihara, S. Suzuki, N. Ishihara, K. Yamazaki, T. Akiyama, Y. Ishizuka, *Synthesis* **2017**, *49*, 2009–2014.

[276] M. Kirihara, J. Yamamoto, T. Noguchi, A. Itou, S. Naito, Y. Hirai, *Tetrahedron* **2009**, *65*, 10477–10484.

[277] M. Kirihara, J. Yamamoto, T. Noguchi, Y. Hirai, *Tetrahedron Lett.* **2009**, *50*, 1180–1183.

[278] M. Kirihara, T. Goto, T. Noguchi, M. Suzuki, Y. Ishizuka, S. Naito, *Chem. Pharm. Bull.* **2013**, *61*, 460–463.

[279] E. V. Rakhmanov, S. V. Baranova, Z. Wang, A. V. Tarakanova, S. V. Kardashev, A. V. Akopyan, E. R. Naranov, M. S. Oshchepkov, A. V. Anisimov, *Pet. Chem.* **2014**, *54*, 316–322.

[280] E. V. Rakhmanov, D. Jinyuan, O. A. Fedorova, A. V. Tarakanova, A. V. Anisimov, *Theor. Found. Chem. Eng.* **2012**, *46*, 552–555.

[281] E. V. Rakhmanov, D. Jinyuan, O. A. Fedorova, A. V. Tarakanova, A. V. Anisimov, *Pet. Chem.* **2011**, *51*, 216–221.

[282] B. W. Yoo, J. Park, H. J. Shin, C. M. Yoon, *J. Sulfur Chem.* **2017**, *38*, 597–603.

[283] B. W. Yoo, M. K. Lee, C. M. Yoon, *Phosphorus, Sulfur Silicon Relat. Elem.* **2016**, *191*, 807–810.

[284] B. W. Yoo, H. M. Kim, D. Kim, *Synth. Commun.* **2013**, *43*, 2057–2061.

[285] A. Spurg, G. Schnakenburg, S. R. Waldvogel, *Chem. - Eur. J.* **2009**, *15*, 5–10.

[286] P. Franzmann, S. B. Beil, P. M. Winterscheid, D. Schollmeyer, S. R. Waldvogel, *Synlett* **2017**, *28*, 957–961.

[287] P. Franzmann, S. B. Beil, D. Schollmeyer, S. R. Waldvogel, *Chem. - Eur. J.* **2019**, *25*, 1936–1940.

[288] G. van Koten, K. Vrieze, in *Adv. Organomet. Chem.*, **1982**, pp. 151–239.

[289] L. Guo, H. Gao, Q. Guan, H. Hu, J. Deng, J. Liu, F. Liu, Q. Wu, *Organometallics* **2012**, *31*, 6054–6062.

[290] A. Raghavan, A. Venugopal, *J. Coord. Chem.* **2014**, *67*, 2530–2549.

[291] B. E. Cole, J. P. Wolbach, W. G. Dougherty, N. A. Piro, W. S. Kassel, C. R. Graves, *Inorg. Chem.* **2014**, *53*, 3899–3906.

[292] V. Lorenz, C. G. Hrib, D. Grote, L. Hilfert, M. Krasnopolski, F. T. Edelmann, *Organometallics* **2013**, *32*, 4636–4642.

[293] C. J. Allan, B. F. T. Cooper, H. J. Cowley, J. M. Rawson, C. L. B. Macdonald, *Chem. - Eur. J.* **2013**, *19*, 14470–14483.

[294] E. Uhlig, *Pure Appl. Chem.* **1988**, *60*, 1235–1240.

[295] B. G. Shestakov, T. V. Mahrova, J. Larionova, J. Long, A. V. Cherkasov, G. K. Fukin, K. A. Lyssenko, W. Scherer, C. Hauf, T. V. Magdesieva, et al., *Organometallics* **2015**, *34*, 1177–1185.

[296] T. K. Panda, H. Kaneko, K. Pal, H. Tsurugi, K. Mashima, *Organometallics* **2010**, *29*, 2610–2615.

[297] K. Takao, S. Tsushima, T. Ogura, T. Tsubomura, Y. Ikeda, *Inorg. Chem.* **2014**, *53*, 5772–5780.

238

[298] S. J. Kraft, U. J. Williams, S. R. Daly, E. J. Schelter, S. A. Kozimor, K. S. Boland, J. M. Kikkawa, W. P. Forrest, C. N. Christensen, D. E. Schwarz, et al., *Inorg. Chem.* **2011**, *50*, 9838–9848.

[299] M. Trincado, V. Sinha, R. E. Rodriguez-Lugo, B. Pribanic, B. De Bruin, H. Grützmacher, *Nat. Commun.* **2017**, *8*, 1–11.

[300] R. E. Rodríguez-Lugo, M. Trincado, M. Vogt, F. Tewes, G. Santiso-Quinones, H. Grützmacher, *Nat. Chem.* **2013**, *5*, 342–347.

[301] I. Pappas, S. Treacy, P. J. Chirik, *ACS Catal.* **2016**, *6*, 4105–4109.

[302] W. N. Palmer, J. V. Obligacion, I. Pappas, P. J. Chirik, *J. Am. Chem. Soc.* **2016**, *138*, 766–769.

[303] R. Wang, X. Sui, W. Pang, C. Chen, *ChemCatChem* **2016**, *8*, 434–440.

[304] W. Kaim, *Eur. J. Inorg. Chem.* **2012**, 343–348.

[305] C. Mealli, A. Ienco, A. D. Phillips, A. Galindo, *Eur. J. Inorg. Chem.* **2007**, 2556–2568.

[306] D. A. Matveev, E. F. Sagitova, P. B. Kraykivskii, S. K. Petrovskii, N. S. Gurinovich, V. V. Saraev, *Russ. J. Electrochem.* **2014**, *50*, 239–242.

[307] K. Dreisch, C. Andersson, C. Stålhandske, *Polyhedron* **1993**, *12*, 1335–1343.

[308] K. Dreisch, C. Andersson, C. Stålhandske, *Polyhedron* **1993**, *12*, 303–311.

[309] A. J. L. Pombeiro, M. F. N. N. Carvalho, *Rev. Port. Quìmica* **1981**, *23*, 23–32.

[310] K. M. Clark, J. W. Ziller, A. F. Heyduk, *Inorg. Chem.* **2010**, *49*, 2222–2231.

[311] J. Scholz, B. Richter, R. Goddard, C. Krüger, *Chem. Ber.* **1993**, *126*, 57–61.

[312] Y. Zhao, Y. Xue, W. Xu, J.-H. Su, B. Wu, X.-J. Yang, *Eur. J. Inorg. Chem.* **2016**, *2016*, 5411–5417.

[313] P. J. Daff, M. Etienne, B. Donnadieu, S. Z. Knottenbelt, J. E. McGrady, *J. Am. Chem. Soc.* **2002**, *124*, 3818–3819.

[314] H. Nishiyama, H. Ikeda, T. Saito, B. Kriegel, H. Tsurugi, J. Arnold, K. Mashima, *J. Am. Chem. Soc.* **2017**, *139*, 6494–6505.

[315] H. Tsurugi, T. Saito, H. Tanahashi, J. Arnold, K. Mashima, *J. Am. Chem. Soc.* **2011**, *133*, 18673–18683.

[316] H. Tanahashi, H. Ikeda, H. Tsurugi, K. Mashima, *Inorg. Chem.* **2016**, *55*, 1446–1452.

[317] H. Tanahashi, H. Tsurugi, K. Mashima, *Organometallics* **2015**, *34*, 731–741.

[318] N. Bartalucci, M. Bortoluzzi, T. Funaioli, F. Marchetti, G. Pampaloni, S. Zacchini, *Dalton Trans.* **2017**, *46*, 12780–12784.

[319] M. Bortoluzzi, F. Marchetti, G. Pampaloni, C. Pinzino, S. Zacchini, *Inorg. Chem.* **2016**, *55*, 887–893.

[320] S. I. Gorelsky, A. B. Ilyukhin, P. V. Kholin, V. Y. Kotov, B. V. Lokshin, N. V. Sapoletova, *Inorganica Chim. Acta* **2007**, *360*, 2573–2582.

[321] U. Siemeling, S. Tomm, C. Bruhn, *J. Organomet. Chem.* **2006**, *691*, 5056–5059.

[322] K. Woźniak, T. M. Krygowski, *J. Mol. Struct.* **1989**, *193*, 81–92.

[323] H. J. Keller, D. Nöthe, M. Werner, *Can. J. Chem.* **1979**, *57*, 1033–1036.

[324] M. S. Kim, S. B. Lee, *Materials (Basel).* **2014**, *7*, 5581–5590.

[325] K. Şendil, B. Özgün, *Phosphorus, Sulfur Silicon Relat. Elem.* **2006**, *181*, 959–964.

[326] N. Değirmenbaşi, B. Özgün, *Monatshefte fur Chemie* **2002**, *133*, 1417–1421.

[327] S. Kundu, A. Banerjee, A. De, A. Y. Khan, G. S. Kumar, R. Bhadra, P. Ghosh, *J. Fluoresc.* **2015**, *25*, 1645–1654.

[328] A. K. Parhi, Y. Zhang, K. W. Saionz, P. Pradhan, M. Kaul, K. Trivedi, D. S. Pilch, E. J. LaVoie, *Bioorg. Med. Chem. Lett.* **2013**, *23*, 4968–4974.

[329] M. Ishtiaq, I. Munir, M. Al-Rashida, Maria, K. Ayub, J. Iqbal, R. Ludwig, K. M. Khan, S. A. Ali, A. Hameed, *RSC Adv.* **2016**, *6*, 64009–64018.

[330] D. Schelz, N. Rotzler, *Dye. Pigment.* **1989**, *11*, 147–161.

[331] D. Schelz, *Helv. Chim. Acta* **1978**, *61*, 2452–2462.

[332] N. Bartalucci, M. Bortoluzzi, S. Zacchini, G. Pampaloni, F. Marchetti, *New J. Chem.* **2018**, *42*, 8503–8511.

[333] M. Zettlitzer, H. tom Dieck, E. T. K. Haupt, L. Stamp, *Chem. Ber.* **1986**, *119*, 1868–1875.

[334] H. Rojas-Sáenz, G. V. Suárez-Moreno, I. Ramos-García, A. M. Duarte-Hernández, E. Mijangos, A. Peña-Hueso, R. Contreras, A. Flores-Parra, *New J. Chem.* **2014**, *38*, 391–405.

[335] E. Wissing, M. Kaupp, J. Boersma, A. L. Spek, G. van Koten, *Organometallics* **1994**, *13*, 2349–2356.

[336] M. Kaupp, H. Stoll, H. Preuss, W. Kaim, T. Stahl, G. van Koten, E. Wissing, W. J. J. Smeets, A. L. Spek, *J. Am. Chem. Soc.* **1991**, *113*, 5606–5618.

[337] L. Weber, J. Förster, H. G. Stammler, B. Neumann, *Eur. J. Inorg. Chem.* **2006**, 5048–5056.

[338] A. A. Trifonov, E. A. Fedorova, G. K. Fukin, N. O. Druzhkov, M. N. Bochkarev, *Angew. Chem., Int. Ed.* **2004**, *43*, 5045–5048.

[339] A. Hinchliffe, F. S. Mair, E. J. L. McInnes, R. G. Pritchard, J. E. Warren, *Dalton Trans.* **2008**, 222–233.

[340] F. S. Mair, R. Manning, R. G. Pritchard, J. E. Warren, *Chem. Commun.* **2001**, *93*, 1136–1137.

[341] I. E. Buys, S. Elgafi, L. D. Field, T. W. Hambley, B. A. Messerle, *Inorg. Chem.* **1994**, *33*, 1539–1542.

[342] D. Walther, S. Liesicke, L. Böttcher, R. Fischer, H. Görls, G. Vaughan, *Inorg. Chem.* **2003**, *42*, 625–632.

[343] D. Walther, S. Liesicke, R. Fischer, H. Görls, J. Weston, A. Batista, *Eur. J. Inorg. Chem.* **2003**, *2003*, 4321–4331.

[344] J. Beck, K. Müller-Buschbaum, F. Wolf, *Z. Anorg. Allg. Chem.* **1999**, *625*, 975–981.

[345] G. V. Khvorykh, S. I. Troyanov, A. I. Baranov, A. A. Serov, *Z. Anorg. Allg. Chem.* **1998**, *624*, 1026–1030.

[346] E. Hey, F. Weller, K. Dehnicke, *Z. Anorg. Allg. Chem.* **1984**, *508*, 86–92.

[347] F. Stoffelbach, D. Saurenz, R. Poli, *Eur. J. Inorg. Chem.* **2001**, *2001*, 2699–2703.

[348] A. V. Butcher, J. Chatt, *J. Chem. Soc. A Inorganic, Phys. Theor.* **1970**, 2652.

[349] E. A. Allen, B. J. Bridson, G. W. A. Fowles, *J. Chem. Soc.* **1964**, 4531.

[350] N. Bartalucci, M. Bortoluzzi, G. Pampaloni, C. Pinzino, S. Zacchini, F. Marchetti, *Dalton Trans.* **2018**, *47*, 3346–3355.

[351] W. Levason, G. Reid, W. Zhang, *J. Fluorine Chem.* **2015**, *172*, 62–67.

[352] W. Levason, M. E. Light, G. Reid, W. Zhang, *Dalton Trans.* **2014**, *43*, 9557–9566.

[353] V. C. Gibson, T. P. Kee, A. Shaw, *Polyhedron* **1988**, *7*, 2217–2219.

[354] T. V. Laine, M. Klinga, A. Maaninen, E. Aitola, M. Leskelä, O. Mønsted, J. C. Rasmussen, H. Toftlund, *Acta Chem. Scand.* **1999**, *53*, 968–973.

[355] W. Levason, G. Reid, J. Trayer, W. Zhang, *Dalton Trans.* **2014**, *43*, 3649–3659.

[356] D. Pugh, J. A. Wright, S. Freeman, A. A. Danopoulos, *Dalton Trans.* **2006**, 775–782.

[357] J. Poitras, A. L. Beauchamp, *Can. J. Chem.* **1994**, *72*, 1675–1683.

[358] T. Spaniel, H. Görls, J. Scholz, *Angew. Chem., Int. Ed.* **1998**, *37*, 1862–1865.

[359] F. Marchetti, G. Pampaloni, S. Zacchini, *Dalton Trans.* **2009**, *5*, 6759.

[360] J. Beck, J. Bordinhão, *Z. Anorg. Allg. Chem.* **2005**, *631*, 1261–1266.

[361] J. A. Canich, F. A. Cotton, S. A. Duraj, *Inorganica Chim. Acta* **1989**, *156*, 41–46.

[362] V. G. Nenajdenko, *Isocyanide Chemistry*, Wiley-VCH Verlag GmbH & Co. KGaA, Weinheim, Germany, **2012**.

[363] M. Suginome, Y. Ito, in *Categ. 3, Compd. with Four Three Carbon Heteroat. Bond.* (Ed.: Murahashi), Georg Thieme Verlag, Stuttgart, **2004**.

[364] J. Campo, M. García-Valverde, S. Marcaccini, M. J. Rojo, T. Torroba, *Org. Biomol. Chem.* **2006**, *4*, 757–765.

[365] A. Dömling, I. Ugi, *Angew. Chem.* **2000**, *39*, 3168–3210.

[366] M. Minozzi, D. Nanni, P. Spagnolo, *Curr. Org. Chem.* **2007**, *11*, 1366–1384.

[367] C. P. Kubiak, in *Compr. Organomet. Chem. II*, Elsevier, **1995**, pp. 1–27.

[368] M. V. Baker, D. H. Brown, M. Tamm, R. J. Baker, in *Compr. Organomet. Chem. III*, Elsevier, **2007**, pp. 391–512.

[369] M. V. Baker, D. H. Brown, in *Compr. Organomet. Chem. III*, Elsevier, **2007**, pp. 597–722.

[370] R. Aumann, *Angew. Chem., Int. Ed. Eng.* **1988**, *27*, 1456–1467.

[371] M. V. Barybin, V. G. Young, J. E. Ellis, *J. Am. Chem. Soc.* **1999**, *121*, 9237–9238.

[372] S. Prashar, M. Fajardo, A. Garcés, I. Dorado, A. Antiñolo, A. Otero, I. López-Solera, C. López-Mardomingo, *J. Organomet. Chem.* **2004**, *689*, 1304–1314.

[373] M. I. Alcalde, J. de la Mata, M. Gomez, P. Royo, M. A. Pellinghelli, A. Tiripicchio, *Organometallics* **1994**, *13*, 462–467.

[374] N. Bartalucci, L. Belpassi, F. Marchetti, G. Pampaloni, S. Zacchini, G. Ciancaleoni, *Inorg. Chem.* **2018**, *57*, 14554–14563.

[375] S. L. Benjamin, Y.-P. Chang, C. Gurnani, A. L. Hector, M. Huggon, W. Levason, G. Reid, *Dalton Trans.* **2014**, *43*, 16640–16648.

[376] P. J. McKarns, M. J. Heeg, C. H. Winter, *Inorg. Chem.* **1998**, *37*, 4743–4747.

[377] M. Jura, W. Levason, R. Ratnani, G. Reid, M. Webster, *Dalton Trans.* **2010**, *39*, 883–891.

[378] M. Bortoluzzi, E. Ferretti, F. Marchetti, G. Pampaloni, S. Zacchini, *Dalton Trans.* **2016**, *45*, 6939–6948.

[379] M. Bortoluzzi, E. Ferretti, F. Marchetti, G. Pampaloni, S. Zacchini, *Chem. Commun.* **2014**, *50*, 4472–4474.

[380] K. F. Hirsekorn, A. S. Veige, M. P. Marshak, Y. Koldobskaya, P. T. Wolczanski, T. R. Cundari, E. B. Lobkovsky, *J. Am. Chem. Soc.* **2005**, *127*, 4809–4830.

[381] G. S. McGrady, A. Haaland, H. P. Verne, H. V. Volden, A. J. Downs, D. Shorokhov, G. Eickerling, W. Scherer, *Chem. - Eur. J.* **2005**, *11*, 4921–4934.

[382] N. C. Tomson, J. Arnold, R. G. Bergman, *Organometallics* **2010**, *29*, 2926–2942.

[383] M. Schormann, S. P. Varkey, H. W. Roesky, M. Noltemeyer, *J. Organomet. Chem.* **2001**, *621*, 310–316.

[384] C. D. Abernethy, G. M. Codd, M. D. Spicer, M. K. Taylor, *J. Am. Chem. Soc.* **2003**, *125*, 1128–1129.

[385] Z. Wei, W. Zhang, G. Luo, F. Xu, Y. Mei, H. Cai, *New J. Chem.* **2016**, *40*, 6270–6275.

[386] A. Bondi, *J. Phys. Chem.* **1964**, *68*, 441–451.

[387] G. Ciancaleoni, L. Belpassi, F. Marchetti, *Inorg. Chem.* **2017**, *56*, 11266–11274.

[388] L. Belpassi, I. Infante, F. Tarantelli, L. Visscher, *J. Am. Chem. Soc.* **2008**, *130*, 1048–1060.

[389] G. Ciancaleoni, L. Biasiolo, G. Bistoni, A. Macchioni, F. Tarantelli, D. Zuccaccia, L. Belpassi, *Chem. - Eur. J.* **2015**, *21*, 2467–2473.

[390] C. A. Gaggioli, G. Bistoni, G. Ciancaleoni, F. Tarantelli, L. Belpassi, P. Belanzoni, *Chem. - Eur. J.* **2017**, *23*, 7558–7569.

[391] G. Bistoni, S. Rampino, F. Tarantelli, L. Belpassi, *J. Chem. Phys.* **2015**, *142*, 084112.

[392] E. D. Glendening, J. K. Badenhoop, A. E. Reed, J. E. Carpenter, J. A. Bohmann, C. M. Morales, C. R. Landis, F. Weinhold, *NBO 6 (Theoretical Chemistry Institute, University of Winsconsin, Madison, WI, 2013); Http://Nbo6.Chem.Wisc.Edu/*, **n.d.**

[393] G. Bistoni, S. Rampino, N. Scafuri, G. Ciancaleoni, D. Zuccaccia, L. Belpassi, F. Tarantelli, *Chem. Sci.* **2016**, *7*, 1174–1184.

[394] N. Bartalucci, L. Biancalana, M. Bortoluzzi, G. Pampaloni, L. Giordano, S. Zacchini, F. Marchetti, *ChemistrySelect* **2018**, *3*, 8844–8848.

[395] P. H. Lacy, D. C. C. Smith, *J. Chem. Soc. Perkin Trans. 1* **1974**, *23*, 2617.

[396] A. S. Pankova, A. Y. Stukalov, M. A. Kuznetsov, *Org. Lett.* **2015**, *17*, 1826–1829.

242

[397] V. C. Gibson, T. P. Kee, A. Shaw, *Polyhedron* **1990**, *9*, 2293–2298.

[398] M. Bortoluzzi, C. Evangelisti, F. Marchetti, G. Pampaloni, F. Piccinelli, S. Zacchini, *Dalton Trans.* **2016**, *45*, 15342–15349.

[399] T. Chanda, S. Chowdhury, S. Koley, M. S. Singh, *Tetrahedron* **2016**, *72*, 5903–5908.

[400] A. L. Bednowitz, W. C. Hamilton, R. Brown, L. G. Donaruma, P. L. Southwick, R. Kropf, R. A. Stanfield, *J. Am. Chem. Soc.* **1968**, *90*, 291–296.

[401] D. G. Hendry, D. Schuetzle, *J. Am. Chem. Soc.* **1975**, *97*, 7123–7127.

[402] M. Bobrowski, A. Liwo, S. Ołdziej, D. Jeziorek, T. Ossowski, *J. Am. Chem. Soc.* **2000**, *122*, 8112–8119.

[403] A. Sinhamahapatra, A. Sinha, S. K. Pahari, N. Sutradhar, H. C. Bajaj, A. B. Panda, *Catal. Sci. Technol.* **2012**, *2*, 2375.

[404] M. M. Hashemi, Y. A. Beni, *J. Chem. Res. - Part S* **2000**, *45*, 196–197.

[405] C.-L. Lin, C.-C. Wang, *Appl. Energy* **2016**, *164*, 1043–1051.

[406] Y. V. Plyuto, J. Stoch, I. V. Babytch, A. A. Chuyko, *J. Non. Cryst. Solids* **1990**, *124*, 41–47.

[407] J. J. Cruywagen, in *Adv. Inorg. Chem.*, **1999**, pp. 127–182.

[408] J. Schwarz, B. König, *Green Chem.* **2018**, *20*, 323–361.

[409] N. A. Till, R. T. Smith, D. W. C. MacMillan, *J. Am. Chem. Soc.* **2018**, *140*, 5701–5705.

[410] W. I. Dzik, P. P. Lange, L. J. Gooßen, *Chem. Sci.* **2012**, *3*, 2671.

[411] M. O. Miranda, A. Pietrangelo, M. A. Hillmyer, W. B. Tolman, *Green Chem.* **2012**, *14*, 490–494.

[412] S. Maetani, T. Fukuyama, N. Suzuki, D. Ishihara, I. Ryu, *Organometallics* **2011**, *30*, 1389–1394.

[413] G. Kraus, S. Riley, *Synthesis* **2012**, *44*, 3003–3005.

[414] A. John, M. O. Miranda, K. Ding, B. Dereli, M. A. Ortuno, A. M. Lapointe, G. W. Coates, C. J. Cramer, W. B. Tolman, *Organometallics* **2016**, *35*, 2391–2400.

[415] S. Maetani, T. Fukuyama, I. Ryu, *Org. Lett.* **2013**, *15*, 2754–2757.

[416] M. A. Ortuño, B. Dereli, C. J. Cramer, *Inorg. Chem.* **2016**, *55*, 4124–4131.

[417] A. John, M. A. Hillmyer, W. B. Tolman, *Organometallics* **2017**, *36*, 506–509.

[418] M. Lesslie, Y. Yang, A. J. Canty, E. Piacentino, F. Berthias, P. Maitre, V. Ryzhov, R. A. J. O'Hair, *Chem. Commun.* **2018**, *54*, 346–349.

[419] P. Hermange, A. T. Lindhardt, R. H. Taaning, K. Bjerglund, D. Lupp, T. Skrydstrup, *J. Am. Chem. Soc.* **2011**, *133*, 6061–6071.

[420] Y. Obora, Y. Tsuji, T. Kawamura, *J. Am. Chem. Soc.* **1995**, *117*, 9814–9821.

[421] N. Bartalucci, M. Bortoluzzi, S. Zacchini, G. Pampaloni, F. Marchetti, *Dalton Trans.* **2019**, *48*, 1574–1577.

[422] P. M. Cook, L. F. Dahl, D. W. Dickerhoof, *J. Am. Chem. Soc.* **1972**, *94*, 5511–5513.

[423] F. Calderazzo, P. Pallavicini, G. Pampaloni, P. F. Zanazzi, *J. Chem. Soc. Dalt. Trans.* **1990**, 2743.

[424] J. Zhou, S. J. Lancaster, D. A. Walker, S. Beck, M. Thornton-Pett, M.

Bochmann, *J. Am. Chem. Soc.* **2001**, *123*, 223–237.

[425] A. Kraft, N. Trapp, D. Himmel, H. Böhrer, P. Schlüter, H. Scherer, I. Krossing, *Chem. - Eur. J.* **2012**, *18*, 9371–9380.

[426] G. A. Olah, M. Alemayehu, A. Wu, O. Farooq, G. K. S. Prakash, *J. Am. Chem. Soc.* **1992**, *114*, 8042–8045.

[427] G. Pampaloni, N. Bartalucci, F. Marchetti, S. Zacchini, *Dalton Trans.* **2019**, DOI 10.1039/C9DT00551J.

[428] G. A. Olah, W. S. Tolgyesi, S. J. Kuhn, M. E. Moffatt, I. J. Bastien, E. B. Baker, *J. Am. Chem. Soc.* **1963**, *85*, 1328–1334.

[429] M. Bortoluzzi, G. Bresciani, F. Marchetti, G. Pampaloni, S. Zacchini, *Dalton Trans.* **2015**, *44*, 10030–10037.

[430] I. Pauls, K. Dehnicke, D. Fenske, *Chem. Ber.* **1989**, *122*, 481–483.

[431] C. D. Garner, P. Lambert, F. E. Mabbs, T. J. King, *J. Chem. Soc. Dalt. Trans.* **1977**, 1191.

[432] C. Limberg, M. Büchner, K. Heinze, O. Walter, *Inorg. Chem.* **1997**, *36*, 872–879.

[433] D. L. Kepert, R. Mandyczewsky, *J. Chem. Soc. A Inorganic, Phys. Theor.* **1968**, 530.

[434] B. Modec, M. Šala, R. Clérac, *Eur. J. Inorg. Chem.* **2010**, *4*, 542–553.

[435] R. Aguado, J. Escribano, M. R. Pedrosa, A. De Cian, R. Sanz, F. J. Arnáiz, *Polyhedron* **2007**, *26*, 3842–3848.

[436] J. Köhler, A. Simon, L. Van Wüllen, S. Cordier, T. Roisnel, M. Poulain, M. Somer, *Z. Anorg. Allg. Chem.* **2002**, *628*, 2683–2690.

[437] M. Bortoluzzi, F. Marchetti, G. Pampaloni, M. Pucino, S. Zacchini, *Dalton Trans.* **2013**, *42*, 13054.

[438] H.-B. Sun, B. Li, R. Hua, Y. Yin, *European J. Org. Chem.* **2006**, *2006*, 4231–4236.

[439] V. López-Carrillo, A. M. Echavarren, *J. Am. Chem. Soc.* **2010**, *132*, 9292–9294.

[440] S. P. Lewis, N. J. Taylor, W. E. Piers, S. Collins, *J. Am. Chem. Soc.* **2003**, *125*, 14686–14687.

[441] T. W. Toone, E. Lee-Ruff, P. G. Khazanie, A. C. Hopkinson, *J. Chem. Soc., Perkin Trans. 2* **1975**, 607–609.

[442] M. Ma, K. E. Johnson, *J. Am. Chem. Soc.* **1995**, *117*, 1508–1513.

[443] G. A. Olah, A. H. Wu, O. Farooq, G. K. S. Prakash, *J. Org. Chem.* **1990**, *55*, 1792–1796.

[444] G. Sauvet, J. P. Vairon, P. Sigwalt, *J. Polym. Sci. Polym. Symp.* **2007**, *52*, 173–187.

[445] G. A. Olah, Y. Halpebn, *J. Org. Chem.* **1971**, *36*, 2354–2356.

[446] G. A. Olah, C. U. Pittman, E. Namanworth, M. B. Comisarow, *J. Am. Chem. Soc.* **1966**, *88*, 5571–5581.

[447] R. A. McClelland, C. Chan, F. Cozens, A. Modro, S. Steenken, *Angew. Chem., Int. Ed. Eng.* **1991**, *30*, 1337–1339.

[448] R. A. McClelland, V. M. Kanagasabapathy, S. Steenken, *J. Am. Chem. Soc.*

1988, *110*, 6913–6914.

[449]   P. Wan, E. Krogh, *J. Am. Chem. Soc.* **1989**, *111*, 4887–4895.

[450]   J. L. Faria, S. Steenken, *J. Phys. Chem.* **1992**, *96*, 10869–10874.

[451]   O. C. Fehr, O. Grapenthin, J. Kilian, W. Kirmse, S. Steenken, *Tetrahedron Lett.* **1995**, *36*, 5887–5890.

[452]   G. A. Olah, G. Salem, J. S. Staral, T. L. Ho, *J. Org. Chem.* **1978**, *43*, 173–175.

[453]   J. Chai, S. P. Lewis, S. Collins, T. J. J. Sciarone, L. D. Henderson, P. A. Chase, G. J. Irvine, W. E. Piers, M. R. J. Elsegood, W. Clegg, *Organometallics* **2007**, *26*, 5667–5679.

[454]   L. Hintermann, *Beilstein J. Org. Chem.* **2007**, *3*, 2–6.

[455]   A. J. Arduengo, R. Krafczyk, R. Schmutzler, H. A. Craig, J. R. Goerlich, W. J. Marshall, M. Unverzagt, *Tetrahedron* **1999**, *55*, 14523–14534.

[456]   B. R. Van Ausdall, J. L. Glass, K. M. Wiggins, A. M. Aarif, J. Louie, *J. Org. Chem.* **2009**, *74*, 7935–7942.

[457]   U. Jacquemard, P. Harpainter, S. Roland, *Tetrahedron Lett.* **2013**, *54*, 4793–4795.

[458]   W. Willker, D. Leibfritz, R. Kerssebaum, W. Bermel, *Magn. Reson. Chem.* **1993**, *31*, 287–292.

[459]   R. Ambrosetti, D. Ricci, *Rev. Sci. Instrum.* **1991**, *62*, 2281–2287.

[460]   C. Pinzino, C. Forte, *EPR-ENDOR*, Rome, Italy, **1992**.

[461]   D. R. Duling, *J. Magn. Reson. Ser. B* **1994**, *104*, 105–110.

[462]   E. König, G. König, in *Magn. Prop. Coord. Organomet. Transit. Met. Compd.*, Springer-Verlag, Berlin/Heidelberg, **2005**, pp. 668–681.

[463]   D. A. Skoog, D. M. West, F. J. Holler, *Fundamentals of Analytical Chemistry*, Thomson Learning, Inc., USA, **1996**.

[464]   M. Movsisyan, T. S. A. Heugebaert, R. Dams, C. V. Stevens, *ChemSusChem* **2016**, *9*, 1945–1952.

[465]   C. J. Bartlett, D. P. Day, Y. Chan, S. M. Allin, M. J. McKenzie, A. M. Z. Slawin, P. C. Bulman Page, *J. Org. Chem.* **2012**, *77*, 772–774.

[466]   D. Basavaiah, K. R. Reddy, *Org. Lett.* **2007**, *9*, 57–60.

[467]   C. De Risi, L. Ferraro, G. P. Pollini, S. Tanganelli, F. Valente, A. C. Veronese, *Bioorg. Med. Chem.* **2008**, *16*, 9904–9910.

[468]   M. M. Kayser, J. Salvador, P. Morand, *Can. J. Chem.* **1983**, *61*, 439–441.

[469]   G. M. Sheldrick, *SADABS 2008/1 - Bruker AXS Area Detector Scaling and Absorption Correction*, Bruker AXS Inc, Madison, Wisconsin, USA, **2008**.

[470]   G. M. Sheldrick, *Acta Crystallogr. Sect. C Struct. Chem.* **2015**, *71*, 3–8.

[471]   A. L. Spek, *PLATON - A Multipurpose Crystallographic Tool*, Utrecht University, Utrecht, **2005**.

[472]   A. L. Spek, *J. Appl. Crystallogr.* **2003**, *36*, 7–13.

[473]   A. L. Spek, *Acta Crystallogr. Sect. D Biol. Crystallogr.* **2009**, *65*, 148–155.

[474]   H. D. Flack, *Acta Crystallogr. Sect. A Found. Crystallogr.* **1983**, *39*, 876–881.

[475]   Y. Minenkov, Å. Singstad, G. Occhipinti, V. R. Jensen, *Dalton Trans.* **2012**, *41*, 5526–5541.

[476] J. Da Chai, M. Head-Gordon, *Phys. Chem. Chem. Phys.* **2008**, *10*, 6615–6620.

[477] I. C. Gerber, J. G. Ángyán, *Chem. Phys. Lett.* **2005**, *415*, 100–105.

[478] F. Weigend, R. Ahlrichs, *Phys. Chem. Chem. Phys.* **2005**, *7*, 3297–3305.

[479] D. Andrae, U. Häußermann, M. Dolg, H. Stoll, H. Preuss, *Theor. Chim. Acta* **1990**, *77*, 123–141.

[480] M. Cossi, N. Rega, G. Scalmani, V. Barone, *J. Comput. Chem.* **2003**, *24*, 669–681.

[481] V. Barone, M. Cossi, *J. Phys. Chem. A* **1998**, *102*, 1995–2001.

[482] F. Jensen, *Introduction to Computational Chemistry*, John Wiley & Sons Ltd, Chichester, **2007**.

[483] D. J. Frisch, M. J.; Trucks, G.W.; Schlegel, H. B.; Scuseria, G. E.; Robb, M. A.; Cheeseman, J. R.; Scalmani, G.; Barone, V.;Mennucci, B.; Petersson, G. A.; Nakatsuji, H.; Caricato, M.; Li, X.; Hratchian, H. P.; Izmaylov, A. F.; Bloino, J.; Zheng, G.; Sonnenber, *Gaussian, Inc. Wallingford CT* **2009**.

[484] *SCM, Theoretical Chemistry, Vrije Universiteit*, Amsterdam, The Netherlands, **2008**.

[485] A. D. Becke, *Phys. Rev. A* **1988**, *38*, 3098–3100.

[486] C. Lee, W. Yang, R. G. Parr, *Phys. Rev. B* **1988**, *37*, 785–789.

[487] E. van Lenthe, E. J. Baerends, J. G. Snijders, *J. Chem. Phys.* **1993**, *99*, 4597–4610.

[488] E. van Lenthe, E. J. Baerends, J. G. Snijders, *J. Chem. Phys.* **1994**, *101*, 9783–9792.

[489] E. Van Lenthe, *J. Chem. Phys.* **1999**, *110*, 8943–8953.